

AD-A031 179

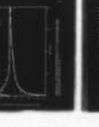
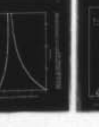
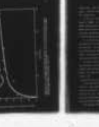
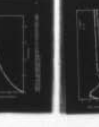
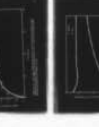
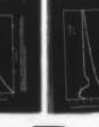
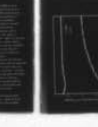
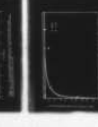
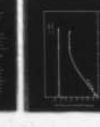
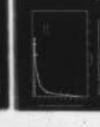
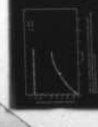
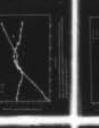
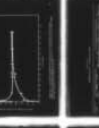
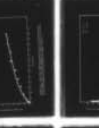
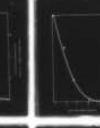
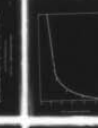
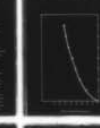
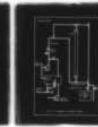
CLEMSON UNIV S C DEPT OF ENVIRONMENTAL SYSTEMS ENGI--ETC F/G 13/2
MATHEMATICAL MODELING OF HETEROGENEOUS SORPTION IN CONTINUOUS C--ETC(U)
APR 76 T M KEINATH, H KARESH, S LOWRY

DADA17-73-C-3154

NL

UNCLASSIFIED

1 OF 2
AD
A031179



AD A031179

CLEMSON UNIVERSITY

Environmental Systems Engineering

MATHEMATICAL MODELING OF HETEROGENEOUS SORPTION IN CONTINUOUS
CONTACTORS FOR WASTEWATER DECONTAMINATION: INFLUENCE OF REVERSIBILITY
AND CHROMATOGRAPHIC EFFECTS ON SYSTEM DESIGN AND OPERATION

by

Dr. Thomas M. Keinath, Principal Investigator
Hyman Karesh, Samuel Lowry, Mohamed Abdo, Investigators

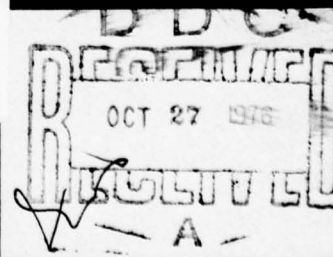


DISTRIBUTION STATEMENT A

Approved for public release;
Distribution Unlimited

Clemson

South Carolina



Approved for public release; distribution unlimited.

The findings in this report are not to be construed as an official Department of the Army position unless so designated by other authorized documents.

| REPORT DOCUMENTATION PAGE | | READ INSTRUCTIONS BEFORE COMPLETING FORM |
|---|--|---|
| 1. REPORT NUMBER (9) Final rept. 1 | 2. GOVT ACCESSION NO. Jul 73-30 | 3. RECIPIENT'S CATALOG NUMBER Jun 74 |
| 4. TITLE (and Subtitle) Mathematical Modeling of heterogeneous sorption in continuous contactors for wastewater decontamination; influence of reversibility and chromatographic effects on system design and operation. | 5. TYPE OF REPORT & PERIOD COVERED Final 7-1-73 to 6-30-74 | |
| 7. AUTHOR (10) Thomas M. Keinath, Hyman Karesh, Samuel Lowry, Mohamed S. Abdo | 6. PERFORMING ORG. REPORT NUMBER | |
| 9. PERFORMING ORGANIZATION NAME AND ADDRESS Environmental Systems Engineering Clemson University Clemson, SC 29631 | 8. CONTRACT OR GRANT NUMBER(s) (15) DADA-17-73-C-3154 NEW | |
| 11. CONTROLLING OFFICE NAME AND ADDRESS US Army Medical R & D Command Washington, DC 20314 | 10. PROGRAM ELEMENT, PROJECT, TASK AREA & WORK UNIT NUMBERS | |
| 14. MONITORING AGENCY NAME & ADDRESS (if different from Controlling Office) | 12. REPORT DATE (11) April 1976 | |
| | 13. NUMBER OF PAGES xi + 169 | |
| | 15. SECURITY CLASS. (of this report) (12) 182p. | |
| | 15a. DECLASSIFICATION/DOWNGRADING SCHEDULE | |
| 16. DISTRIBUTION STATEMENT (of this Report) Approved for public release; distribution unlimited. | | |
| 17. DISTRIBUTION STATEMENT (of the abstract entered in Block 20, if different from Report) | | |
| 18. SUPPLEMENTARY NOTES | | |
| 19. KEY WORDS (Continue on reverse side if necessary and identify by block number) Adsorption, Mathematical Modeling, Decontamination, Reversibility, Chromatographic Effects, Sorption, Wastewater. | | |
| 20. ABSTRACT (Continue on reverse side if necessary and identify by block number) As water quality standards have become more stringent, there has been an increasing interest in the use of activated carbon for the removal of trace contaminants. Accordingly, the objective of this study was to develop a predictive model for adsorption of multiple solutes from solution onto activated carbon using a differential contacting system. To accomplish this goal, two secondary objectives had to be achieved. These were (1) to evaluate existing multi-solute adsorption equilibria models and (2) to determine how adsorption | | |

408598

4B

20. cont.

→ reversibility and chromatographic effects would influence the design and subsequent operation of prototype adsorbers.

Numerous adsorption equilibrium studies were conducted using bi-solute combinations of o-phenylphenol (OPP), dinitro-o-sec-butylphenol (DNOSBP), and 2,4-dichlorophenol (2,4-DCP). Results of these studies were employed to evaluate the utility of the Longmuir Competitive, Longmuir Semi-Competitive Ideal Solution Theory and Graphical Models of competitive adsorption equilibria. Neither of the models was found to adequately describe competitive adsorption effects. Nonetheless, the Graphical approach gave the best estimate of competitive interactions.

Simulations using the dynamic mathematical model showed that:

- (1) the fluidized-bed mode of operation offers distinct advantages over packed-bed operation for minimizing the elution of adsorbed contaminants from adsorbers;
- (2) industrial production schedules should be arranged such that all contaminants are discharged concurrently;
- (3) production schedules should be arranged such that wastewaters containing the highest energy adsorbing contaminants are introduced first to a column of fresh adsorbent while the wastewaters containing the lowest energy adsorbing contaminants are introduced last;
- (4) concentration equilization should be employed ahead of adsorbers to minimize displacement and subsequent elution of adsorbed contaminants.

Columnar laboratory studies generally verified the conclusions drawn from the simulations.

| | |
|--------------------------------|---|
| ADDITION BY | |
| RTW | White Section <input checked="" type="checkbox"/> |
| DOB | Buff Section <input type="checkbox"/> |
| UNANNOUNCED | <input type="checkbox"/> |
| JUSTIFICATION | |
| BY | |
| DISTRIBUTION/AVAILABILITY CODE | |
| Dist. | SCALE, AND/OR SPECIAL |
| A | |

DA _____

MATHEMATICAL MODELING OF HETEROGENEOUS
SORPTION IN CONTINUOUS CONTACTORS FOR
WASTEWATER DECONTAMINATION:
INFLUENCE OF REVERSIBILITY AND CHROMATOGRAPHIC
EFFECTS ON SYSTEM DESIGN AND OPERATION

Final Report

Thomas M. Keinath, Principal Investigator
Hyman Karesh, Investigator
Samuel Lowry, Investigator
Mohamed S. Abdo, Investigator

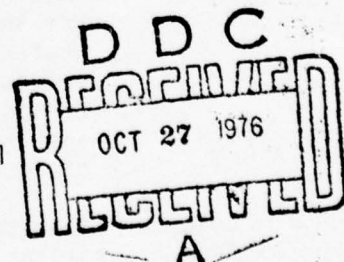
April 1976

Supported by

U. S. ARMY MEDICAL RESEARCH AND DEVELOPMENT COMMAND
Washington, D. C. 20314

Contract No. DADA-17-73-C-3154

Clemson University
Clemson, South Carolina 29631



SUMMARY

As water quality standards have become more stringent, there has been an increasing interest in the use of activated carbon for the removal of trace contaminants. Accordingly, the objective of this study was to develop a predictive model for adsorption of multiple solutes from solution onto activated carbon using a differential contacting system. To accomplish this goal, two secondary objectives had to be achieved. These were (1) to evaluate existing multi-solute adsorption equilibria models and (2) to determine how adsorption reversibility and chromatographic effects would influence and subsequent operation of prototype adsorbers.

Numerous adsorption equilibrium studies were conducted using bi-solute combinations of *o*-phenylphenol (OPP), dinitro-*o*-*sec*-butylphenol (DNOSBP), and 2,4-dichlorophenol (2,4-DCP). Results of these studies were employed to evaluate the utility of the Langmuir Competitive, Langmuir Semi-Competitive Ideal Solution Theory and Graphical Models of competitive adsorption equilibria. Neither of the models was found to adequately describe competitive adsorption effects. Nonetheless, the Graphical approach gave the best estimate of competitive interactions.

Simulations using the dynamic mathematical model showed that:

- (1) the fluidized-bed mode of operation offers distinct advantages over packed-bed operation for minimizing the elution of adsorbed contaminants from adsorbers;
- (2) industrial production schedules should be arranged such that all contaminants are discharged concurrently;
- (3) production schedules should be arranged such that wastewaters containing the highest energy adsorbing contaminants are introduced first to a column of fresh adsorbent while the wastewaters containing the lowest energy adsorbing contaminants are introduced last;
- (4) concentration equilization should be employed ahead of adsorbers to minimize displacement and subsequent elution of adsorbed contaminants.

Columnar laboratory studies generally verified the conclusions drawn from the simulations.

TABLE OF CONTENTS

| | Page |
|---|------|
| TABLE OF CONTENTS | i |
| LIST OF TABLES | iv |
| LIST OF FIGURES | v |
| I. INTRODUCTION | 1 |
| II. OBJECTIVES OF RESEARCH | 4 |
| III. EXPERIMENTAL APPROACH | 8 |
| PHASE I: MODEL MODIFICATION AND REFINEMENT | 8 |
| PHASE II: ACQUISITION OF COMPETITIVE ADSORPTION PARAMETERS | 9 |
| PHASE III: EXPERIMENTAL DETERMINATION OF THE REVERSIBILITY OF COMPETITIVE ADSORPTION | 9 |
| Fluidized-Bed Contactor Studies | 10 |
| Packed-Bed Contactor Studies | 11 |
| Continuous Stirred-Tank Contactor Studies | 12 |
| PHASE IV: SIMULATIONS AND VERIFICATIONS OF THE MATHEMATICAL MODEL | 12 |
| IV. EXPERIMENTAL APPARATUS AND TECHNIQUES | 13 |
| PHYSICAL APPARATUS AND OPERATING PROCEDURE | 13 |
| PACKED AND FLUIDIZED BED SYSTEMS | 13 |
| CONTINUOUS STIRRED TANK REACTOR SYSTEM | 16 |
| ADSORBENT | 18 |
| ADSORBATES | 19 |
| ANALYTICAL TECHNIQUES | 20 |
| SAMPLING PROCEDURE | 22 |
| V. REVIEW OF PERTINENT LITERATURE | 23 |
| VI. MODEL DEVELOPMENT AND IMPLEMENTATION | 28 |
| MATERIAL BALANCE RELATIONSHIPS | 28 |
| Lumped Parameter Approach | 30 |
| ADSORPTION EQUILIBRIA | 33 |
| LANGMUIR COMPETITIVE ADSORPTION MODEL | 34 |
| Semi-Competitive Langmuir Adsorption Model | 35 |
| Ideal Solution Theory Adsorption Isotherm | 36 |
| KINETICS OF INTERPHASE SOLUTE TRANSPORT | 43 |
| Adsorption Rate Step | 44 |
| Pore-Diffusion | 44 |

| | Page |
|--|------|
| Pore-Surface Diffusion | 46 |
| Film or External Diffusion | 47 |
| MODEL IMPLEMENTATION | 49 |
| VII. EXPERIMENTAL RESULTS | 56 |
| ADSORPTION EQUILIBRIA STUDIES | 56 |
| ANALYSIS OF COMPETITIVE ADSORPTION EQUILIBRIA | 56 |
| EXPERIMENTAL COLUMNAR STUDIES | 60 |
| Fluidized-Bed Studies | 60 |
| ... Molar Ratio of 1.0:0.913 DNOSBP to 2,4-DCP | 60 |
| ... Molar Ratio of 1.0:1.53 DNOSBP to 2,4-DCP | 61 |
| ... Molar Ratio of 1.0:1.007 2,4-DCP to DNOSBP | 67 |
| ... Molar Ratio of 1.0:2.086 2,4-DCP to DNOSBP | 70 |
| Fluidized-Bed Studies (OPP/DNOSBP) | 70 |
| ... Molar Ratio of 1.0:2.0 OPP to DNOSBP | 70 |
| ... Molar Ratio of 1.0:1.0 OPP to DNOSBP | 73 |
| ... Molar Ratio of 1.8:1.0 OPP to DNOSBP | 78 |
| ... Molar Ratios of 1.0:2.0, 1.0:1.0, and 1.8:1.0 DNOSBP to OPP | 81 |
| ... Molar Ratio of 0.0:1.0 DNOSBP to OPP | 84 |
| Packed-Bed Studies (2,4-DCP/DNOSBP) | 86 |
| ... Molar Ratio of 1.0:0.92 DNOSBP to 2,4-DCP | 86 |
| ... Molar Ratio of 1.0:1.56 DNOSBP to 2,4-DCP | 90 |
| ... Molar Ratio of 1.0:1.0 2,4-DCP to DNOSBP | 93 |
| ... Molar Ratio of 1.0:2.0 2,4-DCP to DNOSBP | 93 |
| CSTR Studies (2,4-DCP/DNOSBP) | 99 |
| ... Molar Ratio of 1.0:0.96 DNOSBP to 2,4-DCP | 99 |
| ... Molar Ratio of 1.0:2.02 DNOSBP/2,4-DCP | 99 |
| ... Molar Ratio of 1.0:0.96 2,4-DCP to DNOSBP | 105 |
| ... Molar Ratio of 1.0:2.02 2,4-DCP to DNOSBP | 108 |
| SUMMARY | 111 |
| VIII. MATHEMATICAL SIMULATIONS | 112 |
| IX. CONCLUSIONS AND RECOMMENDATIONS | 124 |
| BIBLIOGRAPHY | 125 |
| NOMENCLATURE | 129 |

| | Page |
|--|------|
| APPENDIX A PHYSICAL CHARACTERISTICS OF ADSORBENT | 130 |
| APPENDIX B IDEAL SOLUTION THEORY EQUILIBRIUM COMPUTATION | 133 |
| APPENDIX C LISTING OF COMPUTER PROGRAM | 139 |
| APPENDIX D SINGLE-SOLUTE PRESATURATION STUDIES: SOLUTION AND SOLID-PHASE STUDIES. | 144 |

LIST OF TABLES

| | Page |
|---|------|
| IV-1 Spectrophotometric Characteristics of DNOSBP, OPP, And 2,4-DCP. | 21 |
| VII-1 Summarized Results: Fluidized-Bed Studies | 64 |
| VII-2 Summarized Results: Packed-Bed Studies | 89 |
| VII-3 Summarized Results: CSTR Studies | 102 |
| VIII-1 Synopsis of Simulations | 123 |

LIST OF FIGURES

| | Page |
|--|------|
| IV-1 Apparatus For Columnar Studies | 14 |
| IV-2 Apparatus For CSTR Studies | 17 |
| VI-1 Schematic Drawing Which Shows Use Of Spreading Pressure Curves To Determine Multi-Solute Mole Fraction | .42 |
| VII-1 Adsorption Isotherm For DNOSBP | 57 |
| VII-2 Adsorption Isotherm For OPP | .58 |
| VII-3 Adsorption Isotherm For 2,4-DCP | .59 |
| VII-4 Solid-Phase Concentration Profiles For A Fluidized-Bed System To Which DNOSBP And 2,4-DCP Were Introduced At A Molar Ratio Of 1.0:0.93 After The Activated Carbon Had Been Presaturated With DNOSBP (79.56 μ M) | .62 |
| VII-5 Fluid-Phase Concentration Profiles For A Fluidized-Bed System To Which DNOSBP And 2,4-DCP Were Introduced At A Molar Ratio Of 1.0:0.93 After The Activated Carbon Had Been Presaturated With DNOSBP (79.56 μ M) | .63 |
| VII-6 Solid-Phase Concentration Profiles For A Fluidized-Bed System To Which DNOSBP And 2,4-DCP Were Introduced At A Molar Ratio Of 1.0:1.53 After The Activated Carbon Had Been Presaturated With DNOSBP (80.0 μ M) | .65 |
| VII-7 Fluid-Phase Concentration Profiles For A Fluidized-Bed System To Which DNOSBP And 2,4-DCP Were Introduced At A Molar Ratio Of 1.0:1.53 After The Activated Carbon Had Been Presaturated With DNOSBP (80.0 μ M) | .66 |
| VII-8 Solid-Phase Concentration Profiles For A Fluidized-Bed System To Which DNOSBP And 2,4-DCP Were Introduced At A Molar Ratio Of 1.007:1.0 After The Activated Carbon Had Been Presaturated With 2,4-DCP (80.0 μ M) | .68 |
| VII-9 Fluid-Phase Concentration Profiles For A Fluidized-Bed System To Which DNOSBP And 2,4-DCP Were Introduced At A Molar Ratio Of 1.007:1.0 After The Activated Carbon Had Been Presaturated With 2,4-DCP (80.0 μ M) | .69 |
| VII-10 Solid-Phase Concentration Profiles For A Fluidized-Bed System To Which DNOSBP and 2,4-DCP Were Introduced At A Molar Ratio Of 2.086:1.0 After The Activated Carbon Had Been Presaturated With 2,4-DCP (80.0 μ M) | .71 |
| VII-11 Fluid-Phase Concentration Profiles For A Fluidized-Bed System To Which DNOSBP And 2,4-DCP Were Introduced At A Molar Ratio Of 2.086:1.0 After The Activated Carbon Had Been Presaturated With 2,4-DCP (80.0 μ M) | .72 |

| | | |
|--------|---|----|
| VII-12 | Solid-Phase Concentration Profiles For A Fluidized-Bed System To Which DNOSBP And OPP Were Introduced At a Molar Ratio of 2.0:1.0 After The Activated Carbon Had Been Presaturated With DNOSBP (80.0 μ M) | 74 |
| VII-13 | Fluid-Phase Concentration Profiles For A Fluidized-Bed System To Which DNOSBP And OPP Introduced At A Molar Ratio Of 2.0:1.0 After The Activated Carbon Had Been Presaturated With DNOSBP (80.0 μ M) | 75 |
| VII-14 | Solid-Phase Concentration Profiles For A Fluidized-Bed System To Which DNOSBP And OPP were Introduced At A Molar Ratio of 1.0:1.0 After The Activated Carbon Had Been Presaturated With DNOSBP (80.0 μ M) | 76 |
| VII-15 | Fluid-Phase Concentration Profiles For A Fluidized-Bed System To Which DnOSBP and OPP Were Introduced At a Molar Ratio of 1.0:1.0 After The Activated Carbon Had Been Presaturated With DNOSBP (80.0 μ M) | 77 |
| VII-16 | Solid-Phase Concentration Profiles For A Fluidized-Bed System To Which DNOSBP And OPP Were Introduced At a Molar Ratio Of 1.0:1.8 After the Activated Carbon Had Been Presaturated With DNOSBP (80.0 μ M) | 79 |
| VII-17 | Fluid-Phase Concentration Profiles For A Fluidized-Bed System To Which DNOSBP And OPP Were Introduced At A Molar Ratio of 1.0:1.8 After The Activated Carbon Had Been Presaturated With DNOSBP (80.0 μ M). | 80 |
| VII-18 | Solid-Phase Concentration Profiles For A Fluidized-Bed System To Which DNOSBP and OPP Were Introduced At A Molar Ratio of 1.0:1.0 After The Activated Carbon Had Been Presaturated With OPP (80.0 μ M) | 82 |
| VII-19 | Fluid-Phase Concentration Profiles For A Fluidized-Bed System To Which DNOSBP And OPP Were Introduced At A Molar Ratio of 1.0:1.0 After The Activated Carbon Had Been Presaturated With OPP (80.0 μ M) | 83 |
| VII-20 | Solid-Phase Concentration Profiles For A Fluidized-Bed System To Which DNOSBP and OPP Were Introduced At A Molar Ratio of 0.0:1.0 After The Activated Carbon Had Been Presaturated With DNOSBP (80.0 μ M). | 85 |
| VII-21 | Solid-Phase Concentration Profiles For A Packed-Bed System To Which DNOSBP And 2,4-DCP Were Introduced At A Molar Ratio Of 1.0:0.92 After the Activated Carbon Had Been Presaturated With DNOSBP (81.31 μ M). | 87 |
| VII-22 | Fluid-Phase Concentration Profiles For A Packed-Bed System To Which DNOSBP And 2,4-DCP Were Introduced At A Molar Ratio of 1.0:0.92 After The Activated Carbon Had Been Presaturated With DNOSBP (81.31 μ M). | 88 |

| | | |
|--------|--|-----|
| VII-23 | Solid-Phase Concentration Profiles For A Packed-Bed System To Which DNOSBP And 2,4-DCP Were Introduced At A Molar Ratio Of 1.0:1.56 After The Activated Carbon Had Been Presaturated With DNOSBP (78.52 μ M) | 91 |
| VII-24 | Fluid-Phase Concentration Profiles For A Packed-Bed System To Which DNOSBP And 2,4-DCP Were Introduced At A Molar Ratio Of 1.0:56 After The Activated Carbon Had Been Presaturated With DNOSBP (78.52 μ M) | 92 |
| VII-25 | Solid-Phase Concentration Profiles For A Packed-Bed System To Which DNOSBP And 2,4-DCP Were Introduced At A Molar Ratio Of 1.0:1.00 After The Activated Carbon Had Been Presaturated With 2,4-DCP (80.0 μ M) | 94 |
| VII-26 | Fluid-Phase Concentration Profiles For A Packed-Bed System To Which DNOSBP And 2,4-DCP Were Introduced At A Molar Ratio Of 1.0:1.00 After The Activated Carbon Had Been Presaturated With 2,4-DCP (80.0 μ M) | 95 |
| VII-27 | Solid-Phase Concentration Profiles For A Packed-Bed System To Which DNOSBP And 2,4-DCP Were Introduced At A Molar Ratio Of 2.0:1.00 After The Activated Carbon Had Been Presaturated With 2,4-DCP (80.0 μ M) | 96 |
| VII-28 | Fluid-Phase Concentration Profiles For A Packed-Bed System To Which DNOSBP And 2,4-DCP Were Introduced At A Molar Ratio Of 2.0:1.00 After The Activated Carbon Had Been Presaturated With 1,4-DCP (80.0 μ M) | 97 |
| VII-29 | Solid-Phase Concentration Profiles For A CSTR System To Which DNOSBP And 2,4-DCP Were Introduced At a Molar Ratio of 1.0:0.96 After The Activated Carbon Had Been Presaturated With DNOSBP (82.0 μ M) . . . | 100 |
| VII-30 | Fluid-Phase Concentration Profiles For A CSTR System To which DNOSBP And 2,4-DCP Were Introduced At a Molar Ratio of 1.0:0.96 After The Activated Carbon Had Been Presaturated With DNOSBP (82.0 μ M) | 101 |
| VII-31 | Solid-Phase Concentration Profiles For A CSTR System To Which DNOSBP And 2,4-DCP Were Introduced At A Molar Ratio of 1.0:2.02 After The Activated Carbon Had Been Presaturated With DNOSBP (80.0 μ M) . . . | 103 |
| VII-32 | Fluid-Phase Concentration Profiles For A CSTR System To Which DNOSBP And 2,4-DCP Were Introduced At A Molar Ratio of 1.0:2.02 After The Activated Carbon Had Been Presaturated With DNOSBP (80.0 μ M) . . . | 104 |
| VII-33 | Solid-Phase Concentration Profiles For A CSTR System To Which DNOSBP And 2,4-DCP Were Introduced At A Molar Ratio Of 0.96:1.0 After The Activated Carbon Had Been Presaturated With 2,4-DCP (82.21 μ M) . . | 106 |
| VII-34 | Fluid-Phase Concentration Profiles For A CSTR System To Which DNOSBP And 2,4-DCP Were Introduced At A Molar Ratio Of 0.96:1.0 After The Activated Carbon Had Been Presaturated With 2,4-DCP (82.21 μ M) . . | 107 |

| | | |
|--------|--|-----|
| VII-35 | Solid-Phase Concentration Profiles For A CSTR System To Which DNOSBP And 2,4-DCP Were Introduced At A Molar Ratio of 2.02:1.0 After The Activated Carbon Had Been Presaturated With 2,4-DCP (76.64 μ M). | 109 |
| VII-36 | Fluid-Phase Concentration Profiles For A CSTR System To Which DNOSBP And 2,4-DCP Were Introduced At A Molar Ratio of 2.02:1.0 After The Activated Carbon Had Been Presaturated With 2,4-DCP (76.64 μ M). | 110 |
| VIII-1 | Solution- And Solid-Phase Concentration Profiles For PBP And PNP For A Packed-Bed Adsorber. | 114 |
| VIII-2 | Solution- And Solid-Phase Concentration Profiles For PBP And PNP For A Fluidized-Bed Adsorber. | 115 |
| VIII-3 | Solution- And Solid-Phase Concentration Profiles For PBP And PNP For A Packed-Bed Adsorber. | 117 |
| VIII-4 | Solution- And Solid-Phase Concentration Profiles For PBP And PNP For A Fluidized-Bed Adsorber. | 118 |
| VIII-5 | Solution- And Solid-Phase Concentration Profiles For PBP And PNP For A Packed-Bed Adsorber. | 120 |
| VIII-6 | Solution- And Solid-Phase Concentration Profiles For PBP And PNP For A Fluidized-Bed Adsorber. | 121 |
| D-1 | Fluid-Phase Concentration Profile For DNOSBP (79.56 μ M) In A Fluidized-Bed Adsorber. | 145 |
| D-2 | Solid-Phase Concentration Profile For DNOSBP (79.56 μ M) In A Fluidized-Bed Adsorber. | 146 |
| D-3 | Fluid-Phase Concentration Profile For DNOSBP (80.0 μ M) In A Fluidized-Bed Adsorber. | 147 |
| D-4 | Solid-Phase Concentration Profile For DNOSBP (80.0 μ M) In A Fluidized-Bed Adsorber. | 148 |
| D-5 | Fluid-Phase Concentration Profile For 2,4-DCP (80.0 μ M) In A Fluidized-Bed Adsorber. | 149 |
| D-6 | Solid-Phase Concentration Profile For 2,4-DCP (80.0 μ M) In A Fluidized-Bed Adsorber. | 150 |
| D-7 | Fluid-Phase Concentration Profile For 2,4-DCP (80.0 μ M) In A Fluidized-Bed Adsorber. | 151 |
| D-8 | Solid-Phase Concentration Profile For 2,4-DCP (80.0 μ M) In A Fluidized-Bed Adsorber. | 152 |
| D-9 | Fluid-Phase Concentration Profile For DNOSBP (81.31 μ M) In A Packed-Bed Adsorber. | 153 |
| D-10 | Solid-Phase Concentration Profile For DNOSBP (81.31 μ M) In A Packed-Bed Adsorber. | 154 |

| | | |
|------|--|-----|
| D-11 | Fluid-Phase Concentration Profile For DNCSEP (78.52 μ M) In A Packed-Bed Adsorber. | 155 |
| D-12 | Solid-Phase Concentration Profile For DNOSBP (78.52 μ M) In A Packed-Bed Adsorber. | 156 |
| D-13 | Fluid-Phase Concentration Profile For 2,4-DCP (80.0 μ M) In A Packed-Bed Adsorber. | 157 |
| D-14 | Solid-Phase Concentration Profile For 2,4-DCP (80.0 μ M) In A Packed-Bed Adsorber. | 158 |
| D-15 | Fluid-Phase Concentration Profile For 2,4-DCP (80.0 μ M) In A Packed-Bed Adsorber. | 159 |
| D-16 | Solid-Phase Concentration Profile For 2,4-DCP (80.0 μ M) In A Packed-Bed Adsorber. | 160 |
| D-17 | Fluid-Phase Concentration Profile For DNOSBP (82.0 μ M) In A CSTR Adsorber. . | 161 |
| D-18 | Solid-Phase Concentration Profile For DNCSEP (80.0 μ M) In A CSTR Adsorber. . | 162 |
| D-19 | Fluid-Phase Concentration Profile For DNOSBP (80.0 μ M) In A CSTR Adsorber. . | 163 |
| D-20 | Solid-Phase Concentration Profile For DNOSBP (80.0 μ M) In A CSTR Adsorber. . | 164 |
| D-21 | Fluid-Phase Concentration Profile For 2,4-DCP (82.21 μ M) In A CSTR Adsorber. | 165 |
| D-22 | Solid-Phase Concentration Profile For 2,4-DCP (82.21 μ M) In A CSTR Adsorber. | 166 |
| D-23 | Fluid-Phase Concentration Profile For 2,4-DCP (76.64 μ M) In A CSTR Adsorber. | 167 |
| D-24 | Solid-Phase Concentration Profile For 2,4-DCP (76.64 μ M) In A CSTR Adsorber. | 168 |

CHAPTER I

INTRODUCTION

Use of adsorption technology for the decontamination and renovation of wastewaters has during the past decade and particularly during the past five years been implemented for full-scale systems with increasing frequency. This is because adsorption on both granular and powdered activated carbon has clearly been shown to have rather unique capabilities for removal of trace levels of pollutants, such as pesticides and other surface active organic materials, from wastewaters. Throughout the United States approximately thirty adsorption installations that are to be employed for the treatment of municipal wastewaters are either in the design or construction stages or have, indeed, already been placed on-line. Likewise, numerous industries are currently using adsorption contactors either for processing applications or for removal of certain noxious contaminants from its aqueous waste stream.

Continuous-flow adsorption contactors have heretofore generally been designed for operation in the packed-bed mode. It is to be noted that packed beds of granular active carbon are well suited for the treatment of liquids that contain little or no suspended solids and, with a clear feed stream, can be expected to operate effectively for extended periods without clogging or excessive pressure loss. The presence of suspended solids in aqueous waste streams, however, presents serious problems for the use of activated carbon in packed beds. These solids lead to a progressive clogging of the beds, much as in a deep-bed (sand) filter, with resulting increases in head loss. Conversely, a fluidized-bed adsorber, in which the wastewater which is to be treated is passed upward through a bed of activated carbon at a velocity sufficient to expand

the bed, is not plagued with problems of bed clogging and increasing pressure loss. Whereas, the former contacting scheme serves in a dual capacity as a filter as well as an adsorber, the latter functions only in the singular role as an adsorption process.

Although the performance of packed- and fluidized-bed adsorption contactors has been observed to be virtually identical when employed for the treatment of municipal waste waters, substantial differences in column performance can be anticipated for the two contacting modes when industrial waste waters having a well defined composition of high and low energy adsorbing solutes are treated by the adsorption process. It is clear, therefore, that the choice between the two contacting systems is heavily dependent upon the specific solution and particulate characteristics of the wastewater that is to be treated. The choice cannot be defined by a cursory analysis, but can only be predicted on a detailed investigation of the characteristics of the waste stream that is to be treated and by subsequent simulation of the anticipated column performance.

Both design and operation of adsorption contactors are related to the characteristic breakthrough curves in which the readily measured effluent concentration is plotted as a function of elapsed time. Depending on the ultimate objective of the process, either the breakthrough point or the saturation point represents the design and/or operational target. Prediction of the breakthrough phenomenon has occupied the attention of numerous investigators during recent years. Nonetheless, throughout this period specification of design and operational criteria for full-scale adsorbers has been predicated principally on empirical observations. This is primarily due to the fact that municipal wastewaters have an extremely complex composition

which, in turn, substantially complicates modeling and simulation procedures. For this situation any practicable model must of necessity be of a quasi-empirical nature to be generally applicable.

In contrast, the composition of industrial wastewaters frequently can be explicitly defined. For example, the wastewaters resulting from the manufacture or handling of pesticides would likely consist of several major constituents. While the concentration of each such contaminant would undoubtedly be time variant, the composition could nevertheless be clearly determined. In this case a generalized descriptive model can be employed for accurately simulating the dynamic responses of columnar adsorbers for a variety of operational and systemic conditions including adsorber geometry and configuration, flow rate, composition, concentration, temperature, contacting modes, competitive effects, reversibility, etc. Use of such a model which is wholly fundamental in scope provides one with a rational basis for evaluating design and operational alternatives, for projecting optimal ranges of design and operational criteria, and for simulating process control strategies. Moreover, such a mathematical development is extremely beneficial for specification of the cost effective design of a pilot-scale system if such were indicated. Under certain circumstances, however, use of a fully descriptive model should, indeed, be entirely satisfactory for specifying design and operational parameters without the need to resort to time-consuming and costly pilot-scale studies.

CHAPTER II

OBJECTIVES OF RESEARCH

Numerous research projects have demonstrated the feasibility of utilizing the unit process of adsorption on activated carbon for the removal of pesticides from waters. Others have delineated and characterized process parameters significant to the performance of packed-bed and fluid-bed activated carbon adsorbers. While these investigations have demonstrated the unique utility of the process and have yielded useful information regarding general design and operating criteria for pesticide decontamination applications, there has remained, however, a definite need for the systematization of this information, and for the development of a quantitative rational design procedure for adsorbers for field applications.

Because prediction or simulation of the concentration-time profiles that characterize adsorber performance is paramount to the development of rational design and operational criteria, various theoretical mathematical models have previously been developed for predicting breakthrough profiles for continuous-flow adsorbers in which single-solute solutions were contacted with the solid-phase. Subsequently, a study initiated and directed by the principal investigator resulted in the development of a mathematical model which can be employed to simulate the performance of either packed- or fluidized-bed adsorption contactors when contacted with multiple-solute mixtures such as are commonly encountered in industrial wastewater discharges. This model, in part, accounted for the competitive effects between solutes with regard to adsorption equilibria. Further, according to fundamental thermodynamic principles the model was formulated on the assumption that adsorption on activated carbon was fully reversible. This, of course, had been postulated by numerous previous investigators.

Experimental investigations which were conducted during the latter portion of the contract period, however, showed that the assumption of full reversibility was not entirely valid for description of adsorber column performance in the dynamic state. The results showed neither total reversibility nor total irreversibility in the time-scale that is significant to adsorber operation; although it is anticipated that if an adsorption column were allowed to equilibrate over very extended periods of time one would, indeed, observe a fully reversible condition. While the latter condition is significant with regard to adsorption thermodynamics, it has little practical significance regarding description of the performance of adsorption contactors which would be employed for the removal of residues, such as pesticides, from wastewaters. In this case any fully descriptive model should account for the relative extent of reversibility/irreversibility in the time-scale that has engineering significance. The essence of this research, therefore, is to sufficiently modify the existing mathematical developments to account for all time-dependent reversibility/irreversibility considerations such that mathematical simulations of adsorber column performance accurately predict these time dependent phenomena. Accordingly, the specific aims and objectives of this investigation are enumerated as follows:

- 1) To modify an existing theoretical mathematical model, which was formulated under the direction of the principal investigator to accommodate the effects of time-dependent relative reversibility/irreversibility;
- 2) To conduct batch-system equilibrium studies for single-solute systems using pesticide-type compounds that are of direct interest to the Department of the Army. Single solute adsorption parameters so obtained can then be directly employed for prediction of multiple-solute adsorption equilibria which includes competitive effects;

- 3) To experimentally determine the time-dependent reversible/irreversible interactions between solutes in multi-component systems. These experiments were to be conducted in columnar continuous-flow contactors so as to account for the time-dependent characteristics of reversibility;
- 4) To simulate the multiple-solute adsorption process through use of the model formulated under Part 1. Experimental verification is to be obtained from a series of columnar adsorption studies;
- 5) Upon obtaining satisfactory agreement between the experimental results and model simulations, to conduct an extensive series of simulations to fully evaluate all possible dynamic conditions that might likely be encountered in field applications. This serves a two-fold purpose: (a) to define which design and operational alternatives would provide for optimal performance of activated carbon adsorbers which are subjected to specific and critical dynamic input conditions; and (b) to illustrate how one would proceed to employ the mathematical developments to simulate design, operational, and process control alternatives.

Upon completion of the objectives detailed above, Department of Army scientists and engineers will have at their disposal a relatively straightforward method for design of adsorption contactors, for specifying operational criteria for such adsorbers, and for defining process control strategies. This will under most circumstances obviate the need for lengthy and costly pilot-scale studies which heretofore have been required before design could be initiated. Alternatively, if because of special conditions, pilot studies are indeed indicated, then the model developments can be employed to plan the experimental pilot studies so as to maximize the quantity of useful data obtained per unit of cash expended. Both aspects, obviously,

will serve to minimize the expenditures required of the Department of Army to arrive at a cost effective and fail-safe design of adsorption contactors for specific applications.

CHAPTER III
EXPERIMENTAL APPROACH

The proposed research project was divided into five phases. These are detailed as follows:

PHASE I: MODEL MODIFICATION AND REFINEMENT

Under a previous contract (43) a mathematical model was developed that is general and applicable for the prediction of the performance of adsorbers when treating wastewaters that contained several major contaminants. The model was based on general mass balance relationships and the appropriate rate and equilibrium parameters. With regard to adsorption kinetics the model was formulated assuming that film diffusion was the predominant rate limiting mechanism. This assumption is well supported in the literature (see Chapter 5). If, in contrast, pore-diffusion or pore-surface diffusion were determined to be rate limiting for a specific application, the model was sufficiently general to accommodate these alternate limiting mechanisms. Further, competitive adsorption parameters that were included in the model were based on fundamental thermodynamic principles which were found to accurately predict the competitive effects of adsorption equilibria.

One other assumption that was employed during model formulation was that adsorption on granular activated carbon was fully reversible. Again, this assumption was extensively supported in the literature, particularly in that literature which pertains to chromatography. Nevertheless, several mathematical formulations which had been reported in the literature were based on the assumption of complete irreversibility. This latter assumption, however, was primarily for the purpose of mathematical expediency such that an exact solution of the set of equations could be effected. As was indicated previously, experimental investigations that were conducted under the previous contract clearly showed that, in the dynamic state and in the

time domain of significance in the operation of adsorption columns, adsorption of a variety of pesticides was neither fully reversible nor completely irreversible. Accordingly, the principal focus of this phase of the investigation was to incorporate the reversibility/irreversibility considerations into the model which was previously developed.

PHASE II: ACQUISITION OF COMPETITIVE ADSORPTION PARAMETERS

Because a theoretical interpretation of multicomponent, competitive adsorption equilibria was obtained during the previous contract, the need to perform additional multiple-solute equilibrium experiments was obviated. Consequently, only single-solute experiments were conducted. These provided data that is suitable for prediction of the competitive effects of multi-component adsorption equilibria. These were conducted for three organic herbicides; dinitro-o-sec-butylphenol (DNOSBP), o-phenylphenol (OPP), and 2,4-dichlorophenol (2,4-DCP).

All single-solute adsorption data were obtained using four continuous stirred-tank reactors (CSTR) operated in parallel. Inlet concentrations to the reactors were controlled at predetermined levels. In this manner, the inlet concentration then becomes the equilibrium concentration for the particular solid-solvent-solute system. Equilibrium parameters obtained from this apparatus were incorporated in the basic mathematical model for simulation of effluent-time profiles for columnar flow-through systems.

PHASE III: EXPERIMENTAL DETERMINATION OF THE REVERSIBILITY OF
COMPETITIVE ADSORPTION

This phase of the investigation was conducted to determine the time-dependent reversible/irreversible interactions between solutes in multi-

component systems. The solutes selected in Phase II of the study were also employed in this facet of the investigation. Columnar, continuous-flow contactors which were constructed under a previous contract were used to elucidate the parameters that are required to describe the reversibility phenomena.

With one exception, the experimental procedure involved first saturating the carbon with a single solute in the columnar, continuous-flow contactors employed. When the contactor attained a steady-state operational level (i.e., the effluent concentration of the solute was equal to the influent concentration of that solute), a second solute at the desired concentration level was introduced to the column along with the first solute (concentration was not changed during the step input forcing). The effect of the second solute on the relative column effluent concentrations was then observed. The run was continued until steady-state was again attained.

In one experimental study, however, both solutes (DNOSBP and OPP) were applied as single solutes in consecutive order. That is, DNOSBP was applied to the column initially until steady-state operation was obtained. OPP was subsequently fed to the column as a pure solute. The study was continued until steady-state operation was again attained.

An executive synopsis of the experimental studies conducted follows:

Fluidized-Bed Contactor Studies

- (a) Application of both DNOSBP and 2,4-DCP at a molar ratio of 1.0:0.913 after presaturation with DNOSBP (79.56 μm).
- (b) Application of both DNOSBP and 2,4-DCP at a molar ratio of 1.0:1.53 after presaturation with DNOSBP (80.0 μm).
- (c) Application of both 2,4-DCP and DNOSBP at a molar ratio of 1.0:1.007 after presaturation with 2,4-DCP (80.0 μm).

- (d) Application of both 2,4-DCP and DNOSBP at a molar ratio of 1.0:2.086 after presaturation with 2,4-DCP (80.0 μm).
- (e) Application of OPP at a concentration of 80.0 μm after presaturation with DNOSBP (80.0 μm).
- (f) Application of both OPP and DNOSBP at a molar ratio of 1.0:2.0 after presaturation with DNOSBP (80.0 μm).
- (g) Application of both OPP and DNOSBP at a molar ratio of 1.0:1.0 after presaturation with DNOSBP (80.0 μm).
- (h) Application of both OPP and DNOSBP at a molar ratio of 1.8:1 after presaturation with DNOSBP (80.0 μm).
- (i) Application of both DNOSBP and OPP at a molar ratio of 1.0:2.0 after presaturation with OPP (80.0 μm).
- (j) Application of both DNOSBP and OPP at a molar ratio of 1.0:1.0 after presaturation with OPP (80.0 μm).
- (k) Application of both DNOSBP and OPP at a molar ratio of 1.8:1.0 after presaturation with OPP (80.0 μm).

Packed-Bed Contactor Studies

- (a) Application of both DNOSBP and 2,4-DCP at a molar ratio of 1.0:0.42 after presaturation with DNOSBP (79.88 μm)
- (b) Application of both DNOSBP and 2,4-DCP at a molar ratio of 1.0:1.56 after presaturation with DNOSBP (78.52 μm).
- (c) Application of both 2,4-DCP and DNOSBP at a molar ratio of 1.0:1.0 after presaturation with 2,4-DCP (80.0 μm).
- (d) Application of both 2,4-DCP and DNOSBP at a molar ratio of 1.0:2.0 after presaturation with 2,4-DCP (80.0 μm).

Continuous Stirred-Tank Contactor Studies

- (a) Application of both DNOSBP and 2,4-DCP at a molar ratio of 1.0:0.96 after presaturation with DNOSBP (80.0 μm).
- (b) Application of both DNOSBP and 2,4-DCP at a molar ratio of 1.0:2.02 after presaturation with DNOSBP (80.0 μm).
- (c) Application of both 2,4-DCP and DNOSBP at a molar ratio of 1.0:0.96 after presaturation with 2,4-DCP (80.0 μm).
- (d) Application of both 2,4-DCP and DNOSBP at a molar ratio of 1.0:2.03 after presaturation with 2,4-DCP.

PHASE IV: SIMULATIONS AND VERIFICATIONS OF THE MATHEMATICAL MODEL

Upon completion of Phases I, II, and III the mathematical model as modified in Phase I was utilized to simulate columnar continuous-flow experiments. Once satisfactory agreement between experimental results and model simulations was obtained, a series of simulations was conducted. These serve to fully evaluate possible dynamic conditions that might likely be encountered in field applications. Certainly, this provides guidance for the ultimate users of the mathematical developments and pointed out design and operational targets.

CHAPTER IV:

EXPERIMENTAL APPARATUS AND TECHNIQUES

PHYSICAL APPARATUS AND OPERATING PROCEDURE

All experimental runs were conducted either in fluidized-bed contactors, packed-bed contactors and continuous stirred tank reactors (CSTR). All three modes of contact were used in order to make possible model comparisons for the various systems.

PACKED AND FLUIDIZED BED SYSTEMS

Physically, this experimental apparatus consisted of four pyrex glass columns, two-inches in diameter and five feet in length. Each contained 150 grams of the granular activated carbon. Each column is fitted at its base with a distribution chamber filled with glass beads which serves to dissipate the velocity head at the influent section, thus ensuring steady-state, one-dimensional flow along the length of the column. A process flow diagram of one column is shown in Figure IV - 1.

The make-up water system consisted of a 75 gallon make-up water storage tank, a Chemtrix Incorporated, Model 45 pH controller, and three variable speed Masterflex Model 7545-13 chemical feed pumps, two of which were used in conjunction with the pH controller. These pumps, depending upon the pH signal, fed 0.02M hydrochloric acid and 0.02M sodium hydroxide into the influent line of the make-up water tank at rate of 10 milliliters per minute to maintain the set-point pH. The other chemical feed pump which had the same capacity as the other pumps was used to feed a phosphate buffer to maintain a concentration of 0.002 M. The make-up water was delivered to each of the mixing tanks by gravity through a one-half inch diameter PVC pipe manifold system.

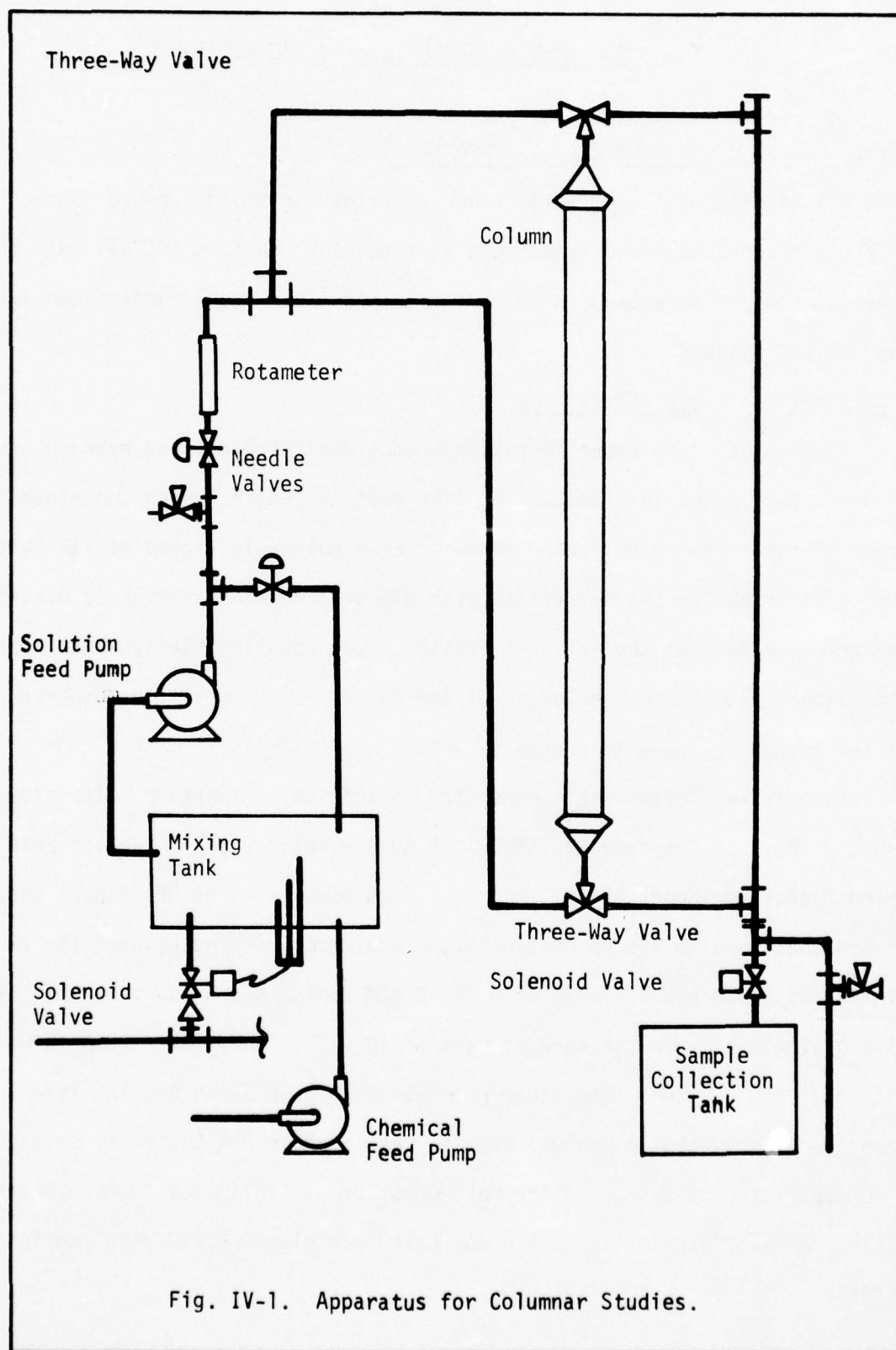


Fig. IV-1. Apparatus for Columnar Studies.

Flow of make-up water into the mixing tank was controlled by a 3/8-inch by 1/8-inch solenoid valve. Operation of this valve was controlled by a level control system. This system consisted of three electrodes in each tank, a low and high water elevation electrode, and a ground.

The sorbate feed system consisted of four variable speed Masterflex pumps (Model 7545-13) which were capable of delivering from 1.8 to 36 milliliters per minute or 0.06 milliliters per pump revolution. Tachometers were attached to each pump to monitor speed which, in turn, was related to volumetric flow rate. Normal operational speeds for these pumps were 120 RPM. This is equivalent to 7.2 milliliters per minute. Stock solutions were supplied to the chemical feed pump at concentrations of either 2500, 5000 or 10,000 micromoles/liter.

Solution was fed to the columns by two variable speed Masterflex pumps Model 7545-17, each of which was equipped with dual pump-heads capable of delivering 84 to 1680 milliliters per minute. This capacity was such that full fluidization of an activated carbon bed of 400 grams could be obtained. For all experimental runs the flow rate through the contactor was maintained constant at 5 gallons/ft²/min (0.413 liters/minute).

The sample collection system consisted of a 30 gallon receiving reservoir, a solenoid valve, and a cam timer.

Composite samples were collected on the basis of 65 milliliters per minute for a twenty-four hour period. The collection vessels were then drained at the end of sampling periods and sampling again initiated. Discrete samples were collected at twelve hour intervals. Since fluctuations in effluent were gradual, there was no need for more frequent sampling.

The packed and fluidized-bed modes of operation were identical with the exception of the direction of flow through the column. For the packed-

bed mode the two three-way valves were positioned such that the flow entered at the top and exited through the bottom of the column. The valve positions were reversed for the fluidized-bed mode of operation.

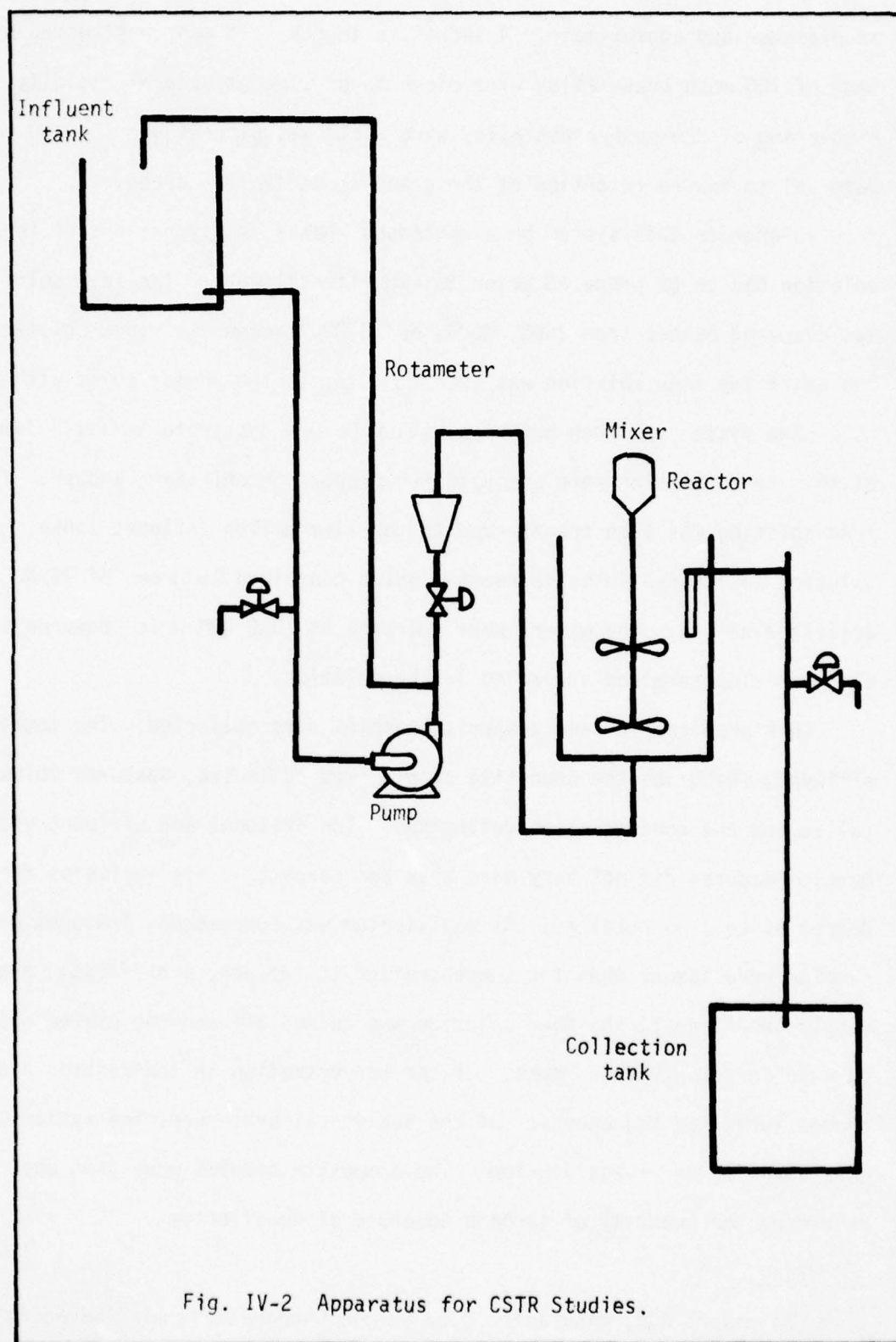
CONTINUOUS STIRRED TANK REACTOR SYSTEM

The apparatus used consisted of four nine-liter baffled-reactors. Figure IV-2 shows the process flow sheet. The feed solution was fed by two variable speed Masterflex pumps Model 7545-15 with dual pumping heads each of which had a rated capacity of 30 to 860 milliliters per minute. At the onset of the runs with the CSTR's, a flow rate of 0.7 liters per hour was selected. Later in the study the rate was increased to approximately 1.3 liters per hour due to the extremely long periods of time required to reach saturation at the lower flows. Some difficulty was experienced in maintaining a steady flow rate at these low levels. For that reason the total volume of effluent collected from the reactor was used to compute the flow rate and complete the solid-phase concentration calculations.

The rotameters were Gilmont Model 3204-2 which were calibrated for flows of 10 to 860 milliliters per minute. The calibration curve for each of these serial numbered rotameters was checked with a NBS calibrated Brooke rotameter. All the calibration curves were found to be accurate.

All fittings and appurtenances used on the apparatus were brass, produced by Imperial Eastman Corporation. All tubing was 3/8 inch diameter polyethylene tubing (poly-flo), manufactured by Imperial Eastman Corporation which met ASTM D-1248 Type 1 Class A, Grade 4 specifications. The mixing system for each reactor consisted of a one-sixth horsepower motor, stainless steel drive shaft, and two three-inch diameter impellers. The impeller consisted of six blades having a pitch of 45 degrees with the vertical.

The effluent system consisted of a cylindrical screen 3/8 inches



in diameter and approximately 4 inches in length. It was constructed of a base of 100 mesh brass alloy wire cloth to provide structural rigidity. A covering of 325-mesh brass alloy wire cloth was placed over the 100 mesh material to ensure retention of the granular activated carbon.

To operate this system on a continuous basis, sixty gallons of feed solution had to be prepared prior to experimental work. The feed solution was prepared either from 2500, 5000, or 10,000 micromolar stock solution. The pH of the feed solution was then adjusted to the pH set-point with 1N HCl. The system was then buffered with a 0.002M phosphate buffer. Samples of this feed solution were analyzed for proper concentration and pH. The feed solution was then transferred to the five gallon influent tanks. The solution was pumped into the reactor which contained 10 grams of 20/40 mesh activated carbon. The mixers were operated at 1000 RPM which ensured that all particles remained suspended in the solution.

Both grab samples and composite samples were collected. The total effluent, which was the composite sample, was collected, measured volumetrically, and the concentration determined. The influent and effluent volumetric measures did not vary more than one percent. This indicates the close degree of control obtained. As equilibrium was approached, frequent grab samples were taken. When the concentration in influent and effluent grab samples were equal, the feed solution was turned off and the system was allowed to stir for twenty-four hours. If the concentration in the reactor did not change more than the accuracy of the analytical procedure, the system was considered to be at equilibrium. The composite samples were then used to determine the quantity of sorbate adsorbed at equilibrium.

ADSORBENT

Filtrisorb 200, manufactured by Calgon Corporation, was the activated carbon used in all studies. Specifications given by the manufacturer have

been detailed in Appendix A.

Prior to using the carbon it was necessary to sieve, wash, and dry the carbon. Since the manufacturer provided a wide range of particle sizes, it was necessary to select a specific particle size range for this study. It was decided that a sieve cut of that passing the 20 mesh sieve and retained on the 40 mesh sieve would be appropriate for the studies.

After the carbon was sieved and the cuts selected, the carbon was washed three times in distilled water to remove the fines. It was then dried at 105°C for twenty-four hours. After allowing the carbon to cool, it was stored in glass containers at 37°C.

ADSORBATES

The solutes 2,4-dinitro-o-sec-butylphenol (DNOSBP), ortho-phenylphenol (OPP), and 2,4-dichlorophenol (2,4-DCP) were used for this study. DNOSBP was selected for use because of the extensive work done with it and its well documented properties. OPP and 2,4-DCP were selected for several reasons including molecular size as compared to DNOSBP and the value of the acid-base equilibrium constant as compared to DNOSBP. This selection provided compounds with markedly different structures and charge characteristics. This, of course, would affect the competition of the solutes for adsorption sites on the activated carbon.

The DNOSBP was obtained in commercial grade and, therefore, required recrystallization for purification. This was accomplished by heating the compound to the melting point in a hot-water bath and then adding an equal volume of 95 percent ethanol. The mixture was heated to boiling. Distilled water was then added until precipitation of the material was observed. The solution was then placed in a freezer and was stirred frequently. As the sorbate precipitated from the ethanol-water mixture, the solution was decanted. Upon total crystallization the precipitate was removed

by filtration and dried under vacuum. The melting point was determined for the DNOSBP which had twice been recrystallized. The melting point curve for the recrystallized DNOSBP had a tolerance of $\pm 1^{\circ}\text{C}$. The OPP and 2,4-DCP were acquired in reagent grade and required no purification. All three solutes are relatively insoluble and, therefore, required high temperatures and pH's to render them soluble. Sodium hydroxide was employed to elevate the pH.

ANALYTICAL TECHNIQUES

All solutions and samples were analyzed spectrophotometrically using a Beckman Acta, Model III, spectrophotometer. To determine the concentrations of the compounds considered it was necessary to establish the maximum adsorption wavelengths of the solutes. DNOSBP in the anion form has a maximum absorbance at a wavelength of 376 nanometers. Similarly, the maximum absorbance wavelength for neutral 2,4-DCP was determined to be 285 nanometers and that for neutral OPP was found to be 282 nanometers.

The compounds were studied as bisolute pairs of DNOSBP and OPP and DNOSBP & 2,4-DCP at system pH's of 7.2 and 6.1, respectively. One of the compounds, DNOSBP, exists in the anion form and the other, 2,4-DCP or OPP, exists in the neutral form at the pH's studied.

Analysis of the DNOSBP/2,4-DCP system was accomplished through the application of Beer's Law as it applies to two solutes. Accordingly, it was necessary to determine the extinction coefficients for each compound at the other competing solute's maximum absorbance wavelength. Table IV-1 lists the applicable spectrophotometric characteristics of DNOSBP, OPP, and 2,4-DCP.

Analysis of the DNOSBP/OPP system was achieved as follows: (1) add a volume of phosphate buffer to one portion of the sample to poise the pH at 7.2; (2) add a volume of sodium hydroxide to another portion of the sample

TABLE IV-1
SPECTROPHOTOMETRIC CHARACTERISTICS OF DNOSBP, OPP, AND 2,4-DCP

| Compound | Wave length of Maximum Absorption (nanometers) | Molar Absorptivity (l/cm-mole) |
|----------|--|--|
| DNOSBP | 376 (Anion) | 13, 950 (Anion @376nm) |
| 2,4-DCP | 285 (Neutral) | 0 (Neutral @376nm) 1,948 (Neutral @285nm) |
| OPP | 282 (Neutral) 310 (Anion) | 4,200 (Neutral @282) 5,000 (Anion @ 310) |

to raise the pH to 11.2; (3) obtain the absorbance reading for the sample at pH = 7.2 at a wavelength of 376 nanometers using a distilled water blank, and (4) obtain the absorbance reading for the sample at pH = 11.2 at a wavelength of 310 nanometers using the sample at pH = 7.2 as the blank. The DNOSBP concentration was determined from the absorbance reading obtained at pH = 7.2 while the OPP concentration was calculated from the adsorbance obtained at pH = 11.2.

SAMPLING PROCEDURE

Samples of approximately 100 milliliters were taken from the influent, effluent, and sample collection tank of the system. Influent and effluent grab samples were taken during a run with the frequency of sampling being greater at the outset of the run. Samples of the composite were taken at the beginning of each day. These were used to keep a "running" check on the solid-phase concentration profiles by having available a 24-hour sample representative of the average effluent for that day. The analysis for the composite samples gave an indication of the validity of each grab sample as the run progressed.

CHAPTER V

REVIEW OF PERTINENT LITERATURE

Mathematical modeling of columnar adsorption reactions for design and operation purposes entails the description of the mass balance for the system and the delineation of the appropriate equilibrium and kinetic relationships. While development of suitable materials balance, equilibrium, and rate equations is simple and straightforward, simultaneous solution of this set of equations is mathematically complex. Frequently, simplifying assumptions and numerical techniques are required to enable an approximate solution of the requisite set of equations.

Although early workers (1) showed that in certain cases equilibrium data alone are sufficient for such mathematical analyses, it is generally necessary to consider also the kinetics of the sorption process to permit accurate calculation of the breakthrough curves. Overall rates of adsorption of solutes from an aqueous stream flowing through a fluidized bed of granular active carbon represent the combined effects of: (a) diffusion through the hydrodynamic boundary layer of fluid surrounding the porous particle (film diffusion); (b) diffusion within the void spaces of the particle (pore diffusion); (c) pore-surface diffusion along the walls of channels within the porous sorbent (solid-phase diffusion); and (d) phase-change in the pores (adsorption). Pore-surface diffusion is distinguished from pore diffusion in that it occurs after phase-change on the solid side of the phase boundary. Under different operating conditions, any combination of these resistances may be operative. Generally, however, only one or two mechanisms are rate-limiting, because of the series relationship between the various resistances. That is, the slowest rate step determines the overall rate of mass transport. For sorption on granular activated carbon, the adsorption step itself is considered to be extremely rapid (2). Consequently, only the diffusional resistances are of import in determining the net rate of

transport.

Most mathematical solutions for systems of equations describing concentration-time profiles for columnar systems are limited to the special case in which only one of these four rate processes controls the overall rate of adsorption. Amundson (3,4), Edeskuty and Amundson (5), Hobson and Thodos (6), Hougen and Marshall (7), Kasten and Amundson (8,9,10), McCune and Wilhelm (11), Resnick and White (12), Richardson and Szekely (13), Tien and Thodos (14), Furnas (15), Goldstein (16), Klinkenberg (17), Kostecky, Manning and Canjar (18), and Vermeulen (19,20), for example, have presented solutions for systems in which either pore diffusion, film diffusion, or pore-surface diffusion is the only significant resistance to mass transport. Several investigators, including Colwell and Dranoff (21), Rosen (22,23), Hall, et al, (24) Masamune and Smith (24), and Tien and Thodos (14) have solved the more general case in which both the external and pore-diffusion or pore-surface diffusion resistances are significant. Masamune and Smith (25) have extended these concepts and presented a solution of the general three-resistance case in integral form. Unfortunately, however, each of the above developments required the use of simplifying assumptions relative to the equilibrium distribution of solute between solution and solid phases. Of the four basic types of isotherms -- irreversible, favorable, linear, and unfavorable -- each respective author assumed that either an irreversible or linear distribution represented the equilibrium conditions, primarily because it was mathematically expedient to do so to enable solution of the sets of partial differential equations. Adsorption isotherms for compounds typical of wastewater pollutants (26), however, are generally of the favorable type. Certainly, therefore, equilibria for such pollutants cannot be approximated adequately by a linear or irreversible type of isotherm.

If approximations to the kinetic parameters are made, such as the quadratic driving-potential approach, solution of the partial differential equations can be effected for non-linear equilibrium systems. Hendricks (27), Acrivos (28), Hall, et al, (24), Lapidus and Rosen (29), and Masamune and Smith (30,31), used various approximations for the rate parameters to obtain solutions for breakthrough profiles for the case of favorable equilibria of the Langmuir type. These solutions, however, are limited to the condition when only one of the possible rate-limiting mechanism is significant. Conversely, the second-order reaction-kinetics development of Thomas (32,33) which also allows the use of a generalized isotherm of the Langmuir type, provides for approximate solutions for the mono-, di-, and tri-resistance cases. Accordingly, the development of Thomas appears particularly suited for description of mass transfer processes for wastewater systems. Hiester and Vermeulen (34) have adapted the Thomas solution to packed-bed adsorbers, and have presented methods for numerical solution of the equations for mass transfer of single-solutes in such systems.

Methods by which rate constants and mass transfer coefficients have been defined by those investigators who provide experimental verification of their models commonly have involved: (a) development of a model based on several assumptions regarding equilibrium and rate parameters; (b) assumption of a succession of incremental rate constants while generating a series of concentration-time profiles; (c) carrying out an experimental column study for any suitable system, subject to the nature of the assumptions involved; and, (d) determination of appropriate rate constants for the system by means of curve-matching techniques. It is to be noted that this approach is not truly predictive in nature, as it must resort to preliminary experiments of a long-term pilot-plant scale. The investigations of Allen, et al, (35,36), provide an excellent example of one such approach of empirical determination of rate

constants.

One of the principal investigators (37,38,39) adapted the methods of Hiester and Vermeulen (34) for accurate description of mass transfer processes in columns of fluidized active carbon. The development involved correlation of experimental kinetic and equilibrium data for agitated non-flow systems with those of continuous flow fluid-bed systems. The model that was developed permits prediction of concentration-time profiles for systems of the latter type from measurements of selected adsorption parameters in critically designed non-flow systems. Measurements in simple, non-flow batch experiments can of course be accomplished much more readily and with greater ease than can those in relatively complex and time consuming continuous flow column tests. Cookson (40) recently developed a comparable model that is essentially identical in nature.

While the studies of numerous investigators as detailed above have provided a model which serves as a rational basis for the design of fluidized- and fixed-bed adsorbers for the removal of single components from aqueous solution, only several researchers have mounted the challenge of mathematically describing adsorption in multicomponent, competitive systems which, of course, are most commonly encountered in prototype applications. Both Collins and Chao (41) and Gariepy and Zweibel (42) developed models for the adsorption of binary mixtures of the gas-phase for fixed-beds. These researchers described competitive adsorption equilibria either by the competitive Langmuir model or by a thermodynamic, gas-phase approach. While these competitive equilibrium expressions were relatively satisfactory for carefully selected mixtures of gases, they have been shown to be unsatisfactory for description of competitive effects for adsorption in multicomponent aqueous solutions.

Under a previous contract the principal investigator (43) and associates

developed a mathematical model which allows simulation of the performance of adsorbers when treating solutions containing multiple components. That development employed either of two expressions for multiple-solute adsorption equilibria; that of Jain and Snoeyink (44) and that of Radke and Prausnitz (45). Moreover, that development as well as all previous models that describe the performance of adsorption from multicomponent solutions in columnar contactors assumed that adsorption on granular activated carbon was fully reversible. During the latter portion of the study by Keinath (43) this assumption, however, was shown not to be entirely valid. Consequently, there remains a demonstrated need for modification of the existing model to account for all time-dependent reversibility/irreversibility considerations such that mathematical simulations of adsorber column performance accurately predict these time dependent phenomena. Only when those modifications have been incorporated into the existing model will it be generally applicable for simulating design and operational alternatives for decontamination of multicomponent aqueous phase systems by use of adsorbers which contain granular activated carbon or, for that matter, any other similar adsorbent material.

MODEL DEVELOPMENT AND IMPLEMENTATION

MATERIAL BALANCE RELATIONSHIPS

Because adsorption contactors conventionally are of a columnar configuration and, therefore, have concentration profiles in the axial direction, it is necessary to conduct a mass balance over an infinitesimal thickness of bed at a given cross-section. The resultant conservation of mass equation expresses the fact that any loss of solute by the solution passing through that section must equal the gain of solute by the adsorbent contained within that section. For the purpose of this development it has been assumed that concentration gradients in the radial direction are of minor import.

Verbally, the materials balance relationship for the packed bed case may be expressed as:

$$\text{Input to Element} = \text{Output from Element} + \text{Adsorption} + \text{Accumulation} \quad (\text{VI-1})$$

For an infinitesimal thickness of bed of unit cross-sectional area the following mathematical formulations can be made for the solution-phase:

$$\text{Input to Element:} \quad C * U$$

$$\text{Output from Element:} \quad \left(C + \frac{\partial C}{\partial z} dz \right) U$$

$$\text{Adsorption:} \quad \rho \left[\frac{\partial q}{\partial t} \right] dz \, dA$$

$$\text{Accumulation:} \quad \epsilon \left[\frac{\partial C}{\partial t} \right] dz \, dA$$

where:

U = solution volumetric flow rate, liters/hour

C = solution-phase concentration of solute, moles/liter

q = solid-phase concentration of solute, moles/gram

z = axial distance, cm

t = time, hours

A = cross-sectional area of column, sq. cm.

ϵ = void ratio or porosity, dimensionless

ρ = packed-bed density, grams/liter

Equating in accordance with Equation VI-1 and assuming unit cross-sectional area, one obtains:

$$C * U = \left[C + \frac{\partial C}{\partial z} dz \right] U + \rho \left[\frac{\partial q}{\partial t} \right] dz + \epsilon \left[\frac{\partial C}{\partial t} \right] dz$$

which upon simplification becomes:

$$U \frac{\partial C}{\partial z} + \epsilon \frac{\partial C}{\partial t} + \rho \frac{\partial q}{\partial t} = 0 \quad (\text{VI-2})$$

Solution of this partial differential equation (Equation VI-2) is the essence of the problem of mathematical simulation of the performance of packed-bed adsorption contactors. Such solution may be effected by exact solution of the equations, by the method of finite differences, by the method of characteristics, or by the lumped parameter approach to modeling this distributed parameter system. To obtain an exact solution it is necessary to make certain simplifying assumptions regarding adsorption equilibria; such as a linear or irreversible isotherm. Although these assumptions are relatively restrictive, they did permit the development of exact solutions by many early investigators including notable developments of Amundson (4), Kasten, et al. (10), and Rosen (23).

Solutions by the methods of finite differences and characteristics have been explicitly detailed by Crank (46) and Acrivos (28), respectively. Because of certain complexities, however, these are not user oriented. In contrast, the lumped parameter approach is user oriented as it permits the use of the continuous system modeling program, CSMP III, developed by IBM (47). Consequently, all further developments relate to the lumped parameter approach.

Lumped Parameter Approach

Use of the lumped parameter approach requires segmentation of the bed of adsorbent into a discrete number of finite elements as determined by the dispersion characteristics of the columnar reactor. Both the liquid- and solid-phase concentrations of solute are assumed to be uniform throughout each element. Further, continuity of mass flows of the solute between adjoining elements must be maintained for both the liquid and solid phases.

For the case in which an adsorption column is charged with an adsorbent and then operated in the unsteady-state until the adsorbent is entirely exhausted, the following formulations can be made for an element of a packed-bed:

| | <u>Solution-Phase</u> | <u>Solid-Phase</u> |
|----------------------|---|---|
| Input to Element: | $U * C_{n-1}$ | 0 |
| Output from Element: | $U * C_n$ | 0 |
| Adsorption: | $\rho * R_A * V$ | $\rho * R_A * V$ |
| Accumulation: | $\epsilon \left[\frac{dc_n}{dt} \right] V$ | $\rho \left[\frac{dq_n}{dt} \right] V$ |

where:

V = volume of the elements, liters

R_A = rate of adsorption, moles/gram-hour

n = number of elements

and all other parameters are as defined above. As before, equating in accordance with Equation VI-1 for the solution-phase:

$$U * C_{n-1} = U * C_n + \rho * R_A * V + \epsilon \left[\frac{dc_n}{dt} \right] V$$

which yields upon rearrangement for the n -th element,

$$\frac{dc_n}{dt} = \left[\frac{U}{\epsilon V} \right] [C_{n-1} - C_n] - \left[\rho/\epsilon \right] [R_A] \quad (\text{VI-3})$$

Similarly, for the solid-phase the mass balance-relationship for the solute becomes:

$$0 = 0 - \rho * R_A * V + \rho (dq_n/dt) V$$

which simplifies to,

$$dq_n/dt = R_A \quad (\text{VI-4})$$

For the case where several or numerous solutes are competing for the available adsorption sites, mass balances for the solution- and solid-phases must be written for each solute that is introduced in the influent to the column.

Although the foregoing equations were developed for packed-bed adsorbers, they can readily be modified for the fluidized-bed mode of operation. This involved making provision for mixing of the adsorbent solids within the column. For the lumped parameter approach this is easily accomplished through the use of a procedural solids mixing subroutine.

It is important to recognize that the set of differential equations (Equations VI-3 and VI-4) are extremely stiff. That is, the time constant for the liquid-phase equation is small in contrast to the time constant for the solid-phase equation. Numerical integration of the set of equations requires specification of an integration interval that provides for the stable and accurate integration of the equation that responds most rapidly; i.e., the liquid-phase mass balance.

If, however, the time constants for the two equations are different by several orders of magnitude, one can assume that the equation that responds most rapidly is continuously at steady-state. For this case the term dc_n/dt in Equation VI-3 is set to zero and the resulting algebraic equation is solved for C_n . Specification of the integration interval is then contingent only on the remaining differential equation - that which responds most slowly (solid-phase mass balance, Equation VI-4). This serves to materially decrease the computation time required for numerical solution.

ADSORPTION EQUILIBRIA

The distribution of solute between liquid- and solid-phases in an adsorbent-solute-solvent system at equilibrium is commonly termed an adsorption isotherm. Adsorption equilibrium data is conventionally presented and correlated by plotting the quantity of solute adsorbed per unit weight of adsorbent, q , as a function of the concentration of solute remaining in solution at equilibrium, C .

Several mathematical formulations that describe adsorption equilibria and that have been widely adopted since their development include the model isotherm originally proposed by Langmuir,

$$q = \frac{Q * b * C}{1 + b * C} \quad (\text{VI-5})$$

that of Freundlich,

$$q = K * C^{1/n'} \quad (\text{VI-6})$$

and that of Branauer, Emmett and Teller,

$$q = \frac{Q * A * C}{(C_s - C) (1 + [A - 1] C/C_s)} \quad (\text{VI-7})$$

where:

Q = ultimate uptake capacity of adsorbent, moles/gram

b = Langmuir energy term, liters/mole

K = adjustable curve-fitting constant

n' = adjustable curve-fitting constant

A = BET energy term, liters/mole

C_s = saturation concentration of solute in solution, moles/liter

Of these three, the simple empirical Freundlich expression is the most widely used primarily because of its simplicity and because it has

been successfully employed for correlating data for adsorption of solutes on activated carbon over limited concentration ranges. The Langmuir equation, based on the assumption of mono-layer adsorption on a fixed number of equivalent adsorptions sites, has also been useful over limited concentration ranges. In contrast, the BET equation which is based on the assumption of multiple-layer adsorption has not been used as frequently as either the Langmuir or Freundlich models principally because of the difficulty in obtaining suitable values for C_s .

LANGMUIR COMPETITIVE ADSORPTION MODEL

Each of the three models which describe adsorption equilibria, Equations VI-5, VI-6, VI-7, are, of course, limited for application single-solute systems. Only the Langmuir model has been extended to account for competitive adsorption equilibria in multiple-solute systems. For the di-solute case the extent of adsorption for solute A is given by:

$$q_A = \frac{Q_A * b_A * C_A}{1 + b_A * C_A + b_B * C_B} \quad (\text{VI-8})$$

and for solute B the solid-phase equilibrium concentration may be expressed as:

$$q_B = \frac{Q_B * b_B * C_B}{1 + b_A * C_A + b_B * C_B} \quad (\text{VI-9})$$

where the constants, Q_A , Q_B , b_A , and b_B , are those that are measured in mono-solute, pure solution systems. For the general case, where (i) is used to designate the number of solutes in the system, the extent of adsorption for solute (j) is given by:

$$q_j = \frac{Q_j * b_j * C_j}{1 + \sum_{i=0} b_i * C_i} \quad (\text{VI-10})$$

Although this formulation is mathematically simple, it has been experimentally verified only for certain selected di-solute competitive systems (44). Accordingly, it is important to recognize that this relationship should not be employed indiscriminately when simulating the performance of adsorption contactors for competitive, multiple-solute systems. Rather, the relationship must be experimentally validated for the specific multiple-solute/solvent/adsorbent system before its use can be judged appropriate.

Semi-Competitive Langmuir Adsorption Model

Jain and Snoeyink (44) have investigated the competitive interaction of substituted phenols in the concentration range of 10^{-5} to 10^{-2} moles per liter. They determined that the competitive Langmuir expression was not satisfactory for description of results obtained in their studies. They observed a preferential adsorption for one compound in comparison to the other. A fraction of the material which was preferentially adsorbed appeared to respond as though it were a single-solute system. These findings led to the development of the following empirical expressions

$$q_A = \frac{(Q_A - Q_B) b_A C_A}{1 + b_A C_A} + \frac{Q_B b_A C_A}{1 + b_A C_A + b_B C_B} \quad (\text{VI-11})$$

for the preferentially adsorbed material and

$$q_B = \frac{Q_B b_B C_B}{1 + b_A C_A + b_B C_B} \quad (\text{VI-12})$$

for the less readily adsorbed material.

The first term of Equation VI-11 describes that fraction of the adsorbed phase which is preferentially adsorbed. The second term describes that fraction of the adsorbed phase that is competitive in the Langmuir sense with the second solute. The rationale for the development of this expression was based upon steric factors, surface characteristics, and certain physical factors.

Equation III-12 represents the competitive interaction of the second solute. This expression is exactly the same as that of the competitive Langmuir theory.

Theoretically, these expressions have the same general limitations as the Langmuir equations. Jain and Snoeyink (44) however, have shown that these equations describe a much broader spectra of competitive adsorption isotherms than do the competitive Langmuir equations.

Ideal Solution Theory Adsorption Isotherm

Radke and Prausnitz (45) detailed a procedure for the prediction of multi-solute adsorption from dilute solutions. A detailed description of their method is given below.

The thermodynamic framework of the Radke and Prausnitz (45) method was based upon the solution-solid interface as described by Gibbs. Assuming the solid was inert, the differential equation for the Helmholtz energy of the adsorbed phase was written as

$$dA^a = -SdT - pdV + \lambda d\sigma + \sum_i \mu_i^a dn_i^a + \mu_s^a dn_s^a \quad (\text{VI-13})$$

where the subscript (i) represents solute and (s) the solvent. The interfacial tension was represented by λ , the area of solution-solid interface by σ , and moles in the adsorbed phase by n^a .

Integration of Equation VI-13 for isothermal conditions and assuming λ , μ_i^a , μ_s^a , V as constant gave

$$A^a = \lambda\sigma + \sum \mu_i^a n_i^a + \mu_s^a n_s^a \quad (\text{VI-14})$$

which upon differentiation became Gibbs isothermal adsorption expression

$$\lambda d\sigma + \sum n_i^a d\mu_i^a + n_s^a d\mu_s^a = 0 \quad (\text{VI-15})$$

The liquid-phase which was not affected by surface forces was expressed as

$$\sum n_i^l d\mu_i^l + n_s^l d\mu_s^l = 0 \quad (\text{VI-16})$$

At equilibrium the chemical potential of the liquid-phase and the solid-phase are equal. Accordingly, multiplying Equation VI-16 by n_s^a/n_s^l

$$\frac{n_s^a}{n_s^l} \sum n_i^l d\mu_i^l + n_s^a d\mu_s^a = 0 \quad (\text{VI-17})$$

and subtracting from Equation VI-15 the expression became

$$\sigma d\lambda + \sum n_i^a d\mu_i^a - \frac{n_s^a}{n_s^l} \sum n_i^l d\mu_i^a = 0 \quad (\text{VI-18})$$

Since the function $d\lambda/d\mu_i^a$ and $d\lambda/d\mu_s^a$ are the Gibbs excess surface function, then the invariant adsorption (n_i^m) was defined as

$$n_i^m \equiv n_i^a - \frac{C_i}{C_s} n_s^a \quad (\text{VI-19})$$

where the adsorbed moles of solute and solvent n_i^a and n_s^a were the Gibbs surface excess quantities. Therefore, the following expression

$$-\sigma d\lambda = \sum n_i^m d\mu_i^a = \sigma d\pi \quad (\text{VI-20})$$

was valid over the entire solute range where the spreading pressure (π) was represented by

$$\pi \equiv \lambda \text{ (pure solvent-solid)} - \lambda \text{ (solution-solid)} \quad (\text{VI-21})$$

Radke and Prausnitz (45) showed in their work that for dilute solutions n_i^m may be approximated by

$$n_i^m = V \Delta C_i = q_i \quad (\text{VI-22})$$

where ΔC_i was the decrease in concentration or constituent in a known volume (V) of the solution-phase when contacted with a known mass of adsorbent. It was further shown that it was useful to define the adsorbed phase fugacity as

$$dp_i^a = RT d \ln f_i^a \text{ (constant } T) \quad (\text{VI-23})$$

and

$$\lim_{\pi \rightarrow 0} \frac{f_i^a}{Z_i \pi} = 1 \quad (\text{VI-24})$$

where the adsorbed phase mole fraction Z_i was defined as

$$Z_i = \frac{n_i^m}{\sum n_i^m} = \frac{n_i^m}{n_T^m} \quad (\text{VI-25})$$

Considering simultaneous adsorption of the solute species at a constant temperature and spreading pressure, it was assumed that an ideal solution phase was formed. Based upon this assumption, the fugacity f_i^a must be proportional to the mole fraction Z_i

$$f_i^a (T, \pi, Z_i^a) = Z_i^a f_i^{a^\circ} (\pi, T) \quad (\text{VI-26})$$

where $f_i^{a^\circ}$ is the fugacity of that single-solute in dilute solution at the same temperature and spreading pressure of the mixture.

Equation VI-26 shows that n_T^m was only a function of the adsorbed-phase composition Z_i and invariant adsorption of a single solute n_i^{om} , therefore, n_T^m was expressed by

$$\frac{1}{n_i^m} = \sum \frac{z_i}{n_i^{om}} \quad (\text{VI-27})$$

Verification of this equation was accomplished by substituting Equation VI-25 into Equation VI-20 and rearranging the terms

$$\frac{\sigma}{n_i^m} = \sum z_i \frac{\partial \mu_i^a}{\partial \pi} \quad (\text{VI-28})$$

Substitution of Equations VI-26 and VI-23 into Equation VI-28 resulted in

$$\frac{\partial \mu_i^a}{\partial \pi} = \frac{\partial \mu_i^{oa}}{\partial \pi} = \frac{\sigma}{n_i^{om}} \quad (\text{VI-29})$$

which upon substitution into Equation VI-28 yields Equation VI-27.

The chemical potential of solute μ_i^a in the adsorbed-phase must equal that of the liquid-phase at equilibrium. This condition is given by

$$\mu_i^a(T, \pi, Z_i) = \mu_i^l(T, C) \quad (\text{VI-30})$$

The solid-phase chemical potential was expressed as

$$\mu_i^a(T, \pi, Z) = \mu_i^{oa}(T\pi) + RT \ln Z_i \quad (\text{VI-31})$$

which was the integrated form of Equation VI-23. Since T and π established the single-solute concentration C_i^o in a dilute phase, the following substitution for μ_i^{oa} was made

$$\mu_i^{oa} = \mu_i^{*l}[T, C_i^o(\pi)] = \mu_i^{*l}(T) + RT \ln C_i^o(\pi) \quad (\text{VI-32})$$

where (*) denotes the ideal-solution standard state of the liquid-phase. The concentration term $C_i^o(\pi)$ refers to a single-solute adsorbed from solution, at the same temperature and spreading pressure as the mixture, and has the same interpretation as n_i^{mo} .

The dilute liquid mixture was expressed as

$$\mu_i^l(T, C) = \mu_i^{l^o}(T) + RT \ln C_i^l \quad (\text{VI-33})$$

Upon substitution of Equations VI-31, VI-32, and VI-33 into Equation VI-30, the following expressions were obtained

$$C_i = C_i^o(\pi) Z_i \quad (\text{constant } T) \quad (\text{VI-34})$$

and

$$C_i X_i = C_i^o(\pi) Z_i \quad (\text{constant } T). \quad (\text{VI-35})$$

The spreading pressure must be evaluated before the mixture concentration and adsorbed phase may be computed. The spreading pressure may be computed by integration Equation VI-20 to give

$$\pi(C_i^o) = \frac{RT}{\sigma} \int_0^{C_i^o} \frac{n_i^{mo}(C_i)}{C_i^o} dC_i^o \quad (\text{VI-36})$$

Experimental single-solute isotherms are used to develop a curve of n_i^{mo}/C_i^o as a function of C_i^o . These can be either numerically or graphically integrated to determine π . A graphical procedure of Myers and Prausnitz (48) and a numerical method have been described in detail in Appendix B. Because the single-solute data describes π , there is no need for a theoretical model of simplifying or restrictive assumptions to describe the adsorption equilibria.

Multi-solute isothermal equilibria may be calculated using a method described by Myers and Prausnitz (48). The procedure is summarized below:

- (i) Experimental single-solute isotherm data is integrated according to Equation VI-36 to yield the spreading pressure for each solute as a function of concentration. This is given by:

$$\pi_1 = f_1(C_1^o) , \text{ and} \quad (\text{VI-37})$$

$$\pi_2 = f_2(C_2^o) . \quad (\text{VI-38})$$

(ii) The equilibrium relationships are given by:

$$C_T x_1 = C_1^o Z_1 , \text{ and} \quad (\text{VI-39})$$

$$C_T x_2 = C_2^o (1 - Z_1) . \quad (\text{VI-40})$$

These are shown in Figure VI-1.

(iii) The spreading pressure of each constituent is equivalent to that of the mixture, i.e.

$$\pi_1 = \pi_2 = \pi . \quad (\text{VI-41})$$

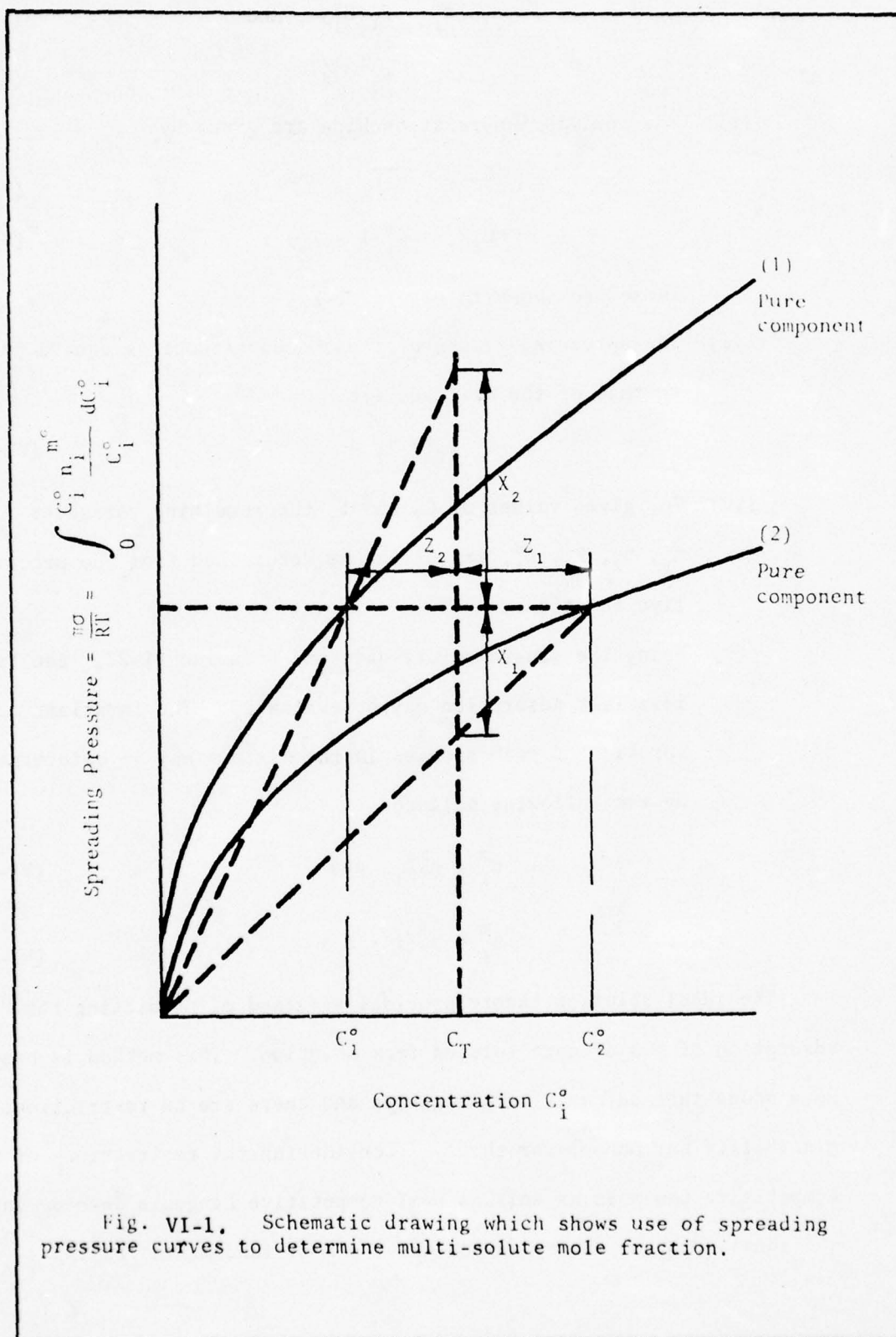
(iv) For given values of C_T and x_1 the remaining variables π_1 , π_2 , Z_1 , C_1^o , and C_2^o may be determined from the preceding five equations.

(v) Using the single-solute data and Equation VI-27, the total invariant adsorption may be evaluated. The invariant adsorption of each species in the mixture may be determined by the following balances

$$n_1^m = n_T^m Z_1 , \text{ and} \quad (\text{VI-42})$$

$$n_2^m = n_T^m (1 - Z_1) . \quad (\text{VI-43})$$

The ideal solution theory provides a method of predicting the adsorption of two or more solutes from solution. This method is based upon sound thermodynamic relationships and there are no restrictions on miscibility nor mono-layer theory. Considering the restrictions of the competitive Langmuir as well as semi-competitive Langmuir developments, the ideal solution theory method has the most fundamental basis.



KINETICS OF INTERPHASE SOLUTE TRANSPORT

To relate the dynamically varying solid- and solution-phase concentrations of solute at any time and position in an adsorption contactor, it is necessary to fully understand the kinetics of solute transport. Consequently, the mechanisms of such transport must be considered in detail.

The overall rate of adsorption of solute, from a solvent stream flowing through a bed of porous, granular adsorbent represents the combined effects of: (1) diffusion through the boundary layer of fluid surrounding the adsorbent particle (film or external diffusion); (2) diffusion within the pores of the particle (pore diffusion); (3) diffusion along the surface of the pores (pore-surface diffusion); and (4) adsorption on the internal pore surfaces (adsorption). Pore-surface diffusion is distinguished from pore diffusion in that it occurs on the solid side of the phase boundary. That is, the solute may enter a particle of adsorbent directly from the exterior surface by movement in a condensed or adsorbed layer along the pore surfaces, or it may diffuse through the fluid-phase held in the pores and then be deposited at a stationary location on the pore surface. In pore diffusion, the mass transfer process occurs before the phase change, while in pore-surface diffusion it occurs afterward. Under different operating conditions, the same particle can exhibit either surface- or pore-diffusion behavior, favoring the former if the concentration level in the pore-fluid is low and the latter if the level is high. Of these two transport processes, the more rapid one will control the overall rate of transport, since they act in parallel. Conversely, for either of the two solute transport pathways, film diffusion/pore diffusion/adsorption or film diffu-

sion/pore-surface diffusion/adsorption, the slowest of the three mass transfer mechanisms will in each case limit the overall rate of adsorption because these rate steps occur in a series relationship.

Adsorption Rate Step

It has been experimentally determined that surface tension attains equilibrium after a disturbance in approximately ten milliseconds. This circumstantial evidence indicates that the adsorption process itself is a relatively rapid process and, therefore, is probably not rate controlling. Considerable experimental evidence exists that supports this supposition. Accordingly, adsorption is generally considered as not limiting the overall rate of adsorption. It will, therefore, not be considered further in this development.

Pore-Diffusion

For a porous adsorbent the rate of diffusion into the liquid in the pores of a spherical particle is given by:

$$D_{\text{pore}} \left[\frac{\partial^2 c}{\partial r^2} + \frac{2}{r} \frac{\partial c}{\partial r} \right] = \chi \left[\frac{\partial c}{\partial t} \right] + \rho_p \left[\frac{\partial q}{\partial t} \right] \quad (\text{VI-44})$$

where:

D_{pore} = pore diffusivity, cm^2/sec

r = radial distance within particle, cm

χ = internal porosity of adsorbent particles, dimensionless

ρ_p = density of adsorbent particle, gm/liter

The mean concentration of the entire particle of diameter, D_p (cm), is obtained by:

$$q = \frac{3}{(D_p/2)^3} \int_0^{D_p/2} q r^2 dr \quad (\text{VI-45})$$

For liquids, the pore diffusivity term (D_{pore}) may be approximated by the relationship:

$$D_{\text{pore}} = \frac{D_{\ell} * X}{2} \quad (\text{VI-46})$$

where:

$$D_{\ell} = \text{diffusivity of solute in solvent, cm}^2/\text{sec}$$

Although Equations VI-44, VI-45, and VI-46 clearly describe the pore-diffusion rate-limiting case, it is to be noted that solution of these equations in conjunction with either Equations VI-2 or VI-3 (materials balance relationships for the columnar adsorption contactor) has not yet been accomplished, either exactly or numerically. This, of course, is due to the fact that an additional independent variable, radial distance within the porous adsorbent particle, is introduced into the mass balance relationship for a packed-bed contactor. Consequently, a linear driving potential is frequently employed as a gross approximation (49). The rate equation then is:

$$R_A = \frac{dq}{dt} = k_p * A_p * (C - C^*) \quad (\text{VI-47})$$

where:

$$k_p = \text{mass-transfer coefficient (pore), cm/hr}$$

$$A_p = \text{external interfacial transfer area for adsorbent, cm}^2/\text{liter}$$

$$C^* = \text{solution-phase concentration of solute considered to be in equilibrium with the outer surface of the adsorbent particle moles/liter.}$$

For this approximation, the term $k_p * A_p$ is evaluated by:

$$k_p * A_p = \frac{60 * D_{\text{pore}}}{D_p^2} (1 - \epsilon) \quad (\text{VI-48})$$

Pore-Surface Diffusion

Diffusion of solute molecules along the surfaces of the pores in a porous adsorbent is described by:

$$D_s \frac{\partial^2 q}{\partial r^2} + \frac{2}{r} \frac{\partial q}{\partial r} = \frac{\partial q}{\partial t} \quad (\text{VI-49})$$

where:

D_s = pore-surface diffusivity, cm^2/sec .

As before, solution of Equation VI-49 in association with Equation VI-2 or VI-3 cannot currently be achieved with the various numerical methods that are available. This equation, therefore, is frequently approximated by the linear-driving force relation of Glueckauf and Coates (50):

$$R_A = \frac{dq}{dt} = k_s * A_p (q^* - q) \quad (\text{VI-50})$$

where:

k_s = mass-transfer coefficient (pore-surface), cm/hr

q^* = solid-phase concentration of solute considered to be in equilibrium with the instantaneous fluid-phase concentration outside the particle, moles/gram

The product $k_s * A_p$ is related to the diffusivity and to the adsorbent particle diameter through the equation:

$$k_s * A_p = \frac{60 * D_s}{D_p^2} \quad (\text{VI-51})$$

Experimentally determined values for D_s are required for solution of Equation VI-51 such that estimates of the term $k_s * A_p$ can be obtained. Methods of obtaining values for D_s have been detailed explicitly by DiGiano (51). For aqueous solutions of various substituted phenols and benzene sulfonates, DiGiano (51) determined ratios of D_s/D_ℓ which varied from 0.1 to 0.3.

A somewhat better approximation to the behavior of Equation VI-49 is given by the quadratic driving potential form postulated by Vermeulen (19):

$$R_A = \frac{dq}{dt} = k_s * A_p * \psi * \left[\frac{q^{*2} - q^2}{2q - q_0} \right] \quad (\text{VI-52})$$

where:

q_0 = initial solid-phase concentration (usually zero), moles/gram

$\psi = 1/(R + 15 (1 - R)/\pi^2)$

R = separation factor, dimensionless

Film or External Diffusion

Transfer of solute molecules from the bulk solution through the hydrodynamic boundary layer surrounding the granular adsorbent particle to its external surface is commonly described by:

$$R_A = \frac{dq}{dt} = k_f * A_p (C - C^*) \quad (\text{VI-53})$$

where:

k_f = film-diffusion controlled mass transfer coefficient, cm/hr

Use of Equation VI-53 does not necessarily imply the existence of a stagnant hydrodynamic boundary layer through which molecular diffusion occurs. Rather, this equation may generally be used for description of mass transfer through the boundary layer. Certainly, this would include the effects of eddy transport in addition to molecular diffusion.

Although various theories including the penetration and free surface models have been advanced to describe transient diffusion through an external boundary layer, the straightforward relationship given by Equation VI-53 is the only form that is generally applicable for simulation of the dynamics of a columnar adsorber. Because of the difficulty

in describing the hydrodynamic conditions in the boundary layer, mass transfer coefficients, k_f are not determined directly but are obtained by correlation of the mass transfer factor, j_d , with the Sherwood number, Reynolds number, and Schmidt number as follows:

$$j_d = N_{Sh} / (N_{Re} * N_{Sc}^{1/3}) \quad (VI-54)$$

where:

$j_d = (k_f/U) * (\nu/D_\ell)^{2/3}$, mass transfer factor, dimensionless

$N_{Sh} = k_f * D_p/D_\ell$, Sherwood number, dimensionless

$N_{Sc} = \nu/D_\ell$, Schmidt number, dimensionless

$N_{Re} = U * D_p/\nu$, Reynolds number, dimensionless

$U = U/A$, velocity of flow, cm/hr

ν = kinematic viscosity of solution, cm^2/sec

Numerous investigators have conducted intensive experimental studies to evaluate the correlation given in the foregoing equation, Equation VI-54, for a variety of different system types including gas-liquid, liquid-solid, and gas-solid two-phase systems. Extensive investigations have also focused on single-particle as well as multiparticle systems which are operated either in the packed, expanded, semifluidized, or fully fluidized-bed modes (52, 53, 54, & 55).

Accordingly, if it has been determined that film diffusion or external transport is rate limiting, then one can obtain a suitable mass transfer coefficient from one of the existing correlations. It is important, however, to pay particular attention to the type of system for which the correlation was obtained and to the procedure employed for calculation of mass transfer coefficients.

MODEL IMPLEMENTATION

Prediction of the performance of adsorption contactors involves the solution of a set of differential equations which describe the fluid- and solid-phase material balances. The computer provides a convenient method of structuring the differential equations for numerical solution. Structure of the model may be directed toward the use of any number of numerical integration procedures. The integration technique selected depends upon the users familiarity with the various techniques as well as convergence criteria of the technique selected. For this reason it was decided to structure the model such that the user might select the integration routine directly from the scientific subroutines stored in the computer library. This would permit the engineer who has minimum programming experience to utilize and understand the function of the model, while allowing the engineer who is more adept in computer programming the versatility of restructuring the model to any other numerical technique he desired.

For this reason the IBM System/360 Continuous System Modeling Program (CSMP III) was used for solution of the differential contacting model. This system is a problem oriented program which permits the problems to be prepared directly from block diagrams or a set of ordinary differential equations. It contains a basic set of 34 functional blocks which may be used to represent components of a continuous system. This basic set of functional blocks includes conventional analog computer components such as integrators, relays, and time delays as well as specialty functions such as logic functions and macro systems. In effect CSMP III does not have to operate within the simulation language framework but may be structured in the symbols characteristic of the language of any specialty field. The program will also accept FORTRAN statements, thereby allowing the user to solve complex nonlinear and time-variant problems.

As was suggested above, solution of the set of differential equations that describe the mass balances for the solution- and solid-phases of an adsorption contactor is facilitated by use of the distributed parameter approach when used in conjunction with CSMP III. Programs formulated in CSMP III generally consist of three segments: INITIAL, DYNAMIC, and TERMINAL. Broadly, the INITIAL segment is intended exclusively for computation of initial condition values. The DYNAMIC segment is normally the most extensive of the model. It includes the complete description of the system dynamics, together with any other computations desired during the run. Conversely, computations which are to be performed only after completion of the dynamic run are placed into the TERMINAL segment of the model. These will often be simple calculations or optimization algorithms based on the final value of one or more model variables.

For an adsorption contactor the differential equations, VI-3 and VI-4 describe the system dynamics or the time-variant performance of each segment of the adsorbent bed. Of course, these require input of the appropriate rate relationship for R_A (Equations VI-47, VI-50, VI-52, or VI-53) and a suitable description of the competitive equilibrium distribution of solute between solution and solid phases. If it is assumed that mass-transfer is rate limiting and that the competitive Langmuir equation adequately represents the pertinent adsorption equilibria, then the system dynamics can be formulated as shown below in the DYNAMIC segment of CSMP III.

DYNAMIC

 *** DIFFERENTIAL EQUATIONS FOR ADSORPTION BED ***

```
QA=INTGRL(ICQA,QADDT,11)
QB=INTGRL(ICQB,QBDJT,11)
```



```

PROCEDURE QADOT,QBDOT=ADS(QA,QB,ISOB,QAMAX,BA,KFA,KFB,A)
DO 10 I=2,11
IF (QB(I).LT.5.E-5) QBINV=2.E+4
IF (QB(I).GE.5.E-5) QBINV=1/QB(I)
CBINV=FUNGEN(ISOB,5,QBINV)
BSLOPE=SLOPE(ISOB,3,QBINV)
QBMAX=1/(QBINV-(1/BSLOPE)*CBINV)
BB=BSLOPE/QBMAX

CSTARA=QBMAX*BB*QA(I)/(QAMAX*QBMAX*BA*BB-QAMAX*QB(I)*BA*BB...
-QBMAX*QA(I)*BA*BB)
CSTARB=QAMAX*BA*QB(I)/(QAMAX*QBMAX*BA*BB-QAMAX*QB(I)*BA*BB...
-QBMAX*QA(I)*BA*BB)
CA(I)=(DUM1*CA(I-1)+DUM2*CSTARA)/(DUM1+DUM2)
CB(I)=(DUM1*CB(I-1)+DUM3*CSTARB)/(DUM1+DUM3)
QADOT(I)=KFA*A*(CA(I)-CSTARA)*1.E-3
QBDOT(I)=KFB*A*(CB(I)-CSTARB)*1.E-3
10 CONTINUE
ENDPROCEDURE

```

Initial conditions for second and fourth equations of each element of the bed are generally specified in the INITIAL segment of the CSMP III program using an INCCN or TABLE label as shown in the program listing which follows:

```

*****
***  INITIAL CONDITIONS FOR SOLID PHASE CONCENTRATION  ***
*****

TABLE ICQA(2-11)=11*0.0
TABLE ICQB(2-11)=11*0.0
***

```

Likewise, parameters which must be specified for the simulation are introduced in the INITIAL segment by use of the PARAM statement as may be observed in the listings below:

```

*****
***  PARAMETER INPUTS REQUIRED ARE DEFINED AS FOLLOWS  ***
*****
***
***  CARBON --- MASS OF CARBON IN BED (GRAMS)  ***
***  A ----- EXTERNAL TRANSFER AREA FOR CARBON (SQ CM/GRAM)  ***
***  DP ----- DIAMETER OF CARBON PARTICLES (CM)  ***
***  RHOPAC --- PACKED BED DENSITY (GRAMS/LITER)  ***
***  EPS ----- PACKED BED POROSITY (DIMENSIONLESS)  ***
***  QAMAX --- LANGMUIR ULTIMATE UPTAKE CAPACITY FOR A (MOLES/GRAM) ***
***  QBMAX --- LANGMUIR ULTIMATE UPTAKE CAPACITY FOR B (MOLES/GRAM) ***
***  BA ----- LANGMUIR ENERGY TERM FOR A (LITERS/MOLE)  ***
***  BB ----- LANGMUIR ENERGY TERM FOR B (LITERS/MOLE)  ***
***  CA(1) --- SOLUTION-PHASE CONCENTRATION OF A (MOLES/LITER)  ***
***  CB(1) --- SOLUTION-PHASE CONCENTRATION OF B (MOLES/LITER)  ***
***  DLA ----- DIFFUSIVITY OF SOLUTE A (SQ CM/SEC)  ***
***  DLB ----- DIFFUSIVITY OF SOLUTE B (SQ CM/SEC)  ***
***  AREA ----- CROSS-SECTIONAL AREA OF COLUMN (SQ CM)  ***
***  U ----- SOLUTION VOLUMETRIC FLOW RATE (LITERS/HOUR)  ***
***  GAMMA --- KINEMATIC VISCOSITY OF WATER (SQ CM/SEC)  ***
***  EXP ----- RATIO: EXPANDED /PACKED BED VOLUME (DIMENSIONLESS) ***
***
*****
***  PARAMETER INPUTS FOLLOW  ***
*****

```

```

PARAM CARBON=36.79
PARAM A=124.6
PARAM DP=9.55E-2
PARAM RHOPAC=253.
PARAM EPS=0.43
PARAM QAMAX=3.4958E-3
PARAM BA=650.
TABLE CA(1)=1.E-3
TABLE CB(1)=1.E-3
PARAM CAO=1.E-3
PARAM CBO=1.E-3
PARAM DLA=8.672E-6
PARAM DLB=8.54E-6
PARAM AREA=4.978
PARAM U=6.12
PARAM GAMMA=9.348E-3
PARAM EXP=(1.0,1.5)

```

Moreover, certain parameters which are non-time-variant and must be calculated prior to the simulation are evaluated in the INITIAL segment.

A listing of those parameters that must be determined by calculation follows:

```

*****
***  CALCULATED INPUT PARAMETERS ARE DEFINED AS FOLLOWS  ***
*****
***
***  RHO ----- EXPANDED BED DENSITY (GRAMS/ LITER)      ***
***  VP ----- TOTAL VOLUME OF PACKED BED (LITERS)       ***
***  V ----- TOTAL VOLUME OF PACKED BED (LITERS)        ***
***  EPSI ----- EXPANDED BED POROSITY (DIMENSIONLESS)    ***
***  UBAR ----- SUPERFICIAL VELOCITY OF FLOW THROUGH BED (CM/SEC) ***
***  NREMOD --- MODIFIED REYNOLDS NUMBER (DIMENSIONLESS)  ***
***  NSCA ----- SCHMIDT NUMBER FOR A (DIMENSIONLESS)    ***
***  NSCB ----- SCHMIDT NUMBER FOR B (DIMENSIONLESS)    ***
***  JD ----- MASS TRANSFER FACTOR (DIMENSIONLESS)      ***
***  KFA ----- MASS TRANSFER COEFFICIENT FOR A (CM/HOUR) ***
***  KFB ----- MASS TRANSFER COEFFICIENT FOR B (CM/HOUR) ***
***  DUM1 ----- DUMMY COEFFICIENT                       ***
***  DUM2 ----- DUMMY COEFFICIENT                       ***
***  DUM3 ----- DUMMY COEFFICIENT                       ***
***
*****
***  INPUT PARAMETER CALCULATIONS FOLLOW  ***
*****

RHO=RHOPAC/EXP
VP=CARBON/(RHOPAC*10.)
V=CARBON/(RHO*10.)
EPSI=(EPS*VP+V-VP)/V
UBAR=(U*0.277777)/AREA
NREMOD=(UBAR*DP)/(GAMMA*(1.-EPSI))
NSCA=GAMMA/DLA
NSCB=GAMMA/DLB
JD=1.34*NREMOD**(-0.468)
KFA=(JD*UBAR/NSCA**(2./3.))*3600.
KFB=(JD*UBAR/NSCB**(2./3.))*3600.
DUM1=U/(EPSI*V)
DUM2=(KFA*A*RHO*1.E-3)/EPSI
DUM3=(KFB*A*RHO*1.E-3)/EPSI

```

If, in contrast, certain parameters are time dependent, they must be included in the DYNAMIC segment of the model, such that at any time during the integration the parameter is evaluated for its current numerical value.

In addition to the foregoing listing in which the dynamic model is fully specified, it is necessary also to provide for several execution and output control statements. Execution control statements are used to specify certain items relating to the actual simulation; e.g. integration method, run time, integration interval, relative error, output times, etc. An example of the execution control statements used in the current simulation studies is shown below.


```
*****
***  EXECUTION CONTROL STATEMENTS  ***
*****
```

```
METHOD RECT
TIMER DELT=.20,FINTIM=48.0,PRDEL=0.2,OUTDEL=0.4
```

The first of two control statement cards specifies the type of integration method which is to be employed during the simulation. For this case the Rectangular Rule (RECT) integration method was utilized. Other integration methods which are available are listed in the CSMP III User's Manual (47). On the Timer statement one specifies the integration interval (DELT), the total duration of the simulation run (FINTIM), and simulation data output intervals (PRDEL & OUTDEL).

For the simulations conducted as part of this study the output was obtained in a graphical form in the format presented by either a line-printer or x-y plotter. An example of the output control statements used in the current simulation studies is shown below:

```
*****
***  OUTPUT CONTROL STATEMENTS  ***
*****

PRINT QA(2-11),QB(2-11)
OUTPUT TIME,CA(11),CB(11)
PAGE GROUP=(0.,2.E-3)
OUTPUT TIME,QAT,QBT
PAGE GROUP=(0.,2.E-3)
OUTPUT TIME,CA(11),CB(11)
PAGE XYPLOT,HEIGHT=5.0,WIDTH=8.0,GROUP=(0.,2.E-3)
OUTPUT TIME,QAT,QBT
PAGE XYPLOT,HEIGHT=5.0,WIDTH=8.0,GROUP=(0.,2.E-3)
```

```
*****
```

To account for the mixing of the granular activated carbon in fluidized beds a procedural solids mixing subrouting is required. The subroutine employed for the current studies is listed as follows:


```

*****
***  TO ACCOUNT FOR MIXING OF CARBON IN FLUIDIZED BEDS (EXP>1.0),  ***
***  AVERAGE SOLID-PHASE CONCENTRATIONS ARE CALCULATED AND QA'S &  ***
***  QB'S ARE REINITIALIZED AT THE AVERAGE VALUES                ***
*****

```

```

      PROCEDURE  QAT,QBT=SORBED(QA,QB)
      QATOT=0.
      QBTOT=0.
      DO 11 J=2,11
      QATOT=QATOT+QA(J)
11  QBTOT=QBTOT+QB(J)
      QAT=QATOT/10.
      QBT=QBTOT/10.
      IF (EXP.EQ.1.0) GO TO 13
      DO 12 K=2,11
      QA(K)=QAT
12  QB(K)=QBT
13  CONTINUE
      ENDPROCEDURE

```

```

*****

```

A complete listing of a typical program employed for the simulations has been attached as Appendix C.

CHAPTER VII

EXPERIMENTAL RESULTSADSORPTION EQUILIBRIA STUDIES

To obtain equilibrium parameters for use in the basic mathematical model for simulation of effluent-time profiles for columnar flow-through systems, it was necessary to obtain single-solute adsorption isotherms. These were obtained for three organic herbicides; dinitro-o-sec-butylphenol (DNOSBP), o-phenylphenol (OPP), and 2,4-dichlorophenol (2,4-DCP). The isotherms are shown in Figures VII-1, VII-2, and VII-3, respectively.

ANALYSIS OF COMPETITIVE ADSORPTION EQUILIBRIA

All columnar, continuous-flow, bisolute competitive adsorption experimental data was analyzed with respect to the steady-state condition (equilibrium) which occurred at the end of each experimental run. The steady-state values were compared with multi-solute adsorption equilibria predictions of the Langmuir competitive and semi-competitive models (previously described) and with a graphical approach termed the Graphical Irreversible Model.

The graphical model is analogous to the Semi-Competitive Langmuir Model in that it accounts for a preferentially adsorbed solute and a competitively adsorbed solute in bisolute systems. The method is based on the assumption that the maximum quantity of both solutes that can be adsorbed is equal to that quantity of the preferentially adsorbed solute that would be adsorbed if it were applied as a single-solute at the reference solution-phase concentration.

The Graphical Irreversible Model is, as might be expected, based on the assumption of irreversibility; that is, once a solute is adsorbed, it remains adsorbed and cannot be displaced by another solute. The method can best be illustrated by example. If an adsorber were initially brought to equilibrium with DNOSBP at a solution-phase concentration of 80 micromoles per liter,

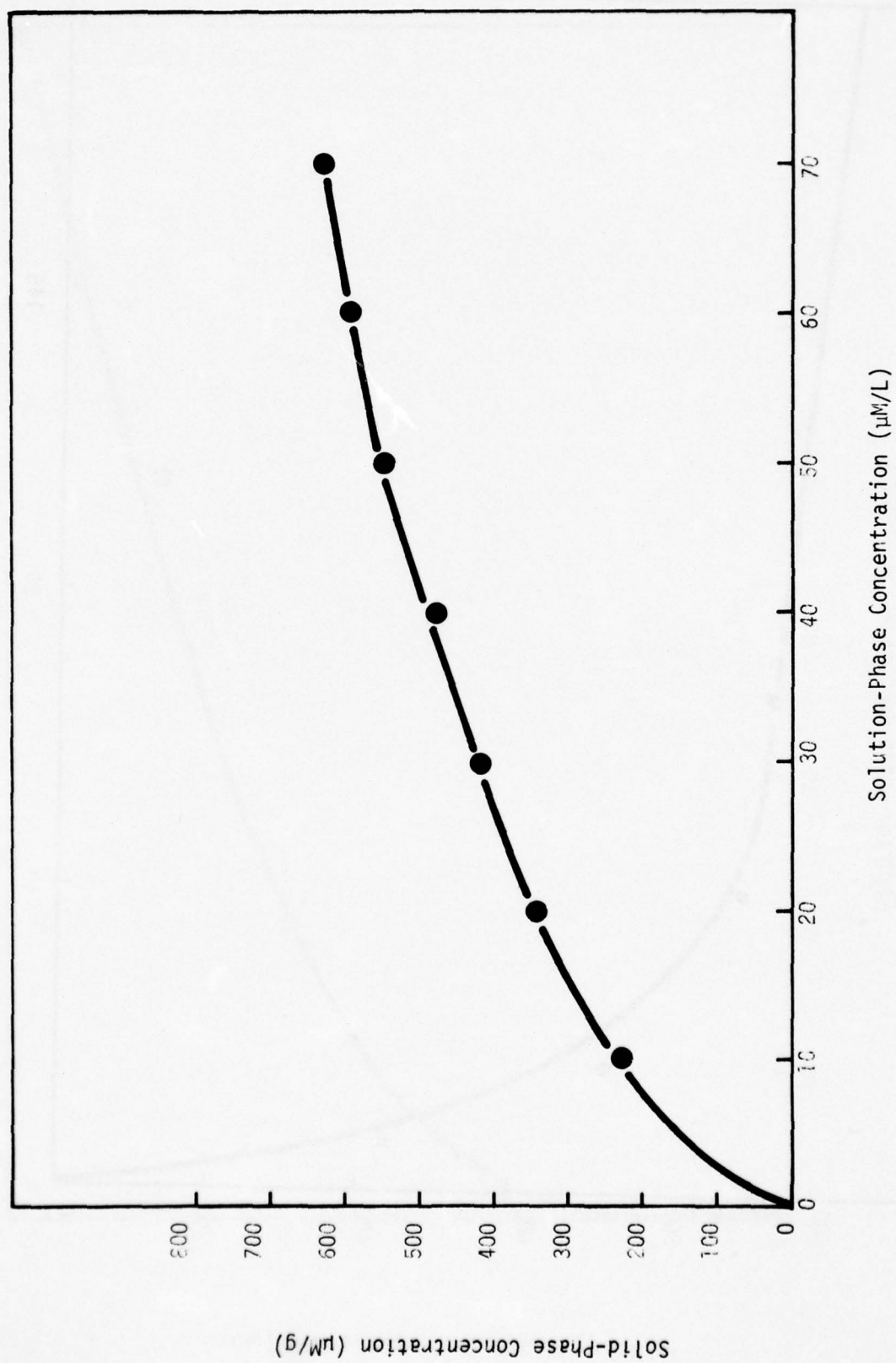


FIGURE VII-1: ADSORPTION ISOTHERM FOR DNOSEP

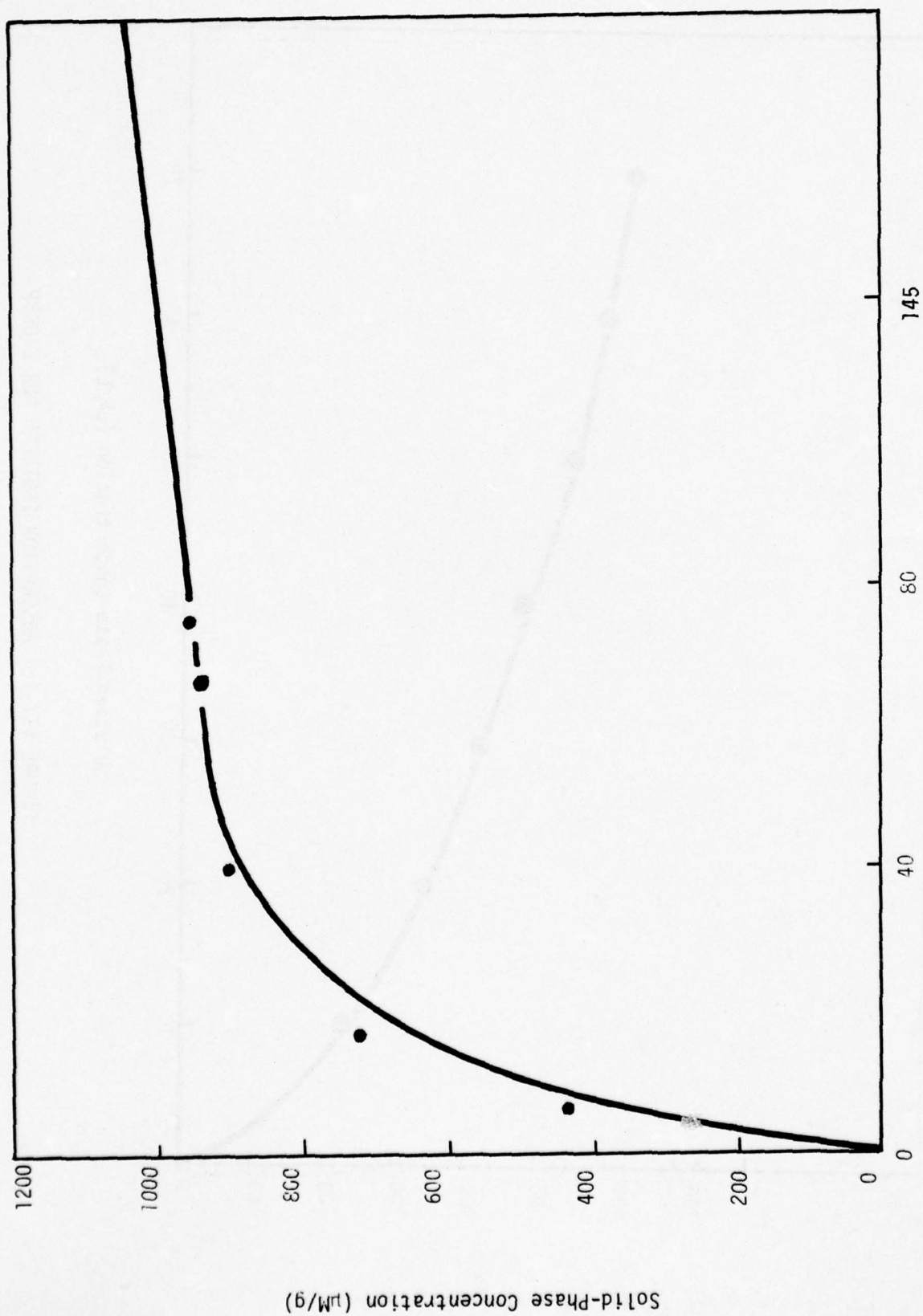
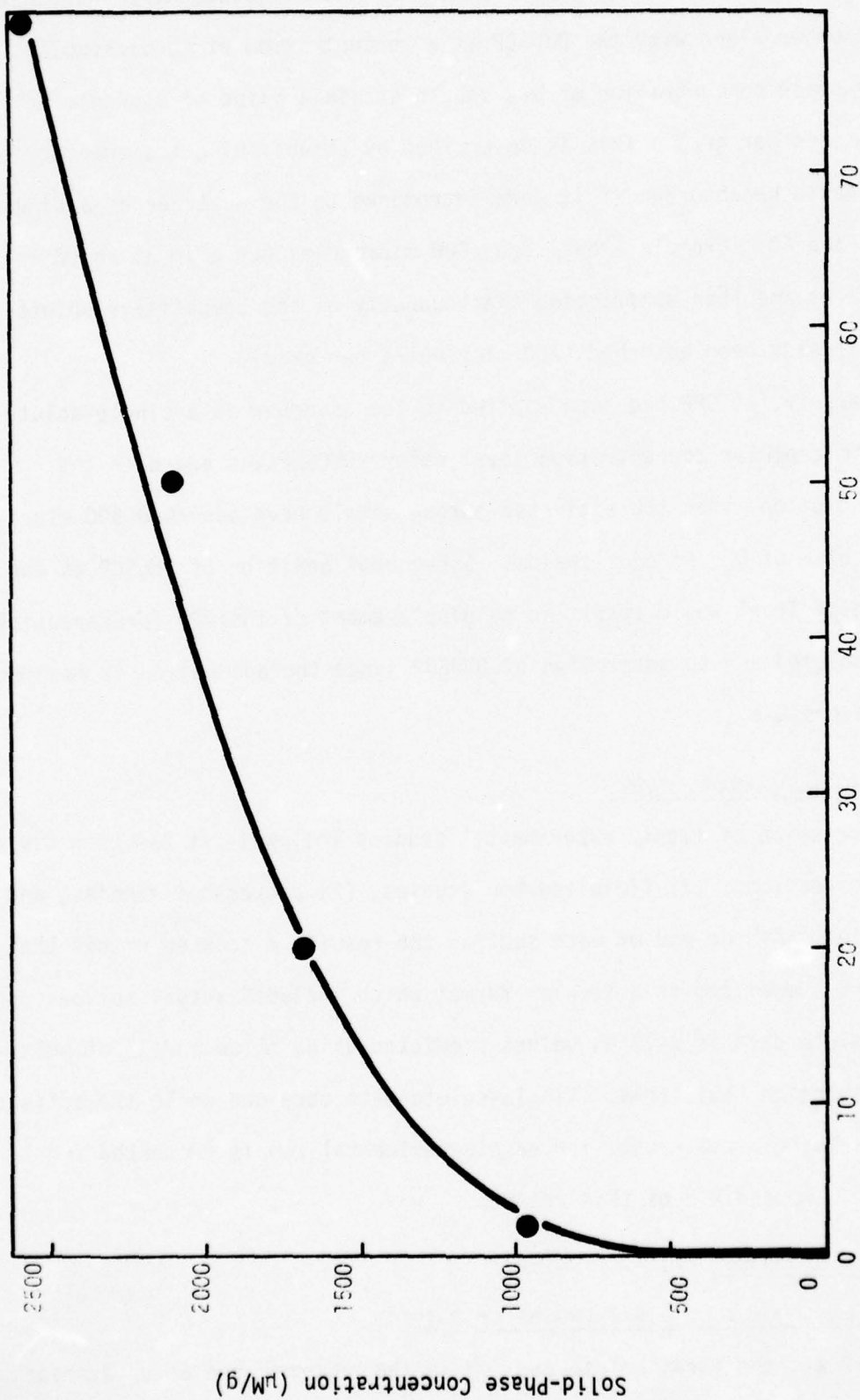
Solution-Phase Concentration ($\mu\text{M/L}$)

FIGURE VII-2: ADSORPTION ISOTHERM FOR OPP



Solution-Phase Concentration ($\mu\text{M/L}$)

FIGURE VII-3: ADSORPTION ISOTHERM FOR 2,4-DCF

then the corresponding solid-phase concentration should attain a value of 700 micromoles per gram (Figure VII-1). If OPP were subsequently introduced to the adsorber along with the DNOSBP at a concentration of 40 micromolar, then the solid-phase concentration of OPP should attain a value of approximately 200 micromoles per gram. This is determined by establishing the quantity of OPP that would be absorbed if it were introduced to the adsorber as a single-solute at the 40 micromolar level (ca. 900 micromoles per gram as noted in Figure VII-2) and then subtracting that quantity of the competitive solute that had already been adsorbed (700 micromoles per gram).

Conversely, if OPP had been applied to the adsorber as a single-solute at the 40 micromolar concentration level before DNOSBP was added to the influent solution, then the activated carbon should have adsorbed 900 micromoles per gram of OPP at equilibrium. Subsequent addition of DNOSBP at the 30 micromolar level would result in no displacement of the OPP (preferentially adsorbed solute) and no adsorption of DNOSBP since the adsorption is assumed to be irreversible.

EXPERIMENTAL COLUMNAR STUDIES

A discussion of twenty experimental studies follows. It has been divided into three sections; (1) fluidized-bed studies, (2) packed-bed studies, and (3) CSTR studies. At the end of each section the results discussed within that section are summarized in a tabular format which includes actual solid-phase bisolute data as well as values predicted using three models of multi-solute adsorption equilibria. Single-solute data obtained while the activated carbon was being presaturated for each experimental run is presented for reference in Appendix D of this report.

Fluidized-Bed Studies (2,4-DCP/DNOSBP)

... Molar Ratio of 1.0: 0.913 DNOSBP to 2,4-DCP

DNOSBP was the first solute applied to the adsorber bed at an average

influent concentration of 79.56 μM . After saturation, 2,4-DCP was added to the influent at an average concentration of 69.37 μM , while the DNOSBP feed was maintained at the same concentration. Figure VII-4 and VII-5 show the solid-phase and fluid-phase concentrations versus time, respectively, for this run. Table VII-1 summarizes actual and predicted solid-phase concentration equilibrium values. Final equilibrium values for the run were 800 and 400 micromoles per gram for DNOSBP and 2,4-DCP, respectively. It is noteworthy that while the bisolute solution was fed to the adsorber, approximately 14.9 percent of the adsorbed DNOSBP was desorbed due to the addition of the 2,4-DCP. The peak solution-phase concentration of DNOSBP noted after introduction of the bisolute solution was approximately 107 micromolar ($C/C_0 = 1.34$) and occurred 1 hour into the run. No re-adsorption of the DNOSBP was observed after the initial desorption occurred.

The Langmuir models used for prediction of final solid-phase equilibrium values gave unrealistic values as shown in Table VII-1. The graphical irreversible procedure predicted values that are smaller by 20 percent than the experimental equilibrium values obtained for DNOSBP.

... Molar Ratio of 1.0:1.53 DNOSBP to 2,4-DCP

After pre-saturation of the fluidized-bed with 79.17 μM DNOSBP, 120.85 μM 2,4-DCP was introduced to the influent. Figure VII-6 shows the solid-phase concentration profile for the run. Figure VII-7 indicates the fluid-phase concentration profile for the run. Table VII-1 summarizes actual experimental and predicted solid-phase concentration equilibrium values. The actual experimental solid phase equilibria values were 520 and 900 micromoles per gram for DNOSBP and 2,4-DCP, respectively.

After application of the 2,4-DCP it can be observed that desorption of

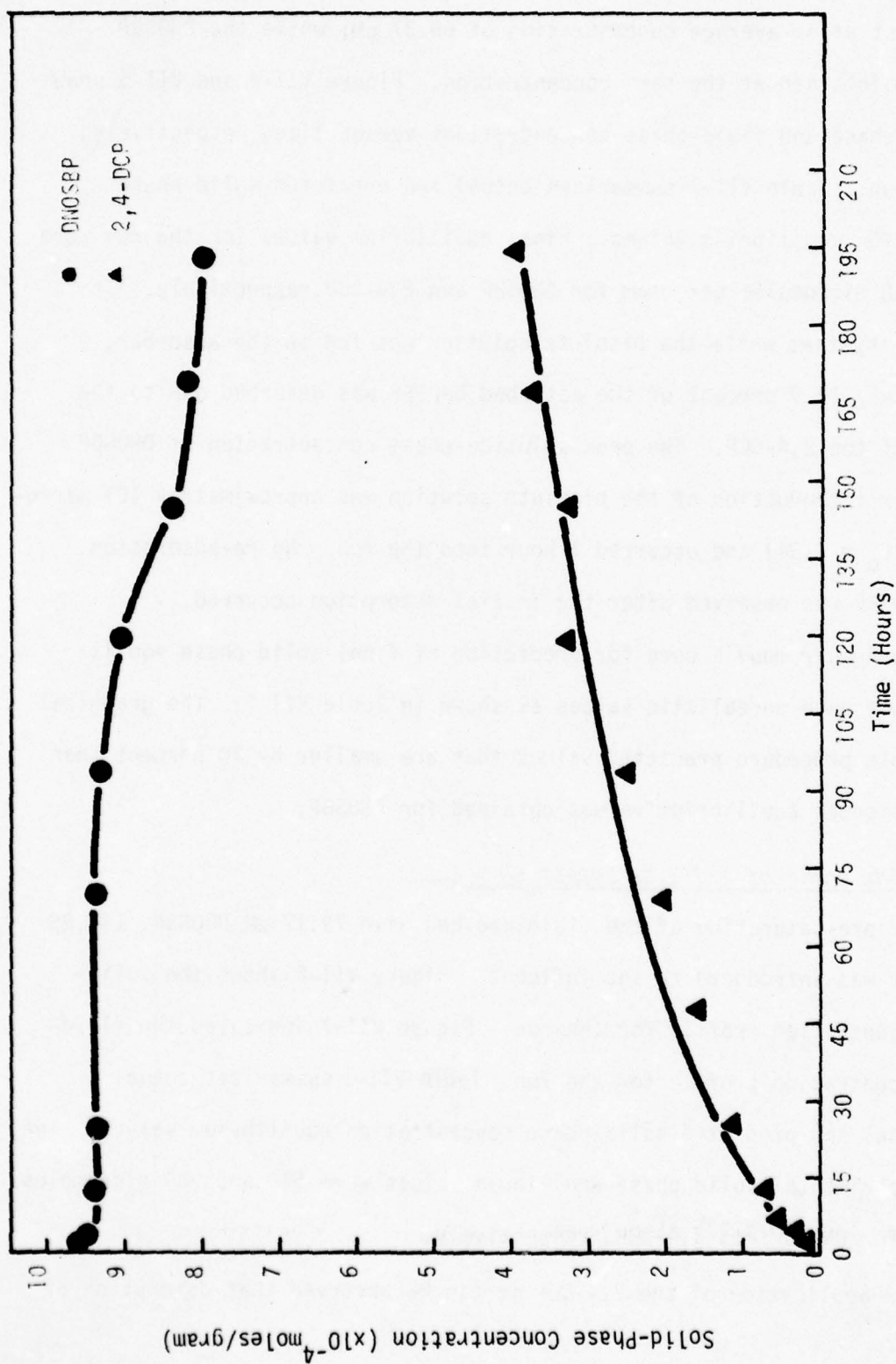


FIGURE VII-4: SOLID PHASE CONCENTRATION PROFILES FOR A FLUIDIZED-BED SYSTEM TO WHICH DNOSEBP AND 2,4-DCP WERE INTRODUCED AT A MOLAR RATIO OF 1.0:0.93 AFTER THE ACTIVATED CARBON HAD BEEN PRESATURATED WITH DNOSEBP (79.56 μ M).

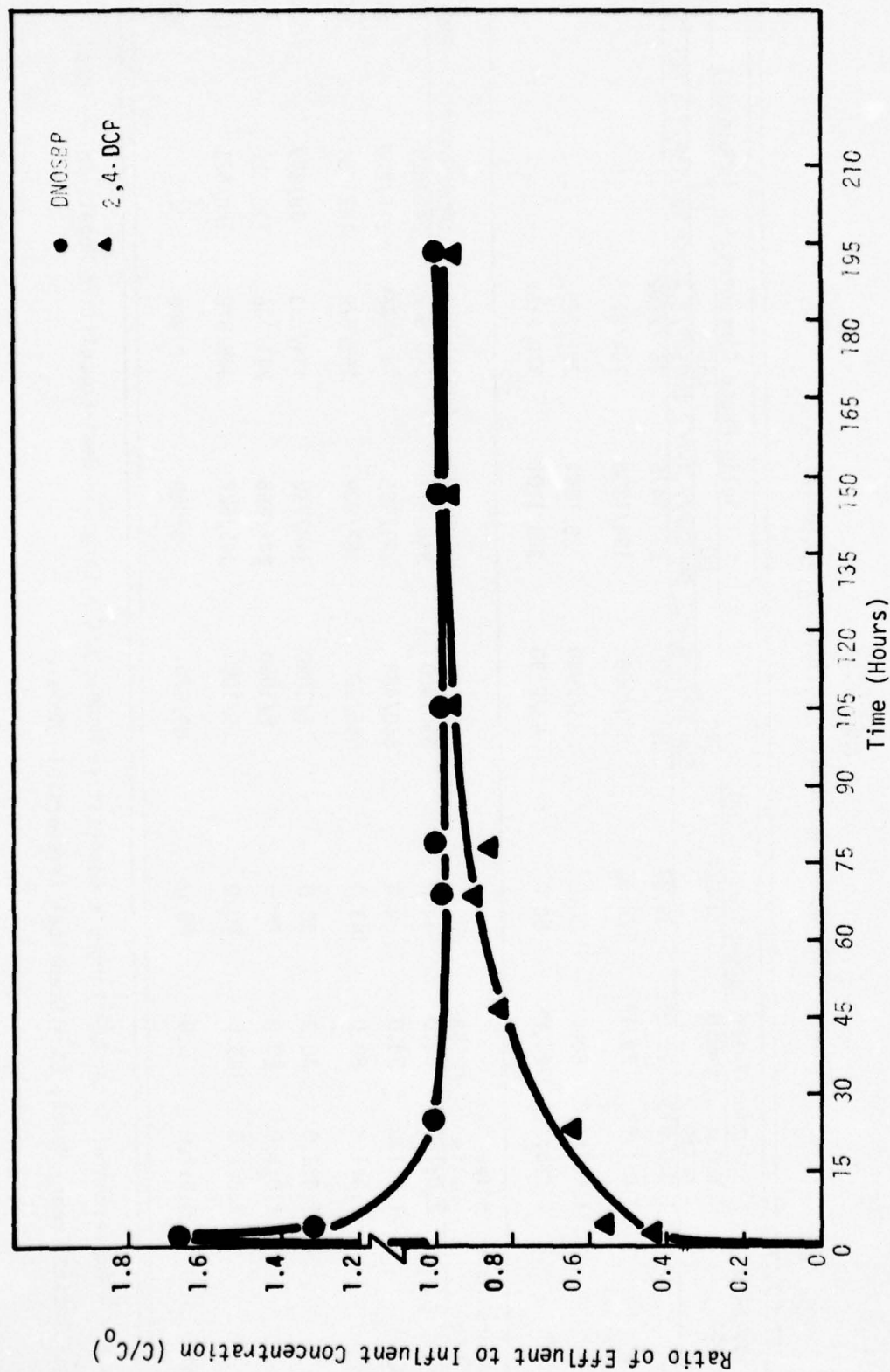


FIGURE VII-5: FLUID-PHASE CONCENTRATION PROFILES FOR A FLUIDIZED-BED SYSTEM TO WHICH DNOSBP AND 2,4-DCP WERE INTRODUCED AT A MOLAR RATIO OF 1.0:0.931 AFTER THE ACTIVATED CARBON HAD BEEN PRESATURATED WITH DNOSBP (79.56 μM).

TABLE VII-1
SUMMARIZED RESULTS: FLUIDIZED-BED STUDIES

| Presaturation Solute | Solution-Phase Concentration (μM) | | EXP | Solid-Phase Concentration ($\mu\text{Moles/g}$) | | | | |
|----------------------|--|--------|---------|---|----------|----------------|---------|----------|
| | Molar Ratio | DNOSBP | | DNOSBP/2,4-DCP | LC | DNOSBP/2,4-DCP | LSC | IST |
| DNOSBP | 1.0:0.913 | 79.56 | 800/400 | 69.37 | 261/1476 | 261/2202 | -/- | 645/1835 |
| DNOSBP | 1.0:1.53 | 79.17 | 520/900 | 120.85 | 194/1838 | 194/2415 | -/- | 645/2204 |
| 2,4-DCP | 1.007:1.0 | 80.6 | 25/2040 | 80.0 | 25/1544 | 251/2257 | -/- | 0/2600 |
| 2,4-DCP | 2.086:1.0 | 166.86 | 53/2130 | 80.0 | 370/1101 | 370/2154 | -/- | 0/2600 |
| Presaturation Solute | Solution-Phase Concentration (μM) | | EXP | Solid-Phase Concentration ($\mu\text{Moles/g}$) | | | | |
| | Molar Ratio | DNOSBP | | DNOSBP/OPP | LC | DNOSBP/2,4-DCP | LSC | IST |
| DNOSBP | 2.0:1.0 | 80.0 | 690/400 | 40.0 | 346/477 | 346/607 | 242/621 | 645/200 |
| DNOSBP | 1.0:1.0 | 80.0 | 660/488 | 80.0 | 241/665 | 241/766 | 215/720 | 645/270 |
| DNOSBP | 1.0:1.8 | 80.0 | 545/500 | 145.0 | 162/809 | 162/879 | 127/851 | 645/320 |
| OPP | 1.0:2.0 | 40.0 | 6/1050 | 80.0 | 144/792 | 144/853 | 79/879 | 0/1050 |
| OPP | 1.0:1.0 | 80.0 | 8/1050 | 80.0 | 241/665 | 241/766 | 215/720 | 0/1050 |
| OPP | 1.8:1.0 | 145.0 | 15/1050 | 80.0 | 346/527 | 346/672 | 248/621 | 0/1050 |
| DNOSBP | 0:0:1.0 | 0.0 | 500/570 | 80.0 | 0/980 | 0/980 | -/- | 645/270 |

KEY: EXP = Experimental Data; LC = Langmuir Competitive Model; LSC = Langmuir Semi-Competitive Model; IST = Ideal Solution Theory Model; GI = Graphical Irreversible Model.

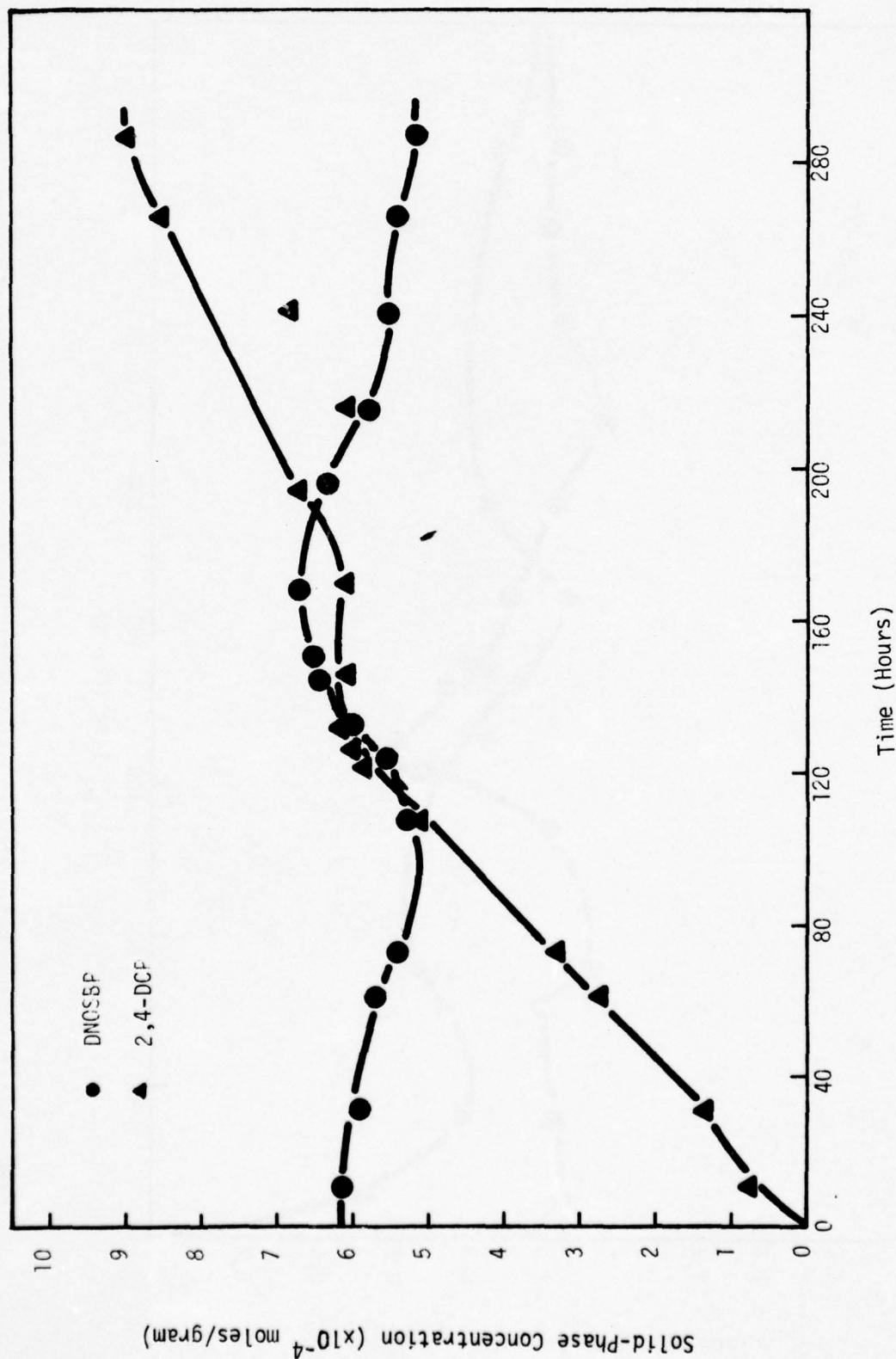


FIGURE VII-6: SOLID-PHASE CONCENTRATION PROFILES FOR A FLUIDIZED-BED SYSTEM TO WHICH DNOSBP AND 2,4-DCP WERE INTRODUCED AT A MOLAR RATIO OF 1.0:1.53 AFTER THE ACTIVATED CARBON HAD BEEN PRESATURATED WITH DNOSBP (80.0 μ M).

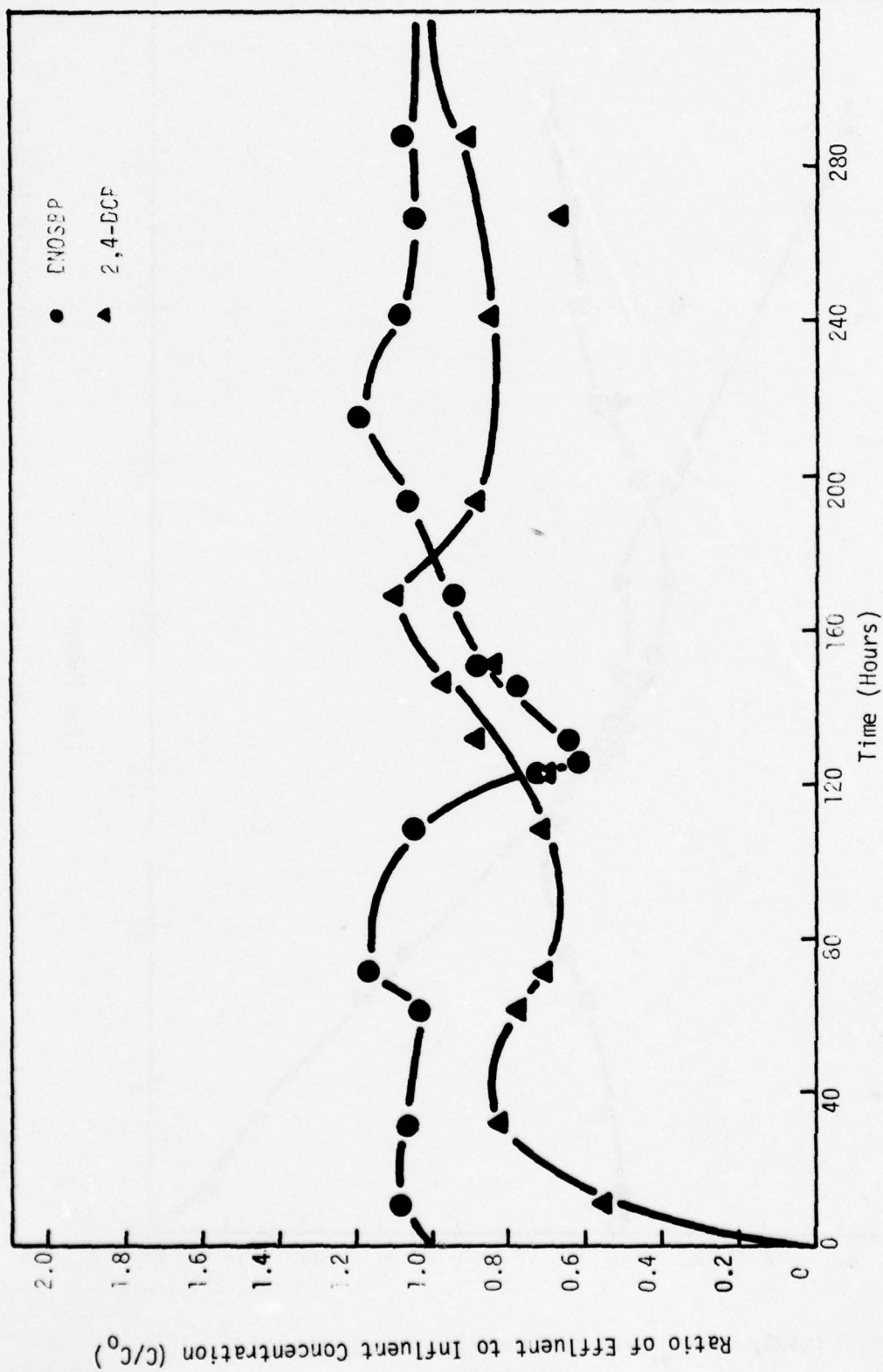


FIGURE VII-7: FLUID-PHASE CONCENTRATION PROFILES FOR A FLUIDIZED-BED SYSTEM TO WHICH DNOSEP AND 2,4-DCP WERE INTRODUCED AT A MOLAR RATIO OF 1.0:1.53 AFTER THE ACTIVATED CARBON HAD BEEN PRESATURATED WITH DNOSEP ($80.0 \mu\text{M}$).

DNOSBP began as adsorption of 2,4-DCP occurred. Desorption of DNOSBP was equal to approximately 19.2 percent of the single solute saturation value. The peak solution-phase concentration of DNOSBP which occurred was 96 micromolar ($C/C_0 = 1.2$) at a bisolute molar ratio of 1.0:1.53 DNOSBP to 2,4-DCP. This peak occurred at approximately 80 hours into the run. Moreover, during the run adsorption and desorption was observed for DNOSBP although desorption predominated at final equilibrium. At 160 hours after introduction of the bisolute mixture, DNOSBP adsorbed to a level 8 percent greater than the presaturation level. The final solid-phase equilibrium value, however, showed a net desorption at steady-state.

As in the previous case the competitive and semi-competitive Langmuir models predicted values that were 100 percent greater than the actual experimental solid-phase equilibrium values obtained for DNOSBP. The graphical irreversible multi-solute procedure over-estimated the actual experimental solid-phase equilibrium values by 24 percent. The Langmuir and graphical predictions for 2,4-DCP did not agree with the actual values.

... Molar Ratio of 1.0:1.007 2,4-DCP to DNOSBP

In this run the fluidized-bed contactor was first equilibrated with 80 μM 2,4-DCP. Thereafter, 80.6 μM DNOSBP was added as a step input to the column. Figures VII-8 and VII-9 shows the solid-phase and fluid-phase concentration profiles, respectively, while Table VII-1 gives a summary of the actual and predicted solid-phase equilibrium values. Final actual solid-phase equilibrium values were 25 and 2040 micromoles per gram for DNOSBP and 2,4-DCP, respectively.

The solid-phase concentration profile for this run shows that no desorption of 2,4-DCP occurred after application of DNOSBP. This may partly be explained by the single-solute isotherms which show 2,4-DCP to adsorb much more strongly than DNOSBP. The competitive and semi-competitive Langmuir models in this case over-estimate the actual solid-phase equilibrium value for

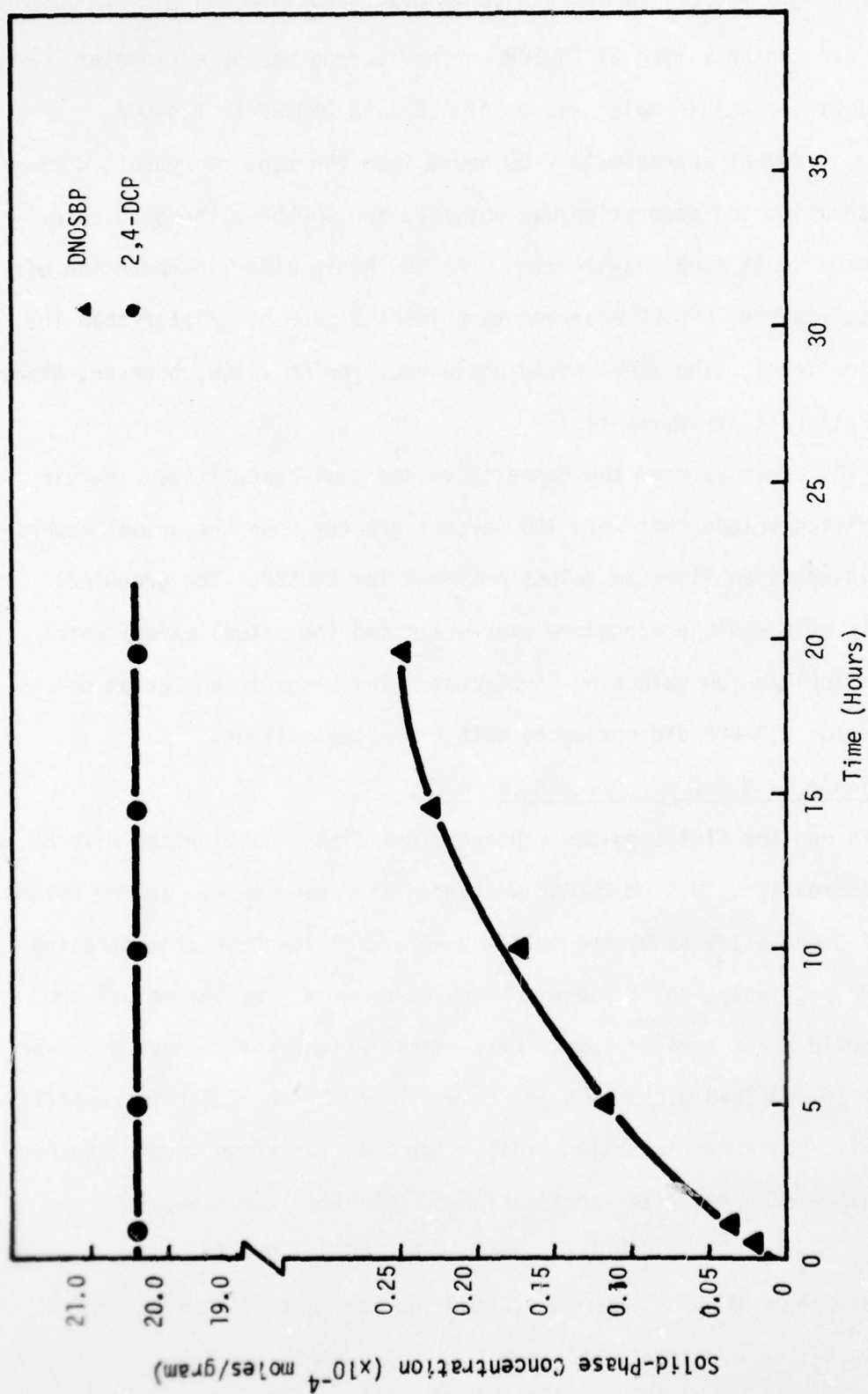


FIGURE VII-8: SOLID-PHASE CONCENTRATION PROFILES FOR A FLUIDIZED-BED SYSTEM TO WHICH DNOSBP AND 2,4-DCP WERE INTRODUCED AT A MOLAR RATIO OF 1.007:1.0 AFTER THE ACTIVATED CARBON HAD BEEN PRESATURATED WITH 2,4-DCP (80.0 μ M).

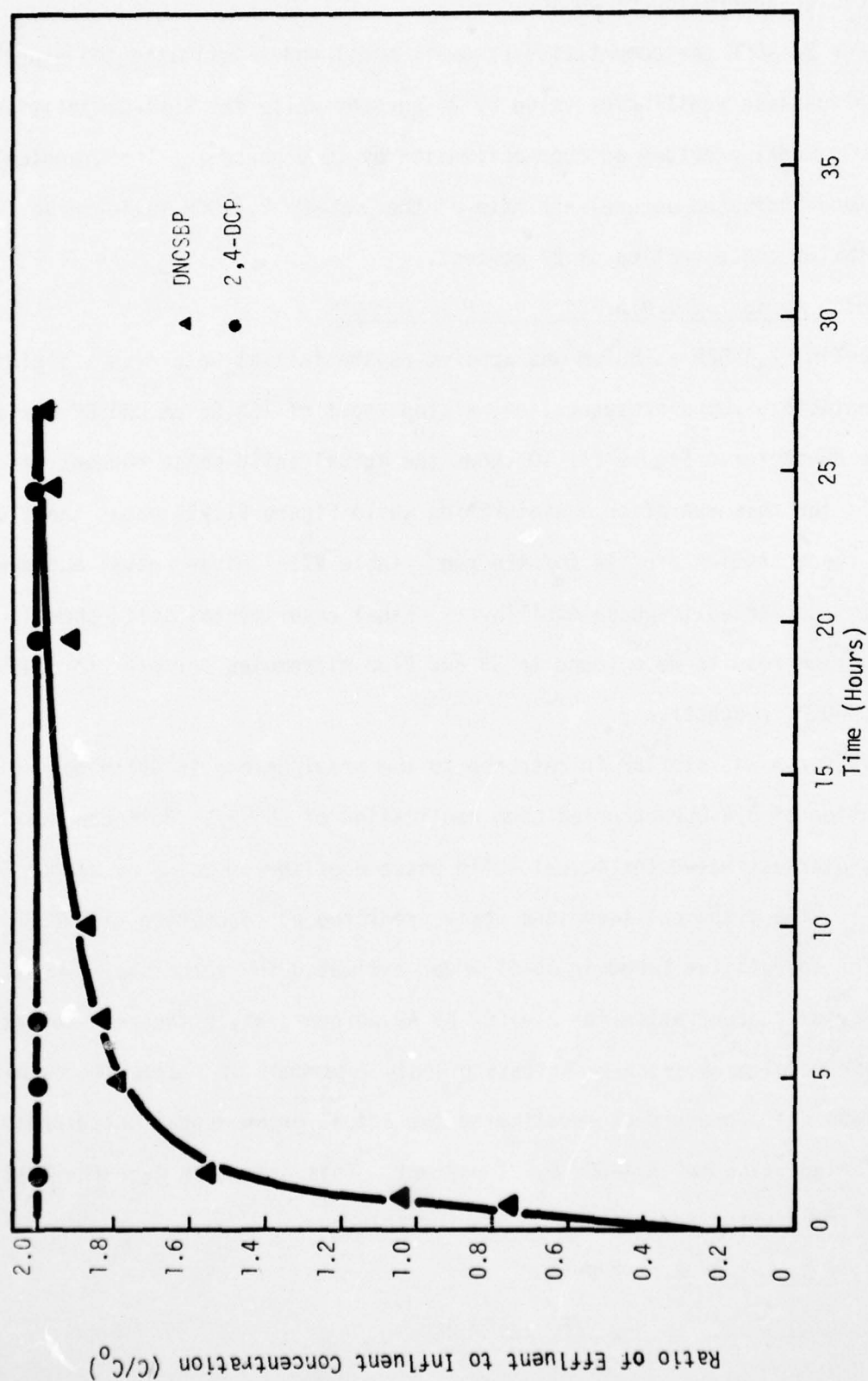


FIGURE VII-9: FLUID-PHASE CONCENTRATION PROFILES FOR A FLUIDIZED-BED SYSTEM TO WHICH DNOSBP AND 2,4-DCP WERE INTRODUCED AT A MOLAR RATIO OF 1.007:1.0 AFTER THE ACTIVATED CARBON HAD BEEN PRESATURATED WITH 2,4-DCP (80.0 μ M).

the adsorption of DNOSBP by a factor of ten while the graphical procedure predicts no adsorption of DNOSBP.

For 2,4-DCP the competitive Langmuir model under-estimated the experimental solid-phase equilibrium value by 24 percent while the Semi-Competitive Langmuir model provided an over-estimation by 10.6 percent. The graphical technique indicated an over-estimate of the actual 2,4-DCP solid-phase equilibrium concentration of 27 percent.

... Molar Ratio of 1.0:2.086 2,4-DCP to DNOSBP

Again, 2,4-DCP at 80 μM was applied as the initial solute to a fluidized-bed contactor. Upon presaturation, a step input of 166.86 μM DNOSBP was applied to the contactor. Figure VII-10 shows the actual solid-phase concentration profile for this run after presaturation while Figure VII-11 shows the fluid-phase concentration profile for the run. Table VII-1 gives actual and predicted information for solid-phase equilibria. Final experimental solid-phase equilibrium results were found to 53 and 2130 micromoles per gram for DNOSBP and 2,4-DCP, respectively.

This run was similar in response to the previous one in which no desorption of 2,4-DCP occurred upon application of DNOSBP. Both Langmuir models over-estimated the actual solid-phase equilibrium value by almost 600 percent. The graphical technique again predicted no adsorption of DNOSBP.

The competitive Langmuir model under-estimated the actual solid-phase equilibrium concentration for 2,4-DCP by 49 percent, while the semi-competitive Langmuir model gave an over-estimate of only 1 percent of the actual value. The graphical procedure over-estimated the actual experimental solid-phase equilibrium value for 2,4-DCP by 22 percent. This procedure gave the best overall prediction for both compounds for this run.

Fluidized-Bed Studies (OPP/DNOSBP)

... Molar Ratio of 1.0:2.0 OPP to DNOSBP

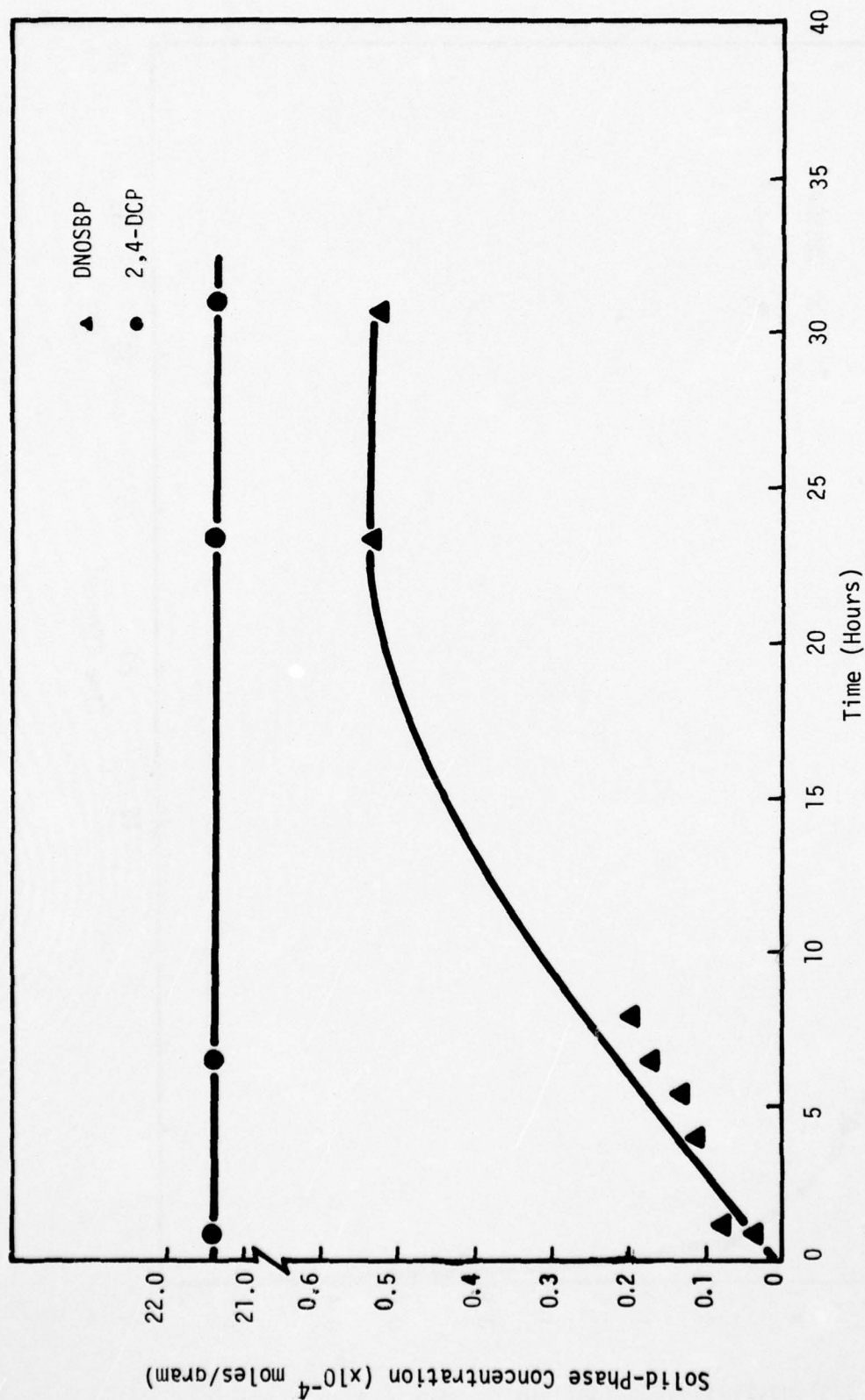


FIGURE VII-10: SOLID-PHASE CONCENTRATION PROFILES FOR A FLUIDIZED-BED SYSTEM TO WHICH DNOSBP AND 2,4-DCP WERE INTRODUCED AT A MOLAR RATIO OF 2.086:1.0 AFTER THE ACTIVATED CARBON HAD BEEN PRESATURATED WITH 2,4-DCP (80.0 μ M).

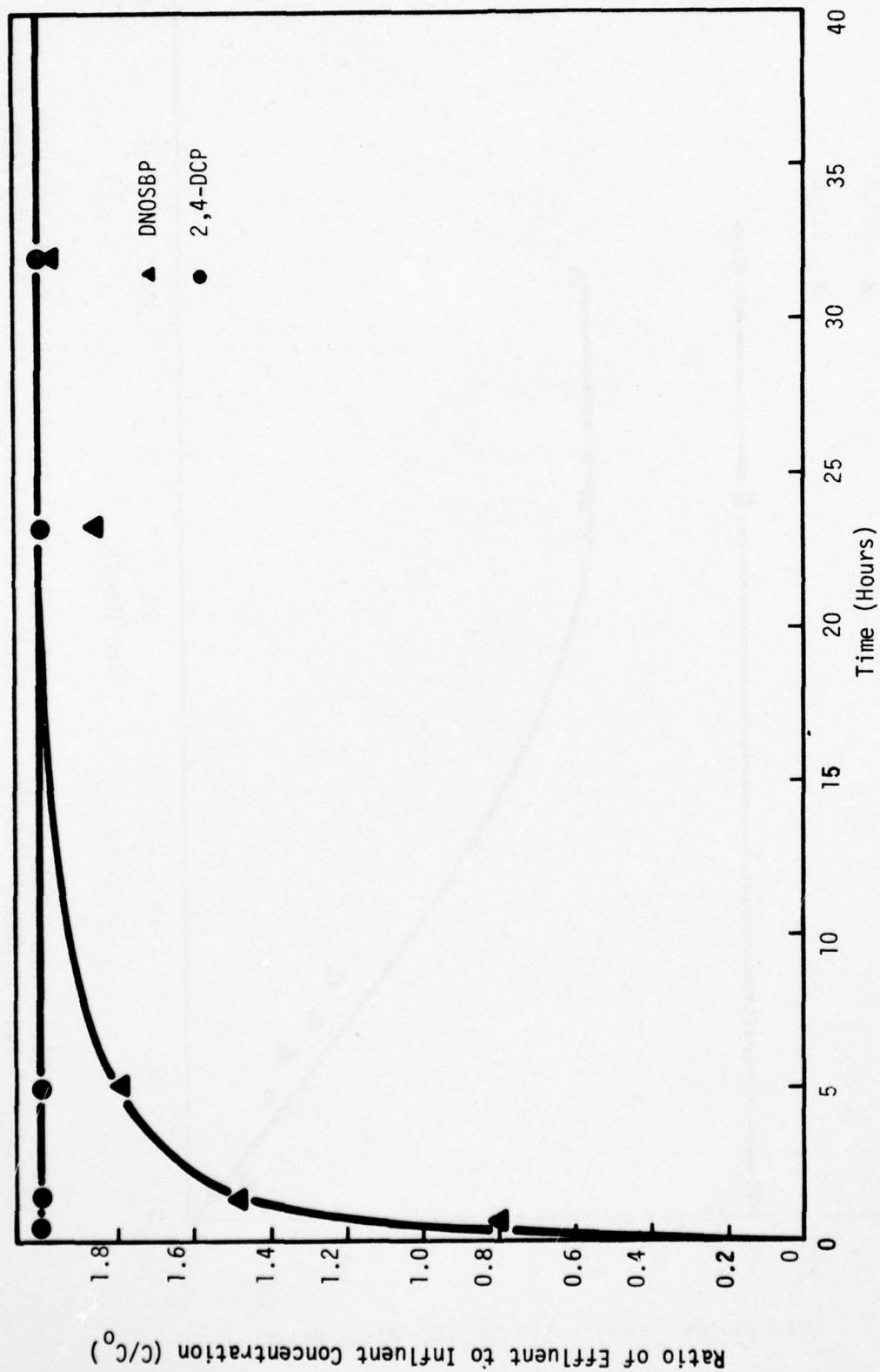


FIGURE VII-11: FLUID-PHASE CONCENTRATION PROFILES FOR A FLUIDIZED-BED SYSTEM TO WHICH DNOSBP AND 2,4-DCP WERE INTRODUCED AT A MOLAR RATIO OF 2.086:1.0 AFTER THE ACTIVATED CARBON HAD BEEN PRESATURATED WITH 2,4-DCP (80 μ M).

After the bed of activated carbon was saturated with DNOSBP at the 80 micromolar solution-phase concentration level, the influent concentration of OPP was stepped up from 0 to 40 micromolar while the DNOSBP concentration was maintained constant. Figure VII-12 shows the solid-phase concentration of OPP and DNOSBP versus time while Figure VII-13 gives the corresponding solution-phase concentrations. Table VII-1 contains a summary of the experimental and theoretical equilibrium values. Steady-state (equilibrium) adsorption values were observed to be 690 and 400 micromoles per gram for DNOSBP and OPP, respectively. It should be noted only a small amount of DNOSBP, less than 2 percent, was desorbed at steady-state. However, as the solid-phase concentration versus time profile for DNOSBP shows, a greater quantity of DNOSBP (about 6.5%) had actually desorbed during the run but was subsequently re-adsorbed. The C/C_0 versus time plot, Figure VII-13, clearly shows this phenomenon. This desorption/re-adsorption phenomenon was also observed in a similar run in which the OPP concentration was 80 micromolar.

The competitive Langmuir model most closely predicted the final OPP solid-phase concentration. The predicted value was only 19 percent above the experimental value. Both the semi-competitive Langmuir and the ideal solution theory over-estimated the adsorption capacity by 51 and 55 percent, respectively. The graphical solution method under-estimated the capacity by the same amount (50 percent).

As expected, the multi-solute models were conservative in predicting equilibrium values for DNOSBP. The competitive Langmuir and semi-competitive Langmuir models were in error by 50 percent. The ideal solution theory model gave an even more conservative value and was in error by 65 percent.

... Molar Ratio of 1.0:1.0 OPP to DNOSBP

After equilibration with 80 micromolar DNOSBP, a 80 micromolar OPP/80 micromolar DNOSBP solution was introduced to the system. Figures VII-14 and VII-15 show the solid-phase and solution-phase profiles for OPP and DNOSBP,

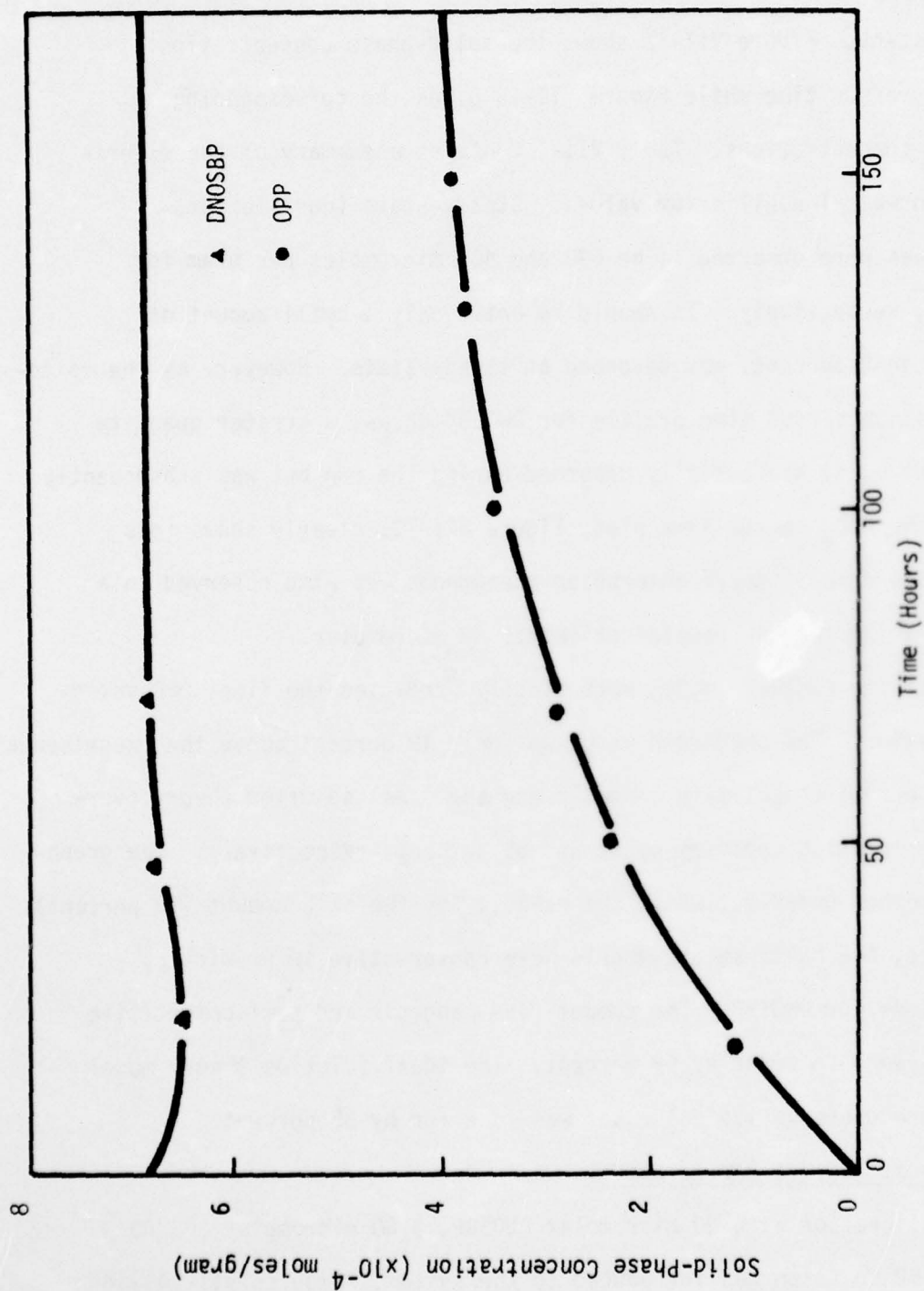


FIGURE VII-12: SOLID-PHASE CONCENTRATION PROFILES FOR A FLUIDIZED-BED SYSTEM TO WHICH DNOSBP AND OPP WERE INTRODUCED AT A MOLAR RATIO OF 2.0:1.0 AFTER THE ACTIVATED CARBON HAD BEEN PRESATURATED WITH DNOSBP (80.0 μ M).

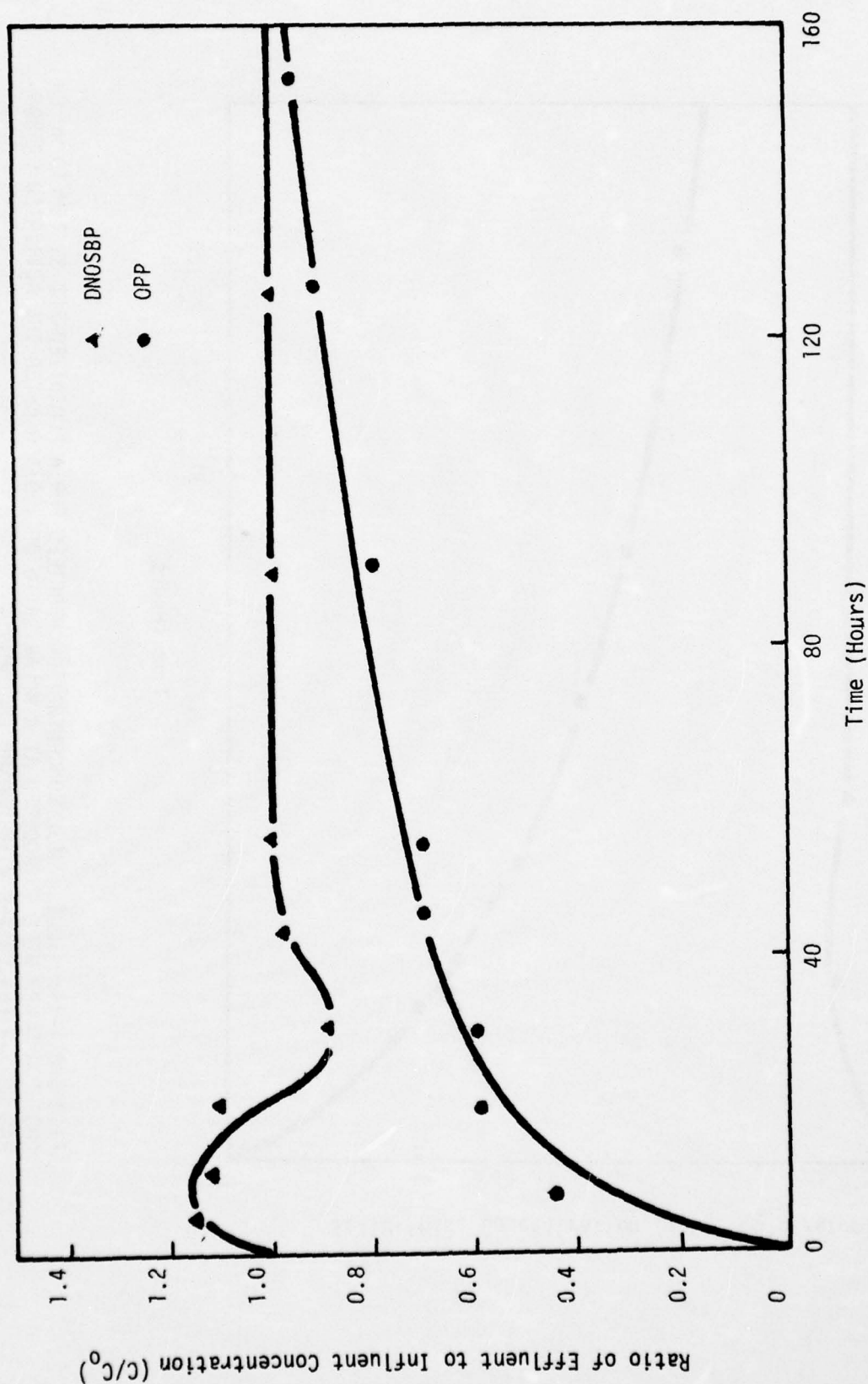


FIGURE VII-13: FLUID-PHASE CONCENTRATION PROFILES FOR A FLUIDIZED-BED SYSTEM TO WHICH DNOSBP AND OPP WERE INTRODUCED AT A MOLAR RATIO OF 2.0:1.0 AFTER THE ACTIVATED CARBON HAD BEEN PRESATURATED WITH DNOSBP (80 μ M).

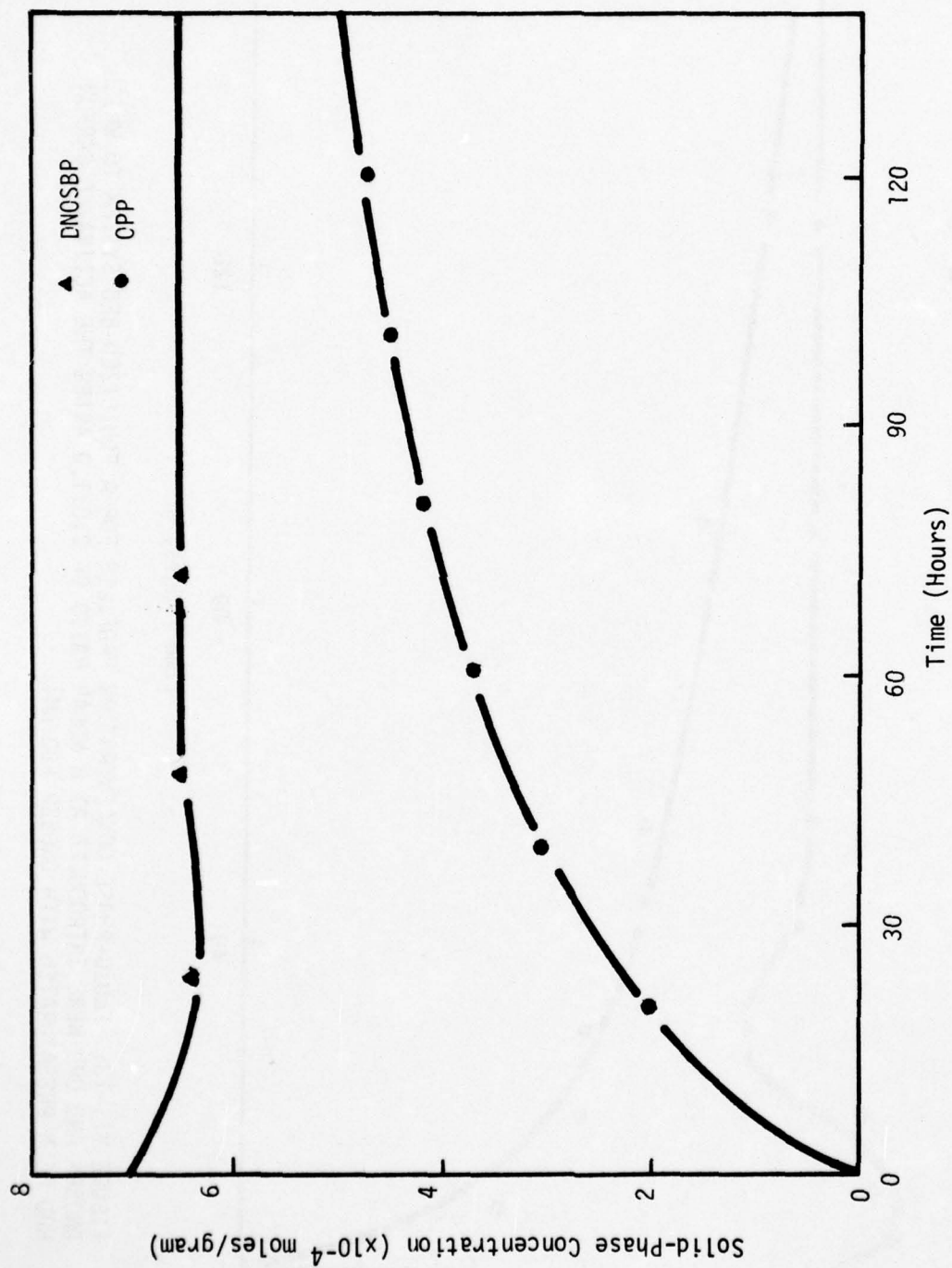


FIGURE VII-14: SOLID-PHASE CONCENTRATION PROFILES FOR A FLUIDIZED-BED SYSTEM TO WHICH DNOSBP AND OPP WERE INTRODUCED AT A MOLAR RATIO OF 1.0:1.0 AFTER THE ACTIVATED CARBON HAD BEEN PRESATURATED WITH DNOSBP (80 μ M).

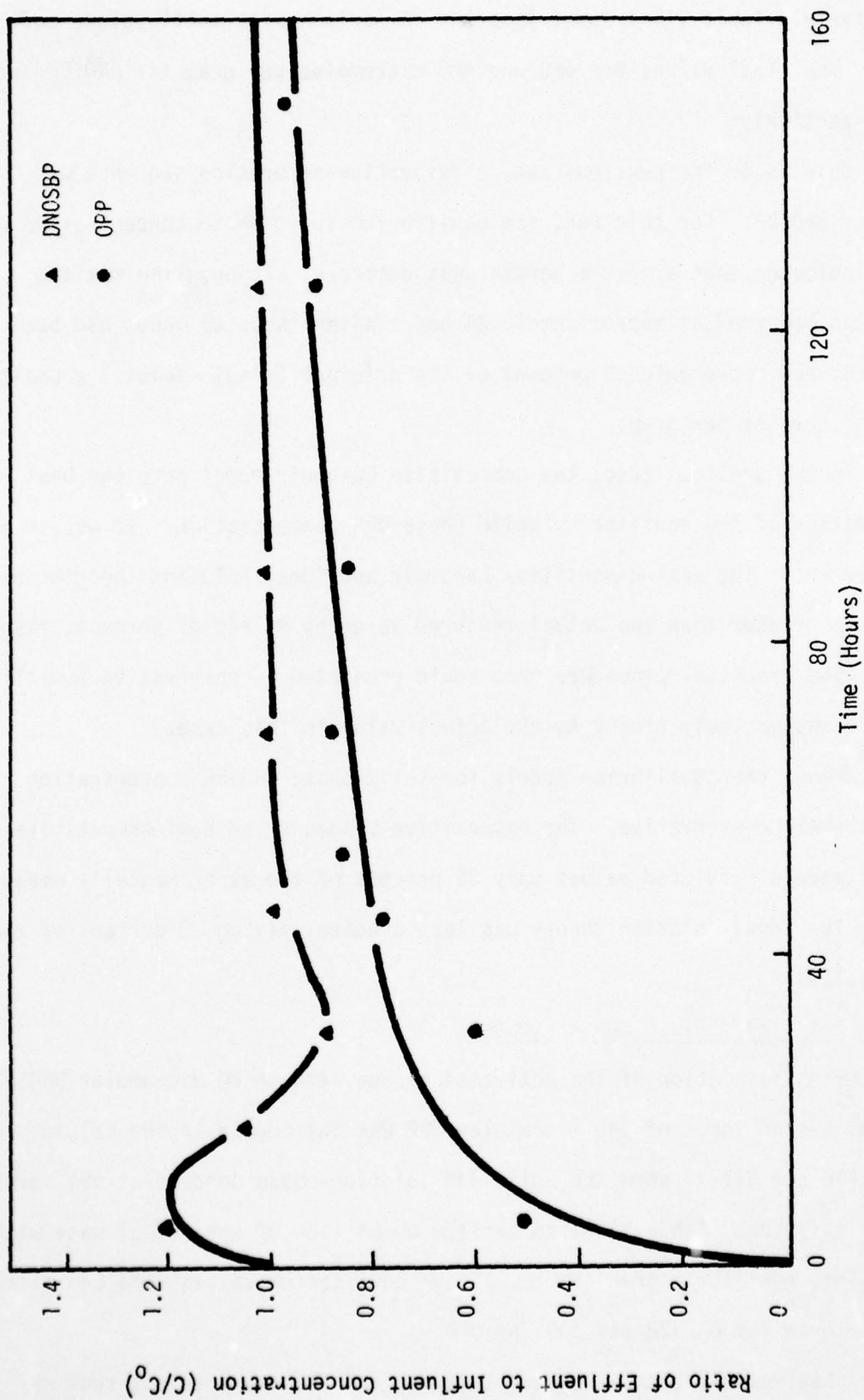


FIGURE VII-15: FLUID-PHASE CONCENTRATION PROFILES FOR A FLUIDIZED-BED SYSTEM TO WHICH DNOSBP AND OPP WERE INTRODUCED AT A MOLAR RATIO OF 1.0:1.0 AFTER THE ACTIVATED CARBON HAD BEEN PRESATURATED WITH DNOSBP (80.0 μ M)

respectively. Table VII-1 summarizes the comparison with multi-solute equilibria models. The final values are 660 and 488 micromoles per gram for DNOSBP and OPP, respectively.

In this as in the previous run, a desorption-adsorption sequence was noted for DNOSBP. For this run, the equilibrium solid-phase concentration of DNOSBP indicated that almost 6 percent was desorbed, although the maximum desorption occurred at approximately 24 hours after the step input had been initiated, and represented 9 percent of the original (single-solute) capacity of 700 micromoles per gram.

As in the previous case, the competitive Langmuir model gave the best approximation of the equilibrium solid-phase OPP concentration. It was in error by 34 percent. The semi-competitive Langmuir and ideal solution theories predicted values greater than the actual measured value by 57 and 47 percent, respectively. The graphical procedure once again predicted a conservative (small) value but was markedly closer to the actual value in this case.

As above, the equilibrium models for solid-phase DNOSBP concentration were extremely conservative. The competitive Langmuir and semi-competitive Langmuir models predicted values only 36 percent of the experimentally measured values. The ideal solution theory was less precise, giving 32 percent of the actual value.

...Molar Ratio of 1.8:1.0 OPP to DNOSBP

After equilibration of the activated carbon with an 80 micromolar DNOSBP solution, a step input of 145 micromolar OPP was introduced to the column. Figures VII-16 and VII-17 show the solid and solution-phase concentrations versus time for this run. Table VII-1 summarized comparison of the actual data with multi-solute equilibria predictions. Final equilibrium values were 545 micromoles per gram for DNOSBP and 500 for OPP.

One observed difference between this run and the two previous runs was

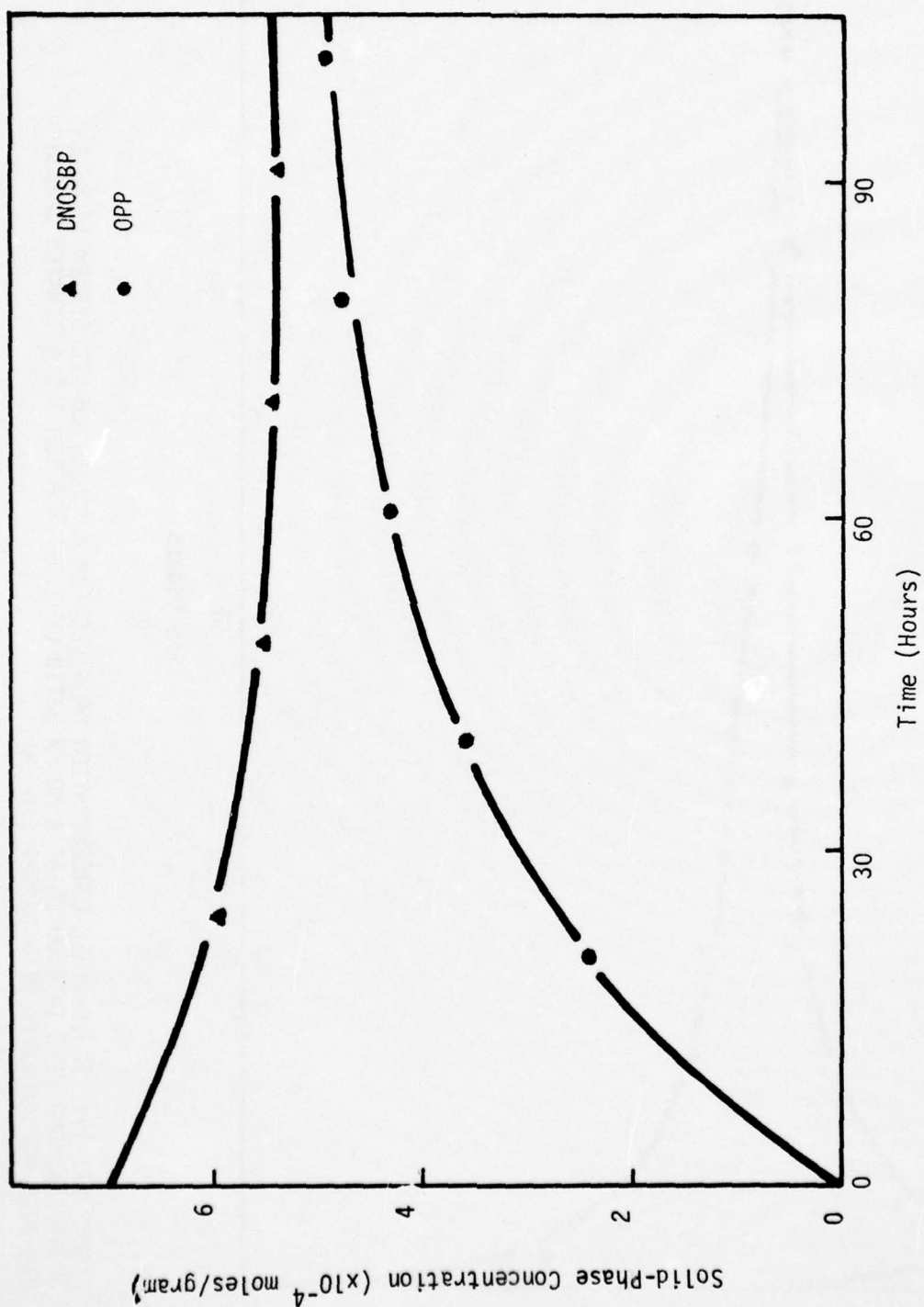


FIGURE VII-16: SOLID-PHASE CONCENTRATION PROFILES FOR A FLUIDIZED-BED SYSTEM TO WHICH DNOSBP AND OPP WERE INTRODUCED AT A MOLAR RATIO OF 1.0:1.8 AFTER THE ACTIVATED CARBON HAD BEEN PRESATURATED WITH DNOSBP (80 μ M).

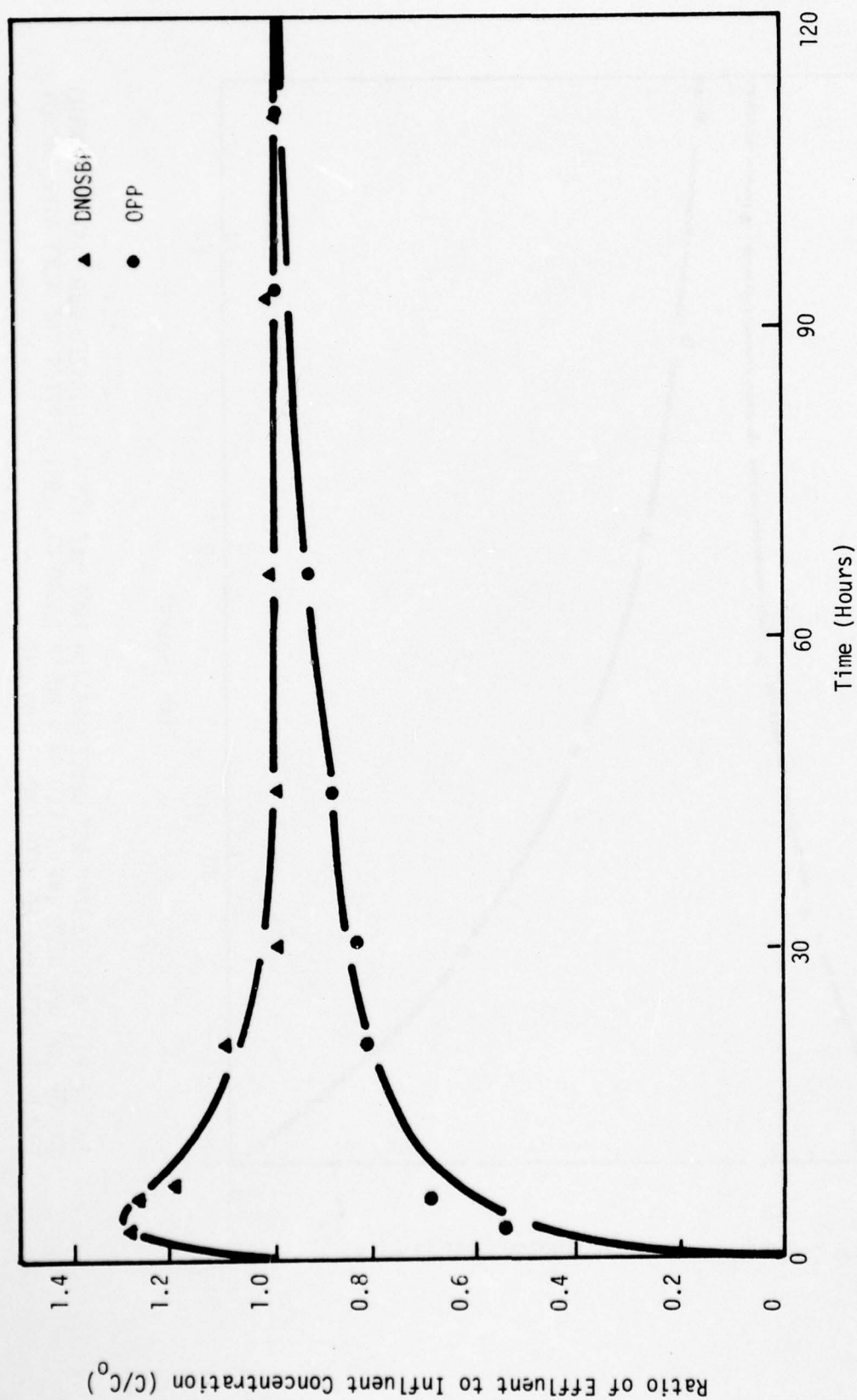


FIGURE VII-17: FLUID-PHASE CONCENTRATION PROFILES FOR A FLUIDIZED-BED SYSTEM TO WHICH DNOSBP AND OPP WERE INTRODUCED AT A MOLAR RATIO OF 1.0:1.8 AFTER THE ACTIVATED CARBON HAD BEEN PRESATURATED WITH DNOSBP (80 μ M).

that no adsorption of DNOSBP occurred after the initial desorption. Also, the amount of DNOSBP desorbed was substantially higher than for the two previous cases. Approximately 155 micromoles per gram of DNOSBP were desorbed; that is, over 22 percent of the solid-phase DNOSBP concentration was displaced by the OPP.

Another difference noted between this run and the others was the period of time required to attain steady-state. The higher concentration of OPP in the influent of this run provided a larger driving force which, in turn, resulted in a more rapid approach to steady-state conditions. This run required approximately 100 hours to reach equilibrium while the three previous runs required 140 to 260 hours.

Following the pattern of the three runs described previously, the competitive Langmuir, semi-competitive Langmuir, and ideal solution theory predicted values for solid-phase OPP concentrations in excess of those experimentally observed. Also, the graphical approach gave values less than those obtained experimentally.

Predicted equilibrium values for DNOSBP again were not accurate. Competitive Langmuir and semi-competitive Langmuir predictions were in error by 70 percent while the ideal solution theory prediction was in error by 77 percent.

...Molar Ratios of 1.0:2.0, 1.0:1.0, and 1.8:1.0 DNOSBP to OPP

Three runs in which OPP was applied as a single-solute at a concentration of 80 micromolar were conducted. After presaturation, DNOSBP was applied at concentrations of 40, 80, and 145 micromolar in addition to maintaining the OPP influent concentration at 80 micromolar. The solid and solution-phase concentration versus time profiles for the 1.0:1.0 molar ratio case are shown in Figure VII-18 and VII-19. Profiles for the other molar ratio cases are essentially identical. Table VII-1 summarizes the experimental results and the values predicted by the multi-solute equilibrium models. The graphical solution

AD-A031 179

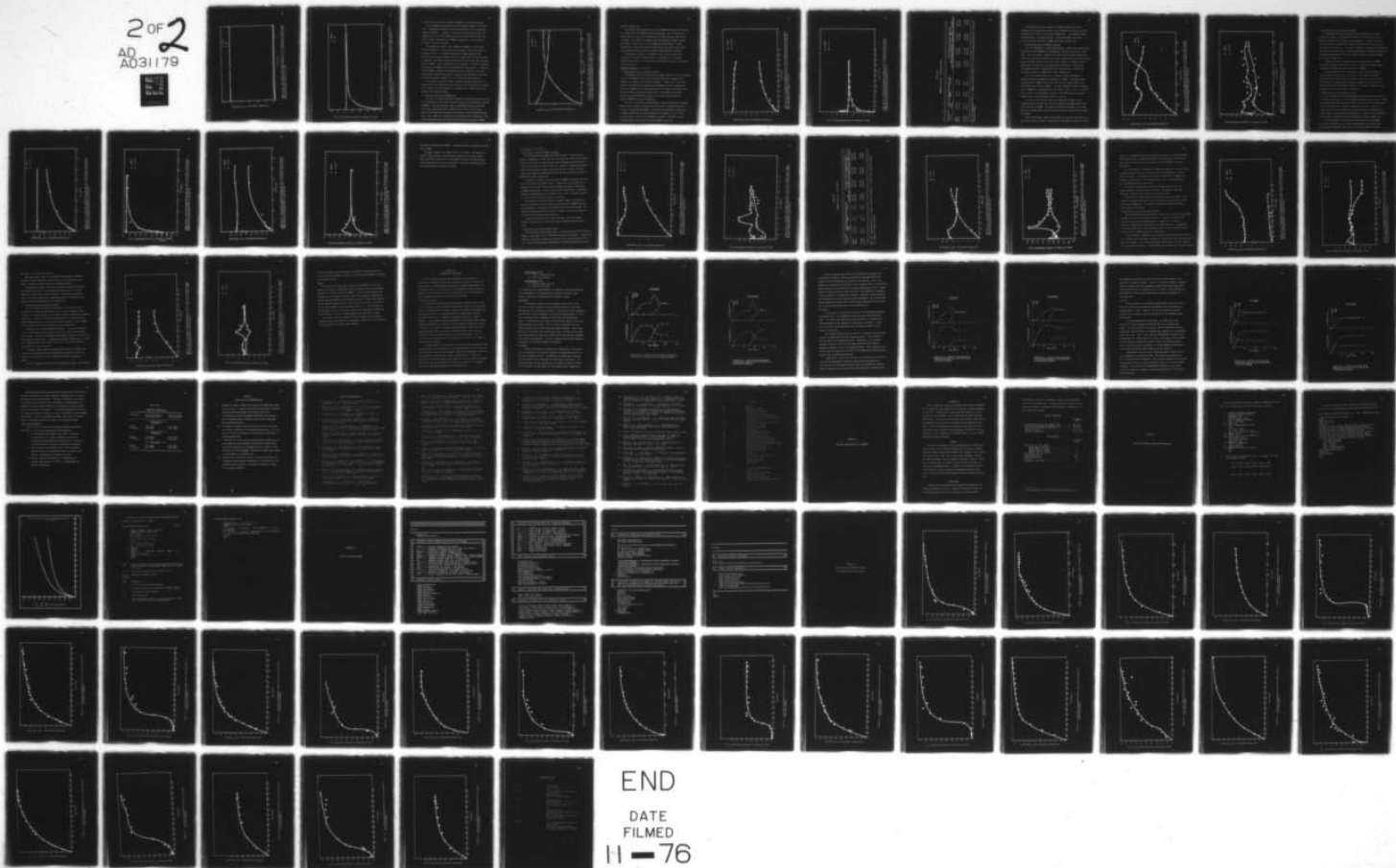
CLEMSON UNIV S C DEPT OF ENVIRONMENTAL SYSTEMS ENGI--ETC F/G 13/2
MATHEMATICAL MODELING OF HETEROGENEOUS SORPTION IN CONTINUOUS C--ETC(U)
APR 76 T M KEINATH, H KARESH, S LOWRY

DADA17-73-C-3154

NL

UNCLASSIFIED

2 OF 2
AD
A031179



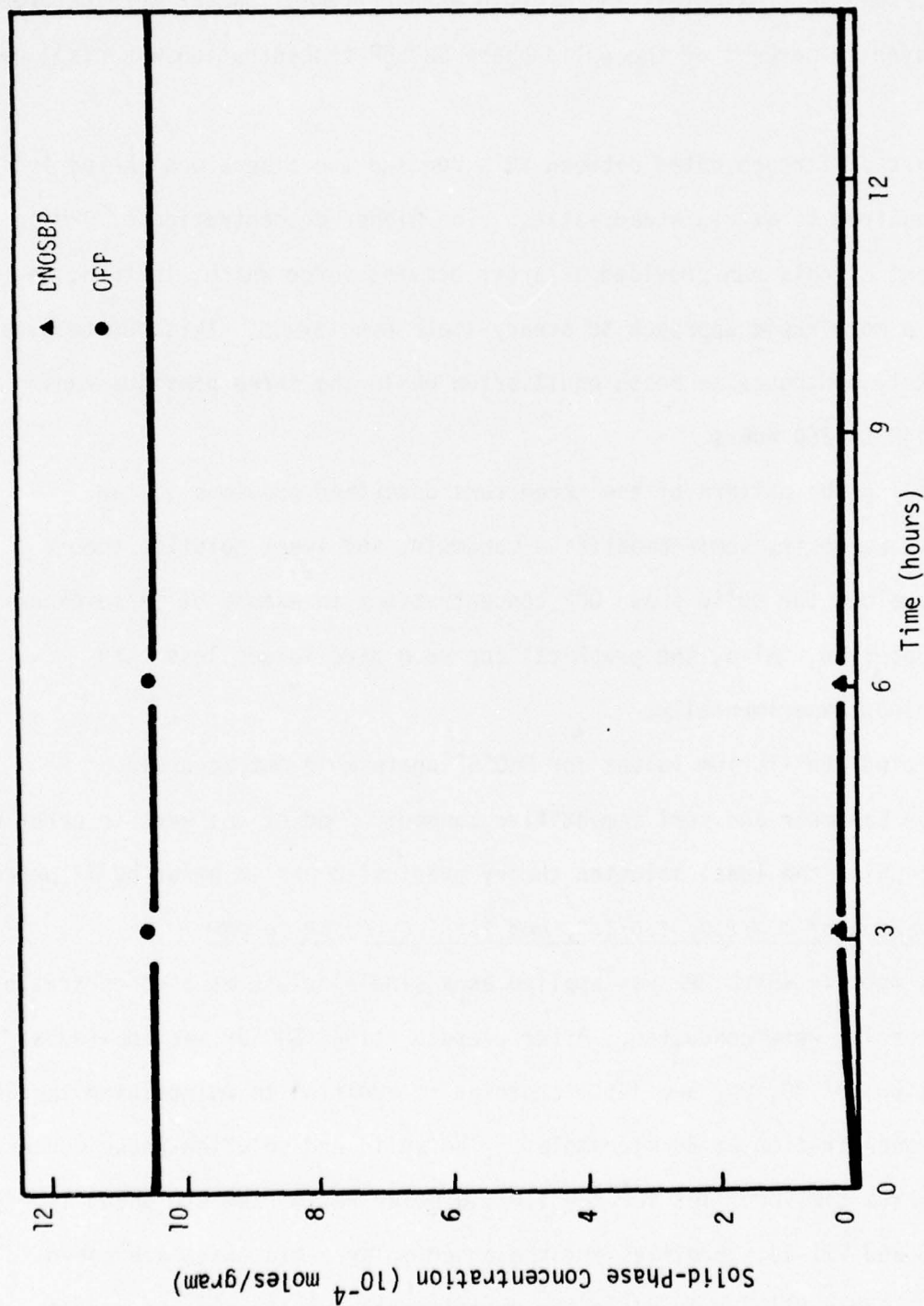


FIGURE VII-18: SOLID-PHASE CONCENTRATION PROFILES FOR A FLUIDIZED-BED SYSTEM TO WHICH DNOSBP AND OPP WERE INTRODUCED AT A MOLAR RATIO OF 1.0:1.0 AFTER THE ACTIVATED CARBON HAD BEEN PRESATURATED WITH OPP ($80 \mu\text{M}$).

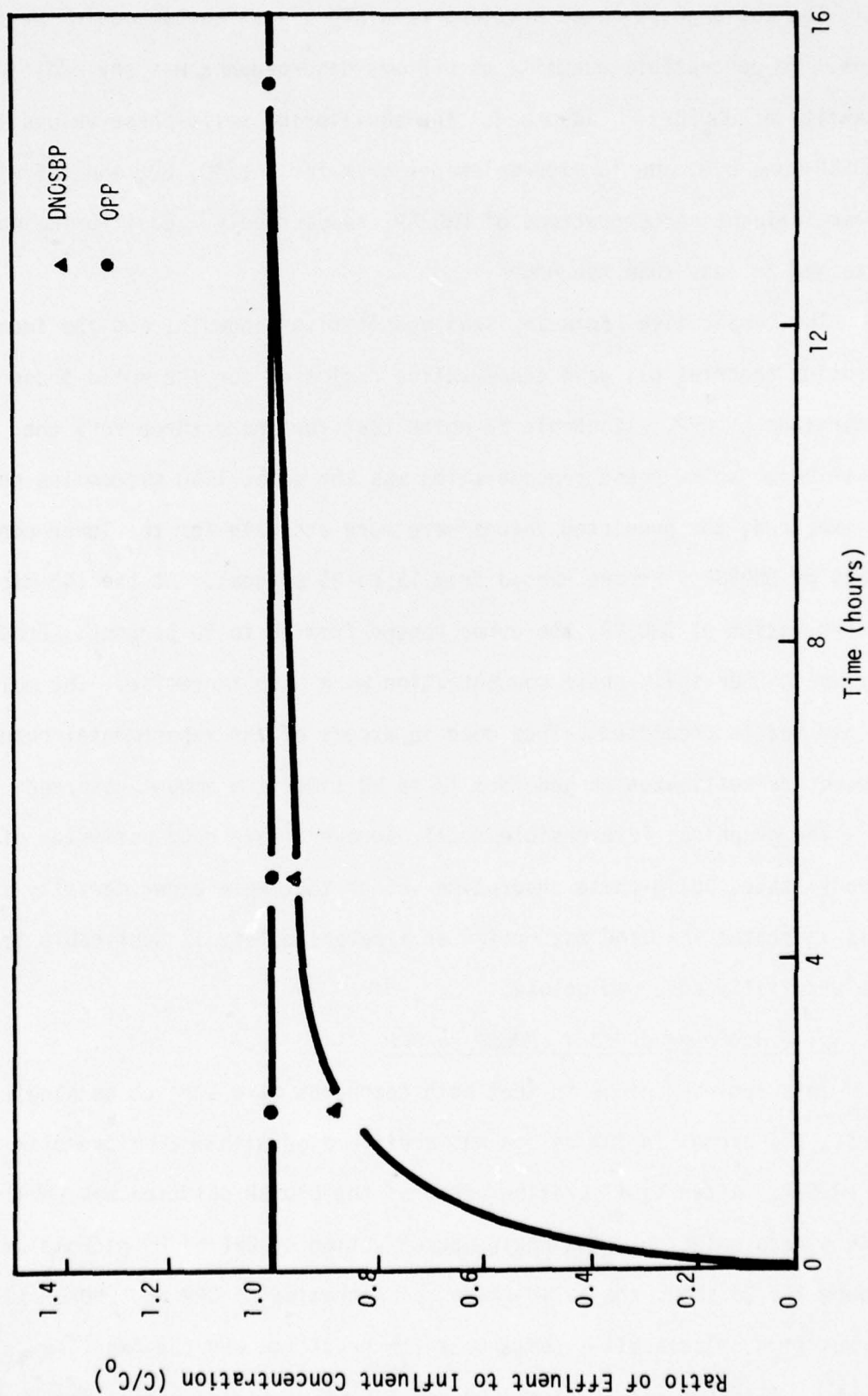


FIGURE VII-19: FLUID-PHASE CONCENTRATION PROFILES FOR A FLUIDIZED-BED SYSTEM TO WHICH DNOSBP AND OPP WERE INTRODUCED AT A MOLAR RATIO OF 1.0:1.0 AFTER THE ACTIVATED CARBON HAD BEEN PRESATURATED WITH OPP ($80 \mu\text{M}$).

is applicable but predicts no uptake of DNOSBP as previously discussed.

The solid-phase concentrations remained almost unchanged in the three runs. No perceptible quantity of OPP was desorbed nor was any additional quantity of DNOSBP adsorbed. The equilibrium solid-phase values for DNOSBP were 6, 8, and 15 micromoles per gram for the 40, 80, and 145 micromolar influent concentrations of DNOSBP, respectively. Equilibrium was attained in less than ten hours.

The competitive Langmuir, semi-competitive Langmuir, and the ideal solution theories all gave conservative estimates for the solid-phase concentration of OPP. It should be noted that for these three runs the equilibrium solid-phase concentration was the same; 1050 micromoles per gram. As expected, the predicted values were more accurate for the lower concentrations of DNOSBP. Errors ranged from 15 to 25 percent. At the 145 micromolar concentration of DNOSBP, the error ranged from 36 to 50 percent. Predictions for the DNOSBP solid-phase concentration were also imprecise. The multi-solute models predicted values much in excess of the experimental quantities. Theoretical estimates ranged from 13 to 23 times the amount observed.

The graphical irreversible model, however, gave good estimates of the steady-state, solid-phase adsorption values that were experimentally measured. This indicates that the assumption of irreversibility is applicable to the preferentially adsorbed solute.

... Molar Ratio of 0.0:1.0 DNOSBP to OPP

This run was unique in that both compounds were applied as single solutes. First, the carbon in the column was equilibrated with an 80 micromolar solution of DNOSBP. After equilibration, feed of the DNOSBP solution was replaced with a feed solution which had a concentration of OPP of 80 micromolar. Figure VII-20 shows the solid-phase concentration of OPP and DNOSBP plotted versus time. Table VII-1 summarizes the predicted and the experimental values. Final equilibrium values were: 500 and 570 micromoles per gram for DNOSBP

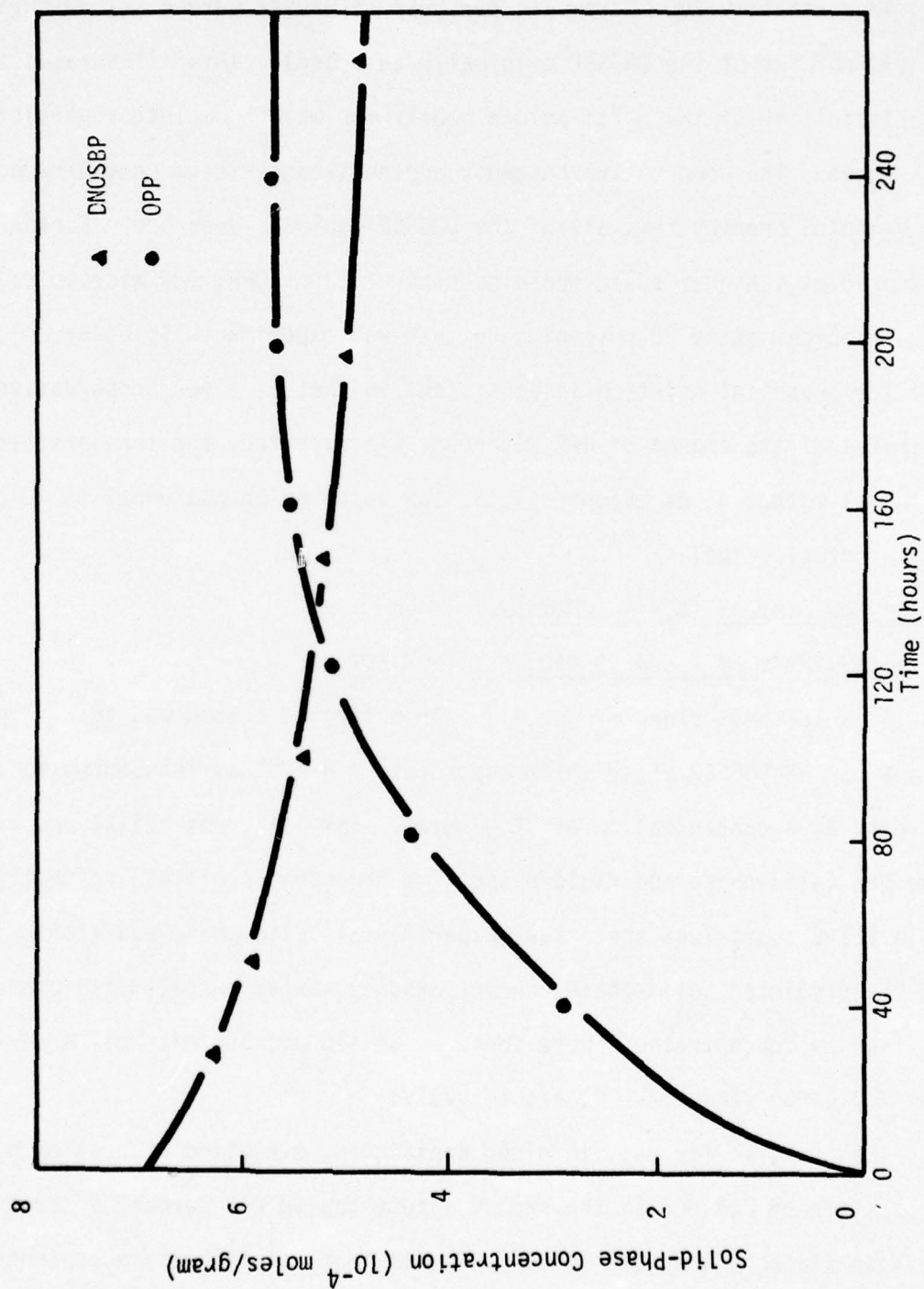


FIGURE VII-20: SOLID-PHASE CONCENTRATION PROFILES FOR A FLUIDIZED-BED SYSTEM TO WHICH DNOSBP AND OPP WERE INTRODUCED AT A MOLAR RATIO OF 0.0:1.0 AFTER THE ACTIVATED CARBON HAD BEEN PRESATURATED WITH DNOSBP ($80 \mu\text{M}$).

and OPP, respectively.

Approximately 200 micromoles per gram of DNOSBP were desorbed during this run (30 percent of the DNOSBP originally adsorbed). This illustrates the inapplicability of the multi-solute models for which complete reversibility is assumed. The competitive Langmuir and semi-competitive Langmuir models, for example, predict that all of the DNOSBP would be desorbed. Further, they predict a higher solid-phase concentration of OPP, 980 micromoles per gram, (approximately 70 percent more than was experimentally observed).

The graphical solution is consistent in that it gives conservative estimates of the amount of OPP adsorbed. As expected, the irreversible graphical method gives an unrealistic low value which was equal to 48 percent of the actual value.

Packed-Bed Studies (2,4-DCP/DNOSBP)

... Molar Ratio of 1.0:0.92 DNOSBP to 2,4-DCP

A packed-bed column of the granular activated carbon was initially saturated with 81.31 μM DNOSBP after which the solute 2,4-DCP was introduced to the influent at a concentration of 78.46 micromolar. Figures VII-21 and VII-22 show the solid-phase and fluid-phase time dependent profiles, respectively. Table VII-2 summarizes the actual experimental solid-phase equilibrium values and the predicted solid-phase concentrations. Experimental solid-phase equilibrium concentrations were found to be 810 and 355 micromoles per gram for DNOSBP and 2,4-DCP, respectively.

This run, as for the fluidized contactors, exhibited desorption of DNOSBP. Application of 2,4-DCP as the second solute caused a 9 percent desorption of the less strongly adsorbed DNOSBP. The maximum solution-phase concentration of DNOSBP observed due to desorption was 105.4 micromolar ($C/C_0 = 1.33$) at a bisolute molar ratio of 1.0:0.92 DNOSBP to 2,4-DCP. This peak occurred at approximately 1 hour into the bisolute segment of the run.

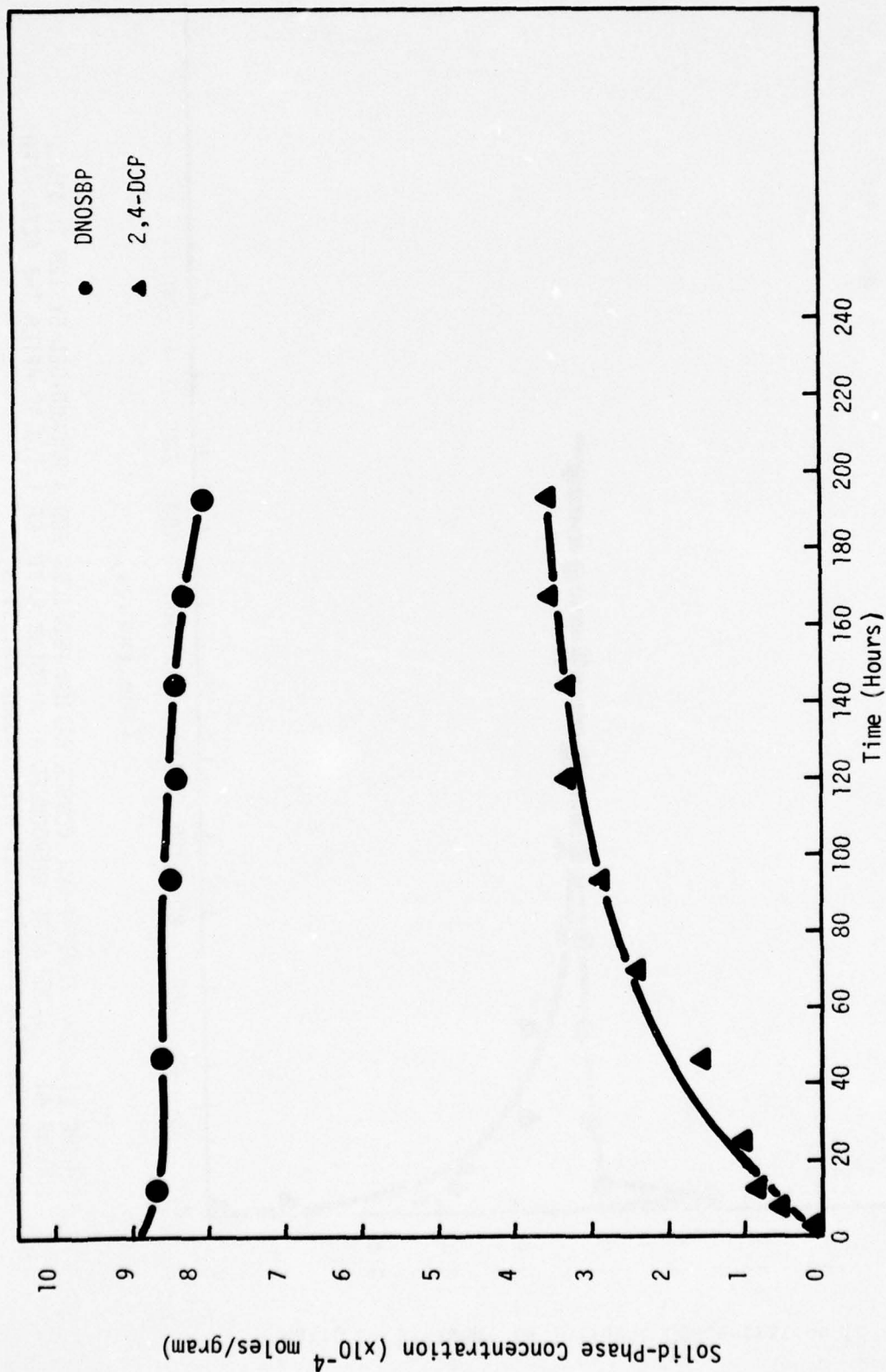


FIGURE VII-21: SOLID-PHASE CONCENTRATION PROFILES FOR A PACKED-BED SYSTEM TO WHICH DNOSBP AND 2,4-DCP WERE INTRODUCED AT A MOLAR RATIO OF 1.0:0.92 AFTER THE ACTIVATED CARBON HAD BEEN PRESATURATED WITH DNOSBP (81.31 μM).

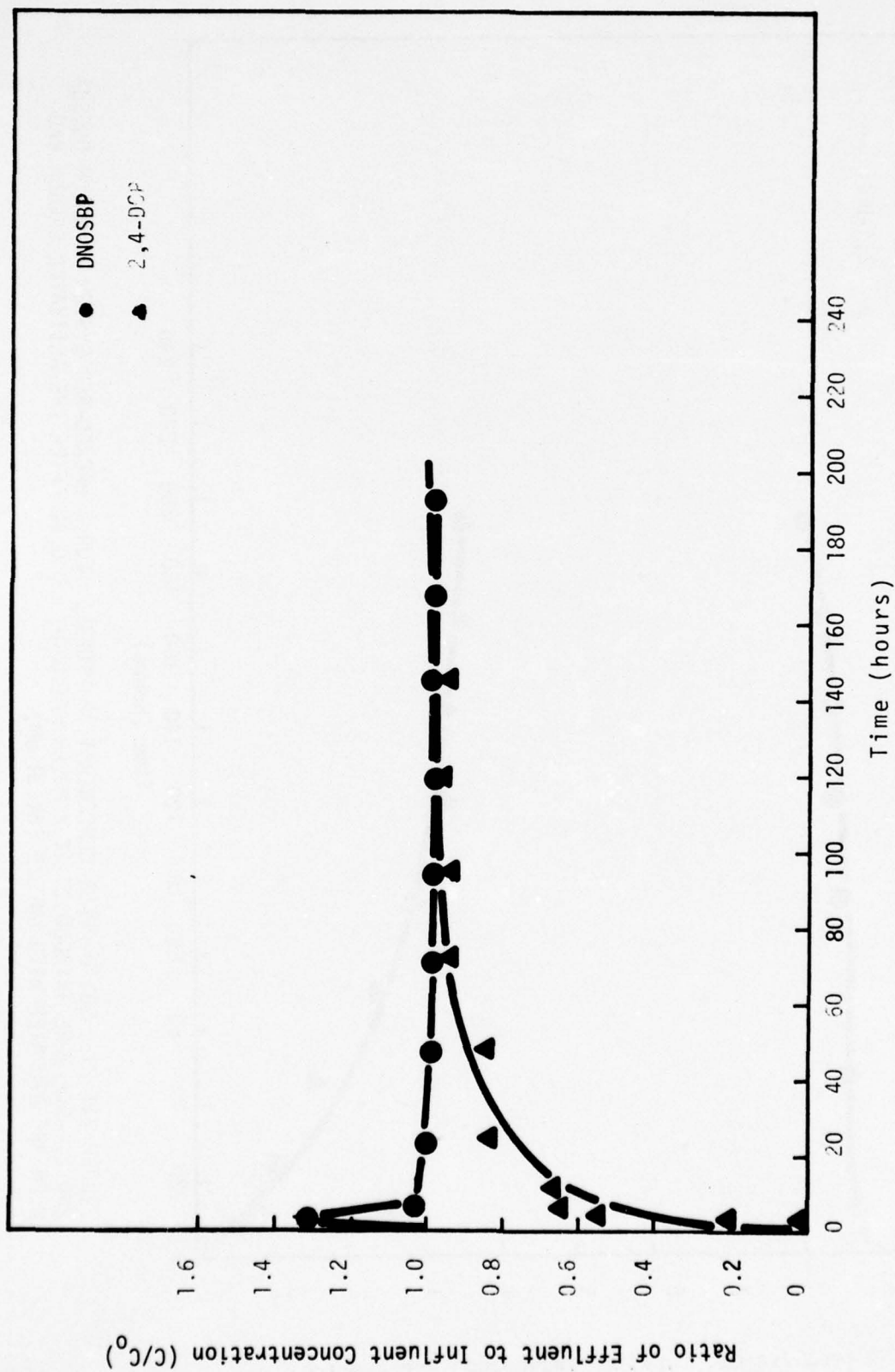


FIGURE VII-22: FLUID-PHASE CONCENTRATION PROFILES FOR A PACKED-BED SYSTEM TO WHICH DNOSBP AND 2,4-DCP WERE INTRODUCED AT A MOLAR RATIO OF 1.0:0.92 AFTER THE ACTIVATED CARBON HAD BEEN PRESATURATED WITH DNOSBP ($81.31 \mu\text{M}$).

TABLE VII-2

SUMMARIZED RESULTS: PACKED-BED STUDIES

| Presaturation Solute | Molar Ratio | Solution-Phase Concentration (μM) | | EXP | Solid-Phase Concentration ($\mu\text{Moles/g}$) | | | |
|-------------------------|----------------|--|---------|----------------|---|----------------|----------------|----------------|
| | | DNOSBP | 2,4-DCP | | LC | LSC | GI | |
| | | | | DNOSBP/2,4-DCP | DNOSBP/2,4-DCP | DNOSBP/2,4-DCP | DNOSBP/2,4-DCP | DNOSBP/2,4-DCP |
| DNOSBP | 1.0:0.92 | 81.31 | 74.86 | 810/355 | 261/1491 | 261/2227 | | 649/1901 |
| DNOSBP | 1.0:1.56 | 78.52 | 122.76 | 630/960 | 191/1854 | 191/2424 | | 643/2207 |
| 2,4-DCP | 1.0:1.0 | 80.75 | 80.0 | 29/1950 | 251/1543 | 251/2256 | | 0/2600 |
| 2,4-DCP | 2.0:1.0 | 160.98 | 80.0 | 90/2110 | 364/1123 | 364/2506 | | 0/2600 |

KEY: EXP = Experimental Data; LC = Langmuir Competitive Model; LSC = Langmuir Semi-Competitive Model; GI = Graphical Irreversible Model.

The competitive and semi-competitive Langmuir models both underestimate the solid-phase equilibrium value of DNOSBP by 210 percent and overestimated the 2,4-DCP value by an even greater error. The graphical method predicted values of 80 and 535 percent of the experimental solid-phase equilibrium values obtained for DNOSBP and 2,4-DCP, respectively.

... Molar Ratio of 1.0:1.56 DNOSBP to 2,4-DCP

This run, conducted in a packed-bed contactor, involved equilibrating the system with 78.52 μM DNOSBP and then adding to the feed solution, as a step input, 122.76 μM 2,4-DCP. Figure VII-23 shows the solid-phase concentration profiles for the bisolute portion of the run. Figure VII-24 gives the solution-phase concentration profile for the run while Table VII-2 summarizes actual experimental and predicted solid-phase equilibrium values. Experimental solid-phase equilibrium concentrations were determined to be 630 and 960 micromoles per gram for DNOSBP and 2,4-DCP, respectively.

As in the previous cases of this sequence of solute application, a desorption-sorption phenomenon was observed for DNOSBP. At steady-state a net desorption of DNOSBP which was 24% less than the single-solute solid-phase saturation value was observed. The peak fluid-phase effluent concentration of DNOSBP due to desorption was 98 micromolar ($C/C_0 = 1.24$) at a bisolute molar ratio of 1.0:1.56 DNOSBP to 2,4-DCP. This peak occurred at approximately 6 hours into the bisolute portion of the run.

For this run the competitive and semi-competitive Langmuir models predicted values that were only 30% of the measured solid-phase equilibrium value obtained for DNOSBP. The graphical procedure predicted a value which was only 2 percent higher than the actual solid-phase concentration obtained for DNOSBP.

Both of the Langmuir models and the graphical technique gave predictions that were in error in excess of 100 percent of the measured value for 2,4-DCP.

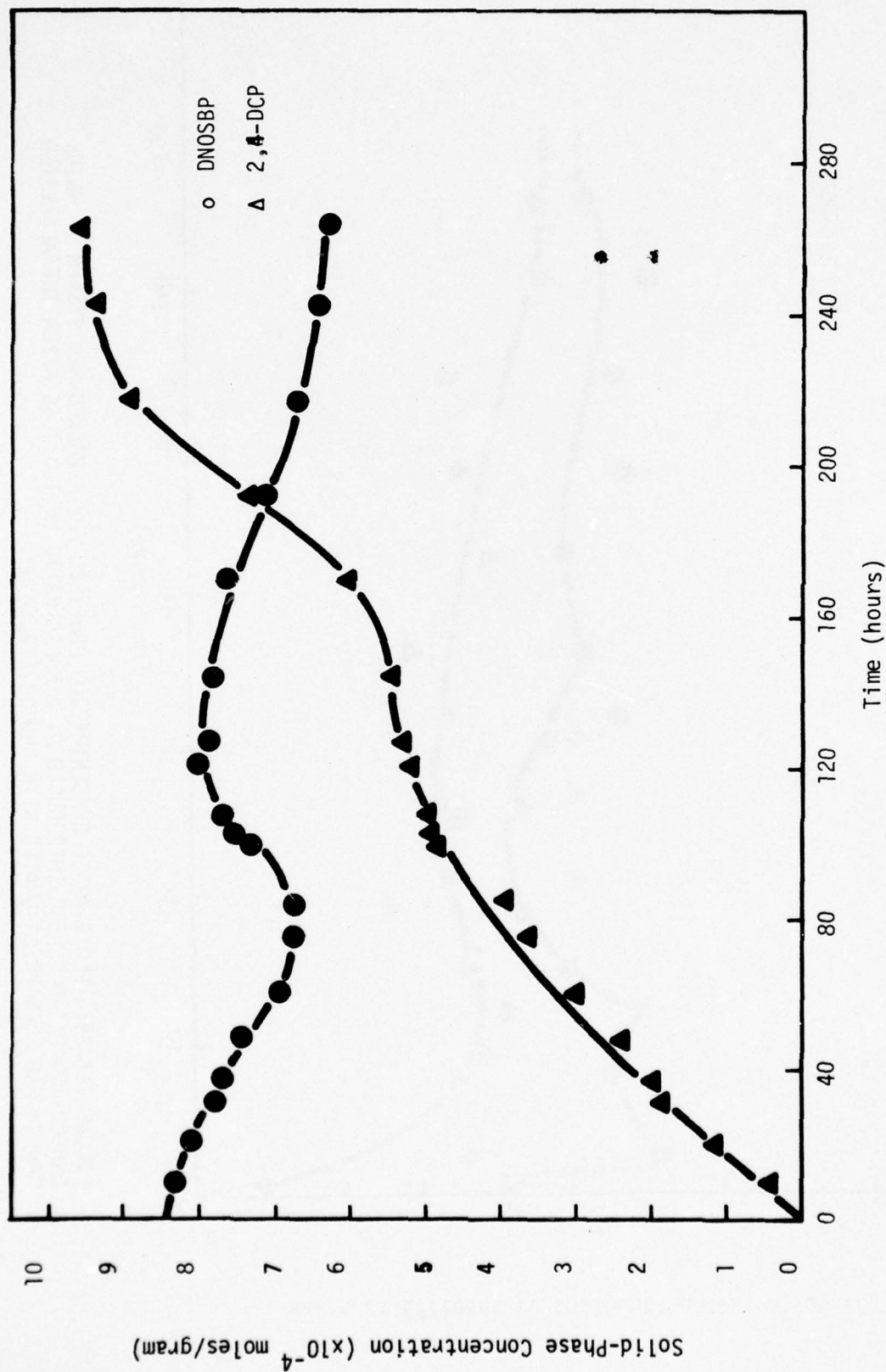


FIGURE VII-23: SOLID-PHASE CONCENTRATION PROFILES FOR A PACKED-BED SYSTEM TO WHICH DNOSBP AND 2,4-DCP WERE INTRODUCED AT A MOLAR RATIO OF 1.0:1.56 AFTER THE ACTIVATED CARBON HAD BEEN PRESATURATED WITH DNOSBP (78.52 μM).

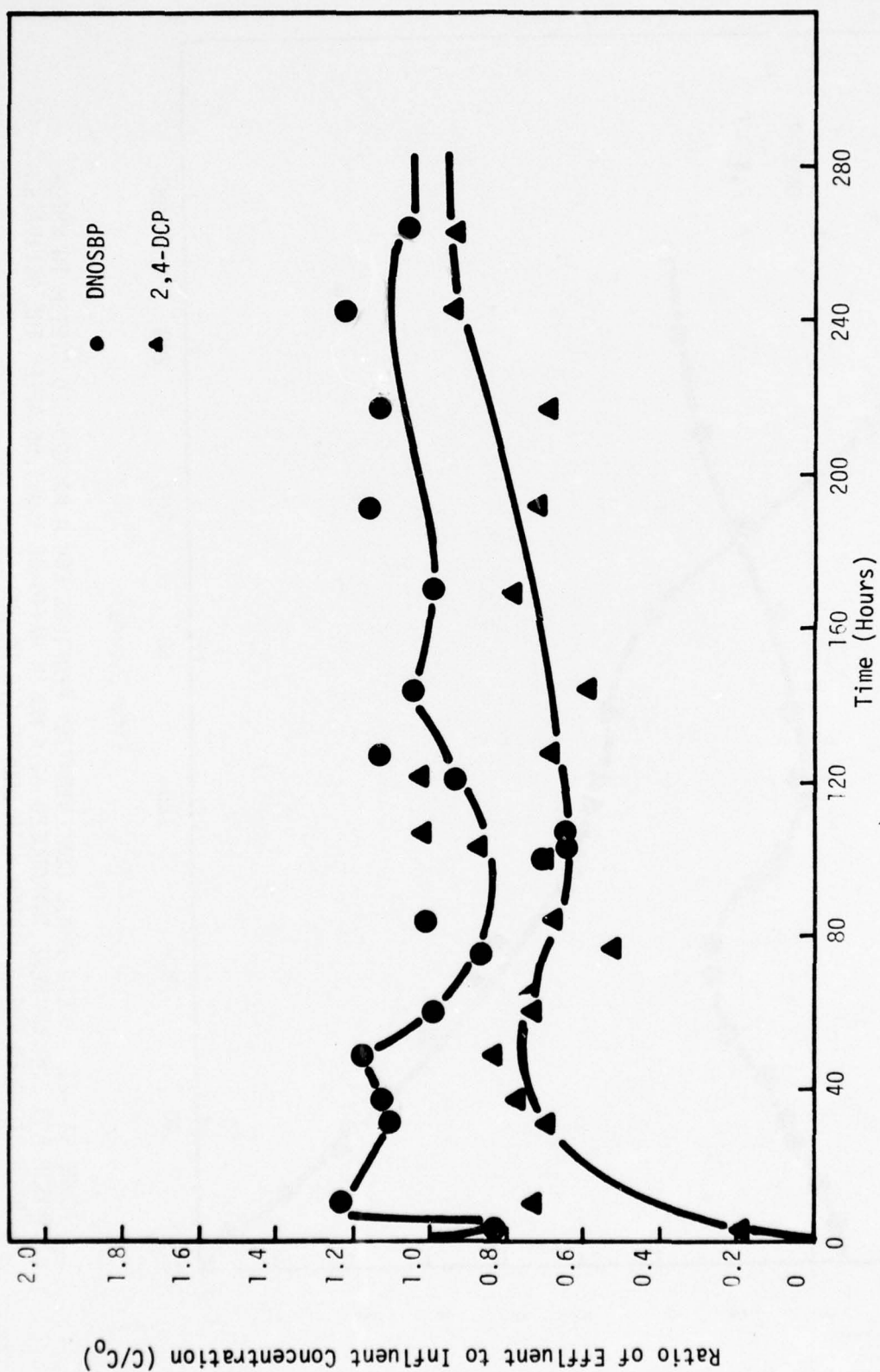


FIGURE VII-24: FLUID-PHASE CONCENTRATION PROFILES FOR A PACKED-BED SYSTEM TO WHICH DNOSBP AND 2,4-DCP WERE INTRODUCED AT A MOLAR RATIO OF 1.0:1.56 AFTER THE ACTIVATED CARBON HAD BEEN PRESATURATED WITH DNOSBP ($78.52 \mu\text{M}$).

...Molar Ratio of 1.0:1.0 2,4-DCP to DNOSBP

A packed-bed contactor was brought to equilibrium with an influent containing 2,4-DCP at a concentration of 80 μM . A step input of 80.75 μM DNOSBP was added to the influent solution thereafter. Figures VII-2 and VII-26 show the solid-phase and fluid-phase concentration profiles for the bisolute portion of the run. Table VII-2 summarizes experimental and predicted solid-phase equilibrium values. Measured experimental solid-phase equilibrium concentrations were found to be 29 and 1950 micromoles per gram for DNOSBP and 2,4-DCP, respectively.

Prediction of the solid-phase equilibrium concentration for DNOSBP was over-estimated by the competitive and semi-competitive Langmuir models. The graphical method predicted no adsorption of DNOSBP.

The model predictions for 2,4-DCP were in much closer agreement with the measured solid-phase equilibrium values. The competitive Langmuir model predicted a value that was 79 percent of the actual value while the semi-competitive Langmuir model predicted a saturation value that was 16 percent higher than experimentally measured. The graphical procedure gave a value that was 33 percent higher than observed.

...Molar Ratio of 1.0:2.0 2,4-DCP to DNOSBP

After pre-saturation of the packed-bed contactor with a 80 μM solution of 2,4-DCP, a step input of 160.98 μM DNOSBP was added to the influent. Figure VII-27 shows the solid-phase concentration profiles for the run while Figure VII-28 illustrates the fluid-phase concentration profiles. Table VII-2 summarizes the actual and predicted solid-phase equilibrium concentrations. Actual steady-state solid-phase concentrations for the run were calculated to be 90 and 2110 micromoles per gram for DNOSBP and 2,4-DCP, respectively.

Slight disproportion of 2,4-DCP occurred upon addition of the DNOSBP, but quickly recovered to its original (single-solute) equilibrium value. The two predictive models again failed to accurately predict the final

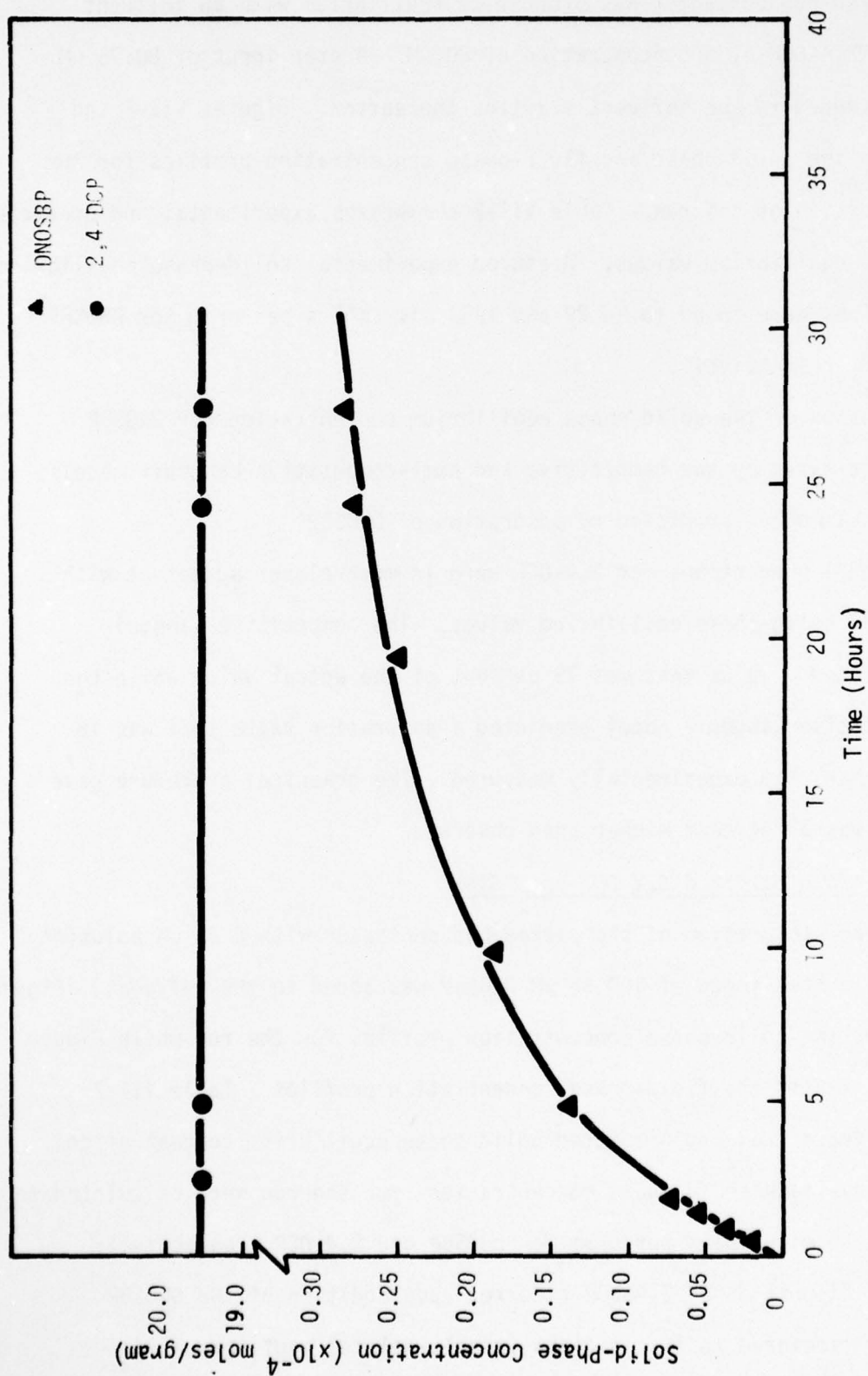


FIGURE VII-25: SOLID-PHASE CONCENTRATION PROFILES FOR A PACKED-BED SYSTEM TO WHICH DNOSBP AND 2,4-DCP WERE INTRODUCED AT A MOLAR RATIO OF 1.0:1.0 AFTER THE ACTIVATED CARBON HAD BEEN PRESATURATED WITH 2,4-DCP (80 μ M).

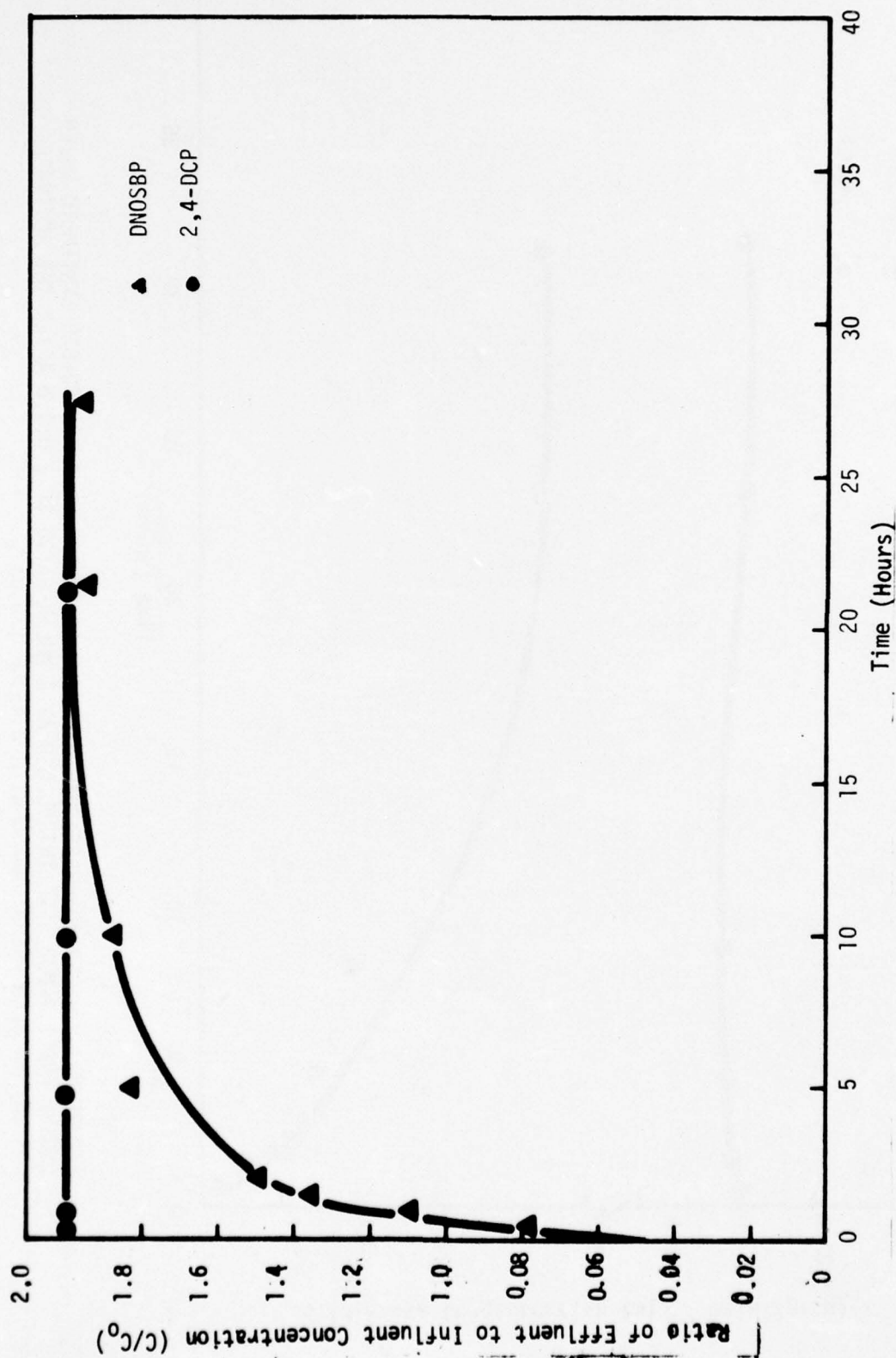


FIGURE VII-26: FLUID-PHASE CONCENTRATION PROFILES FOR A PACKED-BED SYSTEM TO WHICH DNOSBP AND 2,4-DCP WERE INTRODUCED AT A MOLAR RATIO OF 1.0:1.0 AFTER THE ACTIVATED CARBON HAD BEEN PRESATURATED WITH 2,4-DCP (80 μ M).

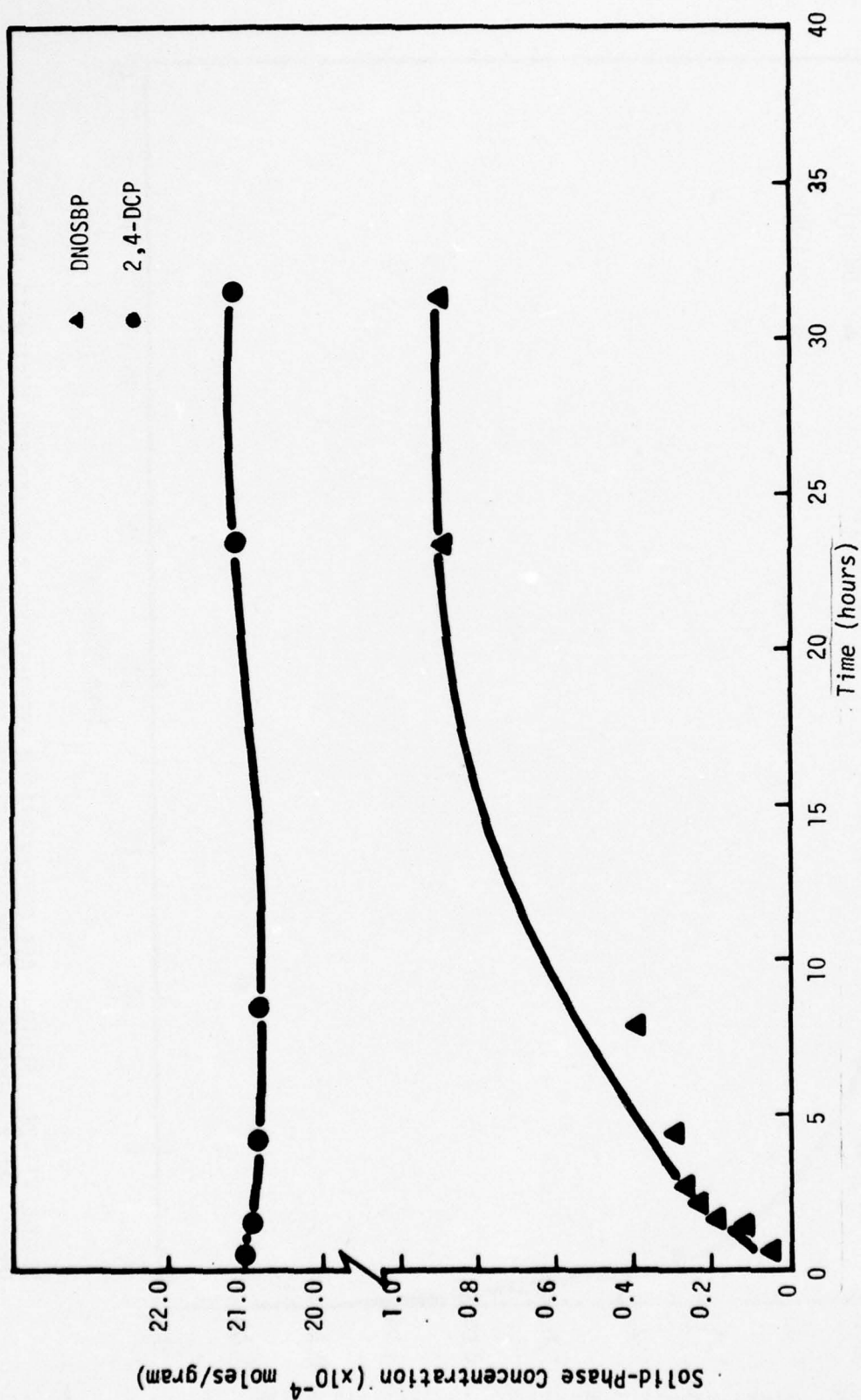


FIGURE VII-27: SOLID-PHASE CONCENTRATION PROFILES FOR A PACKED-BED SYSTEM TO WHICH DNOSBP AND 2,4-DCP WERE INTRODUCED AT A MOLAR RATIO OF 2.0:1.0 AFTER THE ACTIVATED CARBON HAD BEEN PRESATURATED WITH 2,4-DCP (80 μ M).

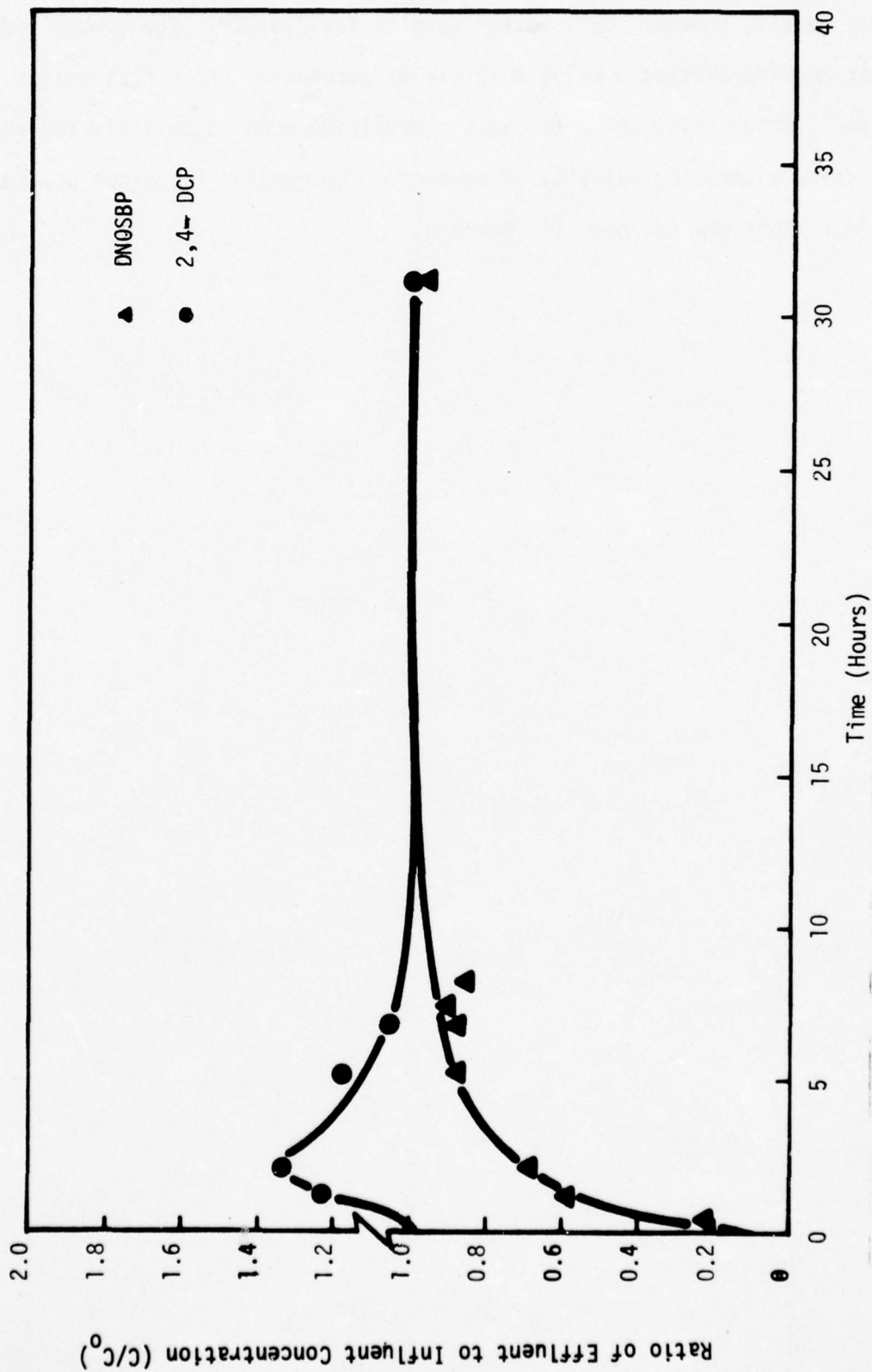


FIGURE VII-28: FLUID-PHASE CONCENTRATION PROFILES FOR A PACKED-BED SYSTEM TO WHICH DNOSBP AND 2,4-DCP WERE INTRODUCED AT A MOLAR RATIO OF 2.0:1.0 AFTER THE ACTIVATED CARBON HAD BEEN PRESATURATED WITH 2,4-DCP ($80 \mu\text{M}$).

solid-phase concentration of DNOSBP. The graphic approach predicted no adsorption of DNOSBP.

The models, however, gave better results for 2,4-DCP. The competitive Langmuir model predicted a value that was 53 percent of the actual solid-phase equilibrium value while the semi-competitive model over-estimated the steady-state adsorption value by 19 percent. The graphic technique provided an estimate that was too high (23 percent).

CSTR Studies (2,4-DCP/DNOSBP)

...Molar Ratio of 1.0:0.96 DNOSBP to 2,4-DCP

A CSTR contactor was brought to equilibrium with a 82 μM solution of DNOSBP. Subsequently, a step input of 79 μM 2,4-DCP was added to the influent. Figures VII-29 and VII-30 show the solid and fluid-phase concentration profiles for the bisolute portion of this run. Table VII-3 summarizes the experimental and predicted solid-phase equilibrium results. Actual solid-phase equilibrium values were determined to be 910 and 550 micromoles per gram for DNOSBP and 2,4-DCP, respectively.

As observed in previous runs desorption of DNOSBP occurred upon the addition of 2,4-DCP to the influent stream. Steady-state values showed that 11 percent of the original single-solute solid-phase saturation concentration of DNOSBP was desorbed. The peak solution-phase concentration of DNOSBP was noted to be approximately 112 micromolar ($C/C_0 = 1.45$). This peak occurred at 150 hours into the bisolute portion of the run.

The competitive and semi-competitive Langmuir models did not provide realistic predictions as both predicted concentrations for DNOSBP that were only 28 percent of the measured solid-phase equilibrium concentration. The graphical technique predicted a value of 71 percent of the actual measured value and thus provided the best prediction.

The actual adsorption of 2,4-DCP was 550 $\mu\text{M/g}$. Both the Langmuir graphical predictions for 2,4-DCP were several hundred percent above this value.

...Molar Ratio of 1.0:2.02 DNOSBP/2,4-DCP

Upon saturating the activated carbon in the CSTR with an 80 μM solution of DNOSBP, a step input of 161.77 μM 2,4-DCP was applied in addition. Figure VII-31 shows the solid-phase concentration profile for the bisolute portion of this run. Figure VII-32 gives the corresponding fluid-phase concentration profile,

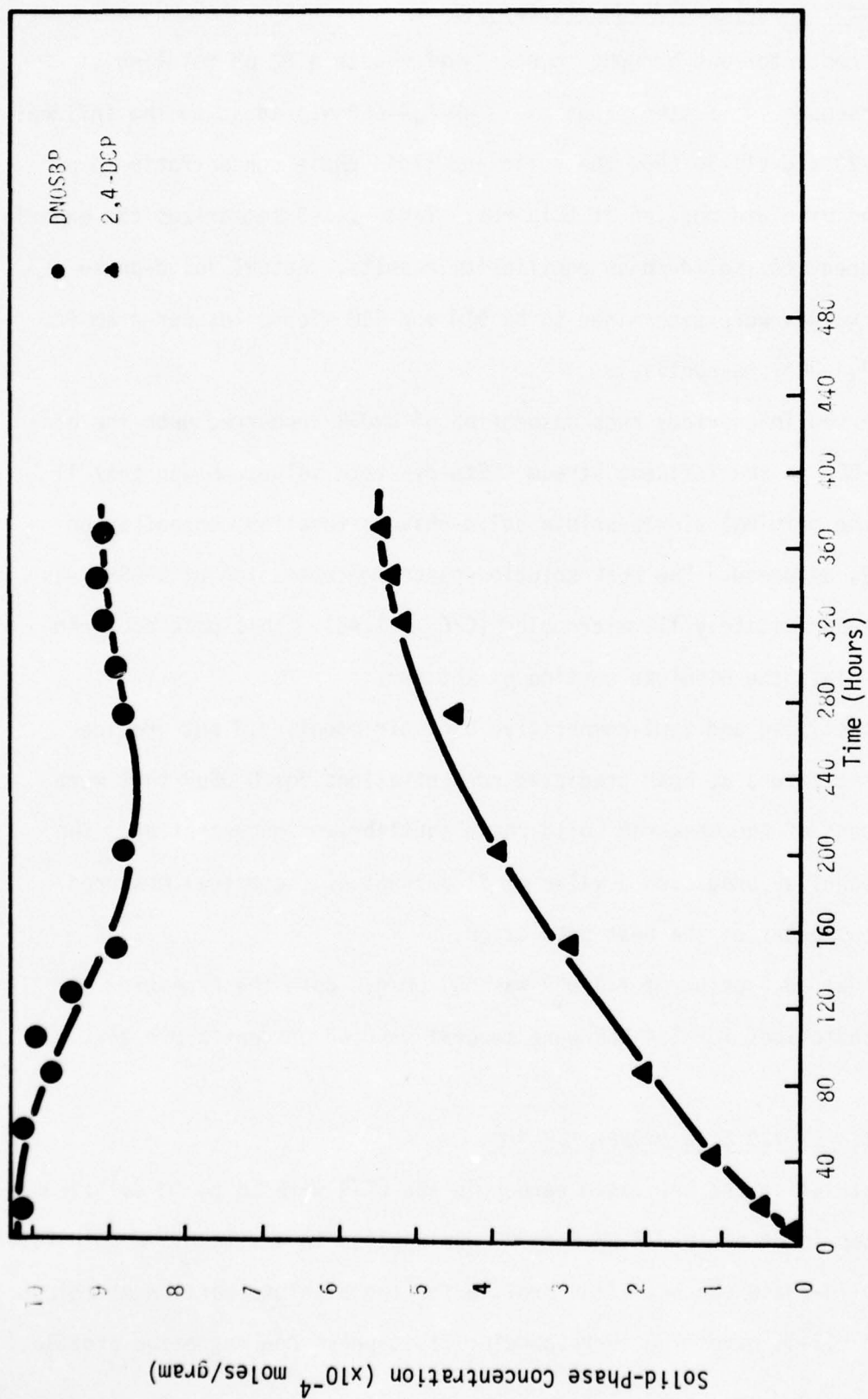


FIGURE VII-29: SOLID-PHASE CONCENTRATION PROFILES FOR A CSTR SYSTEM TO WHICH DNO₃BP AND 2,4-DCP WERE INTRODUCED AT A MOLAR RATIO OF 1.0:0.96 AFTER THE ACTIVATED CARBON HAD BEEN PRESATURATED WITH DNO₃BP (82 μM).

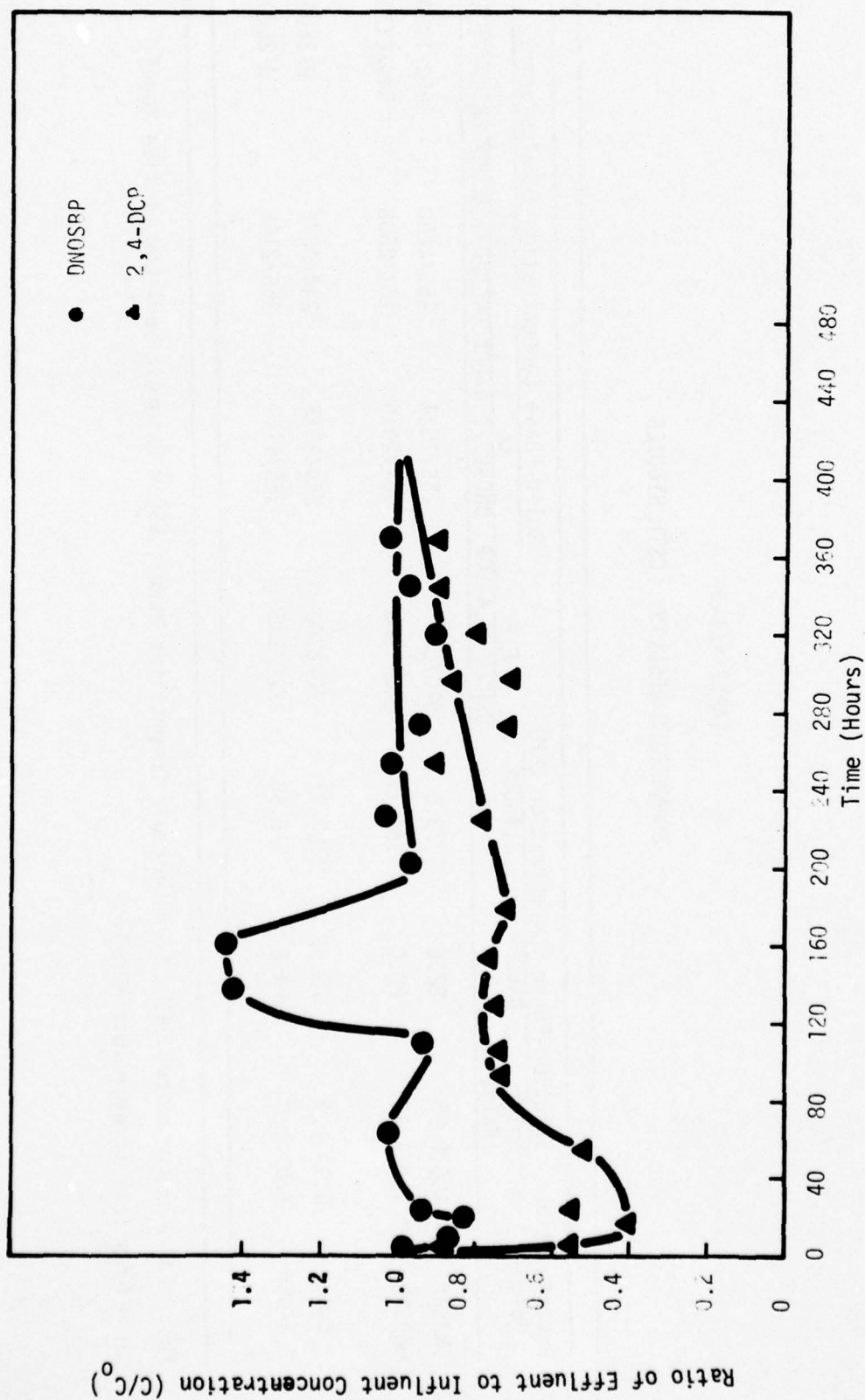


FIGURE VII-30: FLUID-PHASE CONCENTRATION PROFILES FOR A CSTR SYSTEM TO WHICH DNOSBP AND 2,4-DCP WERE INTRODUCED AT A MOLAR RATIO OF 1.0:0.96 AFTER THE ACTIVATED CARBON HAD BEEN PRESATURATED WITH DNOSBP (82 μM).

TABLE VII-3

SUMMARIZED RESULTS: CSTR STUDIES

| Presaturation Solute | Molar Ratio | Solution-Phase Concentration (μM) | | EXP | Solid-Phase Concentration ($\mu\text{Moles/gram}$) | | |
|-------------------------|----------------|--|---------|----------------|--|----------------|----------------|
| | | DNOSBP | 2,4-DCP | | LC | LSC | GI |
| | | | | DNOSBP/2,4-DCP | DNOSBP/2,4-DCP | DNOSBP/2,4-DCP | DNOSBP/2,4-DCP |
| DNOSBP | 1.0:0.96 | 82.0 | 79.0 | 910/550 | 255/1524 | 255/2250 | 650/1950 |
| DNOSBP | 1.0:2.02 | 80.0 | 161.77 | 820/1060 | 161/2016 | 161/2508 | 645/2220 |
| 2,4-DCP | 0.96:1.0 | 78.93 | 82.21 | 70/2700 | 244/1575 | 244/2272 | 0/2600 |
| 2,4-DCP | 2.03:1.0 | 156.0 | 76.64 | 228/2350 | 365/1113 | 365/2146 | 0/2560 |

KEY: EXP = Experimental Data; LC = Langmuir Competitive Model; LSC = Langmuir Semi-Competitive Model;

GI = Graphical Irreversible Model.

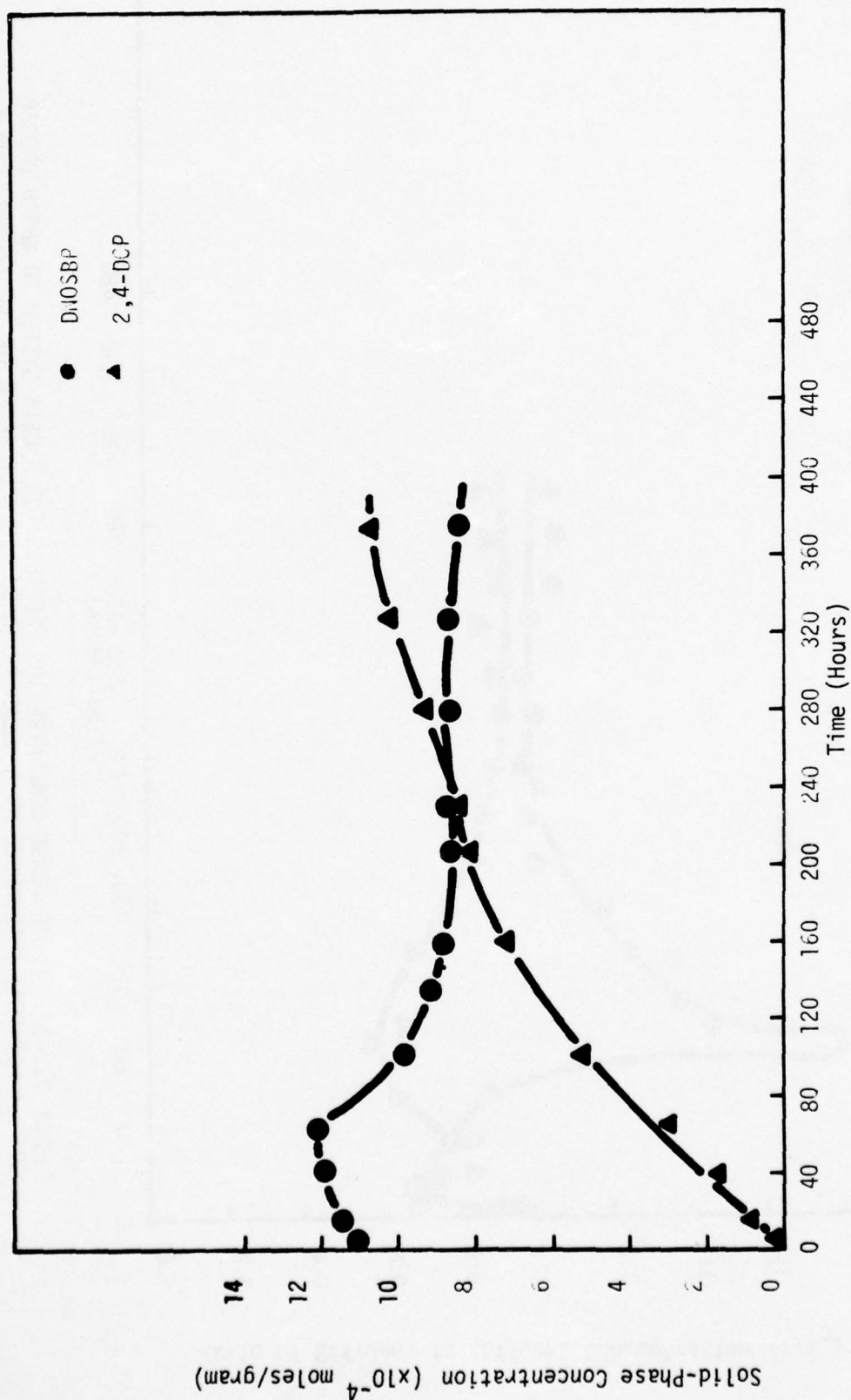


FIGURE VII-31: SOLID-PHASE CONCENTRATION PROFILES FOR A CSTR SYSTEM TO WHICH DNOSBP AND 2,4-DCP WERE INTRODUCED AT A MOLAR RATIO OF 1.0:2.02 AFTER THE ACTIVATED CARBON HAD BEEN PRESATURATED WITH DNOSBP ($80 \mu\text{M}$).

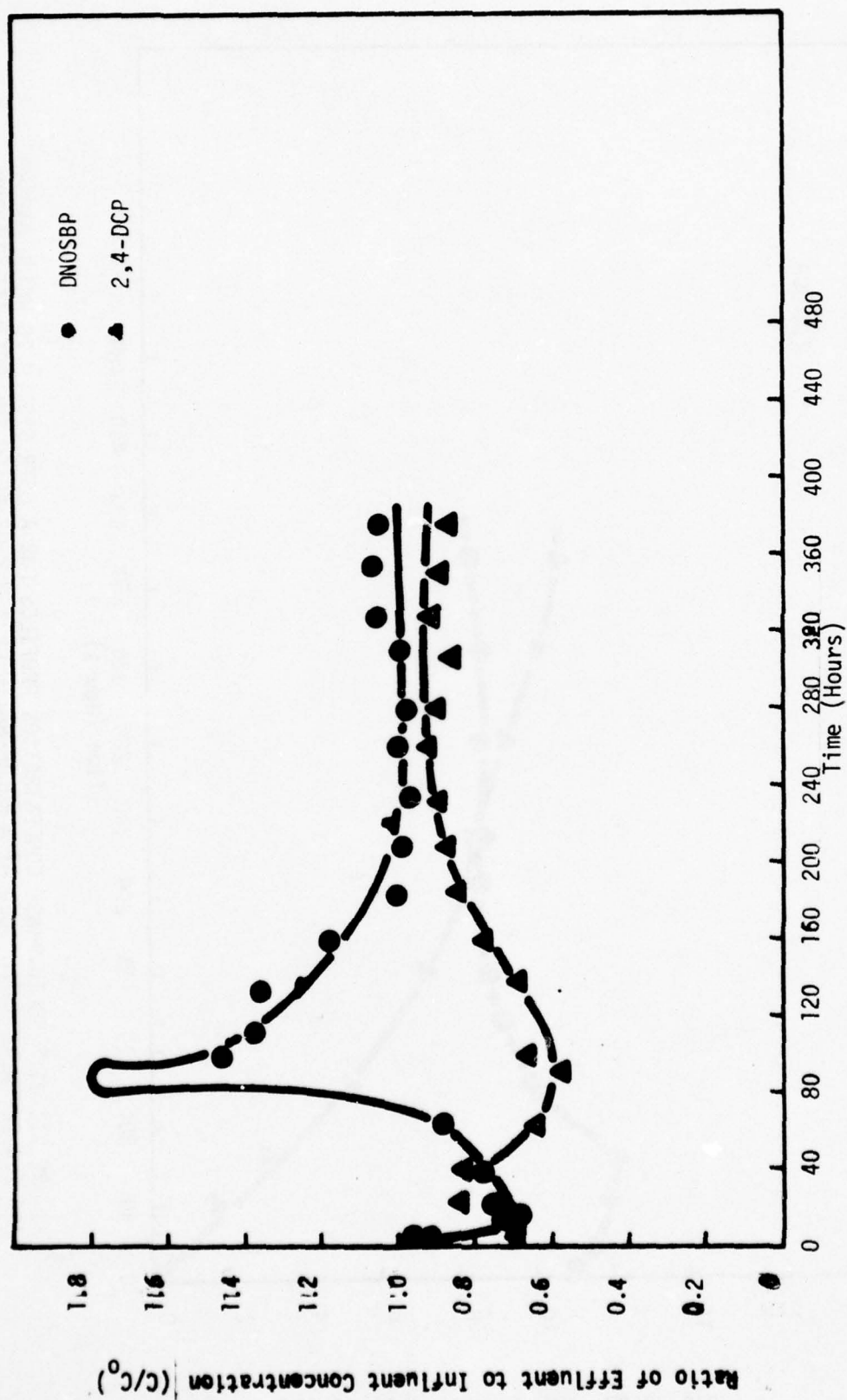


FIGURE VII-32: FLUID-PHASE CONCENTRATION PROFILES FOR A CSTR SYSTEM TO WHICH DNOSBP AND 2,4-DCP WERE INTRODUCED AT A MOLAR RATIO OF 1.0:2.02 AFTER THE ACTIVATED CARBON HAD BEEN PRESATURATED WITH DNOSBP (80 μ M).

Table VII-3 summarizes the solid-phase equilibrium results for the experimental and predicted results. Measured experimental solid-phase equilibrium results were found to be 820 and 1061 micromoles per gram for DNOSBP and 2,4-DCP, respectively.

As in the previous run desorption of DNOSBP was observed. The final solid-phase equilibrium value was 27 percent less than that observed for single-solute saturation. The maximum solution-phase concentration of DNOSBP attributable to desorption was 144 micromolar ($C/C_0 = 1.8$). This peak occurred at approximately 80 hours into the run.

The graphical procedure again provided the best prediction for the observed DNOSBP solid-phase equilibrium value. The Langmuir models gave predictions that were only 20 percent of the actual value.

Predictions of 2,4-DCP adsorption levels were poor for all models. The competitive Langmuir model gave the best results; 90 percent above the actual solid-phase concentration. The graphical procedure predicted a value that was too high by 109 percent.

...Molar Ratio of 1.0:0.96 2,4-DCP to DNOSBP

The CSTR was equilibrated with an 82.21 μM solution of 2,4-DCP before DNOSBP was added at the 70.93 μM concentration level. Figures VII-33 and VII-34 show the solid and solution-phase profiles, respectively, for the run. Table VII-3 summarizes the experimental and predicted results. Experimental solid-phase concentration values obtained for this run were 79 and 2700 micromoles per gram for DNOSBP and 2,4-DCP, respectively.

A small quantity of DNOSBP was adsorbed during the bisolute portion of the run. However, the 2,4-DCP began to adsorb for the 200 hours after the step input of DNOSBP was imposed. The ultimate solid-phase concentration of 2,4-DCP attained the equilibrium listed above. This phenomenon was not observed in any other studies

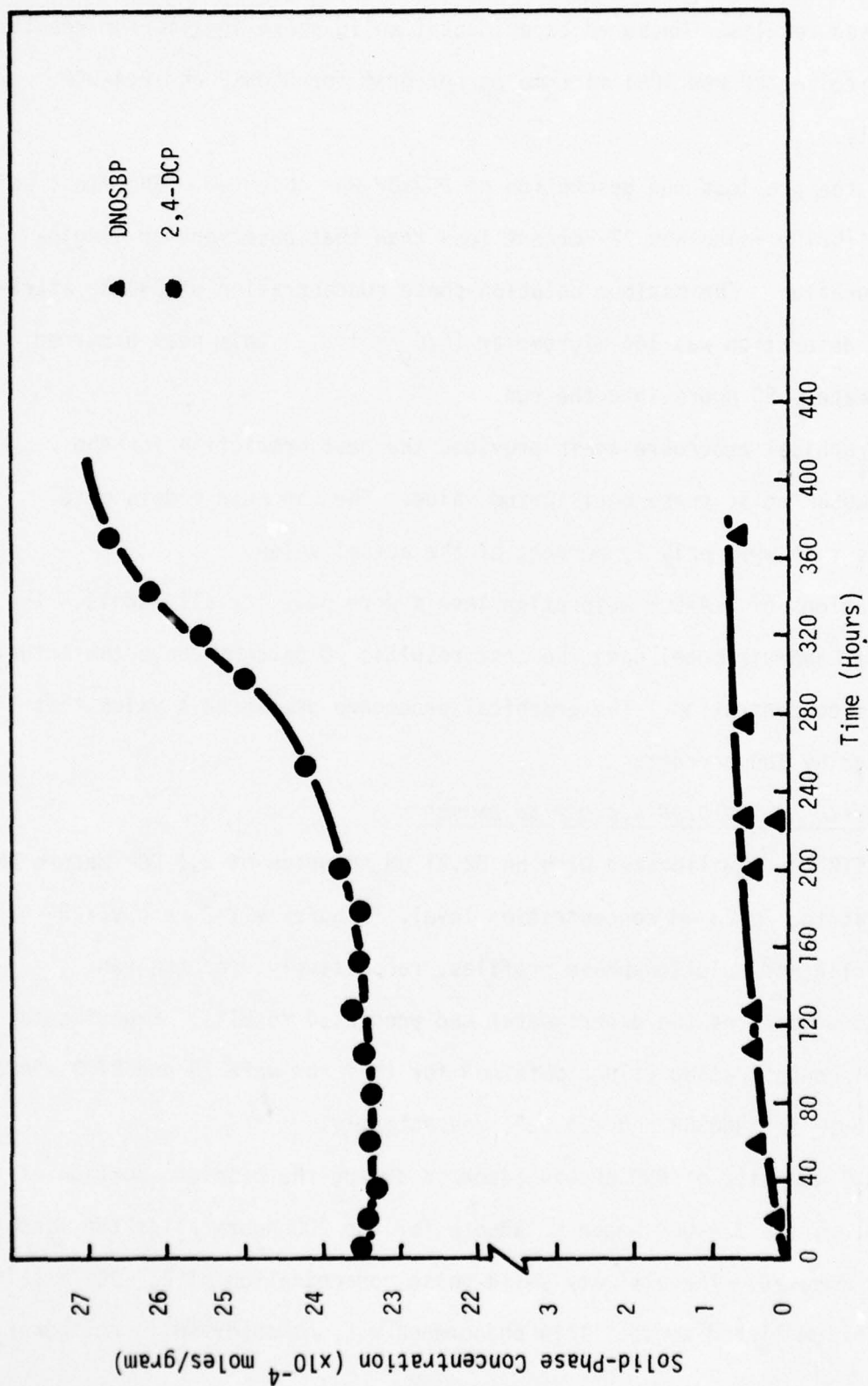


FIGURE VII-33: SOLID-PHASE CONCENTRATION PROFILES FOR A CSTR SYSTEM TO WHICH DNOSBP AND 2,4-DCP WERE INTRODUCED AT A MOLAR RATIO OF 0.96:1.0 AFTER THE ACTIVATED CARBON HAD BEEN PRESATURATED WITH 2,4-DCP (82.21 μ M).

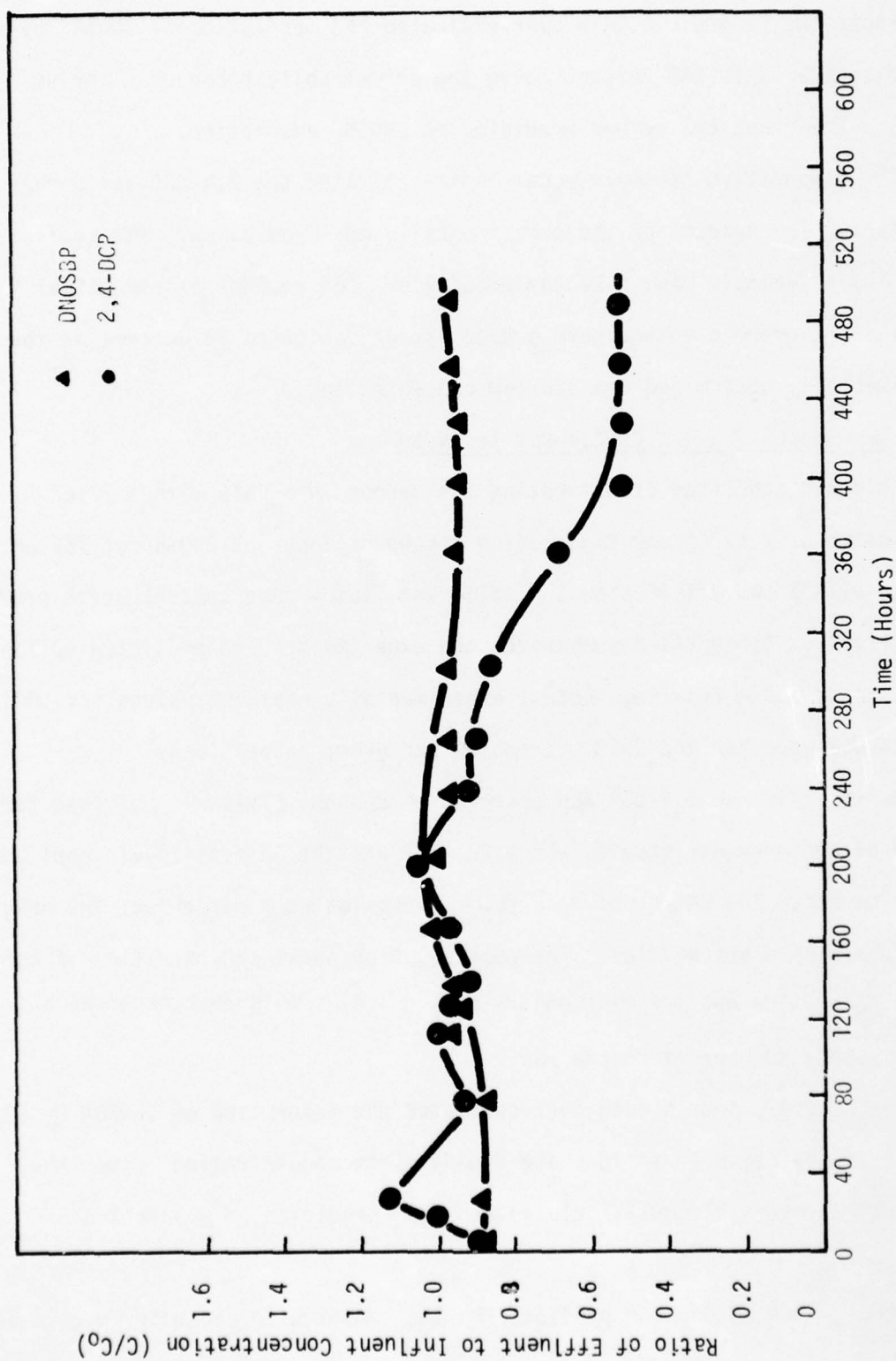


FIGURE VII-34: FLUID-PHASE CONCENTRATION PROFILES FOR A CSTR SYSTEM TO WHICH DNOSBP AND 2,4-DCP WERE INTRODUCED AT A MOLAR RATIO OF 0.96:1.0 AFTER THE ACTIVATED CARBON HAD BEEN PRESATURATED WITH 2,4-DCP (81.21 μM).

and cannot, at this time, be explained.

Again the Langmuir models over-estimated the adsorption of DNOSBP by a significant amount (248 percent above the actual solid-phase equilibrium value). The graphical method predicted no DNOSBP adsorption.

The competitive Langmuir model under-estimated the 2,4-DCP solid-phase equilibrium (58 percent of the experimentally measured value. The semi-competitive Langmuir gave a better prediction (84 percent of the actual value). The graphic method gave a good approximation at 96 percent of the experimentally determined equilibrium concentration.

... Molar Ratio of 1.0:2.02 2,4-DCP to DNOSBP

This run consisted of saturating the carbon in a CSTR with a 76.64 μM solution of 2,4-DCP and then adding a step of input of DNOSBP at 156 μM . Figures VII-35 and VII-36 show the solid and fluid-phase concentration profiles, respectively. Table VII-3 summarizes the experimental and predicted solid-phase steady-state results. Actual experimentally measured values for DNOSBP and 2,4-DCP were 225 and 2350 micromoles per gram, respectively.

During this run 2,4-DCP was observed to desorb. This was not detected in any of the previous studies where 2,4-DCP was the initial solute applied to the carbon. The extent of desorption approximated 3 percent of the original solid-phase saturation value. The peak solution-phase concentration of 2,4-DCP due to desorption was 106 micromolar ($C/C_0 = 1.4$). This peak occurred at approximately 90 hours into the run.

The Langmuir models both over-estimated the adsorption of DNOSBP by 62 percent of the measured solid-phase steady-state concentration value. The graphical irreversible multi-solute technique predicted no adsorption of DNOSBP.

The 2,4-DCP adsorption predicted by the competitive Langmuir model amounted

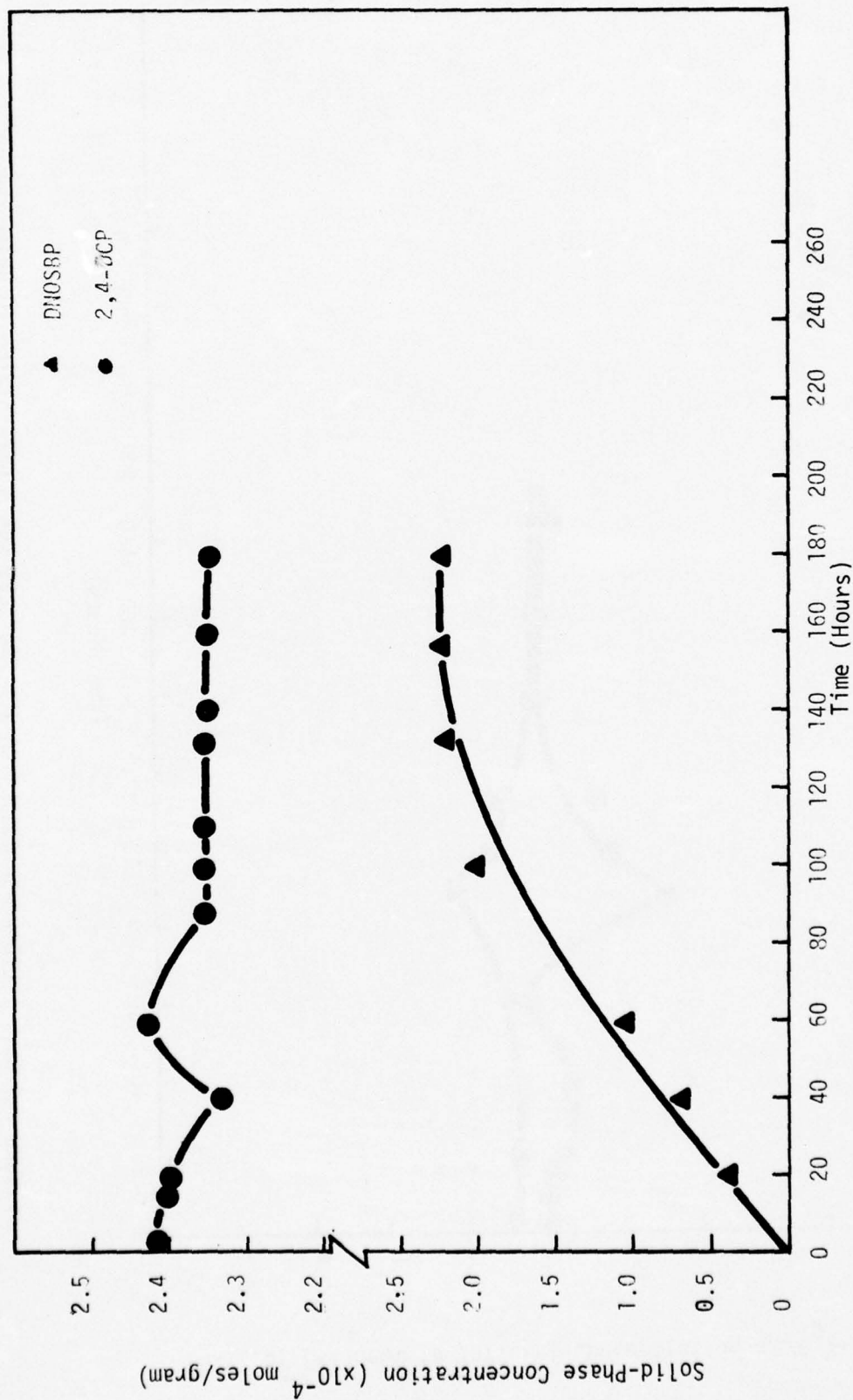


FIGURE VII-35: SOLID-PHASE CONCENTRATION PROFILES FOR A CSTR SYSTEM TO WHICH DNOSBP AND 2,4-DCP WERE INTRODUCED AT A MOLAR RATIO OF 2.02:1.0 AFTER THE ACTIVATED CARBON HAD BEEN PRESATURATED WITH 2,4-DCP (76.64 μM).

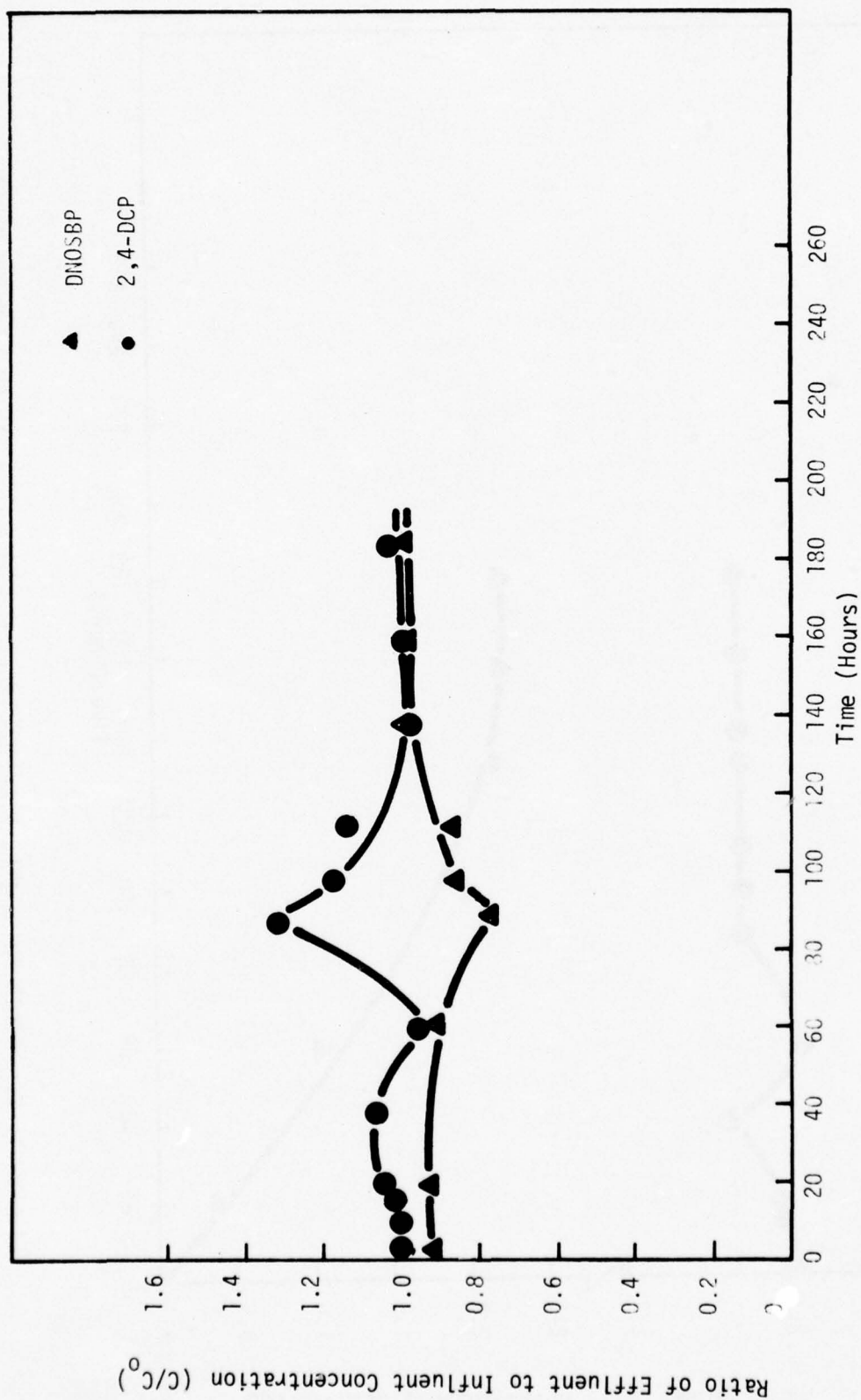


FIGURE VII-36: FLUID-PHASE CONCENTRATION PROFILES FOR A CSTR SYSTEM TO WHICH DNOSBP AND 2,4-DCP WERE INTRODUCED AT A MOLAR RATIO OF 2.02:1.0 AFTER THE ACTIVATED CARBON HAD BEEN PRESATURATED WITH 2,4-DCP ($76.64 \mu\text{M}$).

to only 47 percent of the experimentally measured solid-phase equilibrium value while the semi-competitive model was in much closer agreement (91 percent of the measured value).

SUMMARY

Observation of the experimental results and examination of the solid-phase and fluid-phase concentration profiles indicate a positive preferential adsorption for 2,4-DCP and OPP over DNOSBP. This was to be expected as the isotherms for the compounds indicate 2,4-DCP and OPP adsorb in much greater amounts than does DNOSBP when being applied to carbon in equal concentrations. This preferential adsorption can, in part, explain the ability of 2,4-DCP or OPP to displace DNOSBP from the absorbent during a run. This also explains the observation that 2,4-DCP and OPP, tended to be irreversibly adsorbed and did not desorb as a result of adding DNOSBP to the experimental system.

Calculations using the Langmuir multi-solute models and the graphical procedure, showed that neither can be accepted as logical tools for predicting multi-solute equilibria under dynamic condition.

CHAPTER VIII

MATHEMATICAL SIMULATIONS

A series of model simulations were conducted for the purpose of illustrating the design and operational alternatives one has for minimizing the occurrence of chromatographic displacement of adsorbed contaminants from an adsorber column. This involved use of the mathematical model developed in Chapter VI which consists of a set of dispersed flow mass balance equations and the appropriate kinetic and equilibrium relationships.

SIMULATION CONDITIONS

For the current simulations film diffusion was considered to limit the rate of transport of solute molecules from the bulk solution to the adsorbent surface. Because neither the Langmuir Competitive, Langmuir Semi-Competitive, Ideal Solution Theory, or Graphical adsorption isotherm models adequately described the multi-solute competitive adsorption equilibria as shown in Chapter VII, the Langmuir Competitive Adsorption isotherm model which assumes complete reversibility was employed for the simulations conducted as part of this study. This selection was made because the Langmuir Competitive multi-solute adsorption model allows one to simulate the most critical elution conditions that could potentially occur in prototype adsorbers. This in turn, permits the specification of a conservative (fail safe) set of design and operational criteria.

To simulate the most critical elution conditions from an engineering design and operations criteria viewpoint, all simulations were conducted for the case of two competing solutes, paranitrophenol (PNP) and parabromophenol (PBP) which were introduced to the adsorber column at concentrations of 1.0mM. For simulations the columnar adsorber was assumed to contain a polymeric adsorbent, Duolite A-7, and to be operated at a flow rate of 5 gpm/ft². The Langmuir equilibrium constants employed for the simulations are:

Paranitrophenol (PNP) $Q = 1.515$ millimoles per gram $b = 7457$ liters per moleParabromophenol (PBP) $Q = 3.495$ millimoles per gram $b = 650$ liters per mole

It is noteworthy that parabromophenol is adsorbed to a greater extent than is paranitrophenol at ultimate monolayer saturation, but has a lower energy of adsorption as evidenced by the relative b values.

SIMULATIONS

Six different simulations were conducted as part of this study. The first two were conducted for the operational condition in which the adsorbent was first saturated with PBP as a single-solute. After saturation, both PNP and PBP were introduced to the column at concentrations of 1.0 mM. The two simulations were conducted for the packed- and fluidized-bed cases. For the second set of simulations the order of addition of the competing compounds was reversed. That is, PNP was introduced first as a single-solute and the bisolute mixture was added thereafter. These, again, were run for the packed- and fluidized-bed cases. The final set of simulations were conducted for the case in which both PNP and PBP were introduced to the column simultaneously. As before, these simulations were conducted for packed- and fluidized-bed modes of operation.

PBP \rightarrow PNP

A set of simulations was conducted, as noted above, for the case in which the adsorbent in the columnar adsorber was presaturated with PBP at the 1.0mM concentration level. Subsequently, a solution which contained both PNP and PBP at the 1.0 mM level was introduced to the column. The simulation traces for both solution and solid-phases are given in Figures VIII-1 and VIII-2 for the packed- and fluidized-bed cases, respectively.

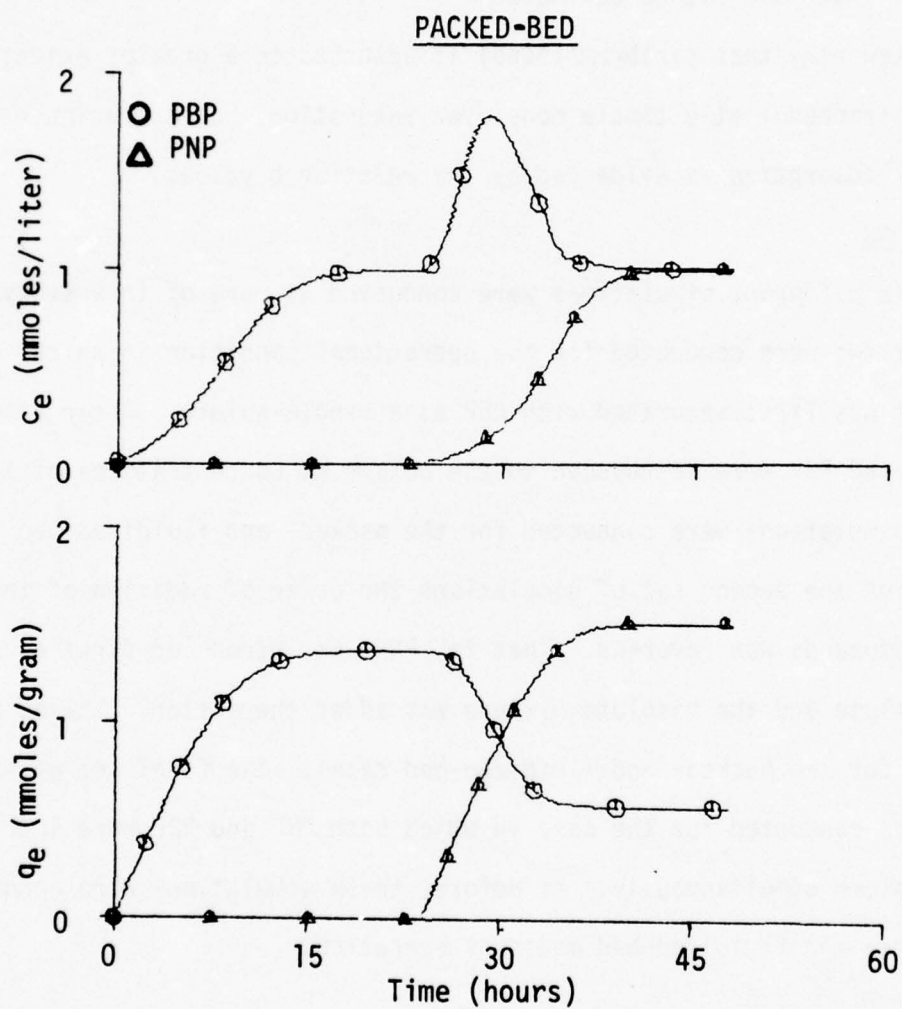


FIGURE VIII-1: SOLUTION- AND SOLID-PHASE CONCENTRATION PROFILES FOR PBP AND PNP FOR A PACKED-BED ADSORBER.

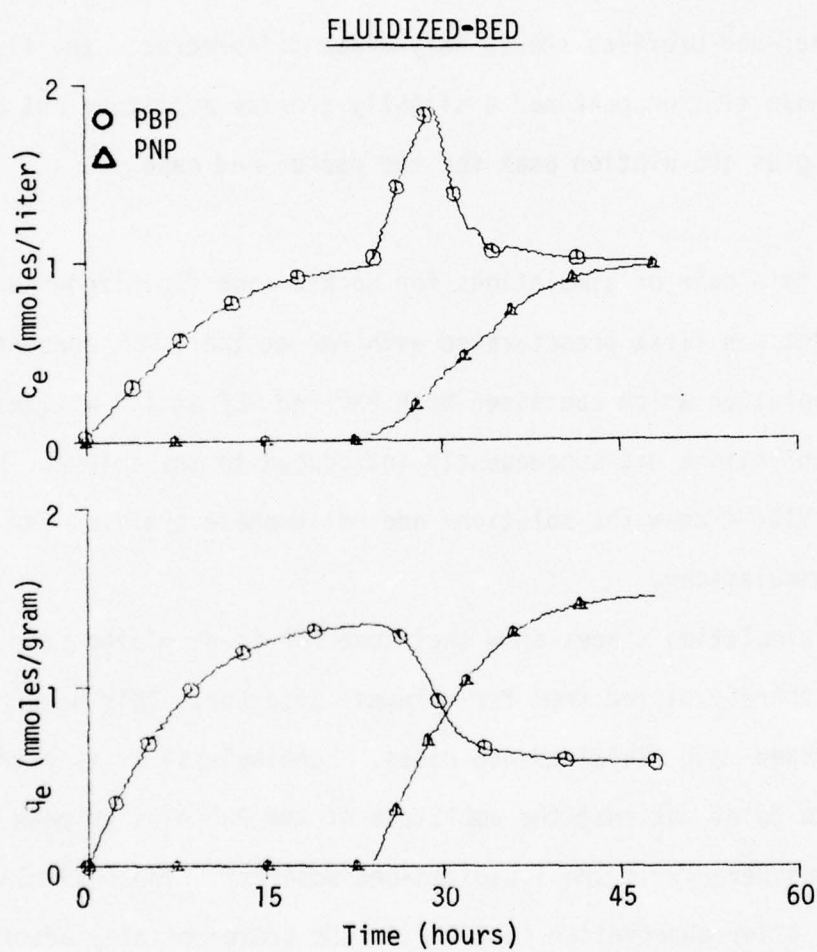


FIGURE VIII-2: SOLUTION- AND SOLID-PHASE CONCENTRATION PROFILES FOR PBP AND PNP FOR A FLUIDIZED-BED ADSORBER

It can be observed that as PNP was introduced to both packed- and fluidized-bed adsorbers a considerable quantity of adsorbed PBP was displaced from the adsorbent and was eluted into the effluent. This is evidenced by the concentration peak which can be observed for PBP in the solution-phase traces and by the decreasing solid-phase concentration of PBP. Further analysis of these simulations shows that PNP is the preferentially adsorbed solute and that PBP is competitively adsorbed. Comparison of the packed-bed and fluidized-bed profiles showed only minor differences: the fluidized-bed solution-phase elution peak had a slightly greater amplitude but did not prevail as long as the elution peak for the packed-bed case.

PNP \rightarrow PBP

For this pair of simulations for packed- and fluidized-bed adsorbers, the adsorbent was first presaturated with PNP at the 1.0mM concentration level. A solution which contained both PNP and PBP at 1.0 millimole per liter concentrations was subsequently introduced to the column. Figures VIII-3 and VIII-4 show the solution- and solid-phase profiles for this series of simulations.

The simulation traces show that some PNP is displaced from the adsorbent and is thereby eluted from the columnar adsorber. This occurred for both the packed- and fluidized-bed cases. Nonetheless, it is extremely important to point out that the amplitude of the PNP elution peak was dampened considerably in the fluidized-bed adsorber. These simulations also confirm the prior observation that PNP is the preferentially adsorbed solute and that PBP is competitively adsorbed.

Comparison of Figures VIII-3 and VIII-4 with Figures VIII-1 and VIII-2 show that the magnitude of the elution peak and the total quantity of solute eluted are diminished considerably when the preferentially adsorbed solute is applied to the column prior to the competitively adsorbed solute.

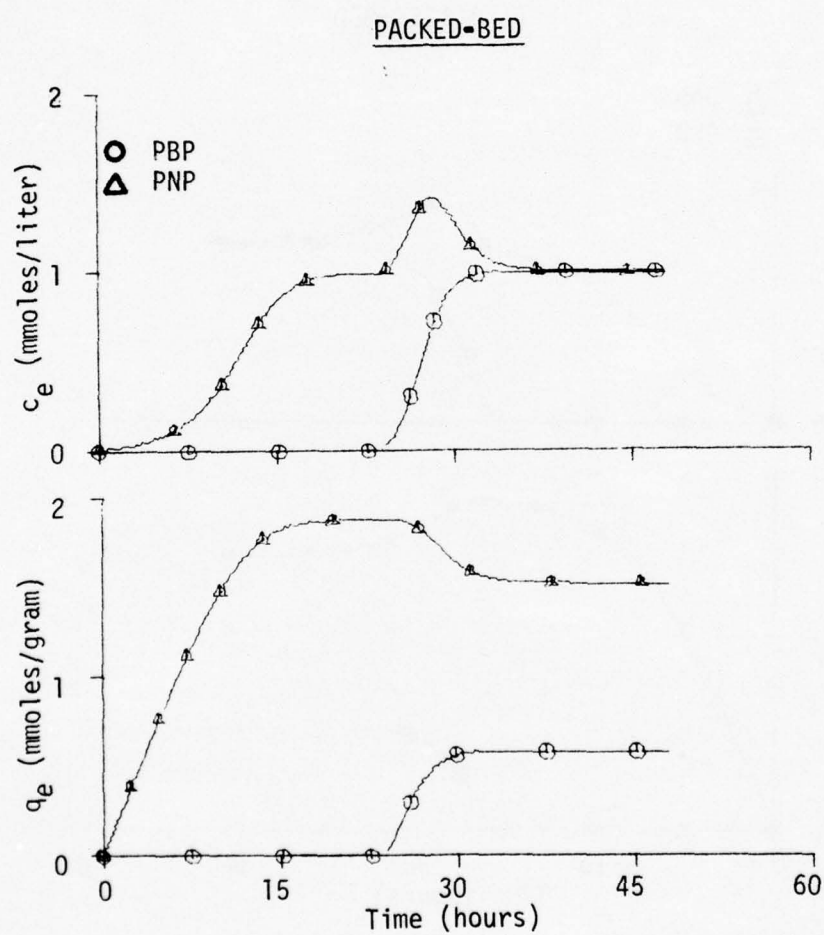


FIGURE VIII-3: SOLUTION- AND SOLID-PHASE CONCENTRATION PROFILES FOR PBP AND PNP FOR A PACKED-BED ADSORBER

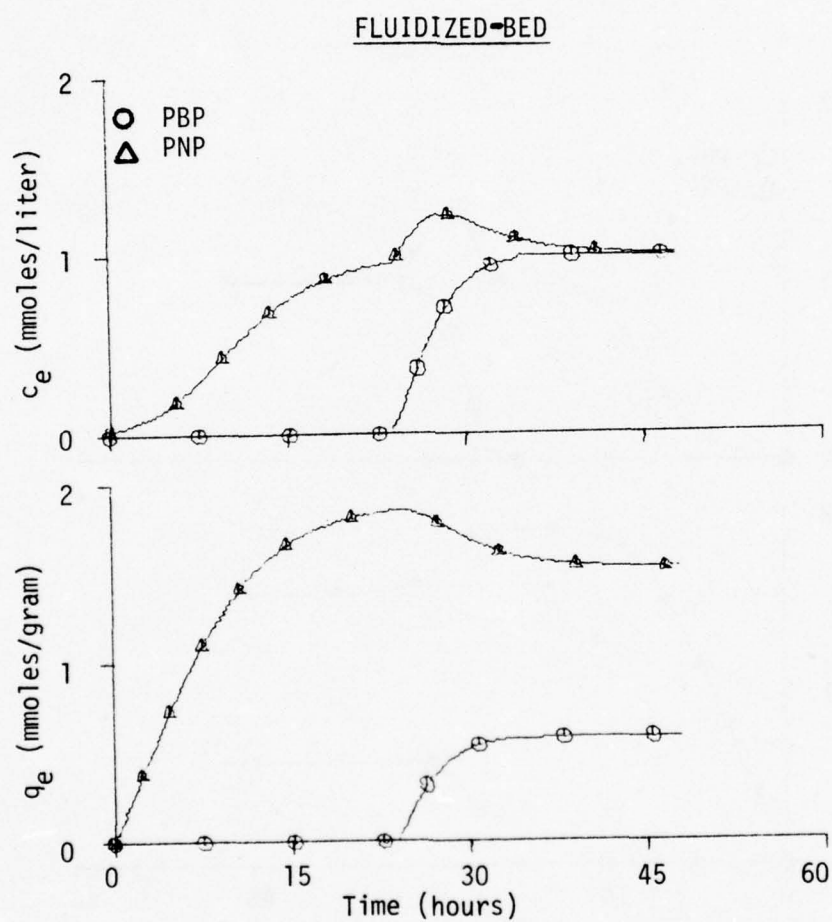


FIGURE VIII-4: SOLUTION- AND SOLID-PHASE CONCENTRATION PROFILES FOR PBP AND PNP FOR A FLUIDIZED-BED ADSORBER

This observation has rather significant implications with respect to the operation of prototype adsorbers. That is, if possible, production schedules should be arranged such that wastewaters containing the highest energy adsorbing contaminants are introduced first to a column of fresh adsorbent and the wastewaters containing the lowest energy adsorbing contaminants are introduced last.

PBP & PNP

The final series of simulations was conducted for the case in which both PBP and PNP were introduced to the adsorber column simultaneously at concentrations of 1.0mM. Figures VIII-5 and VIII-6 show the resultant solution- and solid-phase traces for the packed- and fluidized-bed cases, respectively.

For the packed-bed mode of operation, it is noted that a small quantity of PBP was displaced from the adsorbent and was subsequently eluted. This occurred due to the relative rates of adsorption of the two contaminants which resulted in a chromatographic separation of the compounds within the column. That is, PNP, being the preferentially adsorbed solute, adsorbed near the influent end of the column at the outset of the run while the PBP, being the competitively adsorbed solute, was adsorbed primarily near the effluent end of the adsorber. As time proceeded the PNP moved as a wave front through the column displacing the PBP ahead of it.

Comparing the results for the fluidized-bed mode of operation with those obtained for the packed-bed mode, one observes that essentially no PNP is displaced from the adsorbent. This can be attributed to the fact that the adsorbent solids are virtually completely mixed in a fluidized columnar adsorbent. This prevents the chromatographic separation of the solutes within the column and, therefore, eliminates the possibility for displacement and elution.

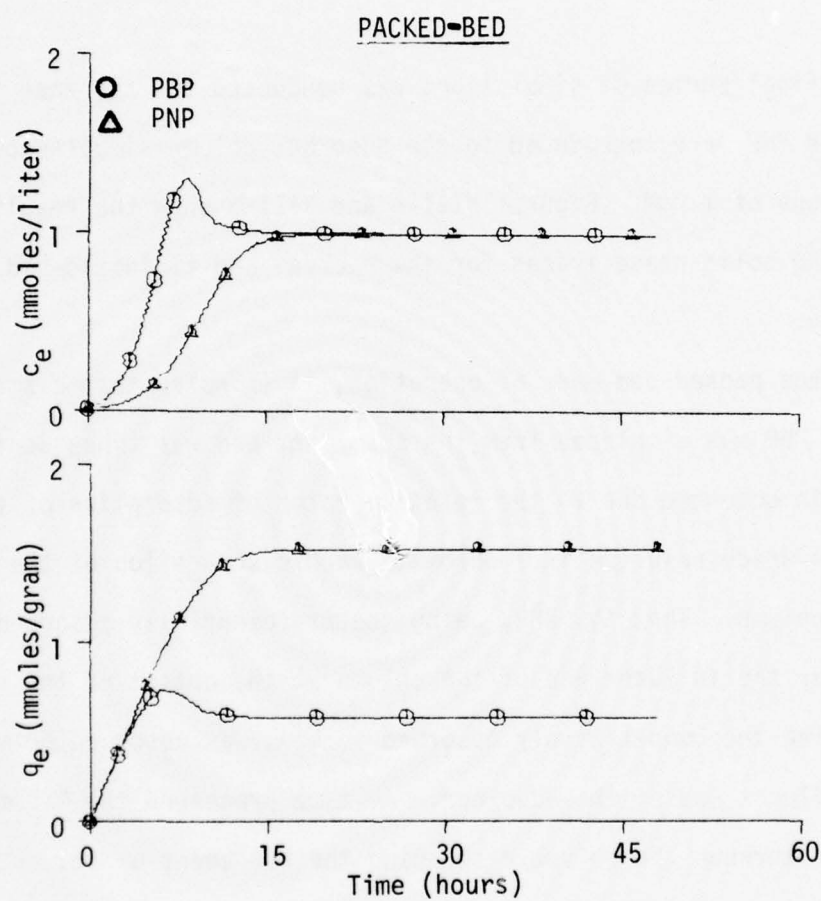


FIGURE VIII-5: SOLUTION- AND SOLID-PHASE CONCENTRATION PROFILES FOR PBP AND PNP FOR A PACKED-BED ADSORBER

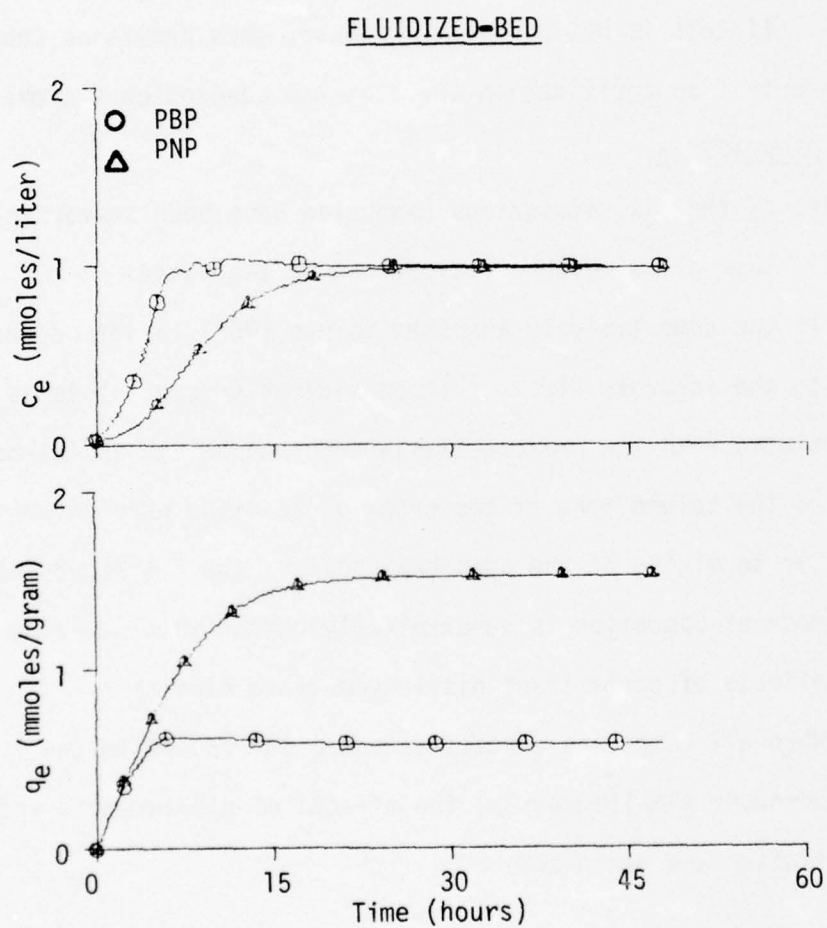


FIGURE VIII-6: SOLUTION- AND SOLID-PHASE CONCENTRATION PROFILES FOR PBP AND PNP FOR A FLUIDIZED-BED ADSORBER

These observations again underscore the conclusion that the fluidized-bed mode of operation has distinct operational advantages over the packed-bed method of solids-liquid contact. Moreover, the results of this series of simulations clearly establish that the effects of chromatographic displacement and elution can be minimized if the competing solutes are introduced to the adsorber simultaneously. This could be accomplished by arranging industrial production schedules such that all contaminants are discharged concurrently. If this is not possible, however, then provision should be made for concentration equilization ahead of the adsorption system.

SYNOPSIS OF SIMULATIONS

Results of the six simulations conducted have been summarized in Table VIII-1. The following observations can be tabulated:

- (1) If the competitively adsorbed solute (PBP) is introduced to the adsorber first, then considerably more solute is eluted when the preferentially adsorbed solute is introduced to the column than if the order of addition were reversed.
- (2) Due to mixing of the adsorbent solids, the fluidized-bed mode of operation is substantially better in minimizing the effects of contaminant displacement and elution.
- (3) When all competing contaminants are introduced to the adsorber simultaneously, the effects of displacement and elution are minimized.

TABLE VIII-1

SYNOPSIS OF SIMULATIONS

| Bed Design | Peak Concentration (millimoles/liter) | Solute Displaced (millimoles/gram) |
|---------------------------------|--|---------------------------------------|
| * * * <u>PBP then PNP</u> * * * | | |
| (low/high) | | |
| Packed | 1.782 (PBP) | 0.792 (PBP) |
| Fluidized | 1.852 (PBP) | 0.770 (PBP) |
| * * * <u>PNP then PBP</u> * * * | | |
| (high/low) | | |
| Packed | 1.411 (PNP) | 0.357 (PNP) |
| Fluidized | 1.226 (PNP) | 0.324 (PNP) |
| * * * <u>PNP and PBP</u> * * * | | |
| Packed | 1.309 (PBP) | 0.155 (PBP) |
| Fluidized | 1.043 (PBP) | 0.045 (PBP) |

CHAPTER IX
CONCLUSIONS AND RECOMMENDATIONS

- (1) Neither the Langmuir Competitive, Langmuir Semi-Competitive, Ideal Solution Theory, or Graphical adsorption isotherm models adequately described multisolute competitive adsorption equilibria.
- (2) To minimize the elution of adsorbed contaminants from adsorbers the fluidized-bed mode of operation offers distinct advantages over packed-bed operation.
- (3) If possible, industrial production schedules should be arranged such that all contaminants are discharged concurrently. This also serves to minimize the effects of chromatographic displacement of adsorbed contaminants.
- (4) If the above (3) is not possible, then production schedules should be arranged such that wastewaters containing the highest energy adsorbing contaminants are introduced first to a column of fresh adsorbent while the wastewaters containing the lowest energy adsorbing contaminants are introduced last.
- (5) Another design option which serves to minimize displacement and subsequent elution adsorbed contaminants is to make provision for concentration equilization in the process configuration ahead of the columnar adsorbers.

SELECTED BIBLIOGRAPHY

1. Vassiliou, B., and Dranoff, J. S. "The Kinetics of Ion Exclusion", *AIChE J.* 8, 248 (1962).
2. Weber, W. J., Jr., and Morris, J. C. "Kinetics of Adsorption on Carbon from Solution", *Proc. Amer. Soc. of Civil Engineers, San. Engr. Div.*, SA2, 31 (1963).
3. Amundson, N. R. "Mathematics of Adsorption in Beds, II," *J. Phys. and Colloid Chem.* 54, 812 (1950).
4. Amundson, N. R. "Solid-Fluid Interactions in Fixed and Moving Beds: Fixed Beds with Small Particles", *Ind. and Engr. Chem.* 48, 26 (1956).
5. Edeskuty, F. J., and Amundson, N. R. "Mathematics of Adsorption IV. Effect of Intraparticle Diffusion in Agitated Static System", *J. Phys. and Colloid Chem.* 56, 148 (1952).
6. Hobson, M., and Thodos, G. "Mass Transfer in the Flow of Liquids Through Granular Solids", *Chem. Engr. Prog.* 45, 517 (1949).
7. Hougen, O. A., and Marshall, W. R., Jr. "Adsorption from a Fluid Stream Flowing Through a Stationary Granular Bed", *Chem. Engr. Prog.* 43, 197 (1947).
8. Kasten, P. R., and Amundson, N. R. "An Elementary Theory of Adsorption in Fluidized Beds", *Ind. and Engr. Chem.* 42, 1341 (1950).
9. Kasten, P. R., and Amundson, N. R. "Analytical Solution for Simple Systems in Moving Bed Adsorbers", *Ind. and Engr. Chem.* 44, 1704 (1952).
10. Kasten, P. R., Lapidus, L., and Amundson, N. R. "Mathematics of Adsorption in Beds, V. Effect of Intraparticle Diffusion in Flow Systems in Fixed Beds", *J. Phys. and Colloid Chem.* 56, 683 (1952).
11. McCune, L. K., and Wilhelm, R. H. "Mass and Momentum Transfer in a Solid-Liquid System: Fixed and Fluidized Beds", *Ind. and Engr. Chem.* 41, 1124 (1949).
12. Resnick, W., and White, R. R. "Mass Transfer of Gas and Fluidized Solids", *Chem. Engr. Prog.* 45, 377 (1949).
13. Richardson, J. F., and Szekely, J. "Mass Transfer in a Fluidized Bed", *Trans. Instn. Chem. Engrs.* 39, 13 (1961).

14. Tien, C., and Thodos, G. "Ion Exchange Kinetics for Systems of Linear Equilibrium Relationships", *AIChE J.* 6, 364 (1960).
15. Furnas, C. C. "Heat Transfer from a Gas Stream to a Bed of Broken Solids", U. S. Bureau of Mines Bull. 361 (1932).
16. Goldstein, S. "The Mathematics of Exchange Processes in Fixed Columns", *Proc. Roy. Soc. (London)*, A219, 151 (1953).
17. Klinkenberg, A. "Heat Transfer in Cross-Flow Heat Exchangers and Packed-Beds -- Evaluation of Equations for Penetration of Heat or Solutes", *Ind. Engr. Chem.* 46, 2285 (1954).
18. Kostecki, J. A., Manning, F. S., and Canjar, L. N. "The Kinetics of Physical Adsorption of a Binary Liquid System in Fixed Beds", *Chem. Engr. Prog., Symp. Ser.* 63, 74, 90 (1967).
19. Vermeulen, T. "Theory for Irreversible and Constant Pattern Solid Diffusion", *Ind. Engr. Chem.* 45, 1664 (1953).
20. Vermeulen, T. "Separation by Adsorption Methods", *Adv. Chem. Engr.* 2, 147 (1958).
21. Colwell, C. J., and Dranoff, J. S. "The Kinetics of Sorption by Ion Exchange Resin Beds", *AIChE J.* 12, 304 (1966).
22. Rosen, J. B. "Kinetics of a Fixed-Bed System for Solid Diffusion into Spherical Particles", *J. Chem. Phys.* 20, 387 (1952).
23. Rosen, J. B. "General Numerical Solution for Solid Diffusion into Fixed Beds", *Ind. Engr. Chem.* 46, 1590 (1954).
24. Hall, K. R., Eagleton, L. C., Acrivos, A., and Vermeulen, T. "Pore and Solid Diffusion Kinetics in Fixed-Bed Adsorption Under Constant-Pattern Conditions", *Ind. Engr. Chem., Fund.* 5, 212 (1966).
25. Masamune, S., and Smith, J. M. "Adsorption Rate Studies -- Interaction of Diffusion and Surface Processes", *AIChE J.* 11, 34 (1965).
26. Weber, W. J., Jr., and Morris, J. C. "Equilibria and Capacities for Adsorption on Carbon", *Proc. Amer. Soc. of Civil Engineers, SED*, SA3, 79 (1964).
27. Hendricks, D. W. "Sorption in Flow-Through Porous Media", Paper presented at the "Symposium on Fundamentals of Transport Phenomena in Flow-Through Porous Media", Haifa, Israel (1969).

28. Acrivos, A. "On the Combined Effect of Longitudinal Diffusion and External Mass Transfer Resistance in Fixed Bed Operations", *Chem. Engr. Sci.* 13, No. 1 (1960).
29. Lapidus, L., and Rosen, J. B. "Experimental Investigations of Ion Exchange Mechanisms in Fixed Beds by Means of an Asymptotic Solution", *Chem. Engr. Prog.*, Symp. Ser. 50, 97 (1960).
30. Masamune, S., and Smith, J. M. "Adsorption Rate Studies -- Significance of Pore Diffusion", *AIChE J.* 10, 246 (1964).
31. Masamune, S., and Smith, J. M. "Transient Mass Transfer in a Fixed Bed", *Ind. Engr. Chem., Fundamentals* 3, 179 (1964).
32. Thomas, H. C. "Heterogeneous Ion Exchange in a Flowing System", *J. Amer. Chem. Soc.* 66, 1664 (1944).
33. Thomas, H. C. "Chromatography: A Problem in Kinetics", *Ann. N. Y. Acad. Sci.* 49, 161 (1948).
34. Hiester, N. K., and Vermeulen, T. "Saturation Performance of Ion Exchange and Adsorption Columns", *Chem. Engr. Prog.* 48, 505 (1952).
35. Allen, J. B., Joyce, R. S., and Kasch, R. H. "Process Design Calculations for Adsorption for Liquids in Beds of Activated Carbon", Paper presented at the Annual Meeting of the Water Pollution Control Federation held at Atlantic City (13 Oct 1965).
36. Allen, J. B., and Joyce, R. S. "Column Calculations for Intraparticle Diffusion Controlled Adsorption", *Chem. Engr. Prog.*, Symp. Ser. 74, 63 (1967).
37. Keinath, T. M. "A Mathematical Model for Prediction of Concentration Time Profiles for Design of Fluid-Bed Adsorbers" Dissert. Abstr. (1968).
38. Keinath, T. M., and Weber, W. J., Jr. "A Predictive Model for the Design of Fluid-Bed Adsorbers", *J. Water Poll. Control Fed.* 40, 741 (1968).
39. Weber, W. J., Jr., and Keinath, T. M. "Mass Transfer of Per-durable Pollutants from Dilute Aqueous Solution in Fluidized Adsorbers", *Chem. Engr. Prog.*, Symp. Ser. 63, 74, 79 (1967).
40. Cookson, J. T. "Design of Activated Carbon Adsorption Beds", Paper presented at the 42d Annual Conference of the Water Pollution Control Federation held at Dallas, Texas (5-10 October 1969).

41. Collins, H. W., Jr., and Chao, K. C. "A Dynamic Model for Multicomponent Fixed-Bed Adsorption", A publication of the School of Chemical Engineering, Purdue University (1971).
42. Gariepy, R. L., and Zwiebel, I., "Adsorption of Binary Mixtures in Fixed Beds", *AIChE Symp. Ser* 67, 117, 17 (1971).
43. Keinath, T. M. "Mathematical Modeling of Heterogeneous Sorption in Continuous Contactors for Wastewater Decontamination", Final Report for Contract No. DADA-17-72-C-2034 of the Department of the Army (1973).
44. Jain, J. S., and Snoeyink, V. L. "Adsorption from Bi-Solute Systems on Active Carbon" *J. Water Poll. Control Fed.* 45, 2463 (1973).
45. Radke, C. J., and Prausnitz, J. M., "Thermodynamics of Multi-Solute Adsorption from Dilute Liquid Solutions", *AIChE J.* 18, 761 (1972).
46. Crank, J. *Mathematics of Diffusion*, Clarendon Press, London (1965).
47. Anon. Continuous System Modeling Program III (CSMP III) Program Reference Manual. Program Number 5734-X59 (SH 19-7001-2) 3rd Ed., IBM Corporation (1972).
48. Meyers, A. L., and Prousmitz, J. M., "Thermo-dynamics of Mixed-Gas Adsorption." *AIChE J.* 11 (1965).
49. Perry, J. H., (ed.), *Chemical Engineers' Handbook*, 4th Ed., McGraw-Hill Book Company, New York (1963).
50. Gleuckauf, E., and Coates, J. I., "Theory of Chromatography", *Jour. Chem. Soc.*, 1315 (1947).
51. DiGiano, F. A., "Mathematical Modeling of Sorption Kinetics in Finite and Infinite Bath Systems." Technical Publication #T-69-1, University of Michigan (1969).
52. Chu, J. C., Kalil, J., and Wetteroth, W. A., "Mass Transfer in a Fluidized Bed," *Chem. Engr. Prog.*, 49, 141 (1953).
53. Pfeffer, R., and Happel, J., "An Analytical Study of Heat and Mass Transfer in Multiparticle Systems at Low Reynolds Numbers," *AIChE J.*, 10, 605 (1964).
54. Fan, L. T., Yang, Y. C., and Wen, C. Y., "Mass Transfer in Semi-Fluidized Beds for Solid-Liquid Systems." *AIChE J.* 3, 482 (1960).
55. Evans, G. C., and Gerald, C. F., *Chem. Engr. Prog.* 49, 135 (1953).

NOMENCLATURE

| <u>Symbol</u> | <u>Description</u> |
|-------------------|---|
| A | BET energy term, liters/mole |
| A | cross-sectional area of column, sq. cm. |
| b | Langmuir energy term, liters/mole |
| C | solution-phase concentration of solute, moles/liter |
| C_s | saturation concentration of solute in solution, moles/liter |
| D_{pore} | pore diffusivity, cm^2/sec |
| f_d | $(K_f/U) * (v/D_e)^{2/3}$, mass transfer factor, dimensionless |
| K | adjustable curve-fitting constant |
| n' | adjustable curve-fitting constant |
| n | number of elements |
| N_{Re} | $U * D_p/v$, Reynolds number, dimensionless |
| N_{Sc} | v/D_e , Schmidt number, dimensionless |
| N_{Sh} | $K_f * D_p/D_e$, Sherwood number, dimensionless |
| Q | ultimate uptake capacity of adsorbent, moles/gram |
| q | solid-phase concentration of solute, moles/gram |
| q_0 | initial solid-phase concentration (usually zero), moles/gram |
| R | separation factor, dimensionless |
| R_A | rate of adsorption, moles/gram-hour |
| r | radial distance within particle |
| t | times, hours |
| U | solution volumetric flow rate, liters/hour |
| \bar{U} | U/A , velocity of flow, cm/hr |
| V | volume of the element, liters |
| z | axial distance, cm |
| <hr/> | |
| ϵ | void ratio or porosity, dimensionless |
| Ψ | $1/(R + 15 (1 - R)/n^2)$ |
| ν | Kinematic viscosity of solution, cm^2/sec |
| ρ | packed-bed density, grams/liter |
| ρ_p | density of adsorbent particle, gm/liter |
| χ | internal porosity of adsorbent particles, dimensionless |

APPENDIX A

PHYSICAL CHARACTERISTICS OF ADSORBENT

DESCRIPTION

Calgon Corporation's granular activated carbon products (Filtrisorb 200) are made from select grades of coal resulting in superior hardness and long life. Produced under rigidly controlled conditions by high temperature steam activation, they are high density carbons with high surface areas. Their pore structures have been carefully controlled for the adsorption of both high and low molecular weight impurities from water. These coal-based carbons wet readily, do not float, and their high density allows convenient backwashing under conventional flow rate conditions. Each is available in a different mesh size to suit specific engineering design requirements.

PURPOSES

Filtrisorb 200 granular activated carbon products are designed for efficient use in water filtration equipment for the removal of organic impurities found in potable and industrial water supplies. These impurities include tastes, odors, color, insecticides, detergents, phenols, and other contaminants from both natural or industrial sources. Furthermore, Filtrisorb 200 is an effective filtration media for removal of turbidity and suspended matter. In addition to the adsorption and filtration functions, they are capable of concurrently removing excess oxidants such as chlorine and permanganate used in pretreatment application.

REACTIVATION

Granular activated carbon has been specifically manufactured for thermal reactivation and re-use. Numerous reactivation installations have demonstrated the feasibility and economy of granular carbon

reactivation. The carbon is handled as a water slurry between the filters and the furnace area. No additional labor or labor skills are required to operate a reactivation facility which is automated to run with minimal surveillance.

PHYSICAL PROPERTIES

| | FILTRASORB 200 |
|--|-------------------|
| Total surface area (N ₂ , BET method) m ² /g | 800 - 900 |
| Bed density backwashed and drained, lbs/ft | 30 approx. |
| Particle density wetted in water g/cc | 1.4 - 1.5 |
| Effective size mm | 0.55 - 0.65 |
| Uniformity coefficient | 1.7 or less |

SPECIFICATIONS

| | FILTRASORB 200 |
|--------------------------------------|-------------------|
| Sieve size U. S. Std. series | |
| Larger than No. 8--Max % | - |
| Larger than No. 14--Max % | 3 |
| Smaller than No. 30--Max % | - |
| Smaller than No. 40--Max % | 1 |
| Mean particle dia. mm | 0.9 |
| Iodine number--Min | 875 |
| Abrasion number--Min | 83 |
| Ash, Max % | 4.0 |
| Moisture as packed, Max % | 0.5 |

APPENDIX B

IDEAL SOLUTION THEORY EQUILIBRIUM COMPUTATION

The following program was used to compute the coefficients for the fifth order polynomial in describing single-solute isotherms:

```

C   PROGRAM FOR SOLVING SIMULTANEOUS
C   ALGEBRAIC EQUATIONS BY USE OF
C   SUBROUTINE SIMQ
      DIMENSION A(100), X(10)
C   READ THE NUMBER OF EQUATIONS
      READ (1,100) INDEX
100  FORMAT (I2)
C   READ THE COEFFICIENTS AND THE X
C   ARRAY
      DO 10 J = 1, INDEX
        IK = INDEX * (INDEX - 1) + J
        READ (1,110) (A(I), I=J, IK, INDEX), X(J)
110  FORMAT (6F12.0)
10   WRITE (3,120) (A(I)=J, IK, INDEX), X(J)
120  FORMAT (1H0,11F12.0)
      CALL SIMQ(A,X,INDEX,KS)
      WRITE(3,130) KS
130  FORMAT(1H,/,3HKS=,I4)
      DO 20 I=1, INDEX
20   WRITE(3,140) I, X(I)
140  FORMAT(1H,10X,2HX(,I2,2H)=,E15.6)
      STOP
      END

```

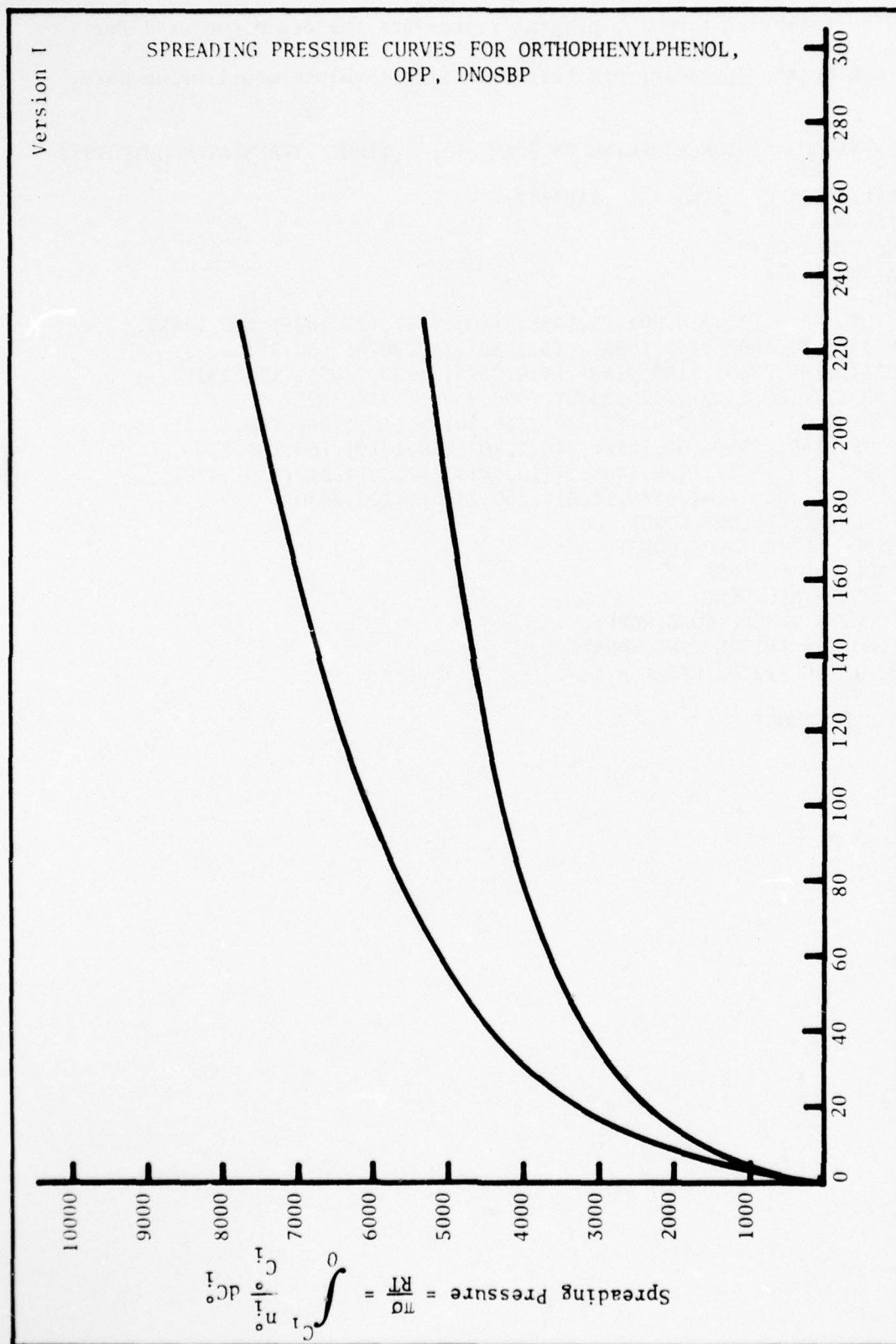
Note: The isotherm is separated into zones. For example, the simultaneous equations were:

$$\begin{aligned}
 (X/m)_1 &= K_1Ce_1 + K_2Ce_1^2 + K_3Ce_1^3 + K_4Ce_1^4 + K_5Ce_1^5 \\
 (X/m)_2 &= K_1Ce_2 + K_2Ce_2^2 + K_3Ce_2^3 + K_4Ce_2^4 + K_5Ce_2^5 \\
 &\quad \cdot \quad \cdot \quad \cdot \quad \cdot \quad \cdot \quad \cdot \\
 &\quad \cdot \quad \cdot \quad \cdot \quad \cdot \quad \cdot \quad \cdot \\
 &\quad \cdot \quad \cdot \quad \cdot \quad \cdot \quad \cdot \quad \cdot \\
 (X/m)_5 &= K_1Ce_5 + K_2Ce_5^2 + K_3Ce_5^3 + K_4Ce_5^4 + K_5Ce_5^5
 \end{aligned}$$

The following computer program represents the technique used for determining the spreading pressure from single-solute equilibrium data:

\$\$\$CONTINUOUS SYSTEM MODELING PROGRAM III VIMO TRANSLATOR OUTPUT\$\$\$

```
* COMPUTATION OF RADKE AND PRAUNITZ
INITIAL
  RENAME TIME= CONC
  INCON CONC =1.E-12
DYNAMIC
  FUNCTION OPP = (0.00,0.00),(5,1385),(10,1545),(15,1655),(20,1745),...
    (25,1820),(30,1880),(35,1938),(40,1988),(50,2070),(60,2140),...
    (80,2234),(90,2260),(100,2280),(110,2295),(120,2305),(130,2310),...
    (140,2318),(160,2320),(180,2325),(200,2325),(220,2325)
  FUNCTION DNOS = (0.0,0.0),(5,870),(10,1015),(15,1100),(20,1155),...
    (25,1195),(30,1225),(35,1255),(40,1280),(50,1310),(60,1340),...
    (80,1380),(90,1395),(100,1405),(110,1415),(120,1420),(130,1428),...
    (140,1430),(160,1440),(180,1450),(200,1450),(220,1450)
    NOC =NLFGEN(OPP,CONC)
    NDC =NLFGEN(DNOS,CONC)
    NOPP = NOC/CONC
    NDNS = NDC/CONC
    OPPT = INTGRL(CONC,NOPP)
    DNST = INTGRL(CONC,NDNS)
  TIMER FINTIM = 225, PRDEL = 1
  METHOD RKS
  PRINT OPPT,DNST
END
STOP
```



The method of solution of multi-solute equilibrium system per
telephonic communication Dr. C. Radke:

FORTRAN COMPILER VERSION 2.3 B.1

15 FEB 71

```

SUBROUTINE NEWTON ( NMAX, X, C1, C2 )
COMMON A1, A2, B1, B2, RN1, RN2
DO 1 I=1,NMAX
CALL FUNC ( I, X, F, DF, C1, C2 )
XN = X - F/DF
S = ( ( XN - X )**2 ) / XN**2
X = XN
IF ( S - 1.E-5 ) 2,2,5
5 IF ( X . GT. 1.0 ) X = 0.95
IF ( X . LT. 0.0 ) X = 0.05
1 CONTINUE
2 PRINT 3
3 FORMAT ( // * I MOLE FRAC FUNCTION ERROR *//)
PRINT 4, I, X, F, X
4 FORMAT ( I4, 3E12.5// )
RETURN
END

```

NMAX Maximum iterations allowed for Newton procedure initial guess
X and final answer for adsorbed phase composition (use a guess
 of X = 0.5)

C1, C2 Given mixture concentrations of solutes 1 and 2.

A1, A2, Constants in equations B2 (32).
B1, B2,
RN1, RN1

FUNC Subroutine

I The i^{th} iteration of Newton procedure.

F The function whose root is desired $f(Z_1)=0=F\left|\frac{C_1}{Z_1}\right|-f_2\left|\frac{C_2}{1-Z_1}\right|$

DF The derivative of that function.

XN The next best root.

S Test of convergence. When $S < 10^{-5}$, X is the answer you may
 want another test other than percentage error.

FORTRAN COMPILER VERSION 2.3 B.1

```
SUBROUTINE FUNC ( I, X, F, DF, C1, C2 )  
COMMON A1, A2, B1, B2, RN1, RN2  
Z = X  
F = Z/(A1*C1) - (1.-Z)/(A2*C2) + ( (Z/C1)**RN1)/B1 - ( ( (1.-Z)/  
1 C2)**RN2)/B2  
DF = 1./(A1*C1) + 1./(A2*C2) + ( RN1*(Z**(RN1-1.)))/((C1**RN1)*B1)  
1 + ( RN2*((1.-Z**(RN2-1.)))/((C2**RN2)*B2)  
RETURN  
END
```

APPENDIX C

LISTING OF COMPUTER PROGRAM

```
*****
*****
*****
```

INITIAL

```
*****
```

```
FIXED I,J,K
STORAGE CA(11),CB(11)
```

```
*****
```

```
*** PARAMETER INPUTS REQUIRED ARE DEFINED AS FOLLOWS ***
```

```
*****
```

```
***
```

```
*** CARBON --- MASS OF CARBON IN BED (GRAMS) ***
```

```
*** A --- EXTERNAL TRANSFER AREA FOR CARBON (SQ CM/GRAM) ***
```

```
*** DP --- DIAMETER OF CARBON PARTICLES (CM) ***
```

```
*** RHOPAC --- PACKED BED DENSITY (GRAMS/LITER) ***
```

```
*** EPS --- PACKED BED POROSITY (DIMENSIONLESS) ***
```

```
*** QAMAX --- LANGMUIR ULTIMATE UPTAKE CAPACITY FOR A (MOLES/GRAM) ***
```

```
*** QBMAX --- LANGMUIR ULTIMATE UPTAKE CAPACITY FOR B (MOLES/GRAM) ***
```

```
*** BA --- LANGMUIR ENERGY TERM FOR A (LITERS/MOLE) ***
```

```
*** BB --- LANGMUIR ENERGY TERM FOR B (LITERS/MOLE) ***
```

```
*** CA(1) --- SOLUTION-PHASE CONCENTRATION OF A (MOLES/LITER) ***
```

```
*** CB(1) --- SOLUTION-PHASE CONCENTRATION OF B (MOLES/LITER) ***
```

```
*** DLA --- DIFFUSIVITY OF SOLUTE A (SQ CM/SEC) ***
```

```
*** DLB --- DIFFUSIVITY OF SOLUTE B (SQ CM/SEC) ***
```

```
*** AREA --- CROSS-SECTIONAL AREA OF COLUMN (SQ CM) ***
```

```
*** U --- SOLUTION VOLUMETRIC FLOW RATE (LITERS/HOUR) ***
```

```
*** GAMMA --- KINEMATIC VISCOSITY OF WATER (SQ CM/SEC) ***
```

```
*** EXP --- RATIO: EXPANDED /PACKED BED VOLUME (DIMENSIONLESS) ***
```

```
***
```

```
*****
```

```
*** PARAMETER INPUTS FOLLOW ***
```

```
*****
```

```
PARAM CARBON=36.79
```

```
PARAM A=124.6
```

```
PARAM DP=9.55E-2
```

```
PARAM RHOPAC=253.
```

```
PARAM EPS=0.43
```

```
PARAM QAMAX=3.4958E-3
```

```
PARAM BA=650.
```

```
TABLE CA(1)=1.E-3
```

```
TABLE CB(1)=1.E-3
```

```
PARAM CAO=1.E-3
```

```
PARAM CBO=1.E-3
```

```
PARAM DLA=8.672E-6
```

```
PARAM DLB=8.54E-6
```

```
PARAM AREA=4.978
```

```
PARAM U=6.12
```

```
PARAM GAMMA=9.348E-3
```

```
PARAM EXP=(1.0,1.5)
```

 *** CALCULATED INPUT PARAMETERS ARE DEFINED AS FOLLOWS ***

 *** RHO ----- EXPANDED BED DENSITY (GRAMS/ LITER) ***
 *** VP ----- TOTAL VOLUME OF PACKED BED (LITERS) ***
 *** V ----- TOTAL VOLUME OF PACKED BED (LITERS) ***
 *** EPSI ----- EXPANDED BED POROSITY (DIMENSIONLESS) ***
 *** UBAR ----- SUPERFICIAL VELOCITY OF FLOW THROUGH BED (CM/SEC) ***
 *** NREMOD --- MODIFIED REYNOLDS NUMBER (DIMENSIONLESS) ***
 *** NSCA ----- SCHMIDT NUMBER FOR A (DIMENSIONLESS) ***
 *** NSCB ----- SCHMIDT NUMBER FOR B (DIMENSIONLESS) ***
 *** JD ----- MASS TRANSFER FACTOR (DIMENSIONLESS) ***
 *** KFA ----- MASS TRANSFER COEFFICIENT FOR A (CM/HOUR) ***
 *** KFB ----- MASS TRANSFER COEFFICIENT FOR B (CM/HOUR) ***
 *** DUM1 ----- DUMMY COEFFICIENT ***
 *** DUM2 ----- DUMMY COEFFICIENT ***
 *** DUM3 ----- DUMMY COEFFICIENT ***

 *** INPUT PARAMETER CALCULATIONS FOLLOW ***

RHO=RHOPAC/EXP
 VP=CARBON/(RHOPAC*10.)
 V=CARBON/(RHO*10.)
 EPSI=(EPS*VP+V-VP)/V
 UBAR=(U*0.277777)/AREA
 NREMOD=(UBAR*DP)/(GAMMA*(1.-EPSI))
 NSCA=GAMMA/DLA
 NSCB=GAMMA/DLB
 JD=1.34*NREMOD**(-0.468)
 KFA=(JD*UBAR/NSCA**((2./3.))*3600.
 KFB=(JD*UBAR/NSCB**((2./3.))*3600.
 DUM1=U/(EPSI*V)
 DUM2=(KFA*A*RHO*1.E-3)/EPSI
 DUM3=(KFB*A*RHO*1.E-3)/EPSI

 *** INITIAL CONDITIONS FOR SOLID PHASE CONCENTRATION ***

TABLE ICQA(2-11)=11*0.0
 TABLE ICQB(2-11)=11*0.0

 *** LINEARIZED ISOTHERM DATA FOR COMPONENT B (PNP) ***

FUNCTION ISJB=(410.,500.),(530.,1000.),(628.,1500.),...
 (710.,2000.),(783.,2500.),(851.,3000.),(912.,3500.),...
 (970.,4000.),(1075.,5000.),(1170.,6000.),(1347.,8000.),...
 (1523.,10000.),(1700.,12000.),(1877.,14000.),(2054.,16000.),...
 (2230.,18000.),(2407.,20000.),(4000.,38031.),(6000.,60668.),...
 (8000.,83305.),(10000.,105942.),(12000.,128579.),...
 (14000.,151216.),(16000.,173853.),(18000.,196491.),...
 (20000.,219128.)

DYNAMIC

*** DIFFERENTIAL EQUATIONS FOR ADSORPTION BED ***

QA=INTGRL(ICQA,QADDT,11)

QB=INTGRL(ICQB,QBDOT,11)

PROCEDURE QADDT,QBDOT=ADS(QA,QB,ISOB,QAMAX,BA,KFA,KFB,A)

DO 10 I=2,11

IF (QB(I).LT.5.E-5) QBINV=2.E+4

IF (QB(I).GE.5.E-5) QBINV=1/QB(I)

CBINV=FUNGEN(ISOB,5,QBINV)

BSLOPE=SLOPE(ISOB,3,QBINV)

QBMAX=1/(QBINV-(1/BSLOPE)*CBINV)

BB=BSLOPE/QBMAX

CSTARA=QBMAX*BB*QA(I)/(QAMAX*QBMAX*BA*BB-QAMAX*QB(I)*BA*BB...

-QBMAX*QA(I)*BA*BB)

CSTARB=QAMAX*BA*QB(I)/(QAMAX*QBMAX*BA*BB-QAMAX*QB(I)*BA*BB...

-QBMAX*QA(I)*BA*BB)

CA(I)=(DUM1*CA(I-1)+DUM2*CSTARA)/(DUM1+DUM2)

CB(I)=(DUM1*CB(I-1)+DUM3*CSTARB)/(DUM1+DUM3)

QADDT(I)=KFA*A*(CA(I)-CSTARA)*1.E-3

QBDOT(I)=KFB*A*(CB(I)-CSTARB)*1.E-3

10 CONTINUE

ENDPROCEDURE

*** TO ACCOUNT FOR MIXING OF CARBON IN FLUIDIZED BEDS (EXP>1.0), ***

*** AVERAGE SOLID-PHASE CONCENTRATIONS ARE CALCULATED AND QA'S & ***

*** QB'S ARE REINITIALIZED AT THE AVERAGE VALUES ***

PROCEDURE QAT,QBT=SORBED(QA,QB)

QATOT=0.

QBTOT=0.

DO 11 J=2,11

QATOT=QATOT+QA(J)

11 QBTOT=QBTOT+QB(J)

QAT=QATOT/10.

QBT=QBTOT/10.

IF (EXP.EQ.1.0) GO TO 13

DO 12 K=2,11

QA(K)=QAT

12 QB(K)=QBT

13 CONTINUE

ENDPROCEDURE

TERMINAL

*** EXECUTION CONTROL STATEMENTS ***

METHOD RECT

TIMER DELT=.20,FINTIM=48.0,PRDEL=0.2,OUTDEL=0.4

*** OUTPUT CONTROL STATEMENTS ***

PRINT QA(2-11),QB(2-11)

OUTPUT TIME,CA(11),CB(11)

PAGE GROUP=(0.,2.E-3)

OUTPUT TIME,QAT,QBT

PAGE GROUP=(0.,2.E-3)

OUTPUT TIME,CA(11),CB(11)

PAGE XYPLT,HEIGHT=5.0,WIDT4=8.0,GROUP=(0.,2.E-3)

OUTPUT TIME,QAT,QBT

PAGE XYPLT,HEIGHT=5.0,WIDTH=8.0,GROUP=(0.,2.E-3)

END

STOP

ENDJOB

APPENDIX D

SINGLE-SOLUTE PRESATURATION STUDIES:
SOLUTION AND SOLID-PHASE STUDIES

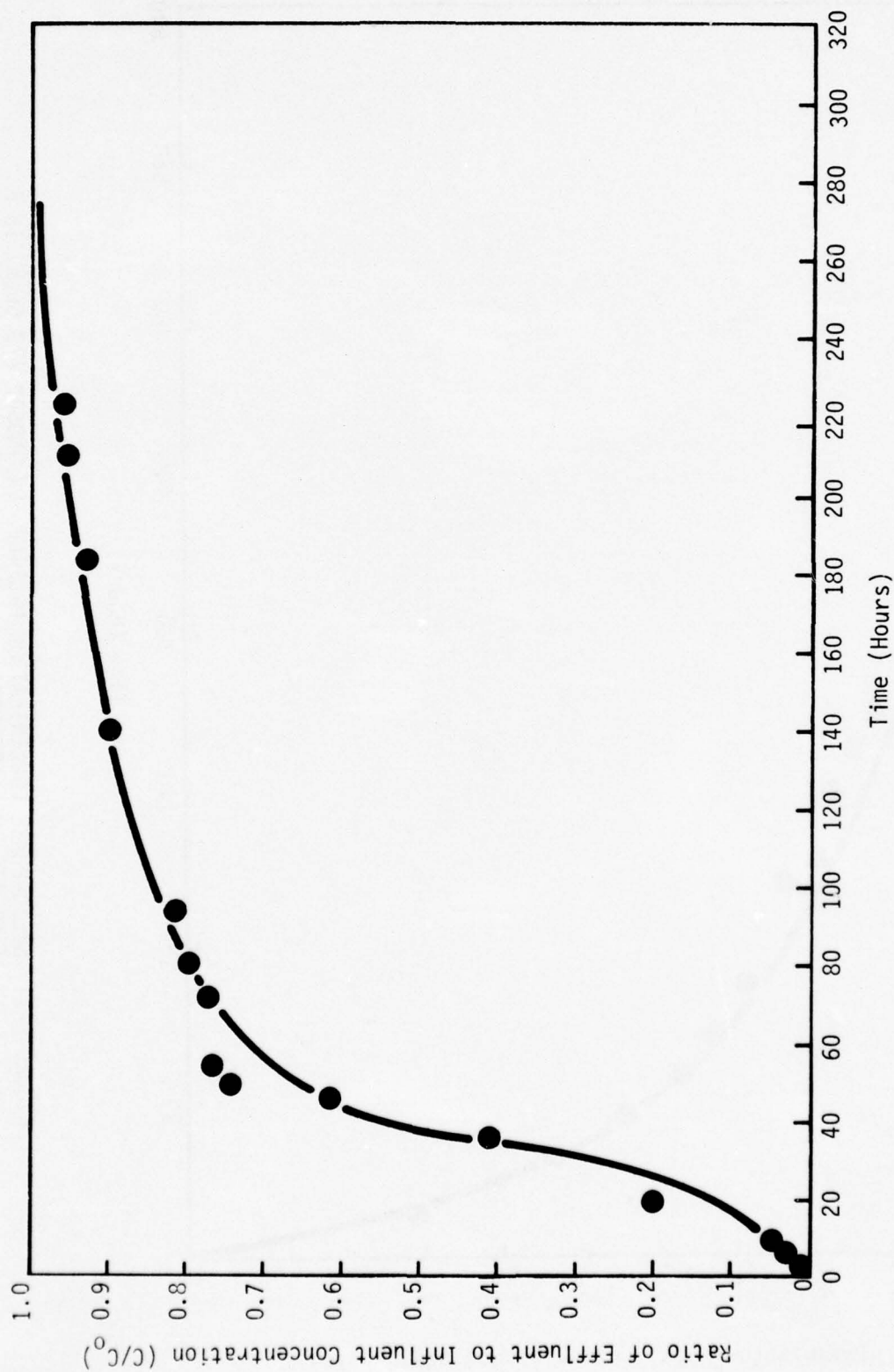


FIGURE D-1: FLUID-PHASE CONCENTRATION PROFILE FOR DNOSBP (79.56 μ M) IN A FLUIDIZED-BED ADSORBER.

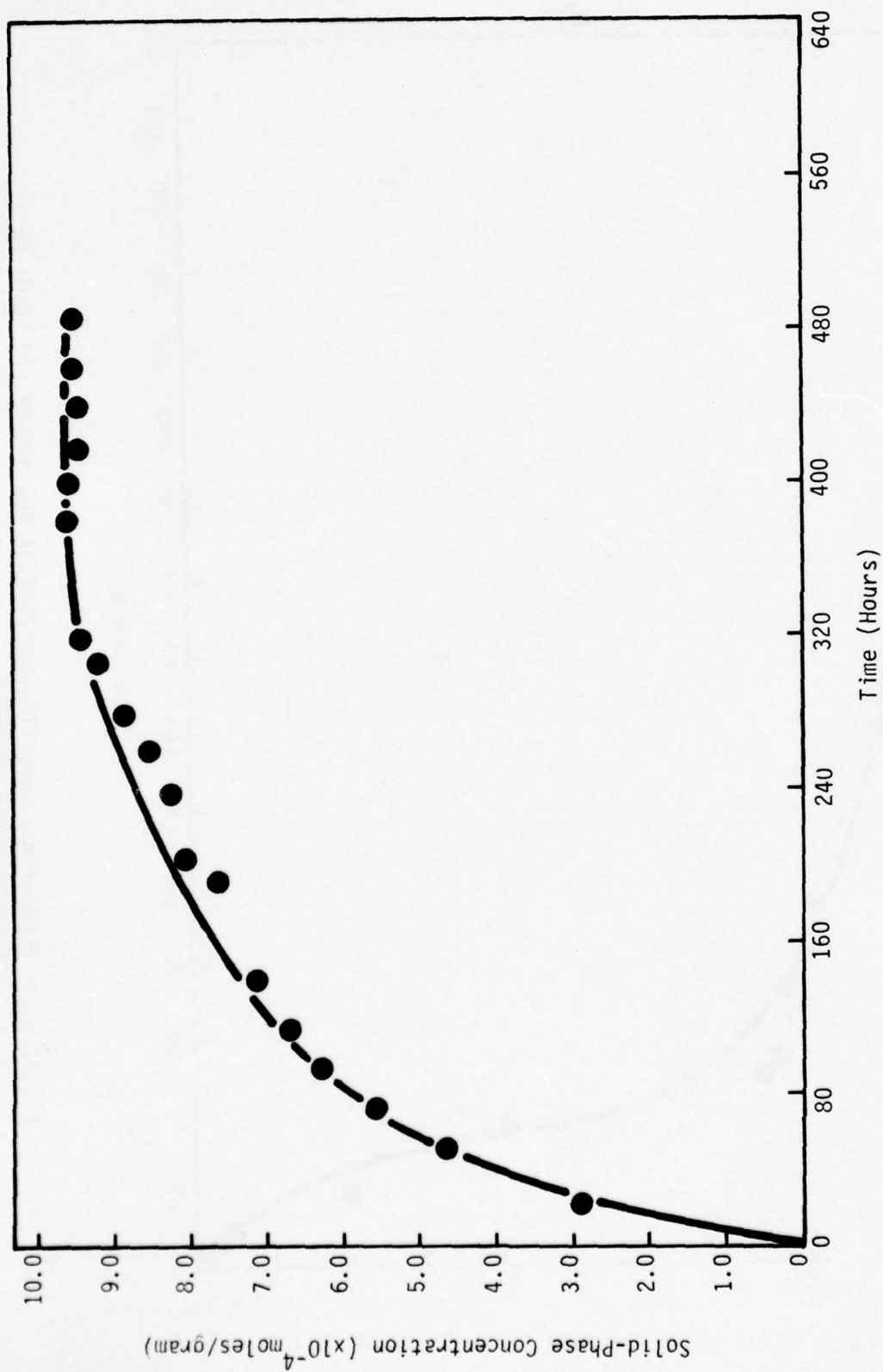


FIGURE D-2: SOLID-PHASE CONCENTRATION PROFILE FOR DNOSBP (79.56 μ M) IN A FLUIDIZED-BED ADSORBER.

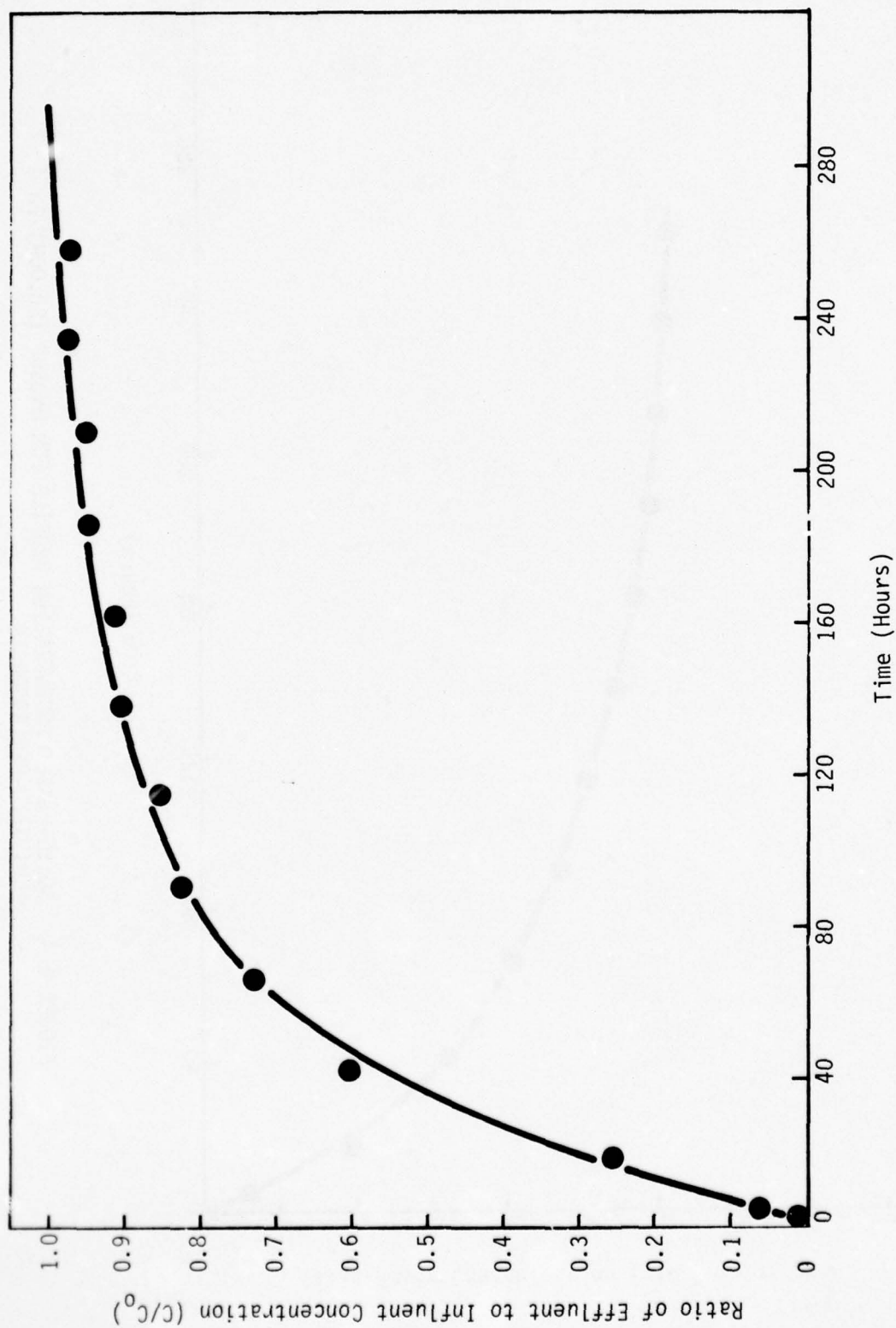


FIGURE D-3: FLUID-PHASE CONCENTRATION PROFILE FOR DNOSBP (80.0 μ M) IN A FLUIDIZED-BED ADSORBER.

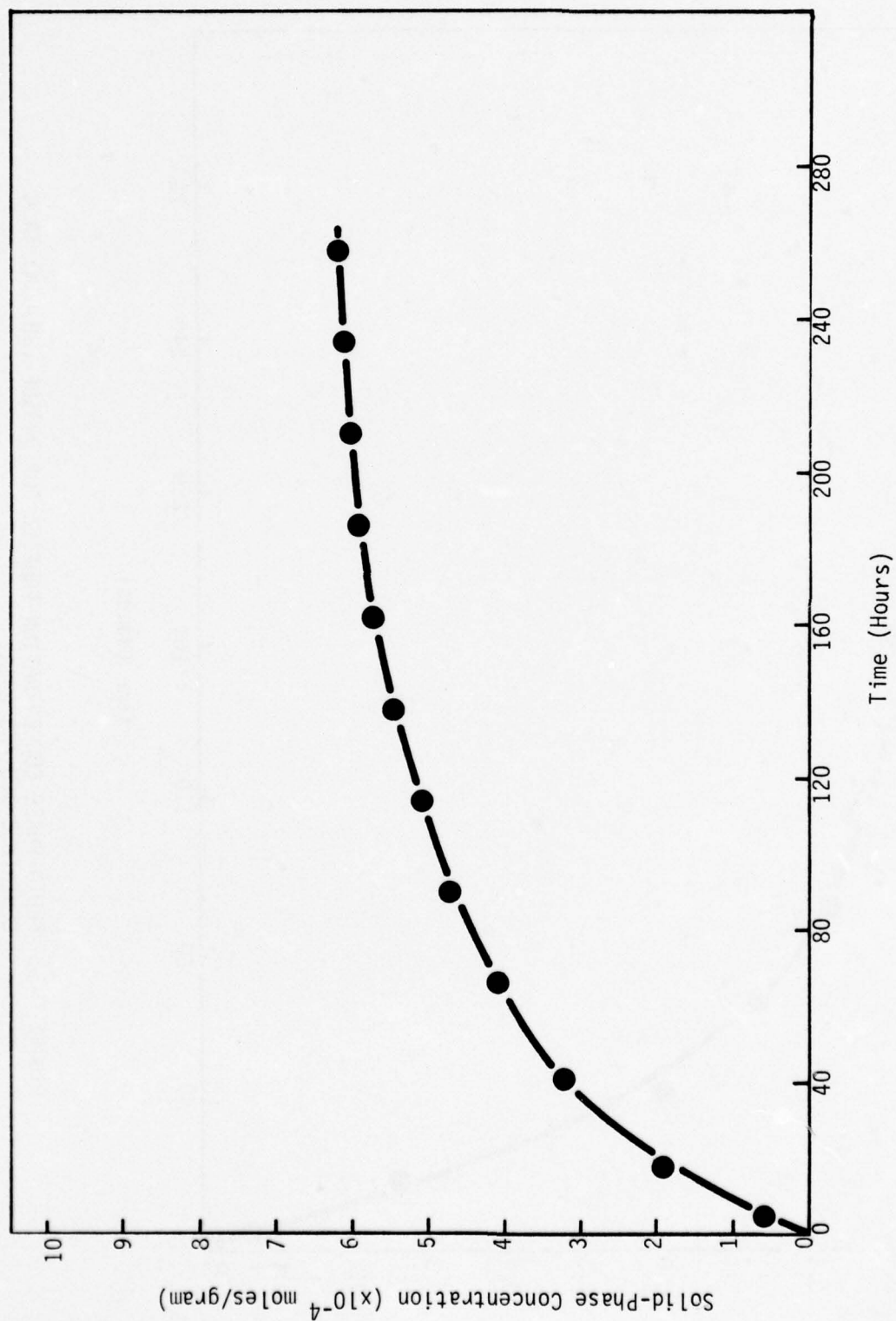


FIGURE D-4: SOLID-PHASE CONCENTRATION PROFILE FOR DNOSBP (80.0 μ M) IN A FLUIDIZED-BED ADSORBER.

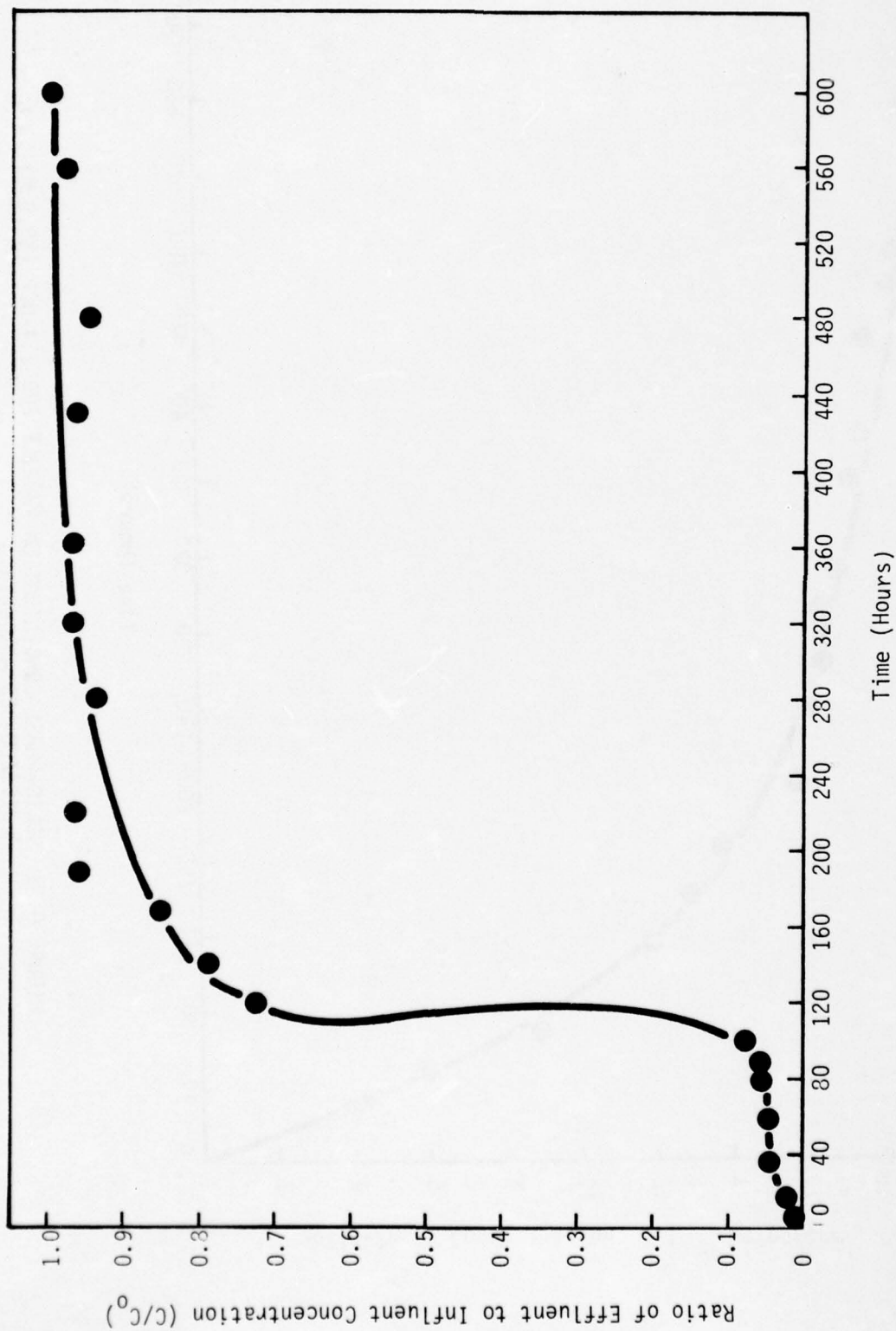


FIGURE D-5: FLUID-PHASE CONCENTRATION PROFILE FOR 2,4-DCP (80.0 μ M) IN A FLUIDIZED-BED ADSORBER.

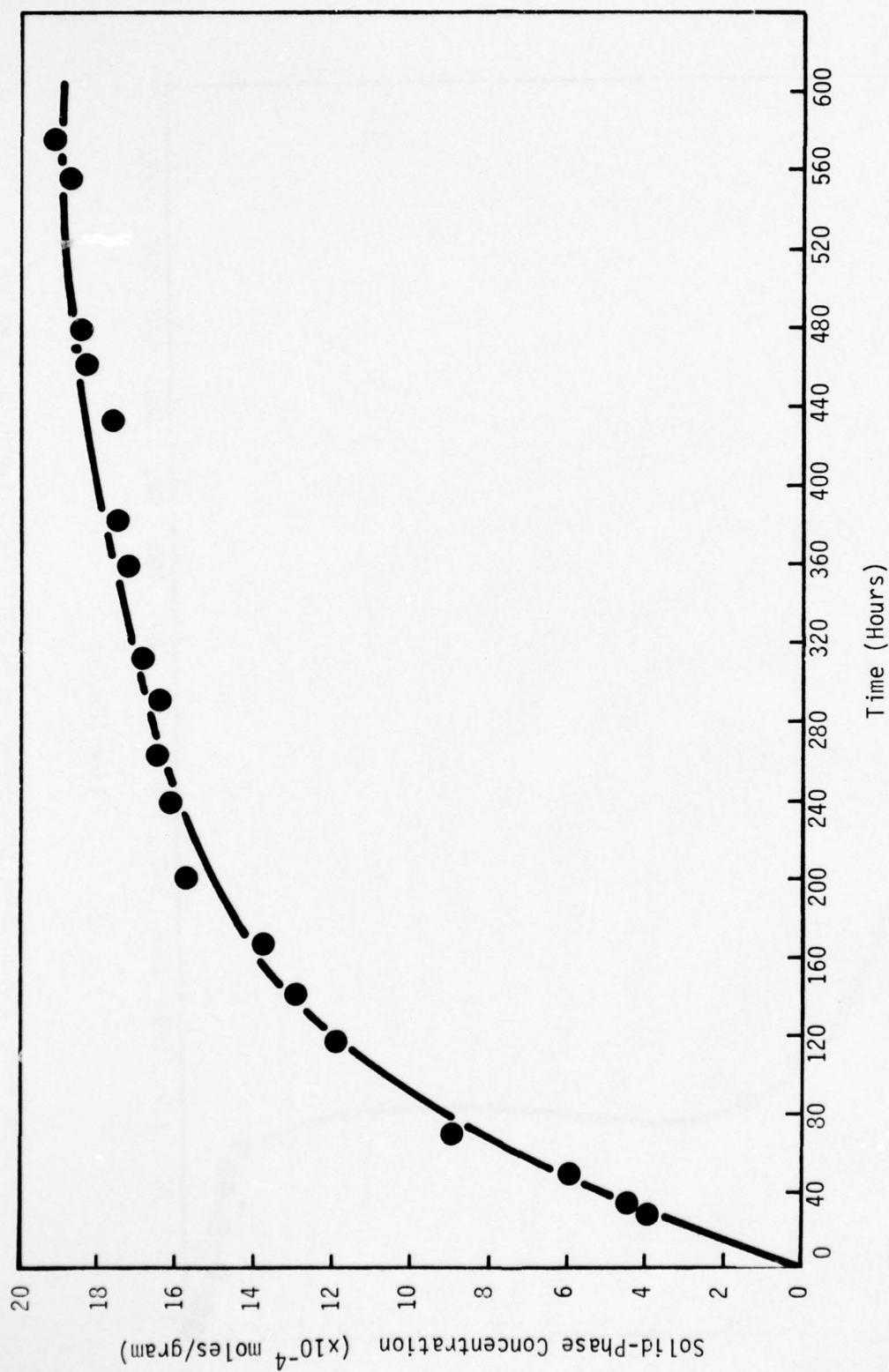


FIGURE D-6: SOLID-PHASE CONCENTRATION PROFILE FOR 2,4-DCP (80.0 μ M) IN A FLUIDIZED-BED ADSORBER.

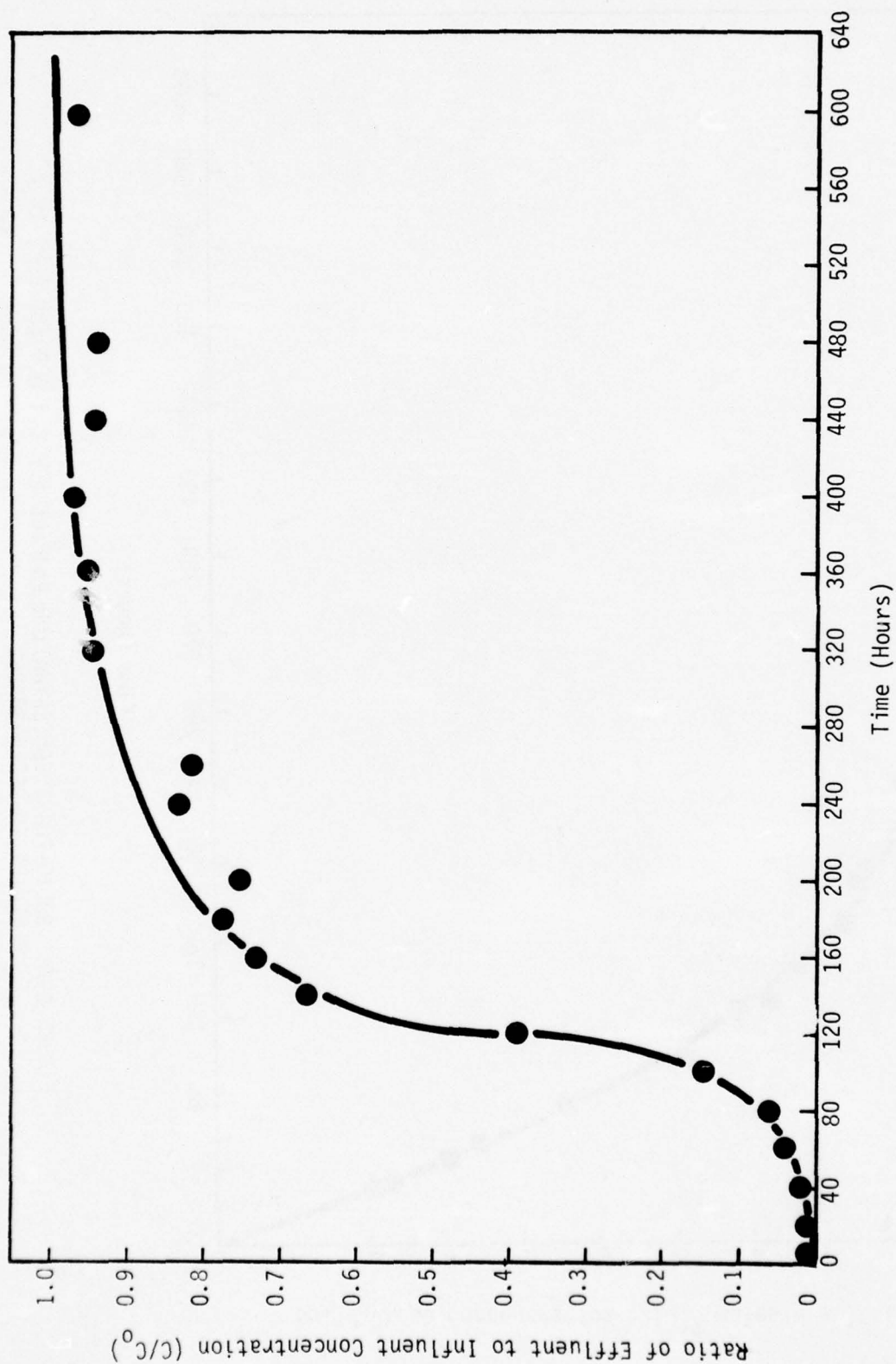


FIGURE D-7: FLUID-PHASE CONCENTRATION PROFILE FOR 2,4-DCP (80.0 μ M) IN A FLUIDIZED-BED ADSORBER.

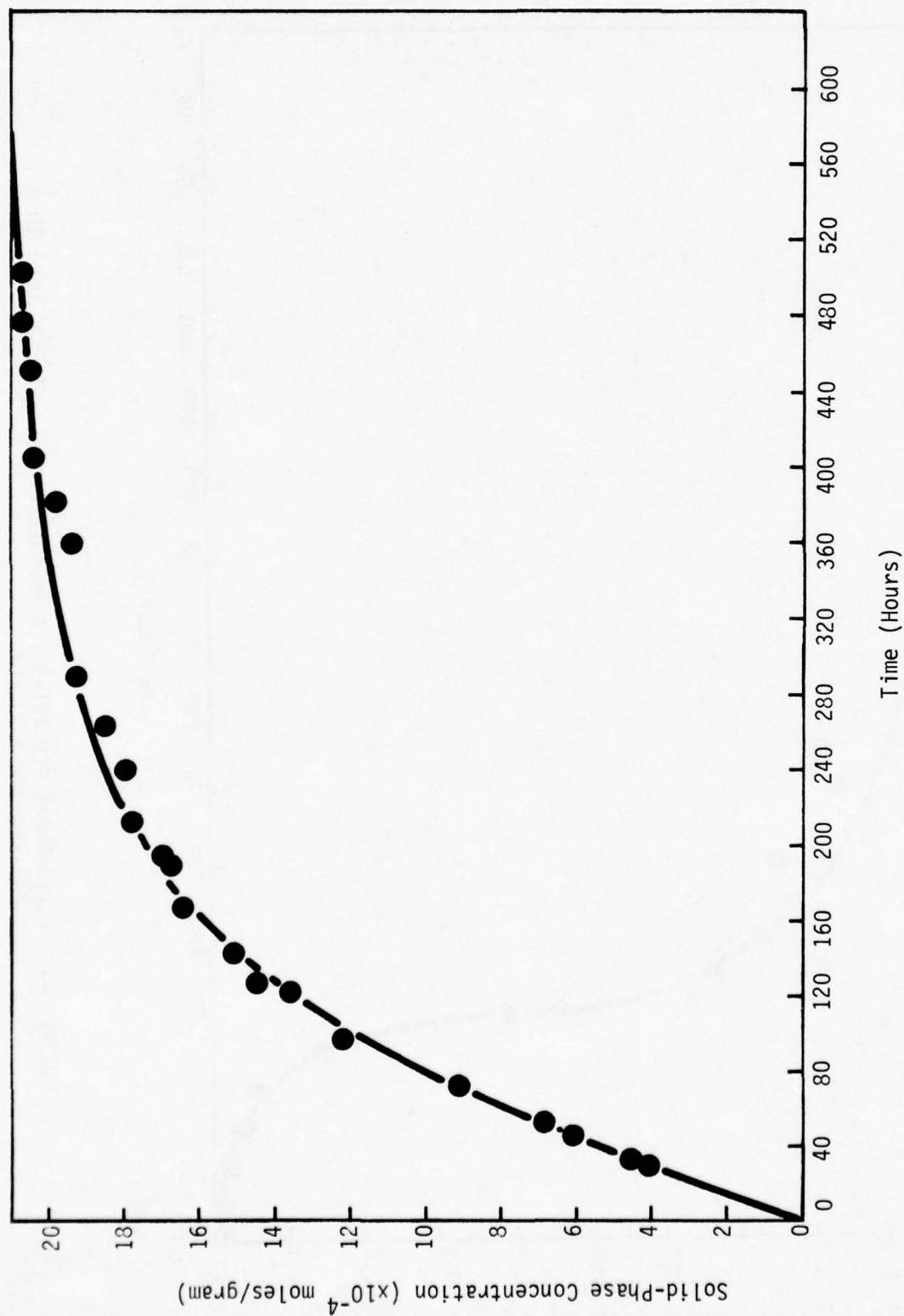


FIGURE D-8: SOLID-PHASE CONCENTRATION PROFILE FOR 2,4-DCP (80.0 μ M) IN A FLUIDIZED-BED ADSORBER.

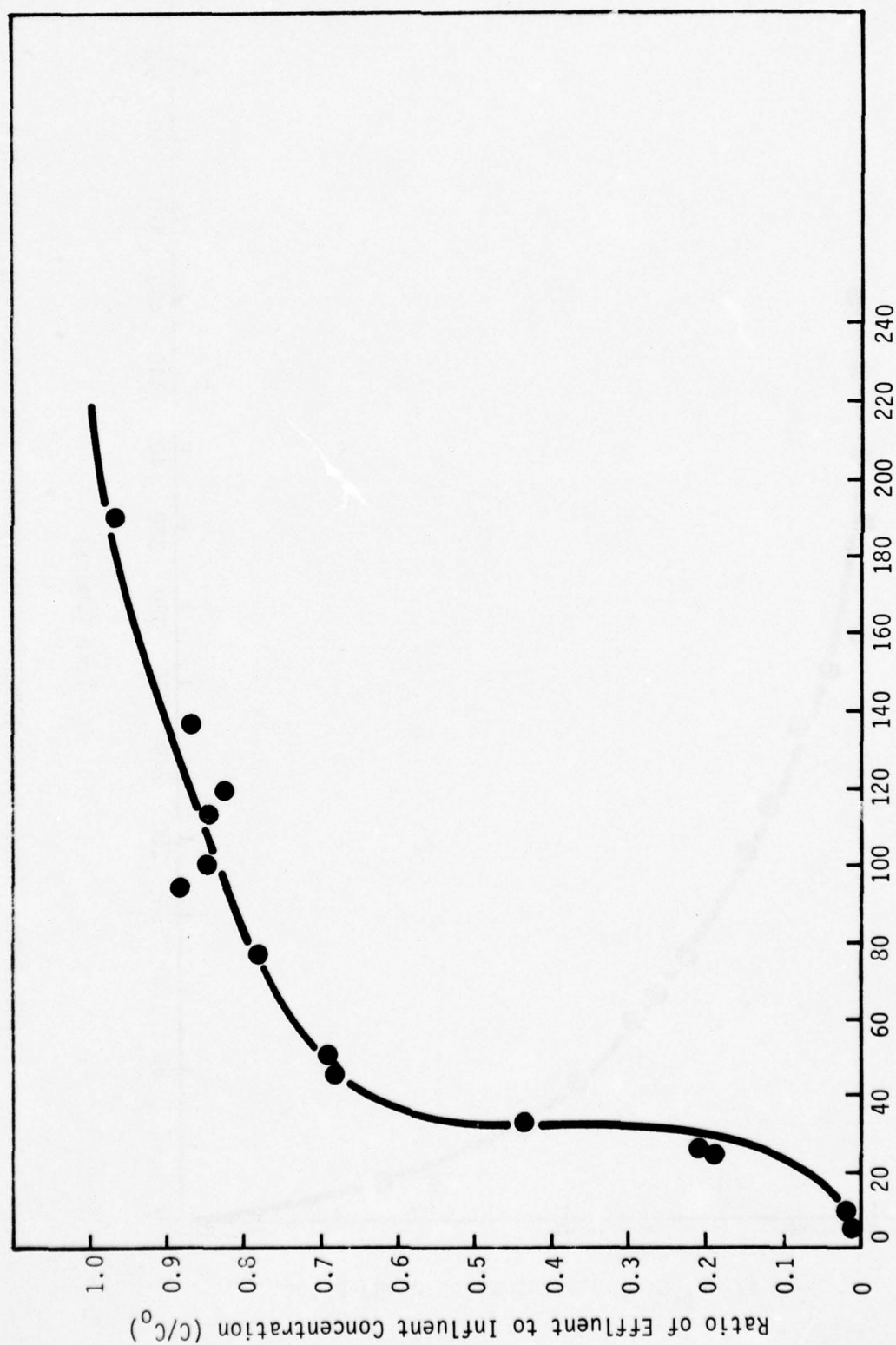


FIGURE D-9: FLUID-PHASE CONCENTRATION PROFILE FOR DNOSBP (81.31 μ M) IN A PACKED-BED ADSORBER.

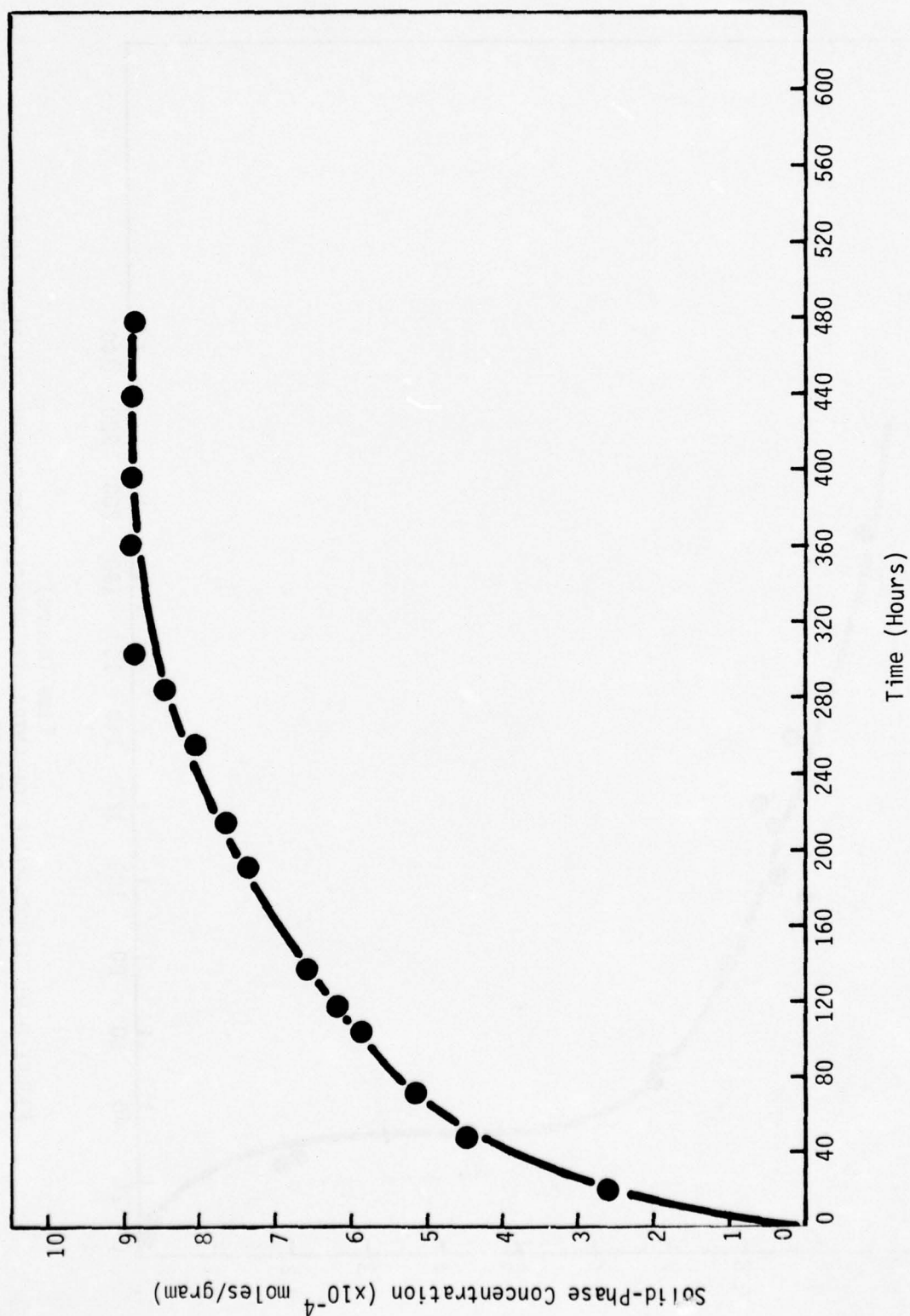


FIGURE D-10: SOLID-PHASE CONCENTRATION PROFILE FOR DNOSBP (81.31M) IN A PACKED-BED ADSORBER.

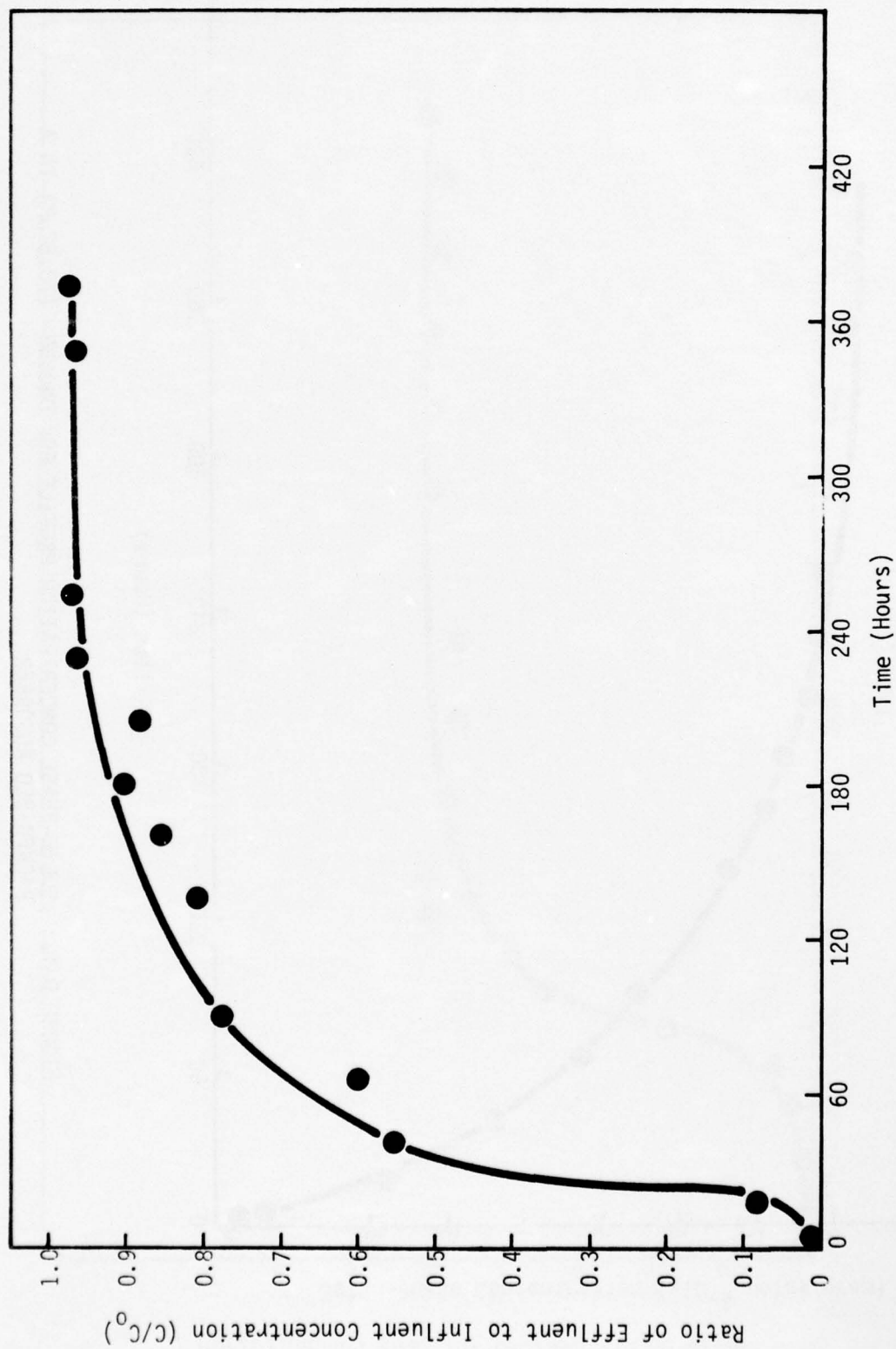


FIGURE D-11: FLUID-PHASE CONCENTRATION PROFILE FOR DNOSBP (78.52 μ M) IN A PACKED-BED ADSORBER.

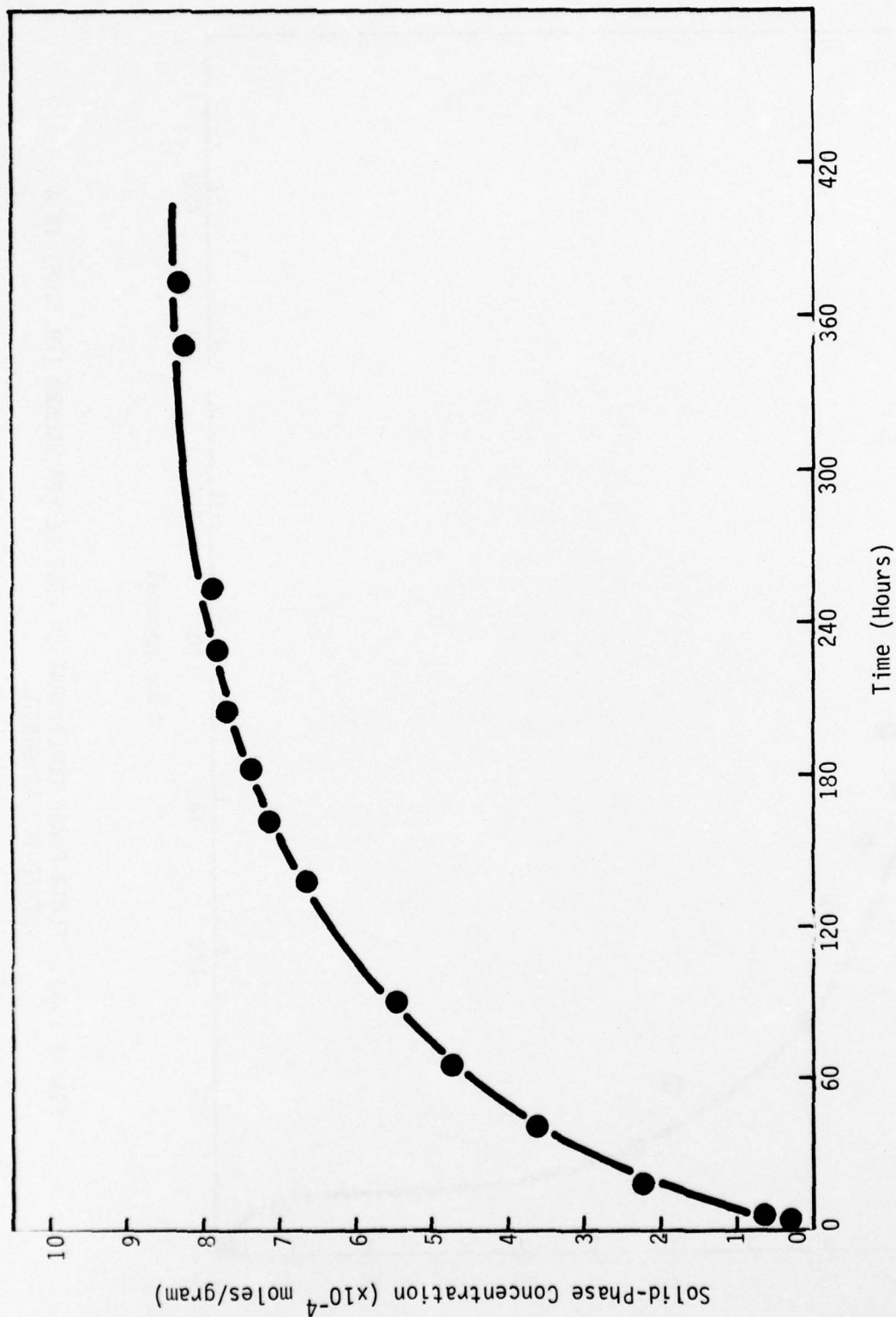


FIGURE D-12: SOLID-PHASE CONCENTRATION PROFILE FOR DNOSBP (78.52 μ M) IN A PACKED-BED ADSORBER.

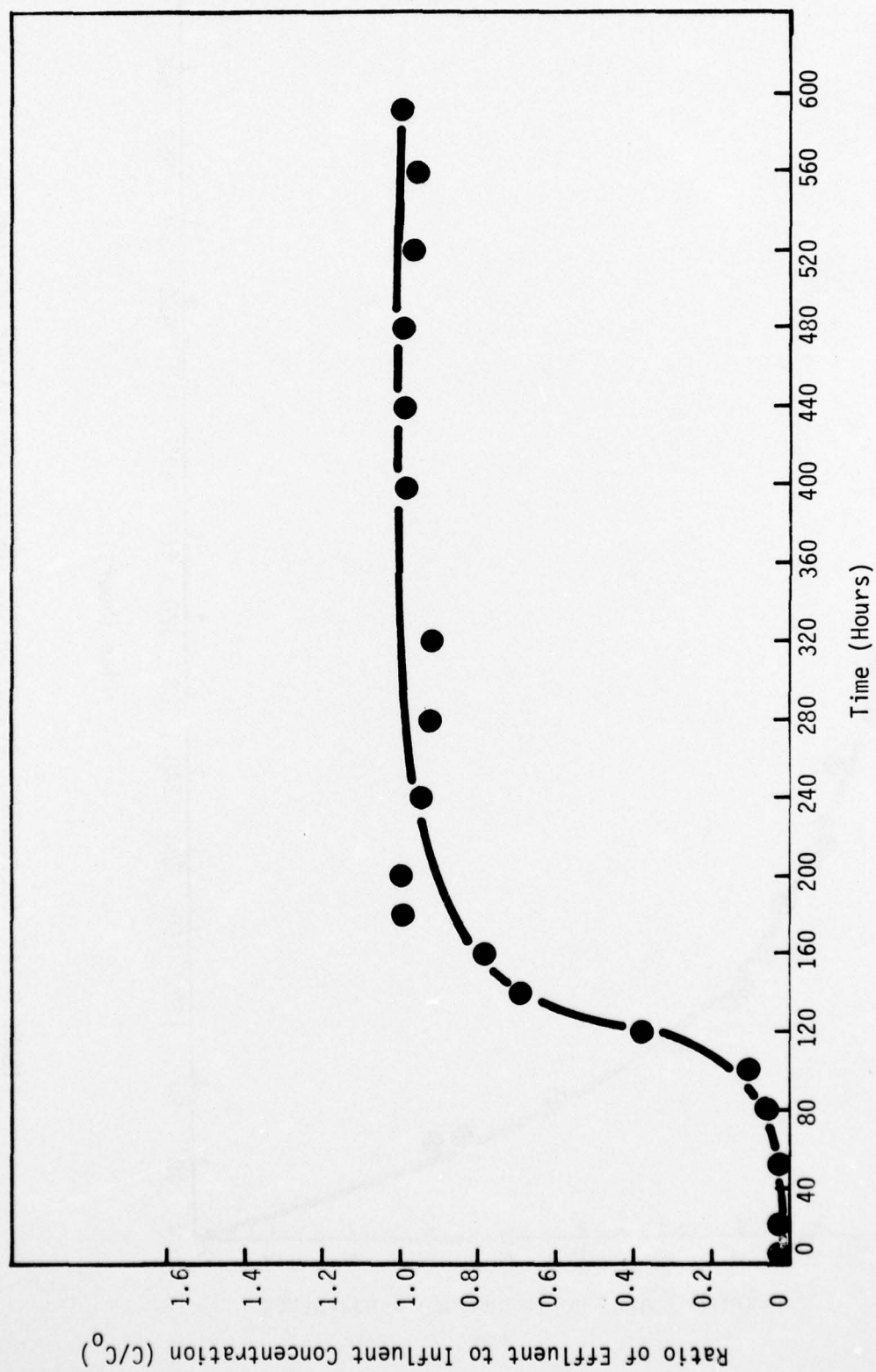


FIGURE D-13: FLUID-PHASE CONCENTRATION PROFILE FOR 2,4-DCP (80.0 μ M) IN A PACKED-BED ADSORBER.

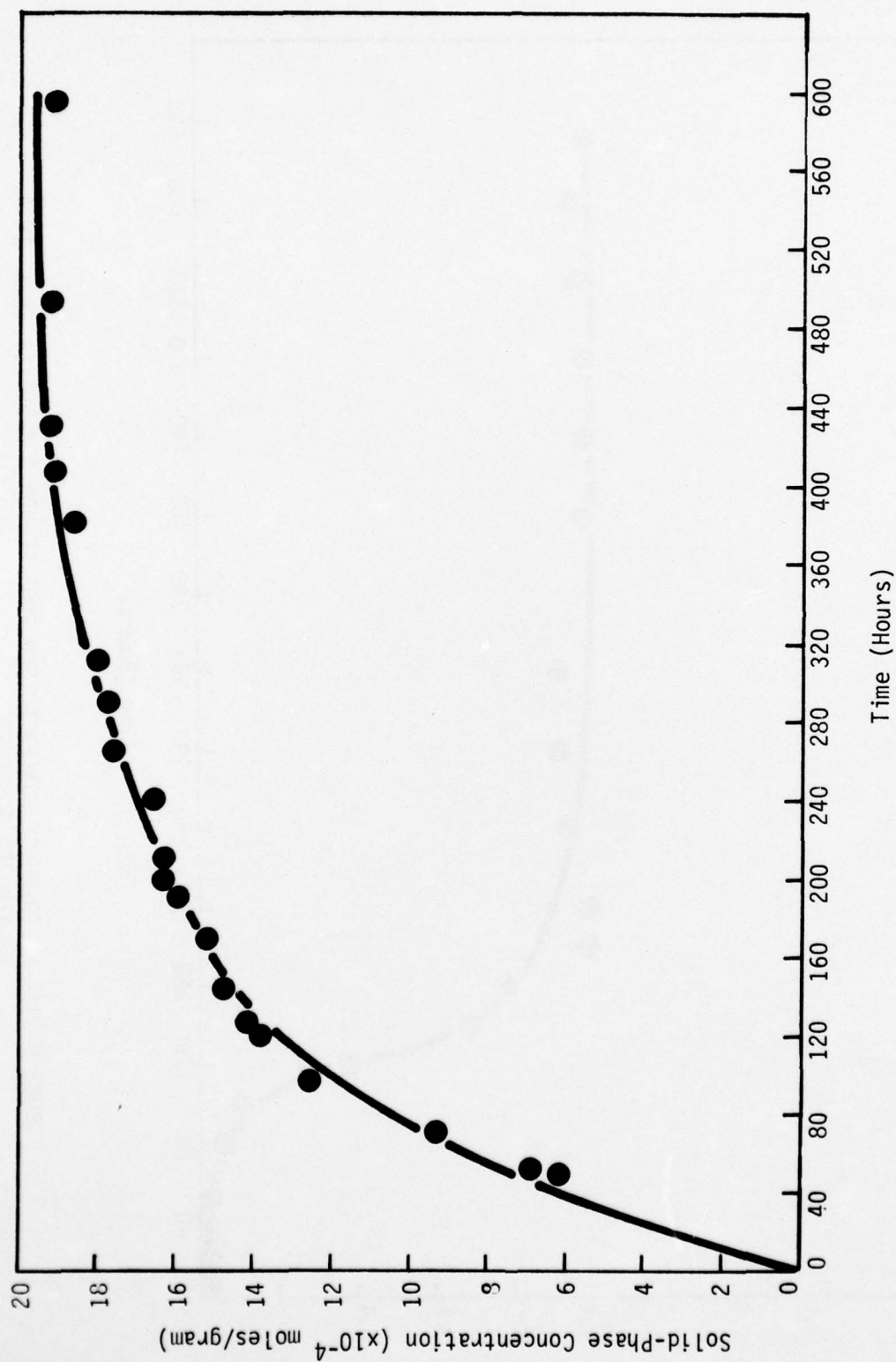


FIGURE D-14: SOLID-PHASE CONCENTRATION PROFILE FOR 2,4-DCP (80.0 μM) IN A PACKED-BED ADSORBER.

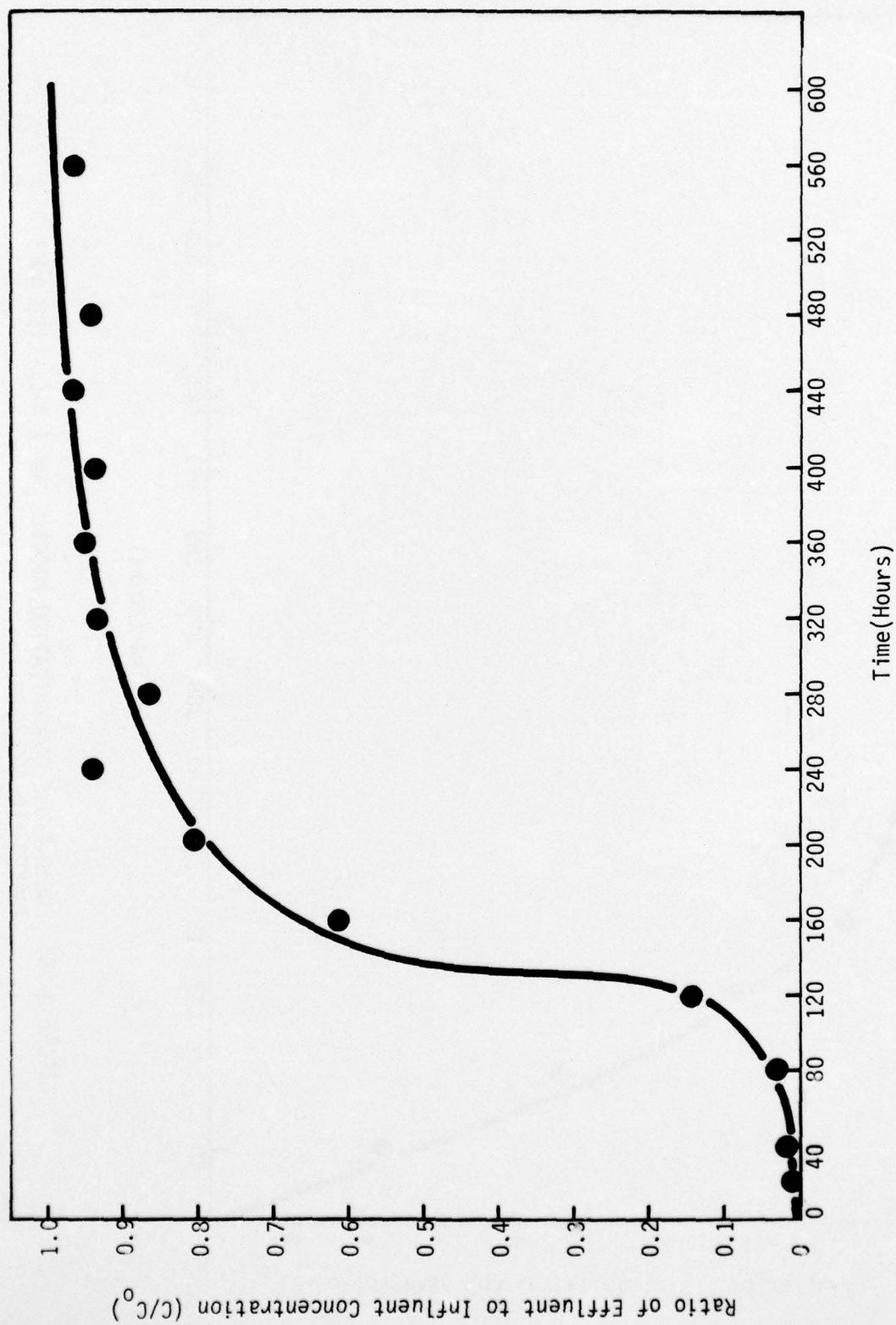


FIGURE D-15: FLUID-PHASE CONCENTRATION PROFILE FOR 2,4-DCP (80.0 μ M) IN A PACKED-BED ADSORBER.

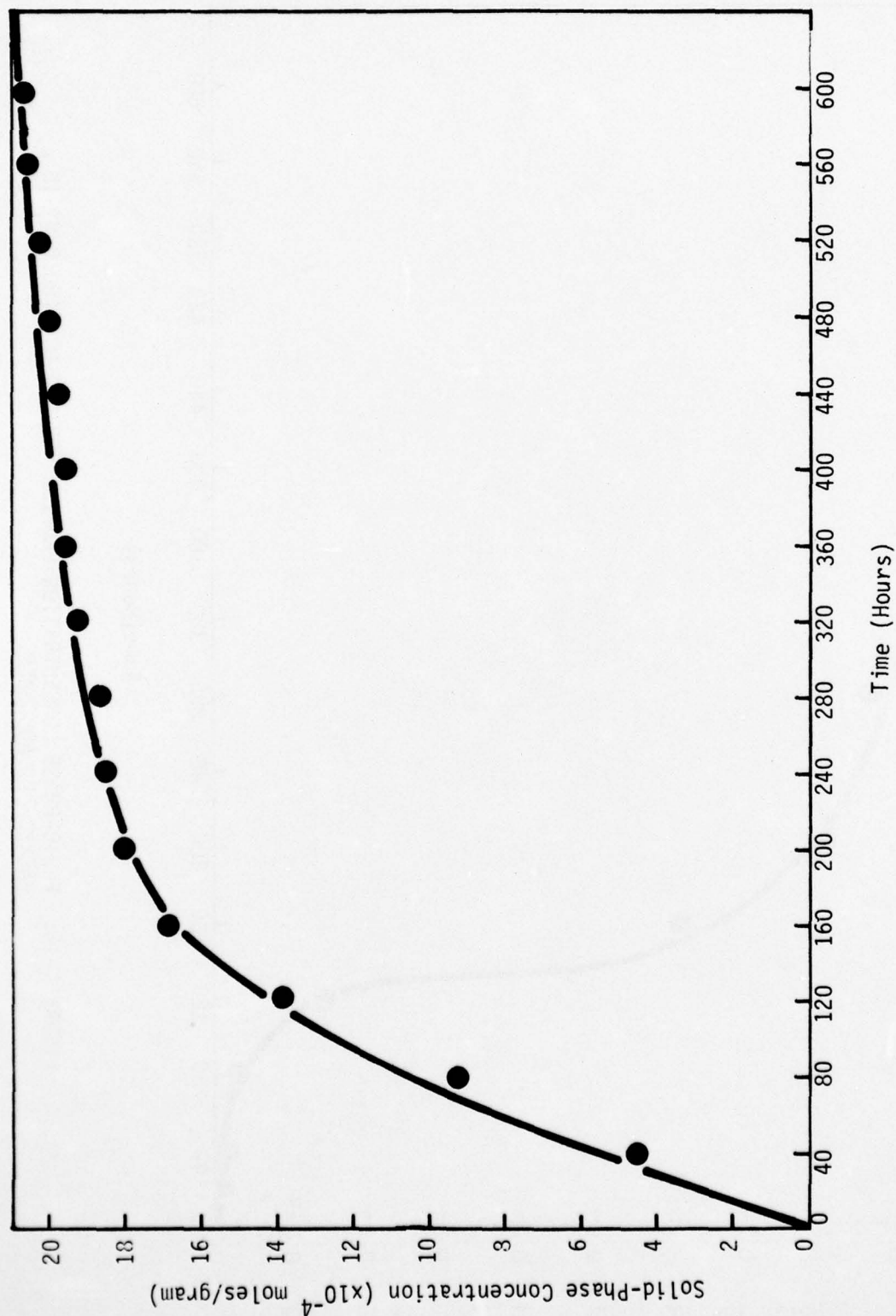


FIGURE D-16: SOLID-PHASE CONCENTRATION PROFILE FOR 2,4-CDP (80.0 μM) IN A PACKED-BED ADSORBER.

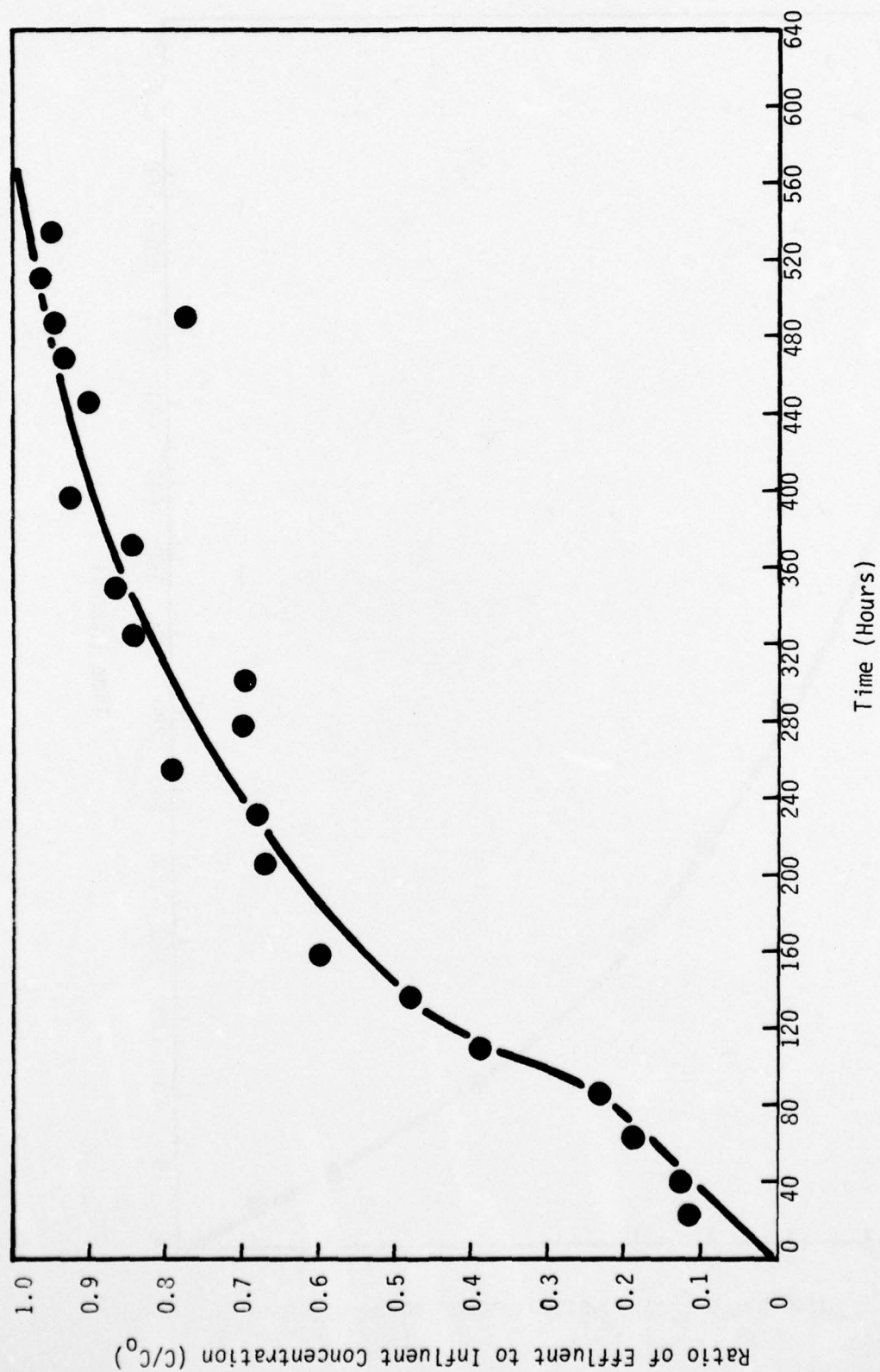


FIGURE D-17: FLUID-PHASE CONCENTRATION PROFILE FOR DNOSBP (82.0 μ M) IN A CSTR ADSORBER.

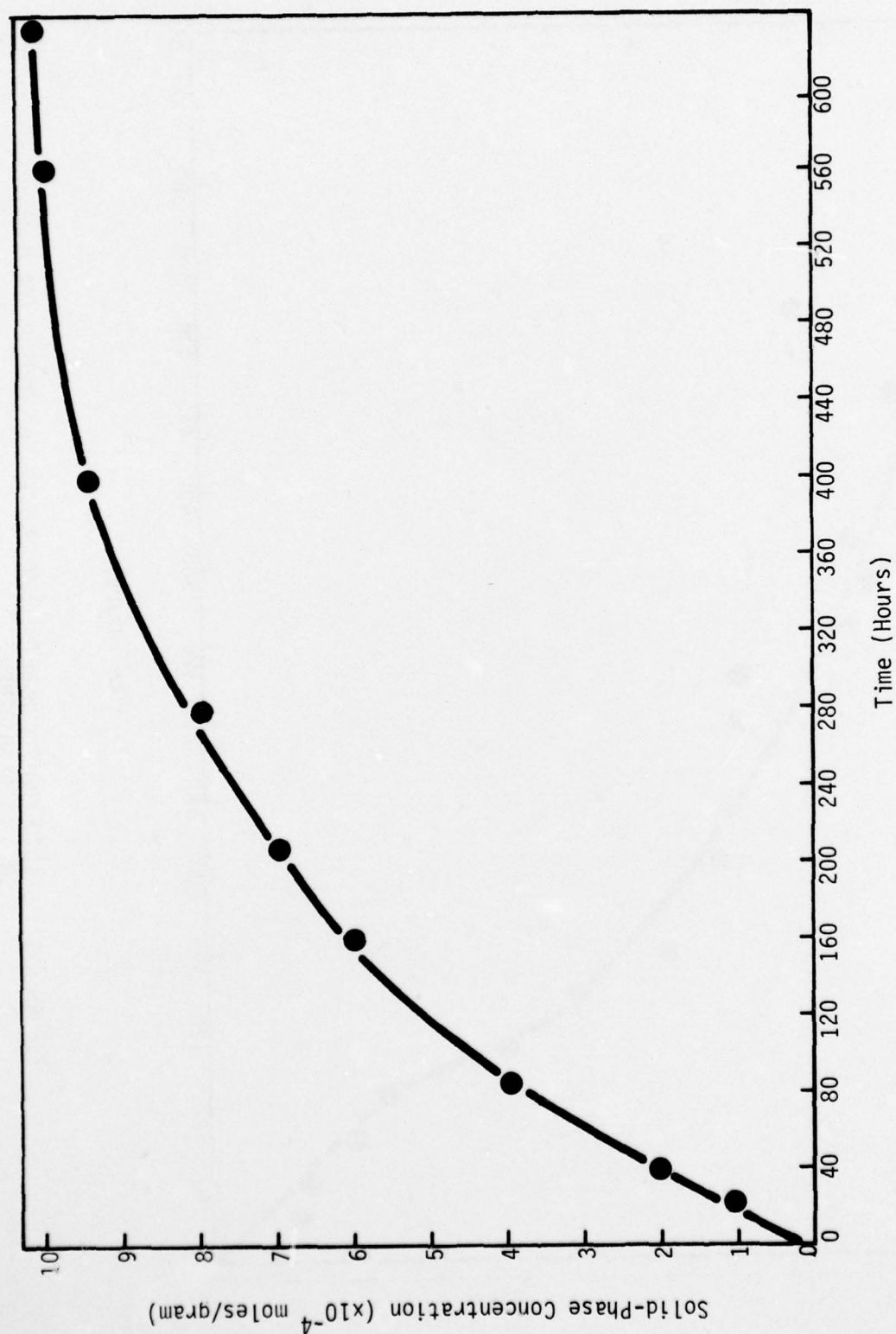


FIGURE D-18: SOLID-PHASE CONCENTRATION PROFILE FOR DNOBP (80.0 μM) IN A CSTR ADSORBER.

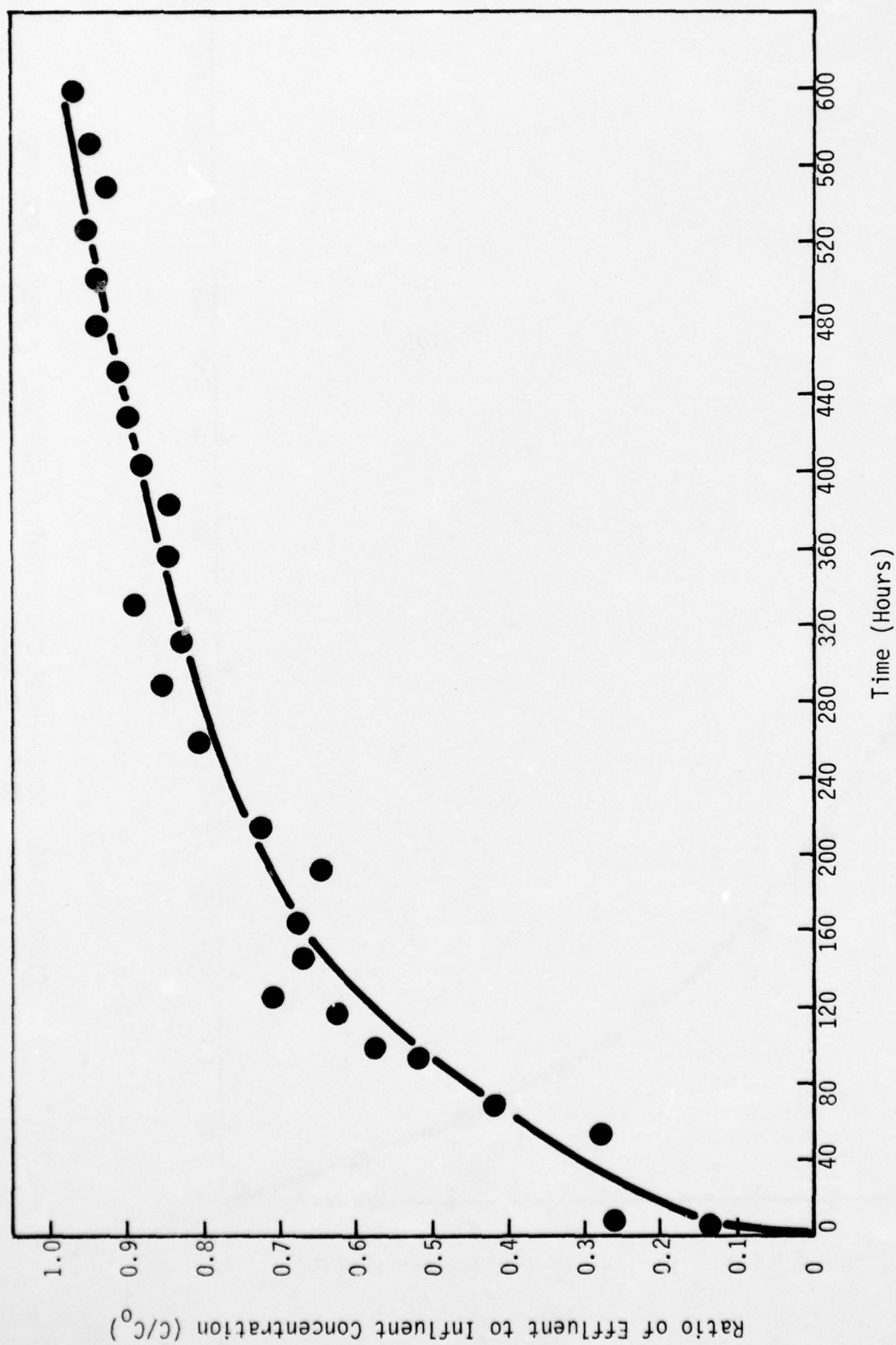


FIGURE D-19: FLUID-PHASE CONCENTRATION PROFILE FOR DNOSBP (80.0 μ M) IN A CSTR ADSORBER.

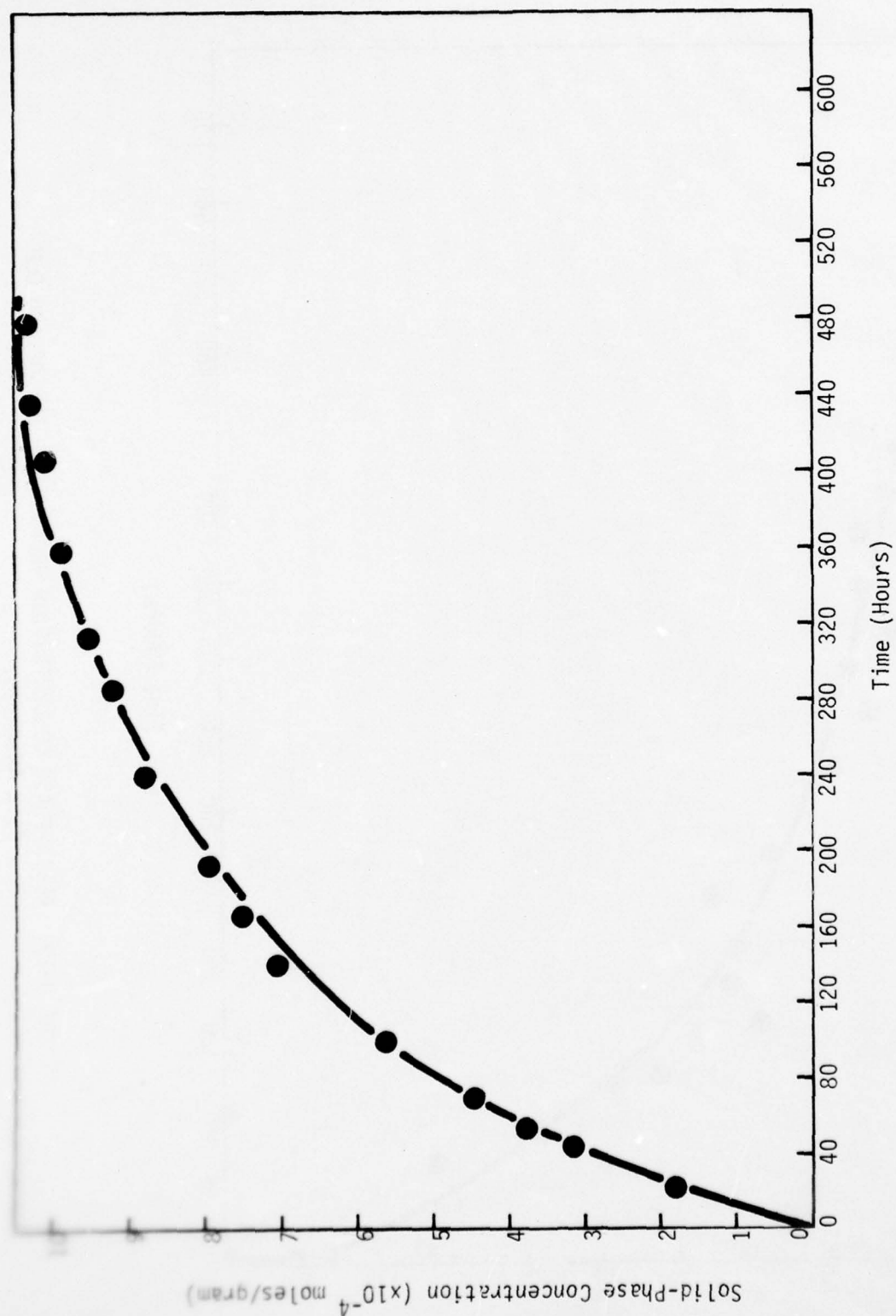


FIGURE D-20: SOLID-PHASE CONCENTRATION PROFILE FOR DNOSBP (80.0 μM) IN A CSTR ADSORBER.

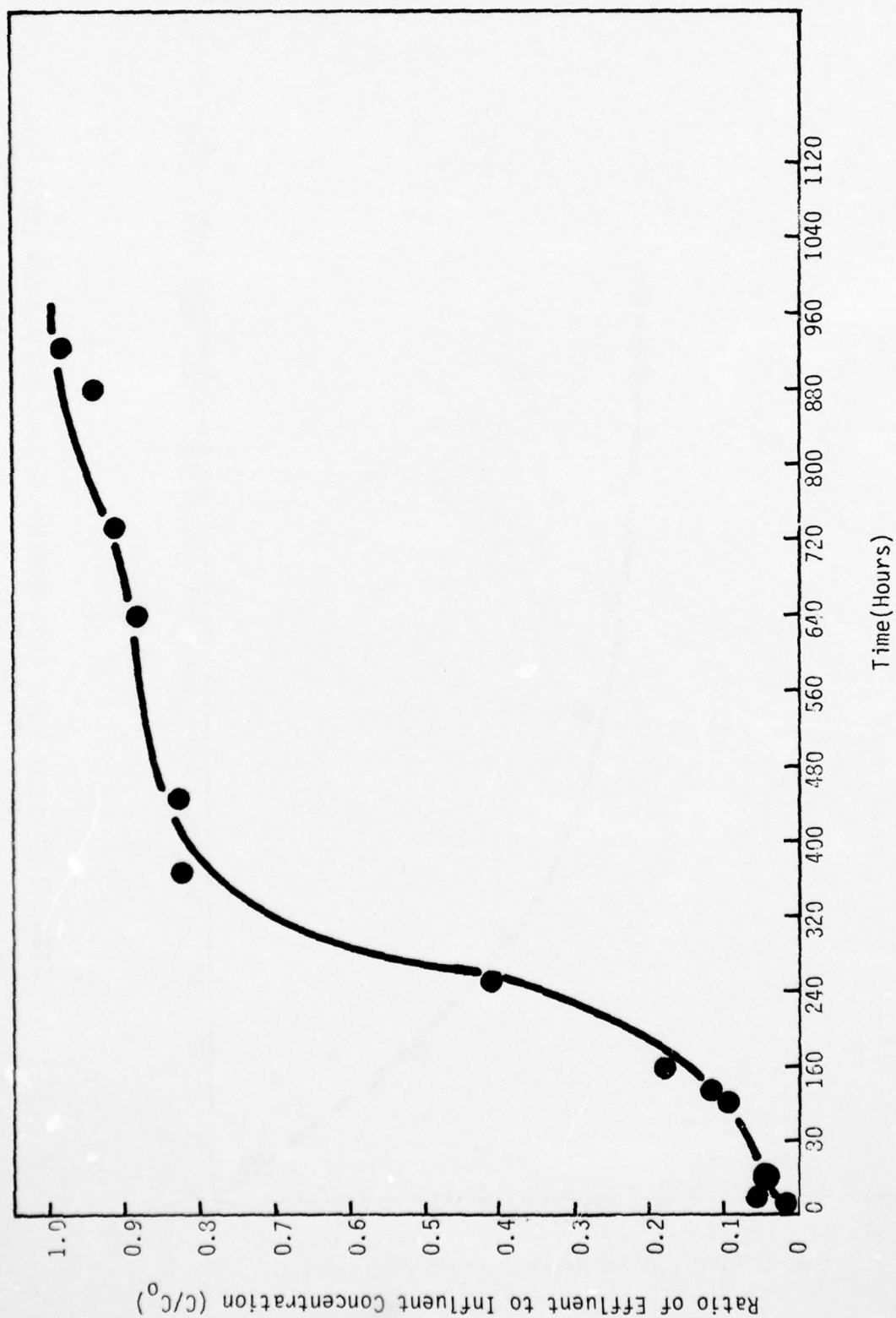


FIGURE D-21: FLUID-PHASE CONCENTRATION FOR 2,4-CDP ($82.21\mu\text{M}$) IN A CSTR ADSORBER.

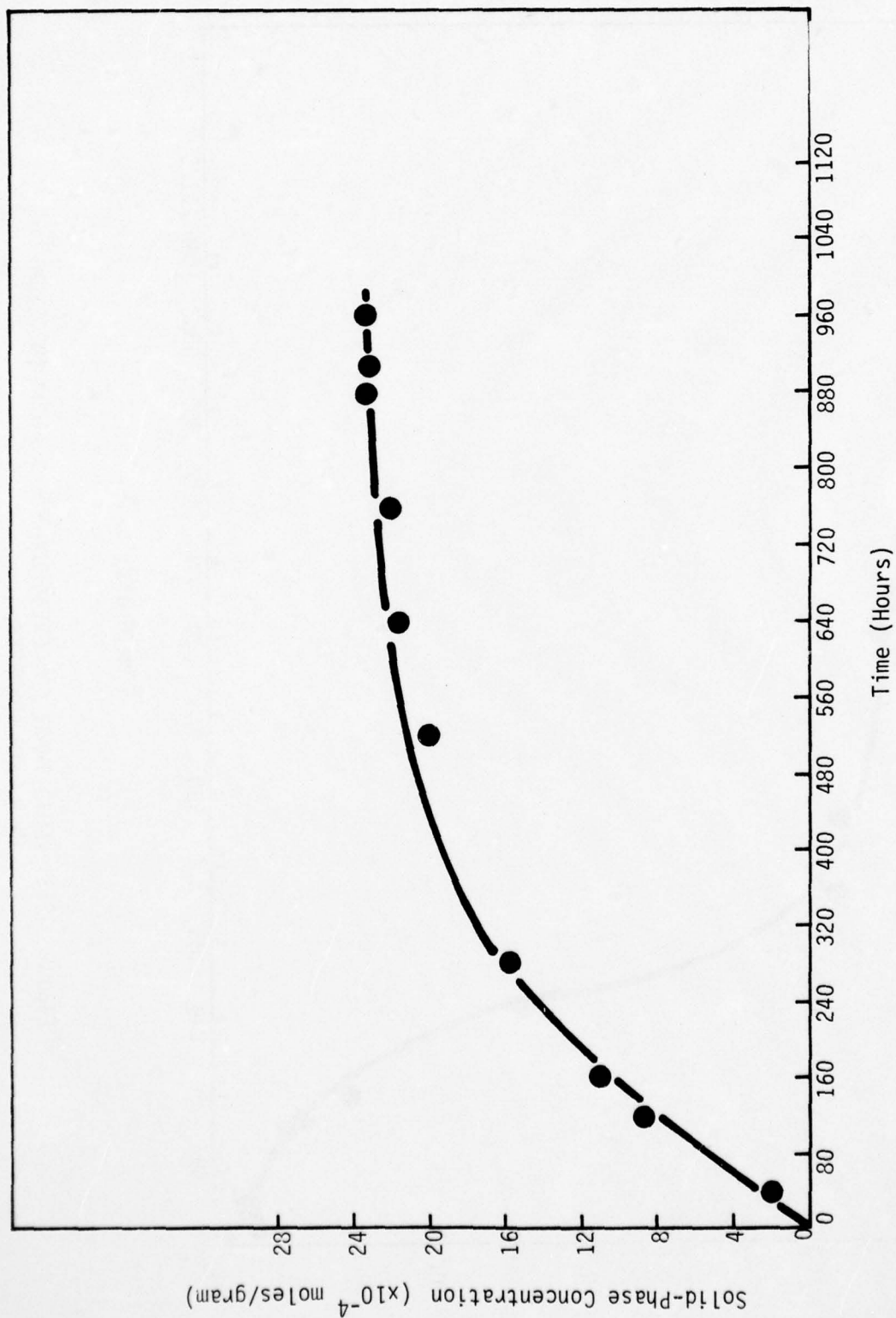


FIGURE D-22: SOLID-PHASE CONCENTRATION PROFILE FOR 2,4-DCP ($82.21\mu\text{M}$) IN A CSTR ADSORBER.

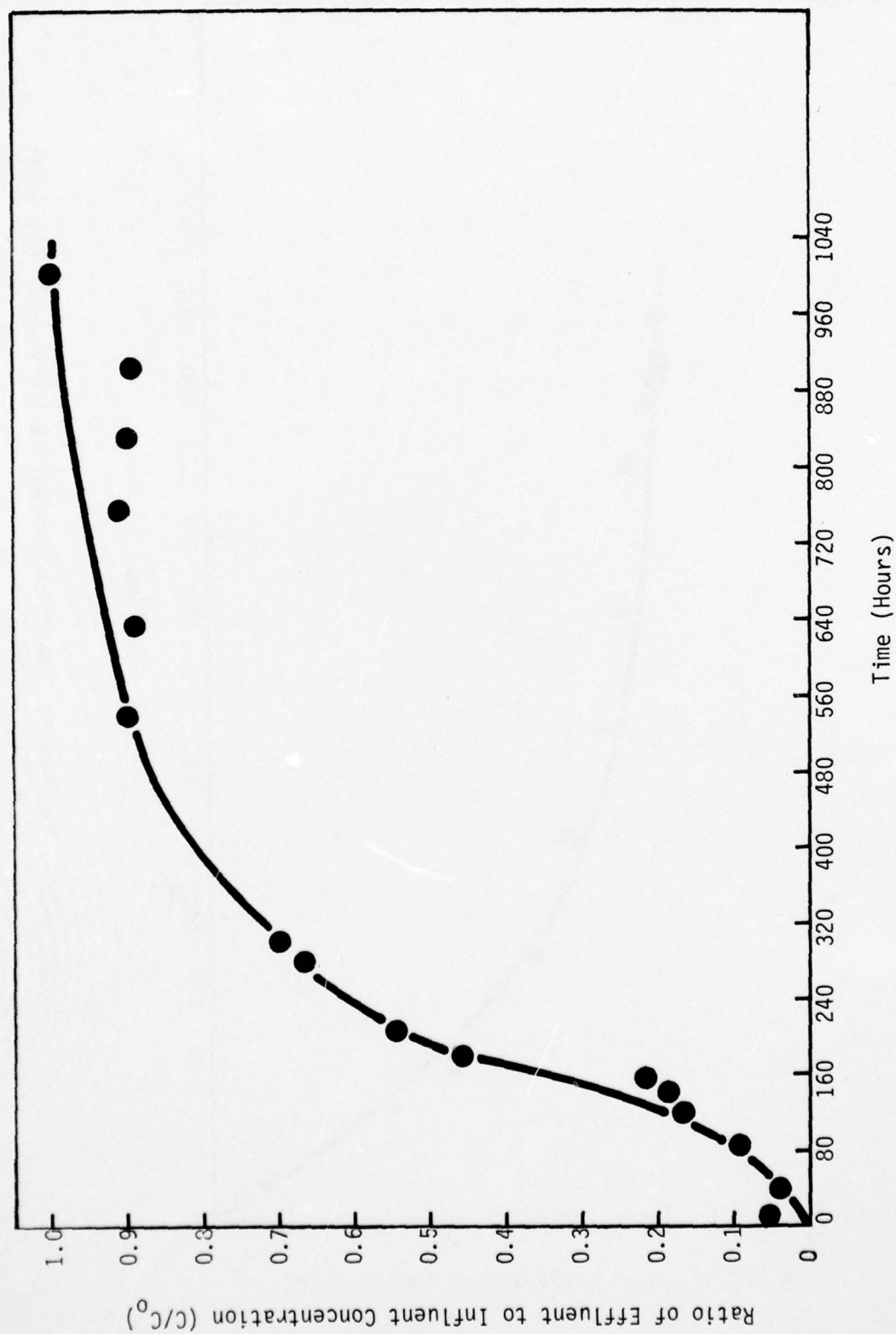


FIGURE D-23: FLUID-PHASE CONCENTRATION PROFILE FOR 2,4-DCP (76.64 μ M) IN A CSTR ADSORBER.

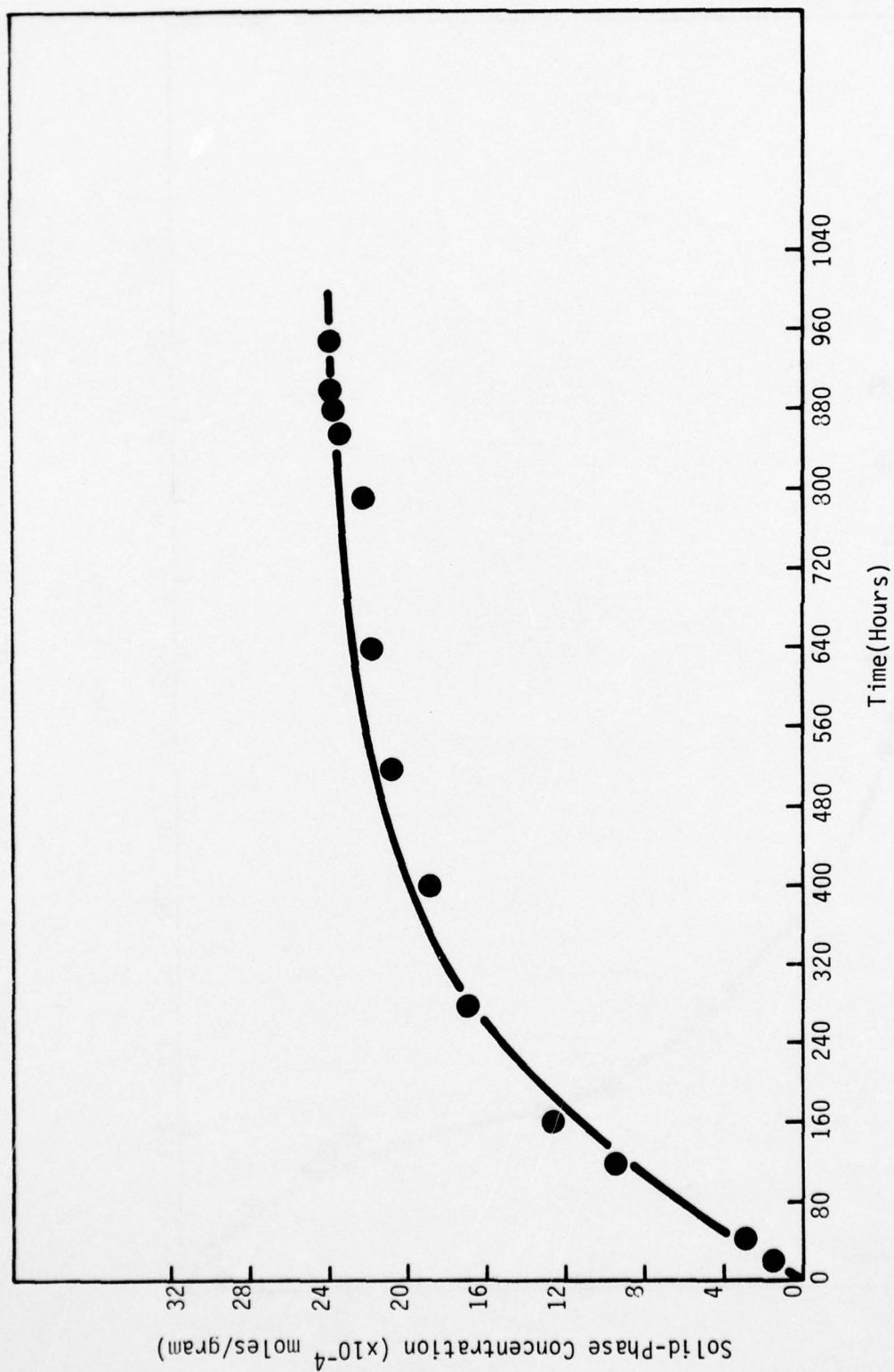


FIGURE D-24: SOLID-PHASE CONCENTRATION PROFILE FOR 2,4-DCP (76.64 μ M) IN A CSTR ADSORBER.

DISTRIBUTION LIST

| | |
|-----------|--|
| 4 copies | HQDA (SGRD-RP) WASH DC 20314 |
| 12 copies | Defense Documentation Center (DDC) ATTN: DDC-TCA Cameron Station Alexandria, Virginia 22314 |
| 1 copy | Superintendent Academy of Health Sciences, US Army ATTN: AHS-COM Fort Sam Houston, Texas 78234 |
| 1 copy | Dean School of Medicine Uniformed Services University of the Health Sciences Office of the Secretary of Defense 6917 Arlington Road Bethesda, MD 20014 |
| 25 copies | Environmental Protection Department ATTN: SGRD-UBG US Army Medical Bioengineering Research and Development Laboratory Fort Detrick, Frederick, MD 21701 |